IMPERIAL COLLEGE LONDON
Division of Cancer, Department of Surgery and Cancer

Identifying New Approaches to the Treatment of Endocrine Resistant Breast Cancer

Kirsty Anushka Balachandran

Thesis submitted for the degree of Doctor of Philosophy

Supervisors: Professors Simak Ali, Laki Buluwela and Charles Coombes

June 2022

Abstract

Estrogen receptor α (ER) plays a key role in the development and progression of breast cancer and is targeted by endocrine therapies used to treat this disease. However, resistance to these therapies remains a major therapeutic challenge. Estrogen receptor gene (*ESR1)* mutations have been implicated as a mechanism of resistance in 20-30% of metastatic, ER-positive breast cancers. The gene-editing system, CRISPR-Cas9, has previously been used to model these mutations in MCF7 cells in my host laboratory. The MCF7-Y537S cell line, with substitution of tyrosine for serine at position 537, has been shown to exhibit estrogen-independent growth, partial resistance to anti-estrogens and upregulation of many ERα target genes, including the progesterone receptor gene (*PGR*). Several reports have demonstrated that, on ligand-activation, the progesterone receptor (PR) reprogrammes the genomic binding pattern and transcriptome of ER into a less tumorigenic profile. Hence PR ligands may have utility in *ESR1* mutant breast cancer. A T47D-Y537S cell line has also previously been created in the laboratory in the same way as MCF7-Y537S cells, using CRISPR-Cas9. Here, I have characterised the T47D-Y537S cell line to check the presence of the Y537S mutation, confirm its ligand-independence and, furthermore, determine its utility for studying PR activity in this setting. I demonstrate that some PR agonists, but not PR antagonists or siRNA-mediated PR knockdown, inhibit the growth of T47D-Y537S cells. To elucidate the role of PR signalling in breast cancer with wildtype (WT) and Y537S ER, I define a set of PR-regulated genes in T47D-WT and T47D-Y537S cells, using RNA-seq. I also identify an anti-migratory effect of a PR agonist on T47D-WT and T47D-Y537S cells, through scratch wound assays and enrichment of Gene Ontology Biological Process pathways related to

motility, which may have implications for the prevention of metastases in endocrine resistant breast cancer.

Statement of Originality

This thesis is submitted in fulfilment of the requirements for the degree of Doctor of Philosophy. I declare that all the work presented in this thesis has been performed by me unless clearly stated otherwise and fully acknowledged.

Kirsty Anushka Balachandran

8th May 2022

Copyright Declaration

The copyright of this thesis rests with the author. Unless otherwise indicated, its contents are licensed under a Creative Commons Attribution-Non Commercial 4.0 International Licence (CC BY-NC).

Under this licence, you may copy and redistribute the material in any medium or format. You may also create and distribute modified versions of the work. This is on the condition that: you credit the author and do not use it, or any derivative works, for a commercial purpose.

When reusing or sharing this work, ensure you make the licence terms clear to others by naming the licence and linking to the licence text. Where a work has been adapted, you should indicate that the work has been changed and describe those changes.

Please seek permission from the copyright holder for uses of this work that are not included in this licence or permitted under UK Copyright Law.

Acknowledgements

There are many people without whom this PhD would not have been possible.

Firstly, I would like to thank my supervisors, Professors Simak Ali, Laki Buluwela and Charles Coombes for their guidance, support and discussions during my studies. Thank you for your generosity with your time - I'm sure you didn't expect to still be supervising me 6 years after I first registered!

Secondly, I would like to thank the past and present members of the lab who have all helped and supported me in different ways. To Dr Alison Harrod, who was instrumental in teaching me the techniques for my first experiments in the early days - I am grateful for your patience, kindness and friendship. I never had the pleasure of meeting Paula Jiminez but I am indebted to her and Professor Laki Buluwela for generating the T47D-Y537S cell line, which formed the basis of so much of my work. Dr Chun Fui Lai has provided humour, support and a wealth of lab experience throughout my time in the group, as well as contributing data to my thesis using the new cell lines that became available to us whilst I was on parental leave. I am also very grateful to Drs Manikandan Periyasamy, Anup Kumar Singh and Carolina Gemma who patiently listened to and answered my many questions on a daily basis before they left the lab. I owe a big thank you to Dr Van Nguyen and Dr Isabella Goldsbrough for their advice and troubleshooting tips when I was learning how to perform bioinformatic analyses. Dr Georgina Sava, Hailing Fan, Kaste Jurgaityte and Georgia Simmons have also supported me during my time in the lab through their discussions and company.

This project would not have begun without Imperial College Healthcare Trust who funded the first year of my PhD, and the Medical Research Council (MRC) who

awarded me a Clinical Research Training Fellowship which funded the remainder of my studies. I am particularly grateful to the MRC Fellows team who have fielded my many queries as my fellowship timelines became slightly extended from the original 3-year plan to account for 2 parental leaves and a global pandemic.

Finally, I would like to thank my friends and family. Liz, as always, has been a constant source of support and understanding throughout. A special thank you must go to my Mum and Dad, who never fail to encourage me in everything I do and to whom I owe everything. And to my husband, Guy, who has supported me in countless ways throughout this time, whilst also completing his own PhD – thank you so much for listening, backing me and, not least, sharing the juggling with me. Finally, thank you to our children, Robyn and Kit (who appeared at various stages of this thesis), for providing fun and perspective when it was most needed!

Table of Contents

Abstract *2*

Statement of Originality *4*

Copyright Declaration *5*

Acknowledgements *6*

List of Figures *14*

List of Tables *17*

1. Introduction *24*

1.1 Breast Cancer **24**

1.1.1 Treatment of Breast Cancer 25

1.1.2 Estrogen and breast cancer 26

1.2 Nuclear Receptor Superfamily **30**

1.2.1 Structure of NRs 30

1.3 Structure and regulation of the Estrogen receptor **33**

1.3.1 Structure and function of the estrogen receptor 33

1.3.2 ER coregulators and pioneer factors 36

1.4 Endocrine therapy for ER positive breast cancer **39**

1.4.1 Ovarian Ablation 39

1.4.2 Tamoxifen 40

1.4.3 Other Selective Estrogen Receptor Modulators 42

1.4.4 Fulvestrant 42

1.4.5 Other Selective Estrogen Receptor Degraders 43

1.4.6 Selective ER Covalent Antagonists and ER PROTAC Protein Degraders 44

1.4.7 Aromatase inhibitors 44

1.4.8 Endocrine therapy plus CDK4/6 Inhibitors 46

1.4.9 Endocrine therapy plus Everolimus 48

1.4.10 Endocrine therapy plus Capivasertib 49

1.4.11 Endocrine therapy plus Alpelisib 50

1.4.12 Endocrine therapy plus HER-2 therapy 50

1.4.13 Neoadjuvant Endocrine therapy and Window Studies of Endocrine Therapy 51

1.5 Mechanisms of endocrine resistance 52

1.5.1 *ESR1* mutations 53

1.5.2 Treatment implications of *ESR1* mutations 63

1.5.3 Other alterations of *ESR1* activity 67

1.5.4 Aberrant regulation of cell cycle and growth signalling pathways 69

1.6 Nuclear Receptor Crosstalk 71

1.6.1 AR in breast cancer 75

1.6.2 GR in breast cancer 76

1.6.3 MR in breast cancer 78

1.7 Progesterone and breast cancer 80

1.7.1 Progesterone biosynthesis and physiological actions 83

1.7.2 Progesterone receptor isoforms and structure 87

1.7.3 Genomic activation and post-translational modifications of PR 91

1.7.4 Non-genomic actions of Progesterone 95

1.7.5 ER and PR in the normal breast 96

1.7.6 PR signalling in breast cancer 104

1.7.7 Modulation of ER activity by PR 110

1.8 PR ligands 111

1.8.1 Progestins 112

1.8.2 PR antagonists 118

1.9 Study Aims 121

2. Materials and Methods 123

2.1 Materials 123

2.1.1 Reagents and Materials 123

2.1.2 Sundries 123

2.1.3 Cell culture equipment and reagents 124

2.1.4 Chemicals 124

2.1.5 General Equipment 125

2.2 Methods 126

2.2.1 Cell Culture 126

2.2.2 Total RNA extraction and complementary DNA synthesis 129

2.2.3 Polymerase Chain Reaction (PCR) and Reverse Transcriptase-Quantitative Polymerase Chain Reaction (RTqPCR) 131

2.2.4 Agarose Gel Electropheresis and DNA sequencing 134

2.2.5 Nuclear localised Green Fluorescent Protein Gene Transduction 135

2.2.6 Cell Growth Assays 136

2.2.7 Scratch Wound Migration Assays 137

2.2.8 Reporter Gene Assays 138

2.2.9 Small interfering RNA (siRNA) Transfection 139

2.2.10 Protein Lysate preparation and Western blotting 140

2.2.11 RNA-sequencing (RNA-seq) 143

2.2.12 Bioinformatic analysis of RNASeq data 144

3. Results 146

3.1 Characterisation of MCF7-Y537S and T47D-Y537S cell lines 146

3.1.1 Confirmation of E2-independent expression of ER target genes in MCF7-Y537S cells 146

3.1.2 Generation and confirmation of Y537S knock-in mutation in T47D-Y537S cells 146

3.1.3 T47D-Y537S cells show estrogen-independent growth and expression of ER-regulated genes 150

3.1.4 Effect of anti-estrogens on ER target gene expression in T47D-Y537S cells 151

3.2 Effect of modulating PR on the growth of *ESR1* mutant cells 155

3.2.1 PR modulating drugs used in this thesis 155

3.2.2 Effect of PR ligands on growth of MCF7-Y537S cells 156

3.2.3 R5020 inhibits the growth of T47D-Y537S cells 158

3.2.4 Effect of siRNA-mediated *ESR1* and *PGR* knock-down on MCF7 and T47D cells 162

3.3 PR target gene expression in ESR1 mutant cells 165

3.3.1 Effect of PR modulating drugs on PR target gene expression in MCF7 and T47D cells 165

3.3.2 Optimisation of conditions for RNA-seq to identify PR regulated gene expression in T47D-Y537S cells 171

3.3.3 T47D-Y537S cells show ligand-independent expression of E2-regulated genes 175

3.3.4 The Y537S mutation confers greater sensitivity to PR ligands 188

3.3.5 Most P4-regulated genes are also R5020-regulated 195

3.3.6 Expression of PR-regulated genes is further stimulated by the presence of E2 199

3.3.7 Genes regulated by R5020 uniquely in the Y537S line 209

3.4 Validation of RNA-seq findings 214

3.4.1 Additional models of the Y537S and D538G mutation modelled in another T47D line 214

3.4.2 R5020 inhibits growth of T47D-WT cells, T47D-Y537S clones #1 and #2 and T47D-D538G clones #49 and #60 218

3.4.3 The effects of R5020 are mediated through PR 221

3.4.4 R5020 reduces migration of T47D and T47D-Y537S cells 225

4. *Discussion* *227*

4.1 The Y537S mutation confers E2-independence in MCF7 and T47D cells 227

4.2 T47D-Y537S cells show greater progestogen-responsiveness than MCF7-Y537S 232

4.3 Investigating the PR transcriptome in ER+ Breast Cancer cells 236

4.4 PR signalling in T47D-Y537S cells 242

4.5 Potential therapeutic strategies for patients with ESR1 mutations 250

4.5.1 PR-targeting therapies for ER+ and *ESR1* mutant breast cancer.....251

4.6 Summary.....**259**

Appendix.....***308***

Appendix I – Generation of Y537S knock-in mutation in T47D-Y537S cells.....**308**

Appendix II – RNA-seq sample read counts and alignment (%) to reference genome (hg38).....**310**

Appendix III – GSEA lists.....**363**

Appendix IV – List of genes in Heatmap clusters.....**372**

List of Figures

Figure 1.1 Hypothalamic-Pituitary-Gonadal (HPG) axis……29

Figure 1.2 Nuclear Receptor Superfamily……33

Figure 1.3 Activation of ER……38

Figure 1.4 Endocrine therapies and their effect on ER activity……52

Figure 1.5 ESR1 mutations……62

Figure 1.6 Nuclear Receptor Crosstalk……..79

Figure 1.7 Challenges in delineating the function of PR signalling……82

Figure 1.8 Steroid Biosynthesis Pathway……86

Figure 1.9 Physiological Progesterone levels……87

Figure 1.10 Structure of PR isoforms and sites of post-translational modifications……...94

Figure 1.11 Classification of Progestins……117

Figure 3.1 ER target genes upregulated in MCF7-Y537S cells……148

Figure 3.2 Characterisation of CRISPR-Cas9 generated ER Y537S mutation in the endogenous ESR1 gene in T47D cells……149

Figure 3.3 T47D-Y537S cells show increased levels of ER protein, estrogen-independent cell growth and increased expression of ER target genes…….153

Figure 3.4 ER target gene expression in the T47D-Y537S line is less sensitive to anti-estrogens than in T47D-WT cells……154

Figure 3.5 Reporter gene assay demonstrating the agonist (PR activating) and antagonist (PR inhibiting) activities of the drugs used in this thesis……157

Figure 3.6 Effect of PR ligands on growth of MCF7 cells carrying ESR1 mutations……158

Figure 3.7 T47D-Y537S cells are sensitive to R5020……161

Figure 3.8 PGR knockdown has only a small effect on growth of MCF7, MCF7-Y537S, T47D-WT and T47D-Y537S cells……..164

Figure 3.9 Human PGR gene and position of siPGR 1-4……..165

Figure 3.10 Low PR activity in MCF7 cells suggested by PR target gene expression……..169

Figure 3.11 Expression of PR regulated genes suggests T47D-WT and T47D-Y537S cells are responsive to Progestin treatment…….170

Figure 3.12 Optimisation of treatment conditions for RNA-seq experiment using 10nM 17β-Estradiol……...173

Figure 3.13 Optimisation of treatment conditions for RNA-seq experiment using P4 and R5020…….174

Figure 3.14 Flowchart detailing RNA-seq pipeline……182

Figure 3.15 Estrogen response pathways are enriched in T47D-Y537S cells in full media…….183

Figure 3.16 ER target genes are differentially expressed in T47D-Y537S cells in hormone deplete conditions…….184

Figure 3.17 Estrogen pathways are enriched in both T47D-WT and T47D-Y537S 17β-Estradiol treated cells…….185

Figure 3.18 Cluster analysis of the 295 differentially expressed genes in T47D-WT and T47D-Y537S cells treated with 17β-Estradiol……186

Figure 3.19 The patterns of gene expression in T47D-WT and T47D-Y537S cells are in keeping with previously published data……..187

Figure 3.20 Flowchart detailing RNA-seq pipeline……192

Figure 3.21 The majority of genes regulated by PR in the T47D-WT line are also regulated in the T47D-Y537S line……..193

Figure 3.22 The magnitude and significance of PR target gene expression is greater with R5020 treatment relative to P4 and in the T47D-Y537S line relative to the T47D-WT……194

Figure 3.23 The majority of genes regulated by R5020 in the T47D-Y537S line are also regulated by P4……197

Figure 3.24 Patterns of PR-regulated gene expression in T47D-WT cells are in keeping with published data……198

Figure 3.25 The addition of E2 further increases the expression of PR-regulated genes……205

Figure 3.26 Cluster analysis of the 371 differentially expressed genes in T47D-WT and T47D-Y537S cells treated with R5020……206

Figure 3.27 Cluster analysis of the 467 differentially expressed genes in T47D-WT and T47D-Y537S cells treated with the combination of R5020 and E2……..207

Figure 3.28 Pathway Enrichment resulting from R5020-upregulated genes in both T47D-WT and Y537S cells……208

Figure 3.29 Differential gene expression between the T47D-WT and T47D-Y537S lines following R5020 treatment……212

Figure 3.30 Genes uniquely R5020-regulated in the T47D-Y537S line, with or without E2……213

Figure 3.31 Validation of RNA-seq results using T47D-WT.SO, T47D-Y537S#1, T47D-Y537S#2 T47D-D538G#49 and T47D-D538G#60 cell lines…….217

Figure 3.32 R5020 inhibits growth of T47D-WT.SO, T47D-Y537S#1/#2 and T47D-D538G#49/60 cells in a dose-dependent manner……..220

Figure 3.33 The effects of R5020 are mediated through PR in T47D-WT.SO, T47D-Y537S#1 and T47D-Y537S#2 cells……224

Figure 3.34 R5020 inhibits migration of T47D-WT and T47D-Y537S cells……226

Figure 4.1 PR Signalling in ER+ Breast Cancer; Findings of this Thesis……260

List of Tables

Table 1.1 Definitions of intrinsic subtypes of breast cancer……25

Table 1.2 Bioavailability, Half-life and Relative Binding Affinity (RBA) of key Progestogens……118

Table 2.1 Estrogen and Progesterone Agonists and Antagonists…….124

Table 2.2 Cell Lines and their Sources……129

Table 2.3 Steroid Hormone content of full and estrogen-depleted media……..131

Table 2.4 Primers for PCR……..132

Table 2.5 Taqman® Gene Expression Assays……...133

Table 2.6 SYBR™ Green Primer Sequences…….134

Table 2.7 SMARTPool and Deconvoluted siRNAs (Dharmacon)……..140

Table 2.8 SDS-PAGE buffers……..142

Table 2.9 SDS-PAGE acrylamide gel solutions……143

Table 2.10 Antibodies for Western Blotting……143

Table 4.1 Summary of studies that have defined PR-regulated genesets in ER+PR+ breast cancer cells……...241

Table 4.2 Summary of studies investigating PR modulating drugs in ER+ Breast Cancer…….259

Abbreviations

ACTH	Adrenocorticotropic hormone
AF1/2	Activation function 1/2
AI	Aromatase Inhibitor
AIB1	Amplified in Breast Cancer 1
AKAP12	A-kinase anchoring protein 12
AKT	Protein kinase B
AP1	Activator protein 1
AP2γ	Activating protein 2 γ
AR	Androgen receptor
AREG	Amphiregulin
ARID1B	AT rich interaction domain 1B
BRCA1/2	Breast Cancer gene 1/2
BSA	Bovine serum albumin
Cas	CRISPR-associated proteins
CBP	CREB-binding protein
CCDC170	Coiled-coil domain containing 170
CCND1	Cyclin D1
CDK	Cyclin-dependent kinase
cDNA	Complementary DNA
cfDNA	Circulating free DNA
ChIP	Chromatin immunoprecipitation
ChIP-seq	Chromatin immunoprecipitation sequencing
CoA	Coactivator
CoR	Corepressor

COSMIC	Catalogue of somatic mutations in cancer
CRISPR	Clustered regularly interspaced short palindromic repeats
CTC	Circulating tumour cell
ctDNA	Circulating tumour DNA
CYP19	Aromatase
DAB2	Disabled-2
DBD	DNA-binding domain
ddH_2O	Double distilled deionised water
DHEA	Dehydroepiandrosterone
DHT	Dihydrotestosterone
ddPCR	Droplet digital PCR
DNA	Deoxyribonucleic acid
DNase	Deoxyribonuclease
DMEM	Dulbecco's modified eagle's medium
DMSO	Dimethyl sulfoxide
DSS	Dextran-coated charcoal-stripped FCS
E1	Estrone
E2	17ß-estradiol
E3	Estriol
ECM	Extracellular matrix
EDTA	Ethylenediaminetetraacetic acid
EGF	Epidermal growth factor
EGFR	Epidermal growth factor receptor
EMT	Epithelial to mesenchymal transition
ER	Estrogen Receptor-α

ERE	Estrogen response elements
EREG	Epiregulin
ERK	Extracellular signal-regulated kinase
FCS	Fetal calf serum
FGFR	Fibroblast growth factor receptor
FISH	Fluorescence *in situ* hybridization
FOXA1	Forkhead box protein A1
FSH	Follicle-stimulating hormone
FULV	Fulvestrant
GATA3	GATA binding protein 3
gDNA	Genomic DNA
GFP	Green fluorescent protein
GnRH	Gonadotropin-releasing hormone
GR	Glucocorticoid receptor
GRIP1	Glutamate receptor interacting protein 1
GSEA	Gene Set Enrichment Analysis
HAT	Histone acetyltransferase
HB-EGF	Heparin-binding-EGF
HDAC	Histone deacetylase complex
HDR	Homology directed DNA repair
HER2	Human epidermal growth factor receptor 2
HPG	Hypothalamic-pituitary-gonadal
HRT	Hormone replacement therapy
IGF	Insulin-like growth factor
IGF-1R	Insulin-like growth factor-1 receptor

IHC	Immunohistochemistry
IL	Interleukin
Indel	Insertion/deletion
IRS-1	Insulin receptor substrate-1
JAK/STAT	Janus kinase/signal transducers and activators of transcription
LBD	Ligand binding domain
LH	Luteinising hormone
LHRH	Luteinising hormone releasing hormone
Log2FC	Log2 fold change
LRH-1	Liver-receptor homolog 1
Luc	Luciferase
LXR	Liver X receptor
MAPK	Mitogen activated protein kinase
Megace	Megestrol acetate
MHT	Menopausal hormone therapy
MMP	Matrix metalloproteinase
MPA	Medroxyprogesterone Acetate
MR	Mineralocorticoid receptor
NCOR1	Nuclear receptor corepressor 1
NFκB	Nuclear factor-κB
NGS	Next-generation sequencing
NR	Nuclear receptor
OHT	4-hydroxytamoxifen
OMP	Oral micronized progesterone
P4	Progesterone

P450aro	Aromatase
padj	adjusted p-value
PAM	Protospacer adjacent motif
PBS	Phosphate buffered saline
PBST	Tween 20 in PBS
PBX1	PBX homeobox 1
PCA	Principal component analysis
PCDH11X	Protocadherin 11 X-linked
PCR	Polymerase chain reaction
PDX	Patient-derived xenograft
PFS	Progression free survival
PI3K	Phosphoinositide 3-kinase
Pol II	RNA polymerase II
Pol III	RNA polymerase III
PR	Progesterone Receptor
PSG	L-glutamine-penicillin-streptomycin
R5020	Promegestone
RARα	Retinoic acid receptor-α
RB	Retinoblastoma protein
RBA	Relative binding affinity
RIPA	Radioimmune precipitation buffer
Rlog	Regularised log transformation
RNA	Ribonucleic acid
RNA-seq	RNA-sequencing
RU486	Mifepristone

RXR	Retinoid X receptors
SDS	Sodium deoxycholate
SDS-PAGE	SDS-polyacrylamide gel electrophoresis
SEM	Standard error of the mean
SERCA	Selective estrogen receptor covalent antagonist
SERD	Selective estrogen receptor downregulator
SERM	Selective estrogen receptor modulator
sgRNA	Single guide RNA
siRNA	short interference RNA
SMRT	Silencing mediator for retinoid and thyroid hormone receptors
SOX9	SRY-Box 9
SP1	Specificity protein 1
SRB	Sulforhodamine B
SRC	Steroid receptor coactivator
StAR	Steroidogenic acute regulatory protein
SWI/SNF	SWItch/Sucrose Non-Fermentable
TBE	Tris-Borate-EDTA
TCA	Trichloroacetic acid
TGF-α	Transforming growth factor-α
TNF-α	Tumour necrosis factor-α
TR	Thyroid receptor
VDR	Vitamin D receptor
WT	Wild-type
YAP1	Yes-associated protein 1

1. Introduction

1.1 Breast Cancer

Breast cancer is the most common cancer in the UK, with over 55,000 cases diagnosed each year and 11,500 associated deaths (Cancer Research UK 2021a). It is also the most commonly diagnosed cancer globally, with 2.3 million women diagnosed in the 5-year period leading up to the end of 2020 (Sung et al. 2021). Although the incidence of breast cancer has been increasing over the last three decades, survival has also improved, in part due to earlier detection through the mammographic screening programme and advances in treatment (Cancer Research UK 2021b).

Breast cancer is a heterogenous disease, which is classified according to the gene expression pattern or 'molecular portrait' of a tumour into one of five intrinsic subtypes, each of which maps to a corresponding surrogate-defined subtype using immunohistochemical measurements of estrogen receptor-α (ER), progesterone receptor (PR), HER-2 and Ki-67 (Table 1.1) (Sørlie et al. 2001; Perou et al. 2000; Goldhirsch et al. 2013). Up to 80% of cases express the estrogen receptor and are classified as luminal A or luminal B (Segal and Dowsett 2014). Prognosis is predicted and treatment dictated by the ER status, together with the histological type, grade, stage and expression of gene mutations such as BRCA1 and BRCA2 (Cardoso et al. 2019).

Table 1.1 Definitions of intrinsic subtypes of breast cancer

Intrinsic Subtype	Definition
Luminal A	'Luminal A-like' ER, PR positive HER2 negative Ki67 low Low risk gene expression signature (if available)
Luminal B	'Luminal B-like (HER2 negative)' ER positive, PR negative or low HER2 negative Ki67 high High risk gene expression signature (if available) 'Luminal B-like (HER2 positive)' ER positive, PR any HER2 positive Ki67 any
HER2 overexpression	'HER2 positive (non-luminal)' HER2 positive ER, PR negative
Basal-like	'Triple negative (ductal)' ER, PR negative HER2 negative

Adapted from the St Gallen Consensus Conference 2013 (Goldhirsch et al. 2013)

1.1.1 Treatment of Breast Cancer

Mortality from breast cancer has fallen by 41% since the 1970s; the reasons for this are multifactorial but include an improvement in treatments available for these patients (Cancer Research UK 2021b). Treatment is based on the individual patient's tumour staging and immunohistochemical status, as well as co-morbidities and any contraindications to treatment. Historically, the treatment of breast cancer has been underpinned by the surgery, radiotherapy, chemotherapy and endocrine therapy, either alone or in combination. In the last couple of decades, targeted therapies have

also been used to treat breast cancer, e.g. Trastuzumab (a monoclonal antibody that targets HER-2) for HER-2 positive breast cancer (Slamon et al. 2001). Chemotherapy may be given either before (neoadjuvant) or after (adjuvant) surgery and enables less invasive surgery (e.g. breast-conserving surgery instead of mastectomy) and reduces the risk of recurrence respectively. Endocrine therapy is discussed in section 1.4.

1.1.2 Estrogen and breast cancer

The role of ovarian steroid hormones in supporting the growth and maintenance of breast cancer was demonstrated by Beatson at the end of the nineteenth century, when bilateral oophorectomy was shown to induce remission of the disease in a premenopausal patient (Beatson 1896). Less than thirty years later in 1923, Allen and Doisy extracted and isolated the so-called 'primary ovarian hormone', (now known as estrogen (E2)) (Allen and Doisy) and in the 1960s, its mediator, the ER was discovered and ER antibodies developed (Jensen et al. 2010; Toft and Gorski 1966).

In premenopausal women, the ovaries are the primary site of E2 production, and are controlled by endocrine feedback loops involving the hypothalamic-pituitary-gonadal (HPG) axis (Figure 1.1) (Clemons and Goss 2001). This release of gonadotropin-releasing hormone (GnRH) from the hypothalamus stimulates luteinising hormone (LH) and follicle-stimulating hormone (FSH) production in the anterior pituitary gland, which in turn results in ovarian release of androgen and stimulation of the expression of the aromatase enzyme (known as CYP19 or P450aro) from theca and granulosa cells respectively (Auchus and Auchus 2012). Androstenedione and testosterone are then converted by aromatase into estrone (E1) and estradiol (E2) respectively (Miller and Auchus 2011) and E1 can be converted to E2 by 17β-hydroxysteroid dehydrogenase (Clemons and Goss 2001). A third native estrogen, Estriol (E3), plays

an important role in pregnancy and is primarily produced by the placenta (Levitz et al. 1984). In postmenopausal women, relatively small amounts of E2 are synthesized, and this occurs through aromatisation of adrenal androgens in extra-gonadal sites, e.g. in hepatic, vascular, brain, bone and adipose tissues (Cui et al. 2013; Simpson and Davis 2001).

E2 plays a wide range of protective roles, as demonstrated by the fact that the lower levels found in postmenopausal women leaves them at greater risk of osteoporosis, cardiovascular disease and cognitive impairment (Simpson and Davis 2001). However, alongside this role in normal physiology, increased lifetime exposure to E2 is associated with a greater risk of developing breast cancer (Lippman et al. 2001) and this is reflected in the established risk factors for the disease including early menarche, late menopause and nulliparity (Clemons and Goss 2001; Paffenbarger et al. 1980). Exposure to combined exogenous E2 and progesterone is also associated with higher rates of breast cancer; the oral contraceptive pill and hormone replacement therapy (HRT), now known as menopausal hormone therapy (MHT) are both well-described risk factors (Clemons and Goss 2001). Many key studies, including the Million Women Study, the Women's Health Initiative trial and the Nurses' Health Studies, have confirmed the risk of breast cancer with MHT use, particularly with combination (E2 and progesterone) treatment (discussed further in section 1.7.6) (Beral et al. 2002; Beral 2003; Chlebowski et al. 2003; Chlebowski et al. 2015; Anderson et al. 2004; Rossouw et al. 2002; Calle et al. 1996; Hunter et al. 2010; Olsson et al. 2003; Ross et al. 2000). More recently, the Collaborative Group on Hormonal Factors in Breast Cancer (CGHFBC) performed a meta-analysis showing that (1) MHT started at the age of menopause increased the risk of breast of cancer relative to women who had

never had MHT, (2) this increase was greater in women who received combination treatment, and (3) although the risk reduced on cessation of MHT, some excess risk remained for >10 years (CGHFBC 2019).

The mechanism by which E2 exposure increases the risk of breast cancer is thought to be through binding of E2 to ER, then direct binding of ER to estrogen response elements (EREs) in ER-regulated genes and recruitment of the general transcriptional machinery, and then activation or suppression of ER target genes that control cancer cell growth and proliferation (discussed in more detail in section 1.3.1) (Clemons and Goss 2001). The efficacy of treatments inhibiting the effects of E2 (discussed in section 1.4) is further evidence of its carcinogenic role in breast cancer (Ali and Coombes 2002).

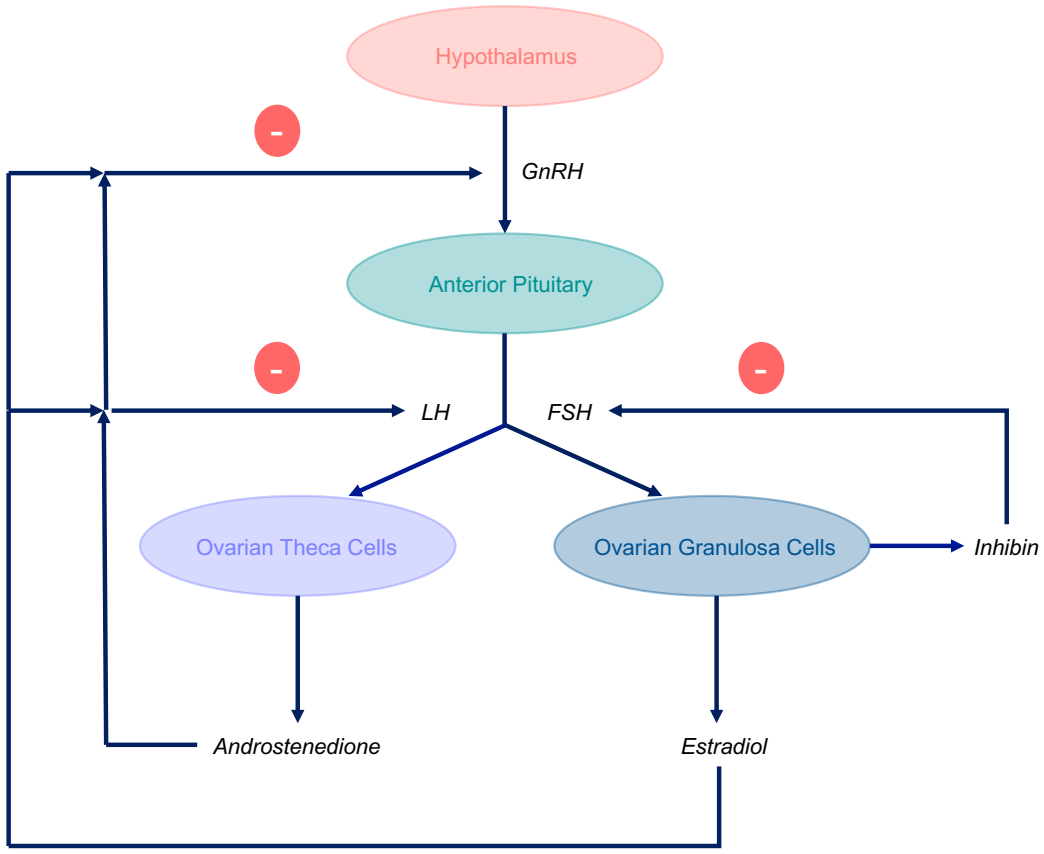


Figure 1.1 Hypothalamic-Pituitary-Gonadal (HPG) axis

Regulation of the HPG axis for the ovary; arrows indicate the actions of the relevant hormones and red symbols denote negative feedback.

1.2 Nuclear Receptor Superfamily

The nuclear receptor (NR) superfamily comprises 48 transcription factor genes, the majority of which contribute to key physiological processes including growth, development, homeostasis and metabolism (Chawla et al. 2001). As well as the classical steroid hormone receptors, such as ER, PR, AR, glucocorticoid receptor (GR) and mineralocorticoid receptor (MR), this group also includes a large number of 'orphan' hormone receptors, which have no known endogenous ligand and unclear functions, although some are likely to act as lipid and metabolic sensors (Figure 1.2A) (Chawla et al. 2001; Huang et al. 2010). Since NRs are most commonly activated upon binding of small molecules to the LBD, the possibility of generating synthetic compounds that compete with the cognate ligand but inhibit rather than activate the NR makes them possible to target for development of therapeutic drugs, as exemplified by anti-estrogens. Indeed, drugs targeting NRs comprise 16% of all human small-molecule drugs in clinical use (Santos et al. 2017). However, the structural homology between NRs does sometimes result in cross-reactivity of drugs across several NRs, which can result in these drugs having undesirable side effects as discussed in section 1.8 (De Bosscher et al. 2020).

1.2.1 Structure of NRs

Although NRs are activated by a diverse range of typically lipophilic ligands (including steroid hormones, thyroid hormones, vitamin D3, retinoic acid and fatty acids), they share structural similarities (Chawla et al. 2001). Each NR is made up of an N-terminal region that is often variable in sequence and length, a highly conserved (i.e. structurally similar for different NRs) DNA binding domain (DBD), a linking "hinge" region, and a conserved ligand binding domain (LBD) (Figure 1.2B) (De Bosscher et

al. 2020). The crystal structure of the DBD and LBD has been resolved for many NRs and structural similarity between LBDs in different NRs is evident. The LBDs are generally comprised of 12 α-helices and contain a central hydrophobic 'pocket' shaped by amino acid residues in helices 3, 7 and 10, the size of which ranges widely between NRs (Li et al. 2003). Transcription activation functions are contained within the N-terminal region (activation function 1 (AF1)) and the LBD (activation function 2 (AF2)) (Figure 1.2B). Helix 12 is critical to AF2 and its position is shifted by ligand-binding, facilitating NR activation (Nagy and Schwabe 2004; de Lera et al. 2007). Upon ligand stimulation, AF2 interacts with coregulators that directly facilitate post-translational modifications, resulting in chromatin remodelling and altered patterns of gene expression (O'Malley et al. 2008; Wolf et al. 2008; Huang et al. 2010; Anbalagan and Rowan 2015). The conformation of agonist-bound NR facilitates recruitment of coactivators through the NR interaction domain, which is an α-helical motif comprising an amino acid sequence with the consensus sequence LXXLL (L=leucine, X=any amino acid). NR antagonists function by altering the position of helix 12 to inhibit coactivator binding and can also stimulate binding of corepressors to AF2 through an elongated α-helical compressor motif with the consensus L/I-X-X-I/V-I ((I=isoleucine, V=valine) (Huang et al. 2010; Hu and Lazar 1999).

The DBD is the most structurally conserved domain across the NR superfamily. It is comprised of 2 zinc finger motifs, each with 4 cysteines co-ordinating one Zn^{2+} ion (De Bosscher et al. 2020). Depending on the NR, monomers, homodimers or heterodimers are formed and bind to consensus DNA response elements accordingly (Chandra et al. 2008; Mangelsdorf and Evans 1995). Retinoid X receptors (RXR) are the most widely reported heterodimerisation partner, pairing with several other NRs (including

retinoic acid receptors (RAR), liver X receptor (LXR), vitamin D receptor (VDR) and the thyroid receptor (TR)). These NRS bind, as heterodimers with RXRs, to direct repeats of the sequence 5'-AGGTCA-3' (Evans and Mangelsdorf 2014; Khorasanizadeh and Rastinejad 2001). Studies have also reported heterodimerisation of ER-α and ER-β, though both can also bind as homodimers to a palindromic repeat sequence, 5'-AGGTCANNNTGACCT-3' (N=any nucleotide) (Cowley et al. 1997; Walker et al. 1984). The other steroid receptors, PR, AR, MR and GR tend to form homodimers and bind to palindromic repeats of the half-site sequence, 5'-AGAACA-3' (Gewirth and Sigler 1995; Khorasanizadeh and Rastinejad 2001). Finally, some NRs bind as monomers, including LRH-1 which binds to sequences with similarity to the motif 5'-YCAAGGYCR-3' (Y=pyrimidine, R=purine) (Seacrist et al. 2020; Fayard et al. 2003).

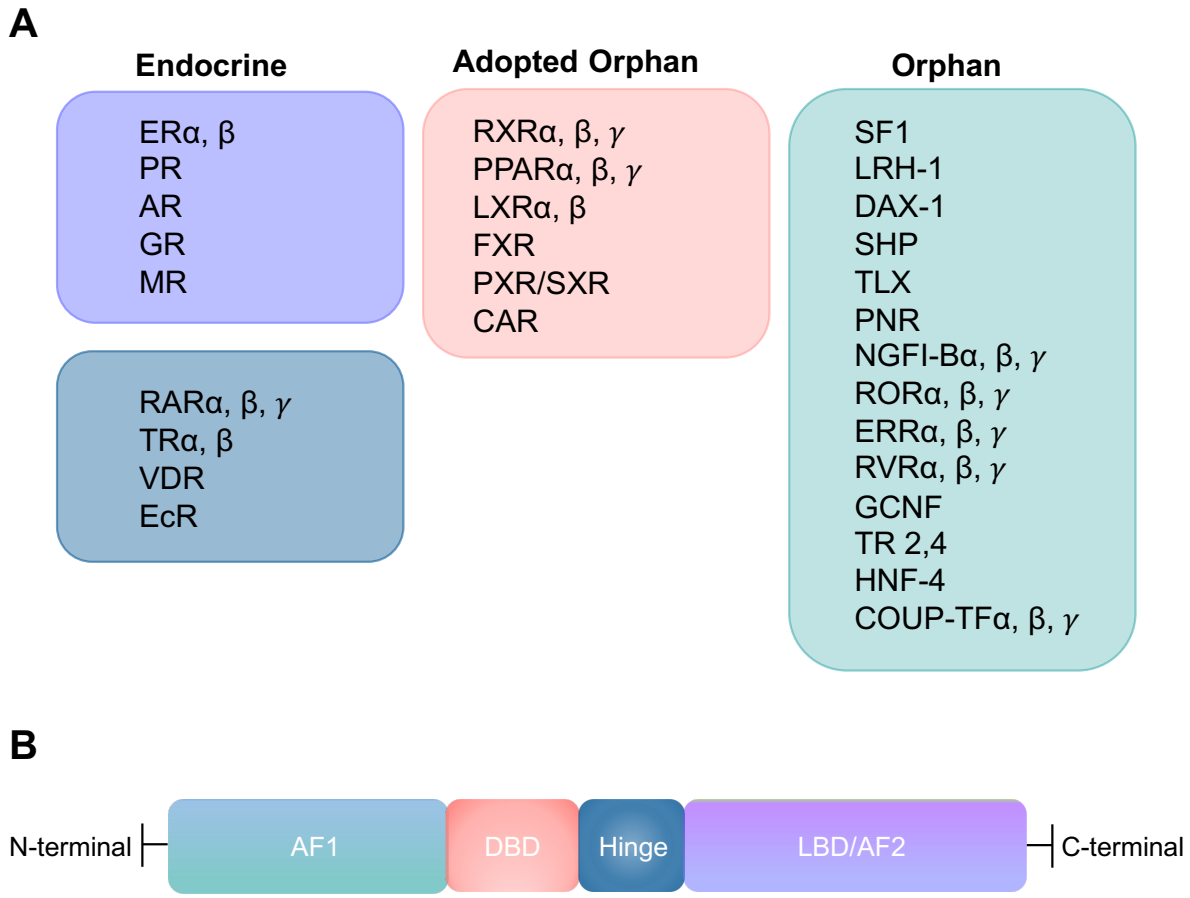


Figure 1.2 Nuclear Receptor Superfamily

(**A**) The 48 members of the nuclear receptor superfamily, categorised according to their class of cognate ligand. (**B**) Schematic of the structure of a nuclear receptor

1.3 Structure and regulation of the Estrogen receptor

1.3.1 Structure and function of the estrogen receptor

The effects of E2 are mediated through two receptors that are members of the nucear receptor superfamily, estrogen receptor-α (ER-α) and estrogen receptor-β (ER-β), the genes for which are located on chromosomes 6 and 14 respectively (Speirs 2002). ER-α and ER-β show strong sequence homology in the DNA-binding domain but differ at the ligand-binding (LBD) and transactivation domains (Kuiper et al. 1997; Speirs

2002). Both are present in the breast (ER-α is predominantly found in epithelial cells and ER-β in epithelial and stromal cells) and bind to E2 with similar affinities (Speirs 2002; Kuiper et al. 1997). ER-α and aromatase knockout models result in impaired mammary gland formation, confirming their importance in the development of the normal breast (Mueller et al. 2002; Mallepell et al. 2006; Fisher et al. 1998). In contrast, knockout of the ER-β gene has no effect on breast structure or lactation (Manavathi et al. 2014). The role of ER-β in breast cancer is unclear with some reports of it being a poor prognosticator with an inverse relationship with the progesterone receptor (PR) and others associating it with favourable outcomes (Dotzlaw et al. 1999; Järvinen et al. 2000; Treeck et al. 2009). ER-α is expressed in 15-25% of normal breast epithelial cells although interestingly, E2 stimulates proliferation of neighbouring ER-negative cells rather than the ER+ epithelial cells (Ali and Coombes 2002; Clarke et al. 1997; Russo et al. 1999). As ER-α has an established role in breast cancer and is the receptor used to define the ER status of tumours clinically, ER-α will be referred to as ER hereafter. Importantly, ER expression is a strong predictor of response to endocrine therapy.

Upon binding of E2 to the LBD of ER, a conformational change is induced that enables interaction with transcriptional coregulators (discussed in section 1.3.2), dimerization of ER, direct binding to EREs within promoters or enhancers of target genes, and recruitment of the general transcription machinery including RNA polymerase II (Pol II) (Ali and Coombes 2002; Schwabe et al. 1993; Métivier et al. 2003). Liganded ER is recruited to enhancer regions of ER-regulated genes, which form chromatin loops and modify target gene expression (Carroll et al. 2005; Ross-Innes et al. 2012; Sanyal et al. 2012). ER can also modulate transcription indirectly through physically interacting

with other transcription factors such as nuclear factor kappa-B (NF-κB), specificity protein 1 (SP1) and activator protein 1 (AP1) (Safe 2001). Further activation of ER occurs through post-translational modifications, including phosphorylation of several residues, primarily serine 118, which is mediated by cyclin-dependent kinase 7 (CDK7), ERK1/2 MAPK and several other kinases (Lannigan 2003; Chen et al. 2000; Anbalagan and Rowan 2015). ER then binds to ER-associated cofactor complexes, resulting in transcription and consequently expression of a wide range of target genes (Carroll 2016). Non-genomic activity of ER has also been described, whereby ER is able to form complexes with a range of tyrosine kinases (such as c-Src) and growth factor receptors (such as epidermal growth factor receptor (EGFR) and insulin-like growth factor-1 receptor (IGF-1R)) and stimulate downstream signalling cascades including the mitogen activated protein kinase (MAPK), janus kinase (JAK)/signal transducer and activator of transcription (STAT) and phosphatidylinositol 3-kinase (PI3K)/protein kinase B (AKT) pathways (Acconcia and Kumar 2006; Razandi et al. 2003). The different mechanisms of activation of ER are summarised in Figure 1.3. In breast cancer, ER continues to function as a transcription factor but it evades the usual regulatory mechanisms resulting in uncontrolled ER-mediated cell proliferation and tumour formation (Carroll 2016). Many of the target genes that ER regulates are involved in cell cycle progression (such as cyclin D1 (CCND1)), angiogenesis (IL-1α and IL-8) and inhibition of apoptosis (Bcl-2 and Bcl-xL); pathways which are all associated with carcinogenesis (Yang et al. 2006; Lindahl et al. 2011; Bendrik and Dabrosin 2009; Gompel et al. 2000).

1.3.2 ER coregulators and pioneer factors

Given the pivotal part coregulators play in ER-regulated transcription, these are an important consideration in the pathogenesis of ER+ breast cancer. Over 200 potential ER coregulators have been identified (Manavathi et al. 2014), which either promote (coactivators) or restrict (corepressors) ER transcriptional activity (Lonard and O'Malley 2006). Several roles have been described, including improving the accessibility of chromatin to facilitate DNA binding by ER, acting as 'platforms' for other key factors and providing enzymatic activity (e.g. acetylation, methylation, ubiquitination) to regulate protein function and chromatin reorganisation (Lonard and O'Malley 2007; Carroll 2016). The most well characterised coactivators include the p160 protein family (SRC1-3, GRIP1, AIB1), the histone acetyltransferase (HAT) complexes (CBP/p300) and the ATPase-dependent chromatin remodelling complexes (SWI/SNF) (Green and Carroll 2007; Lonard and O'Malley 2006). Corepressors, such as NCOR1 and SMRT (Hörlein et al. 1995; Chen and Evans 1995), reduce ER transcription through interacting directly with unliganded ER, competing with coactivators for ER binding and/or recruiting histone deacetylase complexes (HDACs) (Ali and Coombes 2002; Manavathi et al. 2014).

Several transcription factors have been shown to assist in maintaining ER-DNA interactions, and therefore transcription, through direct binding with condensed chromatin (Carroll 2016; Magnani et al. 2011a). This group of ER "pioneer" factors includes FOXA1, GATA3, PBX1 and AP2γ (Carroll et al. 2005; Eeckhoute et al. 2007; Magnani et al. 2011b; Tan et al. 2011). FOXA1 was the first pioneer factor identified, when genome-wide mapping of ER binding using ChIP-chip and ChIP revealed enrichment of forkhead motifs in proximity to ER binding sites in the MCF7 ER+ breast

cancer cell line (Carroll et al. 2005; Carroll et al. 2006). Through “mimicking” histone proteins, FOXA1 can bind to chromatin and change its structure to facilitate ER recruitment and consequently E2-induced transcription of target genes (Cirillo et al. 2002). FOXA1 has been shown to be a downstream target of GATA3 (Kouros-Mehr et al. 2006) and interestingly, inhibition of GATA3 in breast cancer cells, redistributed the ER binding profile to include an increased number of FOXA1 co-occupied sites, suggesting that GATA3 plays an important role in relation to FOXA1 (Theodorou et al. 2013). Both FOXA1 and GATA3 are co-expressed with ER in ER+ breast cancer and each component of this trilogy is essential in forming E2-responsive complexes at the regulatory regions of ER target genes (Kong et al. 2011).

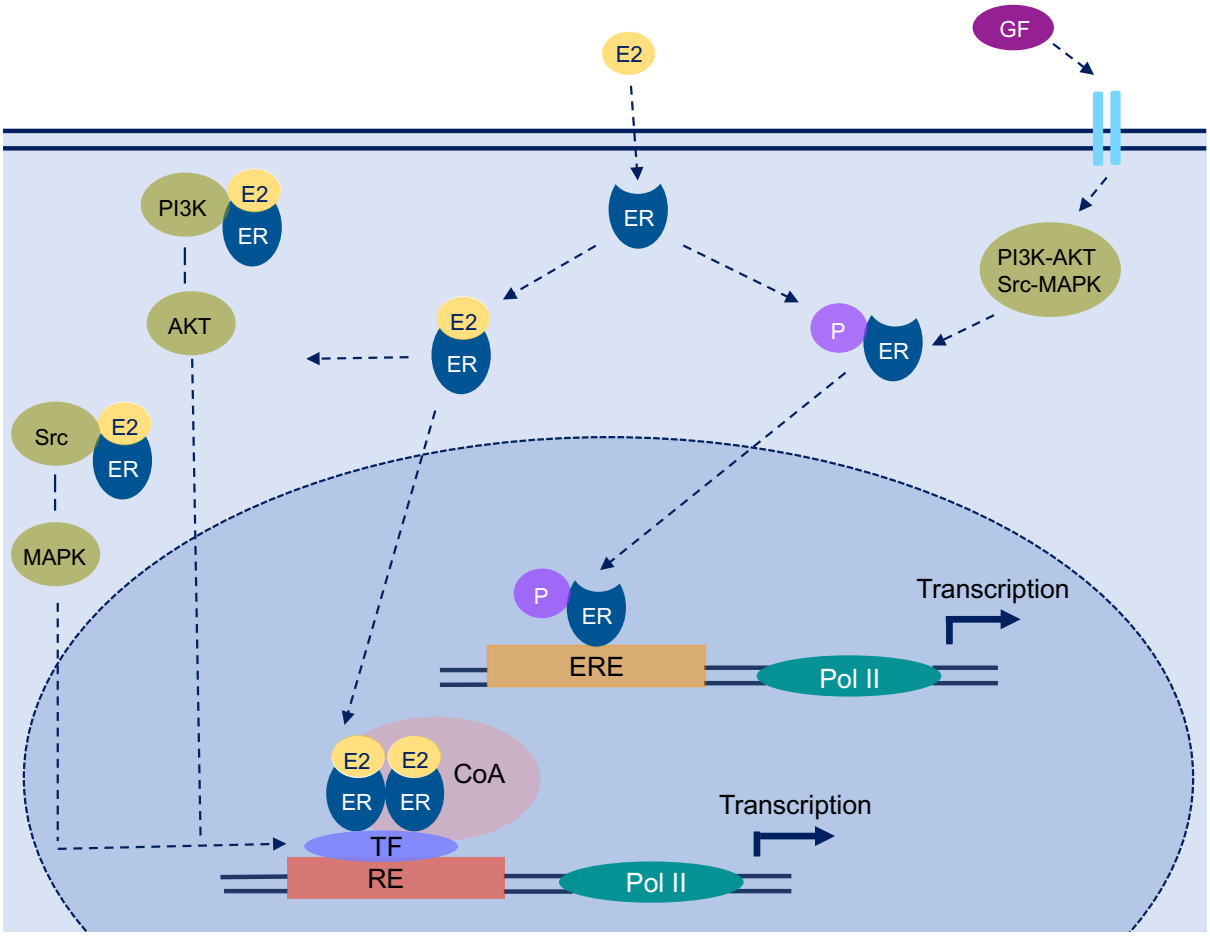


Figure 1.3 Activation of ER

Classical ER signalling occurs through E2-stimulated heterodimerization, binding to transcription factors (TF, e.g. AP1 and SP1) which are bound to their response elements (RE), recruitment of coactivators (CoA) and then transcription of target genes mediated by RNA polymerase II (Pol II). Phosphorylation of ER can further activate it via kinases (e.g. PI3K-AKT, Src-MAPK) that have been stimulated by growth factors (GF). Phospho-ER then binds directly to estrogen response elements (ERE), which facilitates expression of E2-regulated genes. E2-activated ER can also interact with cellular kinases (e.g. PI3K, Src), which stimulates non-genomic activity through downstream signalling pathways involving AKT and MAPK, eventually inducing transcription factor activation.

1.4 Endocrine therapy for ER positive breast cancer

Given the central role of ER in breast cancer, endocrine therapy that is focused on inhibiting the activity of ER and the associated cell proliferation is used adjuvantly in patients with localised breast cancer, and is also the mainstay of maintenance treatment for metastatic ER+ breast cancer, either alone or in combination with targeted therapy, such as CDK 4/6 inhibitors (Yung and Davidson 2021; EBCTCG 2015; Finn et al. 2016). The therapeutic strategies used are outlined below.

1.4.1 Ovarian Ablation

In pre-menopausal women, interrupting ovarian production of E2 is an effective adjuvant treatment, increasing survival relative to chemotherapy alone (EBCTCG 1996). Various modes of achieving ovarian ablation have been used previously including surgery (bilateral oophorectomy) and radiation but these techniques have associated risks (Kennedy 1965; Beatson 1896). LH releasing hormone (LHRH) agonists (e.g. Goserelin) have been used to medically ablate the ovaries by exploiting the negative feedback loops of the HPG axis to reduce pituitary release of gonadotropins and, consequently, downstream ovarian E2 release (Jonat et al. 2002). Several trials have studied the role of LHRH agonists in the adjuvant treatment of pre-menopausal patients with ER+ breast cancer; a meta-analysis of many of these studies reported that LHRH agonists show similar efficacy to adjuvant chemotherapy in terms of the risk of recurrence and death after recurrence (Cuzick et al. 2007). The TEXT and SOFT trials aimed to determine the effect of ovarian suppression (either with LHRH agonist, bilateral oophorectomy or ovarian irradiation) in addition to either tamoxifen or exemestane, and to compare the value of exemestane relative to tamoxifen in women treated with ovarian suppression, respectively (Regan et al.

2013). The addition of ovarian suppression resulted in improved 8-year overall survival (OS) and progression-free survival (PFS) rates for both patients receiving tamoxifen and exemestane; treatment with exemestane and ovarian suppression reduced recurrence rates as compared to tamoxifen and ovarian suppression (Pagani et al. 2014; Francis et al. 2018). Although it is well-tolerated, reversible, and therefore has minimal long-lasting side effects, the use of LHRH agonists is limited to pre-menopausal patients with breast cancer.

1.4.2 Tamoxifen

Tamoxifen is used in both the adjuvant, metastatic and chemopreventative treatment of breast cancer. It is defined as a selective ER modulator (SERM), having both agonistic and antagonistic activity depending on the target tissue site (Jordan 2003). Some of its key side effects can be explained by these opposing properties; hot flushes are a result of antagonistic behaviour in the brain, and endometrial cancer and venous thromboembolic events occur secondary to agonistic activity in the uterus and the cardiovascular system respectively (Benson 2002; Jordan 2003; Lewis and Jordan 2005).

Discovery of Tamoxifen

Tamoxifen was initially developed as a contraceptive drug in the 1960s but although it was shown to inhibit embryo implantation in rats, it actually stimulated ovulation in humans (Klopper and Hall 1971). It was therefore abandoned for this indication but, at around the same time, was found to induce regression of tumours (either measured clinically or radiologically) and be well-tolerated in patients with metastatic breast

cancer (Cole et al. 1971). It has therefore been widely used as a treatment for breast cancer since the 1970s.

Role of Tamoxifen in Metastatic Treatment of Breast Cancer

As a single agent, Tamoxifen has long been known to induce responses (either complete or partial) in patients with metastatic breast cancer (Kiang and Kennedy 1977). Its role in combination with targeted therapies is discussed in sections 1.4.8 and 1.4.9.

Role of Tamoxifen in Adjuvant Treatment of Breast Cancer

Tamoxifen has been commonly prescribed as an adjuvant hormone therapy for premenopausal women since its evaluation as a treatment for breast cancer in the 1970's (Jordan 2003). It also has utility in postmenopausal women, particularly in those for whom adjuvant aromatase inhibitors (AIs) (discussed in section 1.4.7) are contraindicated (Cardoso et al. 2019). Many trials have been undertaken investigating the efficacy of Tamoxfen in the adjuvant setting; meta-analyses of these show that Tamoxifen significantly reduces the annual breast cancer death rate, with the greatest improvements for recurrence seen in the first 5 years of treatment but the improvements in survival seen steadily over the first 10 years (EBCTCG 1998, 2005).

Optimal Duration of Adjuvant Tamoxifen: 5 vs 10 years

Five years of adjuvant Tamoxifen reduces the annual rate of breast cancer-specific mortality by 31% in patients with early stage ER+ breast cancer, regardless of age (EBCTCG 2005). Davies et al. 2013 showed that for years 5-14 after starting treatment, patients who received 10 years of Tamoxifen had both a disease-free

survival advantage (25.1% vs 21.4%) and a reduction in breast cancer mortality (12.2% vs 15%) relative to 5 years of therapy (Davies et al. 2013). The recommended duration of adjuvant Tamoxifen has therefore been increased to 10 years.

Chemopreventative Role of Tamoxifen

Tamoxifen has also been shown to be an effective chemopreventative agent. Long term treatment (8 years) with Tamoxifen has exhibited chemoprophylactic potency in women with a strong family history of breast cancer who are considered at high risk of developing the disease (Powles et al. 2007; Thorat and Cuzick 2017).

1.4.3 Other Selective Estrogen Receptor Modulators

Despite its ability to block the actions of E2 in patients, Tamoxifen has a relatively low binding affinity for ER in vitro; it has been discovered that it is hydroxylated into 4-hydroxytamoxifen (OHT), which is the active form of the drug (Jordan et al. 1977). Other SERMs have since been developed, such as Raloxifene, but despite carrying a lower risk of endometrial cancer, Raloxifene demonstrated just 76% of the efficacy of Tamoxifen in preventing invasive disease (Vogel et al. 2006; Vogel et al. 2010).

1.4.4 Fulvestrant

A second class of anti-estrogens, that function through nuclear export and downregulation of ER, have been developed and are collectively known as Selective ER Degraders (SERDs) (Wakeling and Bowler 1988). Fulvestrant, also known as ICI 182,780 or Faslodex, was the first developed and, unlike SERMs, only possesses ER antagonistic properties (Wakeling et al. 1991; Wakeling and Bowler 1992). In the metastatic setting, several clinical trials have reported that Fulvestrant is at least as effective as an AI or Tamoxifen in patients who have developed resistance to prior

endocrine therapy (Chia et al. 2008; Howell et al. 2002; Osborne et al. 2002; Howell et al. 2005) Fulvestrant has been shown to be superior to Anastrazole as first line treatment for metastatic ER+ breast cancer in the FIRST and FALCON studies (Robertson et al. 2016; Ellis et al. 2015). The CONFIRM trial reported that a dose of 500mg of Fulvestrant is more effective than 250mg in improving the PFS with patients with advanced breast cancer (Di Leo et al. 2010; Di Leo et al. 2014). The main limitation of Fulvestrant is its poor oral bioavailability, resulting in the need for twice weekly (for the first 2 doses) then monthly intramuscular administration (Robertson and Harrison 2004; Harrison et al. 2003).

1.4.5 Other Selective Estrogen Receptor Degraders

Oral SERDs have now been developed, including AZD9833 (Camizestrant), OP-1074 and GDC-9545 (Giredestrant), along with SERM/SERD hybrids Bazedoxifene and RAD1901 (Elacestrant) (De Savi et al. 2015; Fanning et al. 2018a; Kahraman et al. 2018; Wardell et al. 2013; Wardell et al. 2015). The EMERALD phase III trial is currently studying the efficacy of RAD1901 vs endocrine therapy for second and subsequent line treatment of metastatic ER+ breast cancer (Bardia et al. 2019). Amcenestrant, another orally available SERD, and GD-9545 are both being studied relative to the physician's choice of endocrine therapy in Phase II studies of locally advanced or metastatic ER+ breast cancer (in the AMEERA-3 and acelERA trials respectively) (Tolaney et al. 2021; Martin et al. 2021). The Phase II SERENA-2 study is investigating the efficacy of AZD9833 vs Fulvestrant in patients with metastatic ER+ breast cancer (Oliveira et al. 2021). Combination therapy with a SERD and a CDK4/6 inhibitor is also being studied; AZD9833 and GDC-9545 are both currently in phase III clinical trials (SERENA-4 and persevERA respectively) in combination with Palbociclib

for postmenopausal patients with ER+ breast cancer (Im et al. 2021; Turner et al. 2021).

1.4.6 Selective ER Covalent Antagonists and ER PROTAC Protein Degraders

Covalent anti-estrogens have recently been described, including the first selective ER covalent antagonist (SERCA), H3B-6545, which binds covalently to cysteine 530 in the LBD of ER (a residue absent in other NRs, hence its good selectivity) (Rioux et al. 2019). ER PROTAC protein degraders, such as ARV-471, which function in a similar way to SERDs by promoting ER degradation (including that of activating mutant ERs, discussed in section 1.5.1) have also been developed and are in Phase I/II trials (Snyder et al. 2021; Hamilton et al. 2022).

1.4.7 Aromatase inhibitors

AIs are widely used in postmenopausal women, in whom E2 biosynthesis occurs predominantly through peripheral aromatization of adrenal androgens, (EBCTCG 2015; Cui et al. 2013). As AIs may promote ovarian production of E2 through stimulation of the HPG axis in premenopausal patients, they are therefore not recommended for this cohort, except with concurrent ovarian ablation (Dowsett et al. 1992).

Two classes of AI have been developed, non-steroidal (Type 2: Anastrazole and Letrozole) and steroidal (Type 1: Exemestane). Both function by inhibiting ER activity through blocking aromatase function. Steroidal AIs compete with androstenedione and testosterone to bind irreversibly to the aromatase enzyme itself. Non-steroidal AIs also compete for aromatase binding with endogenous androgens but form reversible bonds with the haem iron atom (Buzdar and Howell 2001). Given their different modes of

action, steroidal and non-steroidal AIs may be used sequentially to combat treatment resistance (Harper-Wynne and Coombes 1999; Carlini et al. 2001; Lønning et al. 2000).

Role of AIs in the Metastatic Treatment of Breast Cancer

Letrozole has been shown to have an improved disease progression rate and tolerability compared to Megestrol acetate in patients with metastatic ER+ breast cancer (Dombernowsky et al. 1998; Buzdar et al. 2001). Similarly, Exemestane has been reported to offer an improvement in time to progression compared to Tamoxifen in post-menopausal patients with metastatic ER+ breast cancer (Paridaens et al. 2008). Hence AIs have now supplanted Megestrol acetate and Tamoxifen as the previous standards of care for postmenopausal patients with metastatic disease.

Role of AIs in the Adjuvant Treatment of Breast Cancer

AIs have been reported to significantly reduce the recurrence risk relative to Tamoxifen in the adjuvant setting in postmenopausal women (EBCTCG 2015; BIG1-98 2005). More recently, results from a recent meta-analysis of 4 randomized controlled trials comparing treatment with AIs vs Tamoxifen in pre-menopausal patients with localised ER+ breast cancer receiving ovarian suppression, showed that patients treated with AIs had a lower recurrence rate than those who were given Tamoxifen (Bradley et al. 2022). Data on long-term follow-up is awaited to assess the effect on survival (Bradley et al. 2022).

Chemopreventative role of AIs

As described for Tamoxifen, AIs also exhibit chemopreventative potency for women at high risk of developing breast cancer (Thorat and Cuzick 2017).

Although generally well tolerated, compliance can be a therapeutic challenge with AIs, with quality of life sub-protocols from the ATAC, IES, TEAM and MA-17 trials reporting a wide range of common toxicities, including hot flushes, gastro-intestinal events, arthralgia and weight gain (Fallowfield 2007; Cella et al. 2006; Fallowfield et al. 2012; van Nes et al. 2012; Hilditch et al. 1996). The effects of AIs, Tamoxifen and Fulvestrant on ER activity are outlined in Figure 1.4.

1.4.8 Endocrine therapy plus CDK4/6 Inhibitors

The development of CDK4/6 inhibitors has led to several studies investigating the effect of combining them with endocrine therapy.

AIs and CDK 4/6 inhibitors

All three CDK4/6 inhibitors are now used up front for the treatment of metastatic ER+ breast cancer based on data from the following trials. The Phase II PALOMA-1 and Phase III PALOMA-2 studies showed that the addition of Palbociclib to Letrozole resulted in prolonged PFS rates relative to Letrozole alone for first line treatment in the metastatic setting (Finn et al. 2015; Finn et al. 2016). Shortly afterwards, the Phase III MONALEESA-2 trial showed that Ribociclib and Letrozole combination treatment also had improved PFS rates compared to single agent Letrozole as first line treatment for metastatic disease in postmenopausal patients (Hortobagyi et al. 2018). More recently, the MONALEESA-7 trial has shown longer PFS rates for patients receiving

Ribociclib, a non-steroidal AI and an LHRH agonist in premenopausal patients (Tripathy et al. 2018). Abemaciclib was studied as first line treatment in combination with a non-steroidal AI for metastatic disease and also showed better PFS and overall response rates compared to an AI alone (Goetz et al. 2017).

SERMs and CDK4/6 inhibitors

Tamoxifen and other SERMs have also been studied in combination with CDK4/6 inhibitors and this combination treatment is now used clinically. The MONALESSA-7 study reported an increased PFS when Tamoxifen (or a non-steroidal AI) was combined with the CDK4/6 inhibitor, Ribociclib (and an LHRH agonist) in premenopausal patients with metastatic ER+ breast cancer (Tripathy et al. 2018). A phase Ib/II clinical trial with bazedoxifene and CDK 4/6 also showed good clinical activity for patients with metastatic ER+ breast cancer (Jeselsohn et al. 2019).

Fulvestrant and CDK4/6 inhibitors

Combination treatment with Fulvestrant and Palbociclib was evaluated in the PALOMA-3 trial in postmenopausal patients with ER+ breast cancer, which showed that the median PFS more than doubled with this treatment compared to Fulvestrant and Placebo (Cristofanilli et al. 2016). Similarly, the MONARCH-2 and MONALEESA-3 trials investigated the effect of combining Abemaciclib or Ribociclib with Fulvestrant and reported improved PFS and OS rates relative to Fulvestrant and placebo in patients with metastatic disease (Slamon et al. 2020; Sledge et al. 2020). Hence all three CDK4/6 inhibitors are now used in combination with Fulvestrant for the treatment of metastatic ER+ breast cancer.

1.4.9 Endocrine therapy plus Everolimus

The mTOR inhibitor, Everolimus has been used in combination with endocrine therapies as second line treatment for metastatic ER+ breast cancer based on data from the following studies.

AIs and Everolimus

The BOLERO-2 study reported a nearly 2.5-fold increase in PFS vs Exemestane and Placebo although there was no significant OS benefit (Baselga et al. 2012a; Piccart et al. 2014). More recently, the BOLERO-6 study showed that Everolimus and Exemestane offers a PFS advantage over Everolimus alone; it also showed a PFS benefit with Everolimus and Exemestane treatment over Capecitabine alone, although the authors advise caution in interpretation of this due to variations in baseline characteristics of the cohorts (Jerusalem et al. 2018). Hence, this data supports the continued use of Everolimus combined with endocrine therapy.

SERMs and Everolimus

In patients with metastatic ER+ breast cancer who are resistant to AIs, Tamoxifen in combination with Everolimus has been shown to confer increased response and survival rates in patients compared to Tamoxifen alone in the TAMRAD study (Bachelot et al. 2012). Another Phase II study reported that the addition of Everolimus to the last endocrine therapy on which disease progression last occurred, which included Tamoxifen, AIs or Fulvestrant, resulted in stable disease for 15% (n=48) of patients (Yardley et al. 2017).

Fulvestrant and Everolimus

The addition of Everolimus to Fulvestrant improved the efficacy of Fulvestrant (vs Fulvestrant and placebo) in a phase II study in postmenopausal patients with metastatic ER+ breast cancer who were resistant to non-steroidal AIs (Kornblum et al. 2018). Another Phase II trial (MANTA) studied Everolimus in combination with Fulvestrant vs Fulvestrant alone or Fulvestrant plus Vistusertib (a dual inhibitor of both mTORC1 and mTORC2) and showed a longer PFS with Everolimus and Fulvestrant combination therapy (Schmid et al. 2019).

1.4.10 Endocrine therapy plus Capivasertib

Capivasertib (AZD5363) is a pan-AKT kinase inhibitor, which has shown efficacy in preclinical studies as a single agent or in combination with HER2 targeted therapies or endocrine therapy, in breast cancer cell lines and xenografts, particularly those with PIK3CA or mTOR mutations or alterations (Davies et al. 2012; Ribas et al. 2015; Fox et al. 2013).

In a Phase I study, Capivasertib was reported to have a better overall response rate in combination with Fulvestrant (in patients pre-treated with Fulvestrant) than as a monotherapy in patients with *AKT1*^{E17K}-mutant and *PTEN*-mutant metastatic ER+ HER2-negative breast cancer (Smyth et al. 2020; Smyth et al. 2021). The Phase I/II FAKTION study also showed a PFS benefit (10.3 vs 4.8 months) with Capivasertib plus Fulvestrant therapy vs Placebo plus Fulvestrant in AI-pretreated, metastatic or locally advanced ER+ breast cancer (Jones et al. 2020). CAPItello-291, a phase III clinical trial, is currently continuing to study the role of Capivasertib and Fulvestrant combination therapy in breast cancer (Turner et al. 2020b).

1.4.11 Endocrine therapy plus Alpelisib

PI3K inhibitors have been developed and Alpelisib is an inhibitor of the PI3K alpha (PI3Kα) isoform. The Phase III SOLAR-1 trial evaluated the role of Alpelisib with Fulvestrant in postmenopausal *PIK3CA*-mutated patients who have previously received an AI and showed both PFS (11.0 vs 5.7 months) and OS (39.3 vs 31.4 months) improvements with Alpelisib and Fulvestrant vs Placebo and Fulvestrant (André et al. 2019; André et al. 2021). Alpelisib therapy carries toxicities such as hyperglycaemia, rash and gastrointestinal tract disturbances, which resulted in treatment discontinuation in 25% of patients (André et al. 2019). Given the more favourable toxicity profile of CDK4/6 inhibitors, Alpelisib and Fulvestrant is used after an AI and CDK4/6 combination therapy; the BYLieve study has shown acitivity of Alpelisib and Fulvestrant in patients who have progressed on an AI and CDK4/6 inihibtor (Rugo et al. 2021).

1.4.12 Endocrine therapy plus HER-2 therapy

Following the CLEOPATRA study, first line treatment for patients who have metastatic HER2+ breast cancer is HER2-targeted therapy (Trastuzumab and Pertuzumab) in combination with Docetaxel, irrespective of ER or PR status (Swain et al. 2020; Baselga et al. 2012b). However, the PERTAIN trial showed that after at least 6 upfront cycles of concomitant Docetaxel have been completed, the addition of a non-steroidal AI to trastuzumab-pertuzumab maintenance therapy is effective in patients with metastatic or locally advanced ER+ HER2+ breast cancer (Rimawi et al. 2018).

1.4.13 Neoadjuvant Endocrine therapy and Window Studies of Endocrine Therapy

Neoadjuvant therapy is given to reduce the size of a large or high-risk tumour prior to surgery to enable less invasive surgery (i.e. breast-conserving surgery instead of mastectomy) to be undertaken. Chemotherapy is the most common mode of neoadjuvant therapy but, in patients who are not considered suitable candidates for chemotherapy or surgery (due to comorbidities or general fitness), neoadjuvant endocrine therapy may be used instead as it is well tolerated and effective (Gazet et al. 1994; Mustacchi et al. 2003; Palmieri et al. 2014; Semiglazov et al. 2007).

The POETIC study evaluated the role of perioperative non-steroidal AIs (POAI) given 14 days before and 14 days after surgery; although POAI did not improve long-term treatment outcomes, patients with ER+ tumours with POAI-induced low Ki67 scores did well on adjuvant endocrine therapy alone, relative to those with high Ki67 scores (Smith et al. 2020). The addition of Pictilisib (a PI3K inhibitor) to 14 days of pre-operative anastrazole in a Phase II window study, resulted in greater suppression of mean Ki67 scores than anastrazole monotherapy (Schmid et al. 2016). Similarly, neoadjuvant Everolimus combined with letrozole (4 months of treatment) resulted in better response rates than with letrozole alone in patients with ER+ breast cancer (Baselga et al. 2009).

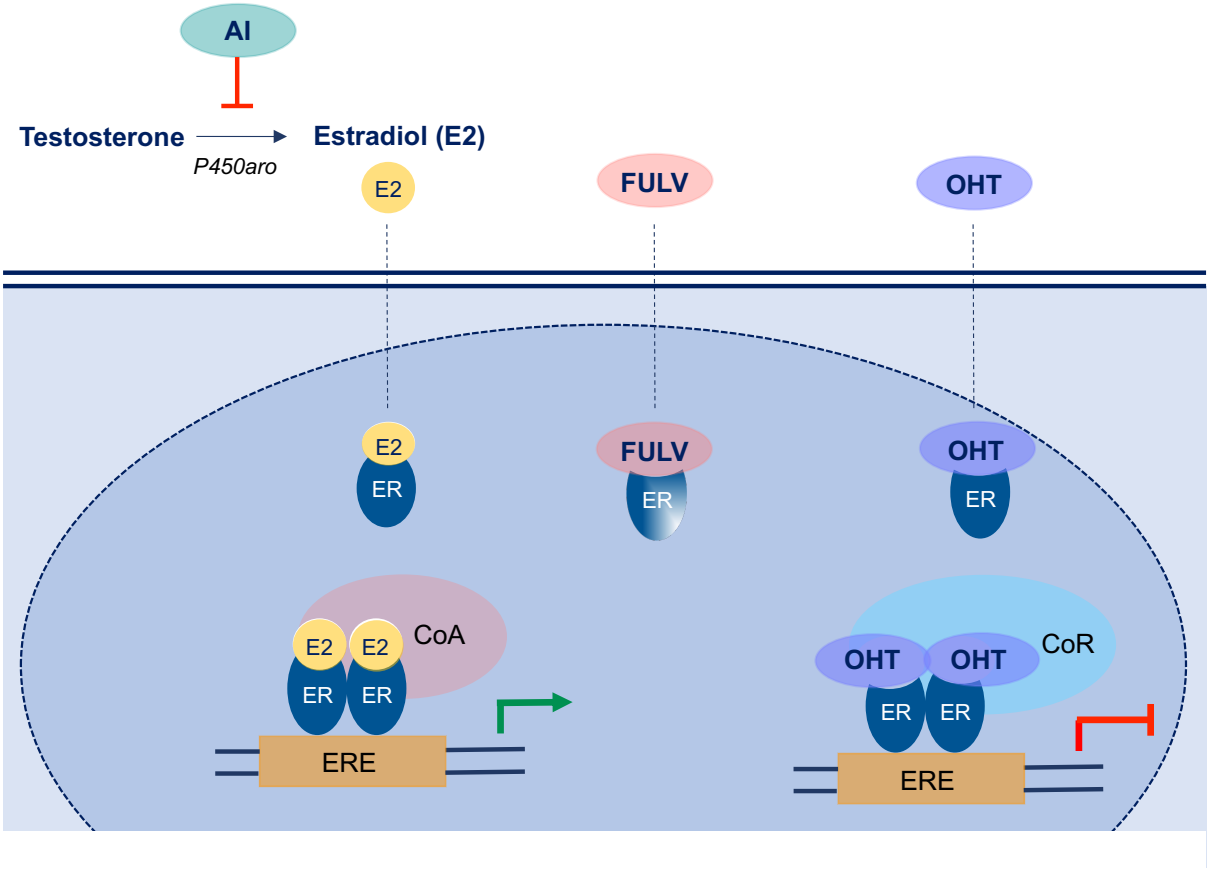


Figure 1.4 Endocrine therapies and their effect on ER activity

Aromatase inhibitors (AI) inhibit CYP enzymes (P450aro) that convert Testosterone to Estradiol (E2). Fulvestrant (FULV) and other SERDs degrade ER. Tamoxifen (OHT) and other SERMs inhibit binding of E2 to ER through competitively binding with ER and inhibiting transcription of ER target genes. Abbreviations - CoA: coactivators, CoR: corepressors, ERE: estrogen response elements.

1.5 Mechanisms of endocrine resistance

Although the endocrine therapies detailed above (section 1.4) have greatly improved the survival of patients with breast cancer, 15-20% of patients with localised disease are intrinsically resistant and unfortunately all patients with metastatic disease (who now receive endocrine therapy with a CDK4/6 inhibitor as first line treatment) will develop resistance to these treatments (Anurag et al. 2018; Gennari et al. 2021). Currently, this is managed by offering further lines of endocrine therapy when resistance develops (Rugo et al. 2016), either as single agents or in combination with targeted therapies (e.g. Fulvestrant and Alpelisib (for patients with PIK3CA mutations)

or Exemestane and Everolimus (Gennari et al. 2021; Baselga et al. 2012a)). However, despite the efficacy of endocrine therapy, most patients with metastatic disease will progress on sequential lines of treatment, hence resistance continues to be a significant therapeutic challenge in the treatment of ER+ breast cancer. The mechanisms of resistance that have been described may be intrinsic or acquired and are outlined below. Although it was previously thought that these may occur in tandem, more recently some of these mechanisms have been found to be mutually exclusive. For example, in a large study of metastatic ER+ breast cancer, 18% of metastatic biopsies were mutated in the ER gene (*ESR1*), while a distinct, non-overlapping 20% had alterations in the EGFR/MAPK pathway (Razavi et al 2018). A further 10% had alterations in MYC; no identified driver mutations were found in the remaining ~50% of cases.

1.5.1 *ESR1* mutations

Activating mutations of *ESR1* have been implicated as a resistance mechanism to endocrine therapy (Dustin et al. 2019). *ESR1* mutations were first studied over 25 years ago in functional studies that investigated the effect of ligand binding and transcriptional activity of ER using site-directed mutagenesis of ER, mainly using reporter gene assays. Using this approach, mutation of key amino acids in the LBD was found to confer ligand independence, replicating activity levels of E2-stimulated wildtype (WT) ER. The mutations identified included substitution of tyrosine at position 537 to serine (Y537S), asparagine (Y537N) and alanine (Y537A), leucine at position 536 to asparagine (L536N), lysine (L536K) or proline (L536P) and glutamic acid at position 380 to glutamine (E380Q) (Carlson et al. 1997; Weis et al. 1996; Zhao et al. 2003; Eng et al. 1997; Pakdel et al. 1993). Interestingly, Zhang et al. (1997) found 3

missense mutations (S47T, K531E, Y537N) in a cohort of 30 patients with metastatic breast cancer (Zhang et al. 1997). They also reported partial resistance to anti-estrogens, with Tamoxifen and ICI 164,384 (a compound similar to Fulvestrant) only slightly inhibiting basal activity of Y537N on E2-responsive reporter genes in the presence of E2 (Zhang et al. 1997). Following these studies, it was proposed that ER mutations may feature in breast cancer and facilitate E2-independent growth and resistance to anti-estrogens. Initially these mutations were found at very low frequencies in studies that often featured only primary, treatment-naïve samples (Zhang et al. 1997; Koboldt et al. 2012).

With the considerable advances in the rapidity and low costs of genomic sequencing, much larger series of metastatic tumour samples have been sequenced, demonstrating that *ESR1* mutations are common in metastatic breast cancer. Frequencies of *ESR1* mutations range from 9-55%, depending on the study, but most of the studies report *ESR1* mutations in around 20-30% of metastatic breast cancer samples (Toy et al. 2013; Robinson et al. 2013; Merenbakh-Lamin et al. 2013; Piccart et al. 2013; Jeselsohn et al. 2014). Consistent with the fact that very few *ESR1* mutations were previously reported in primary, treatment-naïve breast cancer samples, *ESR1* mutations are almost exclusively present in metastatic tumours but not in the matched primary samples (Robinson et al. 2013; Merenbakh-Lamin et al. 2013; Jeselsohn et al. 2014). Furthermore, the vast majority of *ESR1* mutations are detected in patients with metastatic disease who have previously been treated with an AI (Robinson et al. 2013; Jeselsohn et al. 2014; Schiavon et al. 2015). In support of this, patients with recurrent breast cancer who have not previously been treated with AI have very low rates of *ESR1* mutations (<1%), implying that the low levels of

circulating E2 induced by AIs actually select for cells carrying ligand-independent, *ESR1* mutations (Guerrero-Zotano et al. 2018; Leal et al. 2019; Schiavon et al. 2015; Reinert et al. 2020; Jeselsohn et al. 2014). There have, however, been reports of *ESR1* mutations, including Y537S, found in patients treated with Tamoxifen alone but these are much less common than in AI-treated patients (2% vs 28.9% respectively) (Magnani et al. 2017; Toy et al. 2013; Fribbens et al. 2016). As mentioned above, Razavi et al. (2018) sequenced tumour specimens from a large cohort of metastatic breast cancer patients who were either treatment-naïve or who had received prior treatment and found that, overall, 18% (128/692) of those who had received prior endocrine therapy had an *ESR1* mutation (Razavi et al. 2018).

Most *ESR1* mutations are found at a 'hotpot' in the LBD of ER, located in coding exon 8, affecting amino acids 536, 537 or 538 (Figure 1.5) (Robinson et al. 2013; Toy et al. 2013). Following the resolution of the crystal structure of ER, functional modelling of these hotspot mutations using molecular dynamics simulations, established the ligand-independent, constitutive activity of Y537S and D538G (Toy et al. 2013; Nettles et al. 2008). Subsequently, biophysical and structural biology data has been integrated to confirm how the altered structure of ER mutations results in E2-independence and resistance to anti-estrogens (Fanning et al. 2016; Fanning et al. 2018b; Lainé et al. 2021). Helix 12 in the ER LBD acts as a 'molecular switch' that, along with helices 3, 4 and 5, forms part of the coregulator binding site (AF2) (Nettles et al. 2008). In the ligand-bound, agonist conformation, helix 12 is folded across helices 3 and 11 which stabilises the coactivator binding pocket (Nettles et al. 2008). Through forming stable, tight hydrogen bonds with D351, helix 12 of Y537S- and D538G-mutant ER is held fixed in the agonist conformation even in the apo form (Toy et al. 2013;

Katzenellenbogen et al. 2018). On ligand binding of WT ER, the helix 11-12 loop has been shown to have a 'spring-like' property, which fixes it in the agonist conformation (Katzenellenbogen et al. 2018). The D538G mutation results in a 'lengthening' of this helix 11-12 spring, which further contributes to its constitutive activity (Katzenellenbogen et al. 2018). This agonist-like structure of mutant ER persists even when bound to anti-estrogens such as Endoxifen (a SERM) and AZD9496 (Pavlin et al. 2018). In addition, the ER protein structure that results from LBD mutations also promotes transcription through enhanced interaction with coactivators such as members of the SRC family (Gates et al. 2018; Merenbakh-Lamin et al. 2013).

ESR1-mutant breast cancer is resistant or at least less sensitive to standard endocrine therapy and carries worse survival outcomes (Fribbens et al. 2016; Chandarlapaty et al. 2016). Whilst low doses of Tamoxifen, Bazedoxifene and Fulvestrant reduced the activity of Y537S and D538G mutations, higher levels (50-100nM Fulvestrant) were required to suppress the activity to equivalent levels of inhibition of WT ER by these SERMs and SERDs (Toy et al. 2013). LBD mutations have been reported to drive the development of distant metastases, with doxycycline-inducible Y537S and D538G models exhibiting metastatic behaviour, which regressed in Y537S cells on removal of doxycycline (Jeselsohn et al. 2018). The aggressive nature of this disease has made identification of patients carrying *ESR1* mutations essential in order to enable prognostication and guide treatment, i.e. avoiding therapies such as AIs that are likely to be ineffective (Schiavon et al. 2015). Although next generation sequencing (NGS) initially revealed the magnitude of *ESR1* mutations in metastatic disease, digital droplet PCR (ddPCR) has been developed and increased the sensitivity with which *ESR1* mutations can be detected (at frequencies <1%) even in very small numbers of

malignant cells (Dustin et al. 2019; Jeselsohn et al. 2015; Guttery et al. 2015). Importantly, both technologies enable non-invasive detection of *ESR1* mutations from patients' plasma (using circulating tumour DNA (ctDNA)), which is likely to increase the number of samples taken and therefore the chances of identifying a mutation in a population of metastatic patients who have been extensively investigated previously, and may therefore be reluctant to have repeated biopsies, or may have metastases that are technically difficult to biopsy (Schiavon et al. 2015; Shaw et al. 2016). Through analysis of ctDNA, *ESR1* mutations have been detected 6.7 months prior to overt clinical progression in patients with metastatic disease, providing a window of opportunity to change therapeutic strategy (Fribbens et al. 2018). Furthermore, regular ctDNA testing would enables continuous monitoring of patients for emergence of *ESR1* mutations and facilitates prompt switch in therapy at this point.

Given the discrepancy in the frequency of *ESR1* mutations in primary and metastatic disease, improved detection methods have also enabled exploration of their clonal evolution over the full disease course. A small proportion of patients with primary breast cancer (0.05-2.5%) have been identified as having *ESR1*-mutant disease using highly sensitive ddPCR assays (Takeshita et al. 2015; Wang et al. 2016). Hence, the 'acquired resistance' they confer, may be through the development of resistant subclones, present in very small numbers in the original, genetically heterogenous primary tumour, before growing into the dominant clone under the selective pressure of low circulating E2 levels following treatment with AIs (Schiavon et al. 2015). They are predominantly a feature of metastatic disease as it is thought that in early or micro-metastatic disease, the tumour volume is insufficient for these subclones to exist in large numbers (Schiavon et al. 2015). During treatment with AIs, the *ESR1* mutant

variant allele frequency (VAF) was shown to increase using ddPCR testing of circulating tumour DNA (ctDNA), providing further evidence that these mutations are selected for through AI use (Allouchery et al. 2018). ddPCR has also revealed that these mutations are polyclonal, with 21-49.1% of cases carrying more than one *ESR1* mutation (Schiavon et al. 2015; Fribbens et al. 2018; Fribbens et al. 2016; O'Leary et al. 2018; Takeshita et al. 2015). A limitation of ddPCR is that, unlike unbiased NGS, only selected mutations can be studied, which are likely to be the most well characterised and may be unrepresentative of the magnitude and frequency of the true *ESR1* mutational profile.

More recent studies have identified *ESR1* mutations outside the hotspot in pre-malignant and malignant breast lesions in patients. These include those that retain baseline ligand sensitivity (V534E and S432L), those that result in E2 hypersensitivity (E380Q and K303R) and others that have reduced binding to ER coactivators (E380Q and S436P) (Toy et al. 2017; Fuqua et al. 2000) . E380Q is now recognised as one of the most common *ESR1* mutations, reported at frequencies of 9.5-26% in patients pre-treated with AIs, implicating it in treatment resistance (Fribbens et al. 2016; Spoerke et al. 2016). However, Patient-Derived Xenograft (PDX) models harbouring E380Q mutations, failed to exhibit ligand-independence, unlike those with Y537S mutations, suggesting they have different mechanisms of endocrine resistance, reflecting the differences in ligand sensitivity and coactivator recruitment (Li et al. 2013). The K303R mutation, with substitution of lysine for arginine at position 303, is located in the border between the hinge region and the LBD (Fuqua et al. 2000). Its hypersensitivity to E2 and resulting endocrine resistance is thought to be mediated through enhanced affinity for TIF-2 (a member of the SRC family of coactivators) even at low circulating levels

of E2 (Fuqua et al. 2000). K303R also interacts with growth factor signalling pathways, stabilising ER via inhibition of acetylation and the generation of an AKT phosphorylation site at serine 305 (Fuqua et al. 2014). Serine 305 is an important site for the activity of anti-estrogens and partial resistance to Tamoxifen, as well as AIs, has been observed with this mutation (Barone et al. 2010; Giordano et al. 2010). Detection rates of K303R as high as 34% in pre-malignant hyperplasia, 5.7% in primary breast cancer and 50% in invasive disease have been reported (Herynk et al. 2007; Conway et al. 2005; Fuqua et al. 2000) but this mutation has not been identified in many other studies (even with ddPCR), making the significance of this mutation unclear (Koboldt et al. 2012; Li et al. 2013; Toy et al. 2013; Robinson et al. 2013; Merenbakh-Lamin et al. 2013).

An ER fusion gene created through a translocation of the N-terminal end of ER and the C-terminus of yes-associated protein 1 (YAP1), has also been described (Li et al. 2013). The resulting novel fusion gene, *ESR1*-YAP1 lacks the LBD but YAP1 has a transactivation function region, enabling E2-independent transcription (Jeselsohn et al. 2015; Li et al. 2013). Breast cancer cell lines with overexpression of *ESR1*-YAP1, PDX models and the original patient sample show ligand-independent growth and complete Fulvestrant resistance secondary to the *ESR1*-YAP1 fusion gene (Li et al. 2013). Other *ESR1*-fusion genes have since been identified, including translocations with protocadherin 11 X-linked (PCDH11X), coiled-coil domain containing 170 (CCDC170), A-kinase anchoring protein 12 (AKAP12), disabled-2 (DAB2), SRY-Box 9 (SOX9) and AT rich interaction domain 1B (ARID1B) (Lei et al. 2018; Li et al. 2020; Ma et al. 2014; Hartmaier et al. 2018; Gou et al. 2021). The ER LBD is always lost in these fusion proteins, which are present in up to 1% of patients with metastatic breast

cancer, although the exact site of translocation differs between fusion proteins (Hartmaier et al. 2018). These *ESR1* fusion genes have been associated with E2-independent cellular proliferation, migration and invasion, and induction of EMT-related genes (Gou et al. 2021). In addition, the *ESR1* fusion protein is resistant to degradation by Fulvestrant (Gou et al. 2021). The absence of the LBD in these fusion genes also confers resistance to SERMs such as Tamoxifen and will necessitate alternative therapies to overcome this; Palbociclib (a CDK4/6 inhibitor) has shown promise in inhibiting the growth of *ESR1*-YAP1 cells and PDX models (Lei et al. 2018).

A number of studies have described the transcriptomic profiles of WT and mutant ER expressing breast cancer cell lines, identifying mutant-specific patterns of gene expression (Jeselsohn et al. 2018; Bahreini et al. 2017; Harrod et al. 2017; Martin et al. 2017). The majority of these have used CRISPR-Cas9 or lentiviral techniques to create cell line models carrying specific *ESR1* mutations. Interestingly, one study demonstrated enrichment of *ESR1* mutations following ER+ breast cancer cell line adaptation to E2-independence by long term culturing in E2-free culture media (Martin et al. 2017). These authors identified MCF7 cells in which the endogenous gene had been mutated for Y537C, while an independent cell line (SUM44PE) had the Y537S mutation. At least in the latter case, there was a rare pre-existing cell population (~1 in 10^6 cells) with the Y537S mutation, providing *in vitro* evidence for enrichment of rare pre-existing mutations as a mechanism of acquired resistance to hormone therapies. ChIP-seq has shown that the magnitude of ER binding in the absence of E2 is far greater for mutant ER than WT ER (Jeselsohn et al. 2018; Harrod et al. 2017). Mutant ER shares common genomic binding sites with ligand-bound WT ER but also has unique sites, implying that *ESR1* mutations have both hormone dependent and

independent mechanisms of chromatin binding and gene expression (Martin et al. 2017). Using RNA-seq on MCF7-Y537S cells treated with vehicle or E2, Harrod et al. 2017 described ligand-independent expression of several well-known ER target genes including the progesterone receptor (PR) (Harrod et al. 2017). Gene set enrichment analysis (GSEA) revealed enrichment of early and late E2 response pathways in vehicle-treated MCF7-Y537S cells, although interestingly, E2 treatment of these cells further enhanced ER-regulated gene expression (Harrod et al. 2017).

Phenotypic differences between the Y537S and D538G mutations have been reported. Models of Y537S have demonstrated greater resistance to growth inhibition from Tamoxifen and Fulvestrant than D538G and WT ER (Jeselsohn et al. 2018). The D538G mutation has shown greater sensitivity to E2, with an additional 416 genes upregulated by E2 treatment compared to only 12 in Y537S-mutant breast cancer cells (Jeselsohn et al. 2018). In keeping with this, gene expression analyses have shown distinct profiles for the Y537S and D538G mutations in hormone-depleted culture medium (with 18% and 33% overlap with E2-stimulated WT ER respectively) and, to a lesser extent, a number of unique genome binding sites (Jeselsohn et al. 2018). Therefore, these mutations do not just replicate ligand-activated ER but have their own transcriptional profiles.

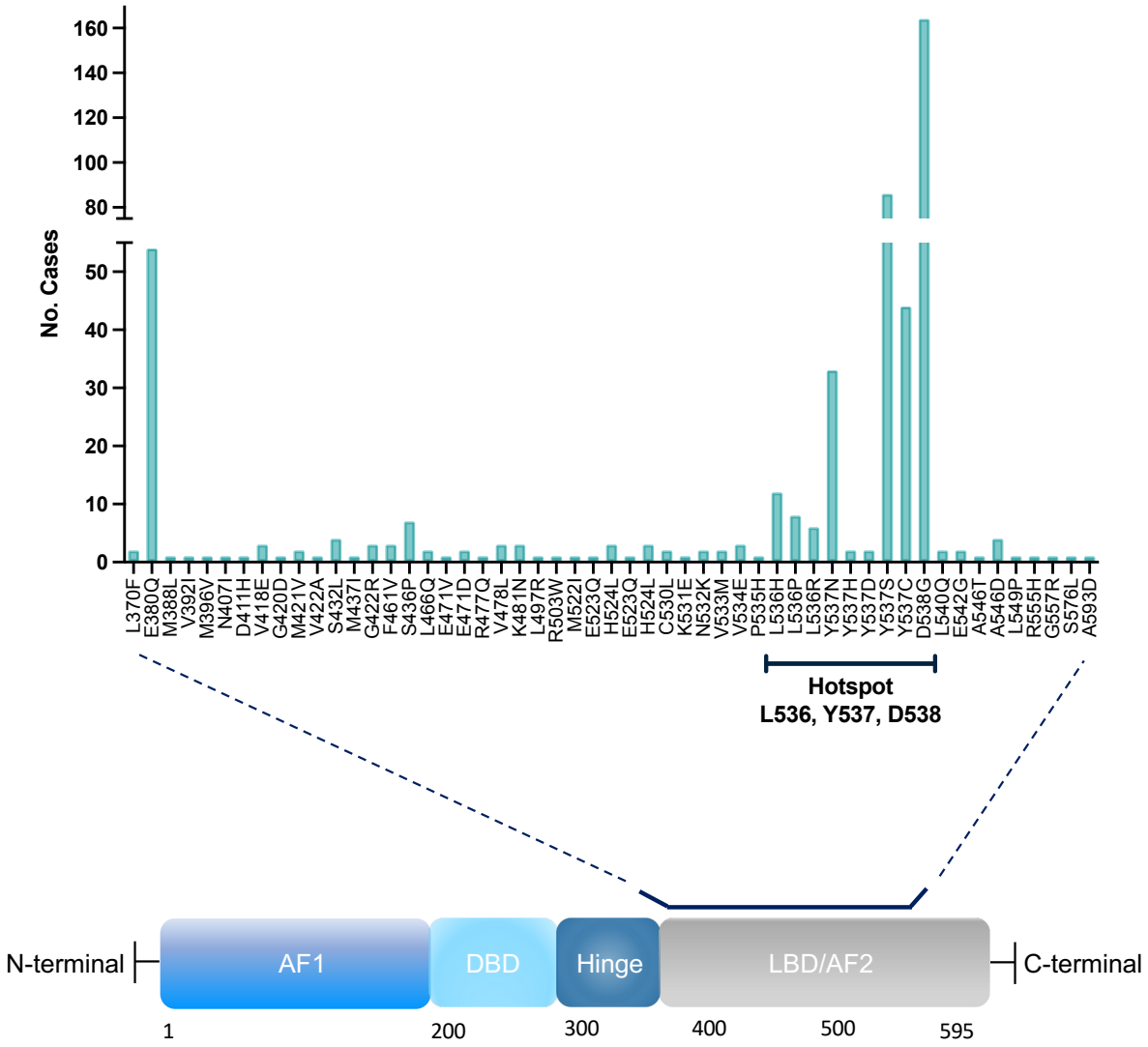


Figure 1.5 ESR1 mutations

ESR1 mutations are predominantly located on the ligand-binding domain, with a hotspot at L536, Y537 and D538. Locations and frequency of ESR1 mutations are displayed; scale of y-axis is altered from 80-160 cases. Data obtained from COSMIC (https://cancer.sanger.ac.uk/cosmic), accessed 07 February 2022. Abbreviations are as follows: AF1: activation function 1, DBD: DNA binding domain, LBD: ligand binding domain, AF2: activation function 2.

1.5.2 Treatment implications of *ESR1* mutations

The availability of metastatic samples in large clinical trials has facilitated retrospective study of the efficacy of standard treatments for ER-mutant metastatic breast cancer.

ESR1 Mutations and Aromatase Inhibitors/Fulvestrant

Combined analyses from the Phase III SoFEA and EFECT trials showed that patients with mutant ER had worse survival outcomes with Exemestane treatment than Fulvestrant; following progression on a non-steroidal AI, patients with mutant ER had shorter PFS rates (2.4 months vs 3.9 months respectively, hazard ratio 0.59, P=0.01) and a worse 1-year OS with Exemestane treatment vs Fulvestrant (62% vs 80% respectively, P=0.04) (Turner et al. 2020a; Chia et al. 2008; Johnston et al. 2013). For the group receiving Exemestane, patients with *ESR1* mutations had worse PFS and OS than those with WT ER (Turner et al. 2020a; Chia et al. 2008; Johnston et al. 2013).

Fulvestrant was reported to have similar efficacy in patients with either mutant or WT ER in the SoFEA and EFECT trials (Johnston et al. 2013; Chia et al. 2008; Turner et al. 2020a). The efficacy of Fulvestrant versus Fulvestrant combined with Pictilisib (a PI3K inhibitor) was also assessed in patients who had received an AI either in the adjuvant or metastatic setting in the FERGI trial. Pictilisib was associated with considerable toxicity but patients with *ESR1* mutations in this study were not more resistant to Fulvestrant than those with ER WT (Krop et al. 2016).

However, in contrast to the data from the SoFEA, EFECT and FERGI trials detailed above, analysis of the PALOMA-3 trial (which investigated Fulvestrant versus the

combination of Fulvestrant and Palbociclib in patients with metastatic disease previously treated with an AI); patients receiving Fulvestrant monotherapy with mutant ER had a poorer PFS than those with WT ER (3.6 vs 5.4 months) (Cristofanilli et al. 2016; Fribbens et al. 2016). The Phase IIa plasmaMATCH study also reported that Fulvestrant may not be effective for heavily pretreated (median of 2 prior lines of endocrine therapy) patients with *ESR1* mutations, as those randomized to receive Fulvestrant had a PFS of just 2.2 months (Turner et al. 2020c). Increasing the dose of Fulvestrant had no benefit in treating patients with *ESR1* mutations (Turner et al. 2020c).

Fulvestrant has proven to be much more effective than Tamoxifen at reducing mutant ER activity down to basal levels, albeit with greater doses than required for equivalent degradation of WT ER (Toy et al. 2013; Jeselsohn et al. 2014).

Hence, there remains some conflict in the literature about the role of Fulvestrant in treating patients with ER mutations.

ESR1 Mutations and Selective Estrogen Receptor Modulators

ESR1 mutations confer partial resistance to Tamoxifen through impaired ligand-binding affinity and the altered helix 12 conformation (Fanning and Greene 2019). However another SERM, Lasofoxifene, has shown retention of its ER antagonism *in vitro* and significant inhibition of tumour growth in xenograft models of Y537S and D538G, which is very promising (Laine et al. 2018). The Phase II ELAINE 2 trial is studying the safety and efficacy of Lasofixifene in combination with Abemaciclib for patients with *ESR1* mutant breast cancer which had progressed on previous endocrine

therapy with or without a CDK4/6 inhibitor, and has currently reported a censored median PFS of 13.9 months and an overall response rate of 33.3% (Damodaran et al. 2022). The Phase II ELAINE 1 trial is also studying the efficacy of Lasofoxifene vs Fulvestrant in a second line setting, following resistance to CDK4/6 inhibitors in patients with ER mutant breast cancer (ClinicalTrials.gov Identifier NCT03781063).

Bazedoxifene is a SERM/SERD hybrid and functions as a pure antagonist; it has been shown to be effective in Tamoxifen-resistance models and inhibits Y537S and D538G mutant ER transcriptional activity in MCF7 cells (Fanning et al. 2018b; Wardell et al. 2013). Interestingly, Bazedoxifene degrades WT and D538G ER but not Y537S ER, again highlighting the distinctions between different ER mutant variants (Fanning et al. 2018b). A Phase II trial of Bazedoxifene in combination with Palbociclib in patients who have progressed on endocrine therapy is ongoing (ClinicalTrials.gov Identifier NCT02448771).

ESR1 Mutations and Oral Selective Estrogen Receptor Degraders

Novel orally bioavailable SERDs, such as AZD9496 have shown promise, with increased potency relative to Fulvestrant in Y537S-mutant, MCF7-derived xenograft tumour models (Toy et al. 2017). RAD1901, another oral SERD, has also shown anti-tumour activity through downregulation of ER signalling, reduced transcription of ER target genes and inhibition of growth in Y537S and D538G mutant cells lines, even those resistant to CDK4/6 inhibitors (Patel et al. 2019). The novel, small molecule SERCA, H3B-6545, has been shown to possess single agent activity in inhibiting the growth of tumours in Y537S xenograft models and its effects have been reported to be further potentiated when combined with CDK4/6 or mTOR inhibitors in an ongoing

Phase I/II study (ClinicalTrial.gov Identifier NCT03250676) (Hamilton et al. 2021; Puyang et al. 2018).

ESR1 Mutations and CDK4/6 Inhibitors

The combination of an AI and CDK4/6 inhibitor is standard first-line treatment for metastatic ER+ disease but this is likely to be suboptimal for patients with *ESR1* mutations, given the associated resistance to AIs. The PALOMA-3 study supports a role for CDK4/6 inhibitors in *ESR1* mutant disease, reporting a PFS advantage of 5.8 months with the addition of Palbociclib to Fulvestrant treatment in patients with *ESR1* mutant positive ctDNA (Fribbens et al. 2016). Analysis of the impact on the emergence of *ESR1* mutations following Abemaciclib monotherapy in patients pre-treated with endocrine and chemotherapy (nextMONARCH1) and Abemaciclib and AI versus AI alone in patients who had not received systemic therapy but may have been previously treated with endocrine therapy (with a disease-free interval >12 months from completion of endocrine therapy) (MONARCH3) has been performed; relatively low levels of ER mutations were detected during the study periods (6% in nextMONARCH1 with Abemaciclib monotherapy and 17% in MONARCH3 with Abemaciclib plus AI), implying that mutant *ESR1* may not be involved in Abemaciclib resistance (Hamilton et al. 2020; Goetz et al. 2020).

ESR1 Mutations and PI3K/mTOR1 Inhibitors

In combination with endocrine therapy, mTOR inhibitors are a standard second line treatment option for metastatic ER+ breast cancer. The BOLERO-2 study compared Exemestane versus Exemestane combined with Everolimus in patients with metastatic breast cancer who had previously received a non-steroidal AI

(Chandarlapaty et al. 2016). Patients with D538G mutations derived a PFS benefit of 5.78 months with the addition of Everolimus; due to small numbers of Y537S-mutant cases, it was not possible to analyse the benefit in these patients.

Utilising the detection techniques and knowledge of resistance mechanisms now available for *ESR1* mutations, the PADA-1 trial is the first to combine serial testing (2-monthly ddPCR) with a treatment intervention (switching to Fulvestrant and Palbociclib) on detection of an emerging *ESR1* mutation in patients treated with first-line AI and Palbociclib (Bidard et al. 2019). The initial results of this show a PFS benefit with Fulvestrant plus Palbociclib therapy vs AI plus Palbociclib (11.9 vs 5.7 months) (Bidard et al. 2022). Long term data from the PADA-1 and future similar trials will be very informative in how best to manage these patients, particularly regarding the uncertainty as to whether switching treatment before clinically overt resistance develops improves outcomes.

Although it is clear that AIs have no role in the treatment of *ESR1* mutant breast cancer, SERMs, SERDs, hybrid SERM/SERDs, CDK4/6 inhibitors and mTOR inhibitors have all shown utility in this setting. It is possible that optimal management of *ESR1*-mutant breast cancer can only be achieved through recurrent testing of cfDNA and blockade of multiple resistance pathways.

1.5.3 Other alterations of *ESR1* activity

Other genomic changes to *ESR1* have been described which alter its activity and contribute to endocrine resistance. Amplification of *ESR1*, resulting in enhanced ER target gene expression, has been demonstrated through fluorescence in-situ

hybridisation (FISH), biochemical assays and NGS of cfDNA, CTCs and patient tumour samples (Jeselsohn et al. 2014; Nielsen et al. 2011; Holst et al. 2007; Moelans et al. 2010). As amplification of the androgen receptor (AR) was reported in 30% of patients who relapsed on androgen-deprivation therapy but not found in matched primary samples, it has been implicated in treatment-resistant prostate cancer and therefore amplification of ER may have a similar function in breast cancer (Visakorpi et al. 1995). Through NGS, amplified *ESR1* has been detected in 1.7% of primary and 1.3% of metastatic ER+ tumours, which is much lower than the rates previously detected (~20%) by less sensitive FISH and microarrays (Jeselsohn et al. 2014; Nielsen et al. 2011; Holst et al. 2007; Tomita et al. 2009). Although *ESR1* amplification has been reported to stimulate E2-independent growth in an endocrine-resistant PDX model, the low frequency of this genomic alteration makes its significance unclear (Li et al. 2013).

Changes in the ER coactivator:corepressor balance have been shown to alter the effects of Tamoxifen in a tissue-specific manner, with overexpression of coactivators and downregulation of corepressors resulting in agonistic activity of Tamoxifen and cellular proliferation through enhanced ER regulated transcription (Jordan and O'Malley 2007; Shang and Brown 2002). The ER coactivator AIB1 is reportedly amplified in 5% of primary breast cancers and, when overexpressed, increases Tamoxifen-induced agonism of ER *in vitro* (Bautista et al. 1998; Smith et al. 1997). Upregulation and increased phosphorylation of AIB1 resulted in enhanced expression of ER target genes and Tamoxifen resistance *in vitro*, and in reduced responsiveness and poorer PFS in patients (Ali and Coombes 2002; Osborne et al. 2003). In addition, crosstalk between AIB1 and HER-2 has been proposed and in MCF7 cells with high

levels of AIB1 and HER-2 overexpression (MCF7-HER2-18 cells), Tamoxifen has been shown to behave as an ER agonist, recruiting coactivators to the ER-regulated pS2 gene promotor (Shou et al. 2004). The EGFR inhibitor, Gefitinib abrogates this crosstalk and restores the interaction of corepressors rather than coactivators to Tamoxifen-bound ER on target gene promoters (Shou et al. 2004). Gefitinib also inhibited growth of MCF7-HER2-18 cells and MCF7-HER2-18 tumour xenografts (Shou et al. 2004).

Loss of ER altogether has also been proposed as another resistance mechanism, through formation of silencing DNA methyltransferase/HDAC complexes in the *ESR1* promoter (Yoshida et al. 2000; Ottaviano et al. 1994; Lapidus et al. 1996; Yang et al. 2001). In combination with an AI, Entinostat (an oral HDAC inhibitor) has shown efficacy in restoring expression of ER and sensitivity to endocrine therapy in cell lines (Yardley et al. 2013; Sabnis et al. 2011). Tamoxifen resistance has been described in this context, with loss of ER reported in 10-17% of patients who initially responded then became resistant to Tamoxifen, suggesting that, in the absence of ER, tumour growth is directed by alternative pathways (Ring and Dowsett 2004).

1.5.4 Aberrant regulation of cell cycle and growth signalling pathways

Cell cycle progression is controlled through regulation of the G1-S checkpoint by cyclin D, CDK4/6 and RB. Alterations in this pathway have been implicated in altering sensitivity to endocrine therapy (Knudsen et al. 2019). CCND1 amplification and/or overexpression is observed in approximately 50% of ER+ breast cancer (Elsheikh et al. 2008). As an ER target gene, CCND1 is also upregulated in the presence of E2 (Eeckhoute et al. 2006). CDK4 gene amplification has been reported in 15.8% of

breast cancers (An et al. 1999). Furthermore, the expression of p16 (a member of the INK4 family of cyclin kinase inhibitors that negatively regulates CDK4/6) inversely correlates with ER positivity (Milde-Langosch et al. 2001). This and other evidence is strongly supportive of aberrant CDK4/6 activity in the G1 phase of the cell cycle. Increased levels of CDK4/6 are also associated with Tamoxifen resistance and the efficacy of CDK4/6 inhibitors in endocrine sensitive and resistant ER+ disease is further evidence of the role cell cycle deregulation plays in endocrine resistance (Finn et al. 2009).

Alteration of growth factor signalling cascades is a well-documented means of providing alternative proliferation stimulus in the presence of ER inhibition (Musgrove and Sutherland 2009). Tyrosine kinases are a group of receptors that, when ligand-activated, enhance signalling through downstream pathways including MAPK, JAK/STAT and PI3K/AKT that can activate ER in an E2-independent manner (Presti and Quaquarini 2019; Campbell et al. 2001). Members of the tyrosine kinase family include the epidermal growth factor receptors (EGFRs), Insulin-like growth factor (IGF) receptors and fibroblast growth factor receptor (FGFR). Inhibitors of these receptors (TKIs) have been used successfully in several malignancies when resistance to other treatments has developed. Overexpression of EGFR is reported to increase the risk of Fulvestrant resistance, which was then reduced again by instigating combination treatment with Fulvestrant and an EGFR inhibitor (Razavi et al. 2018). Upregulation of EGFR ligands (TGF-α, epidermal growth factor (EGF), amphiregulin (AREG), epigen, epiregulin (EREG) and heparin-binding-EGF (HB-EGF)) have been implicated in endocrine resistance through enhanced growth factor pathways; an increase in TGF-α expression has been associated with increased EGFR/HER2 dimerization

(Knowlden et al. 2003). As discussed in section 1.3.1, IGF1R has been implicated in mediating the non-genomic effects of ER. Worse survival outcomes have been associated with higher expression of insulin receptor substrate-1 (IRS-1), a downstream component of the IGF1R pathway (Rocha et al. 1997). This suggests that growth factors may have utility in endocrine resistant disease but clinical trials with EGFR inhibitors have reported varied findings; patients with high expression levels of EGFR or HER2 responded well to Gefitinib or Lapatinib in combination with AIs but in other patients, no benefit was seen and increased toxicity was observed (Polychronis et al. 2005; Johnston 2009; Osborne and Schiff 2011; Burstein et al. 2014). However, some downstream targets, such as mTOR have established efficacy when targeted. Everolimus (an mTOR inhibitor) and Exemestane are used as subsequent lines of therapy after endocrine resistance develops (Gennari et al. 2021).

Therefore, as detailed in this section, multiple mechanisms of endocrine resistance have been proposed. Through genomic sequencing of nearly 2,000 breast cancers (1,501 of which were ER+), Razavi et al. 2018 demonstrated that 20% of acquired resistance involves EGFR, 10% involves MYC and in 50% of cases, the cause is unknown (Razavi et al. 2018). The remaining 20% of cases of acquired resistance were attributed to *ESR1* mutations, confirming the significance of this mechanism of endocrine resistance and the importance of identifying effective treatments for these patients.

1.6 Nuclear Receptor Crosstalk

In contrast to autoregulation (gene expression through activation of a NR by its cognate ligand), cross-regulation or crosstalk of NRs has been described as a

temporal means of coordinating cellular responsiveness to different hormonal stimuli (Bagamasbad and Denver 2011). Crosstalk can be direct or indirect, involving either the presence or absence of physical interaction between NRs respectively, resulting in regulation of target gene sets that may be unique to one of the NRs or shared (Kumar et al. 2021; De Bosscher et al. 2020). The downstream signalling cascades of two or more NRs may also be interlinked, which is termed 'dual NR crosstalk' (De Bosscher et al. 2020). The result of this is that numerous and complex combinations of pathways may be stimulated, leading to potentially unique downstream signalling and transcriptional patterns.

Given the hormonal milieu of malignant, ER+ breast tissue, unsurprisingly crosstalk between ER and several other steroid hormone NRs has been described in this setting (Carroll 2016). PR has long been associated with ER (as discussed in section 1.7) both in normal and malignant physiology of the breast and reproductive systems. In MCF7 and T47D cells cultured in estrogenic media, ligand-activated PR is reportedly recruited to the ER complex and reduces the tumorigenic effects of ER signalling through redistribution of ER-chromatin binding away from a pro-proliferative gene expression pattern (Mohammed et al. 2015). Furthermore, one of the isoforms of PR, PR-B, competes with ER for common coactivators (McDonnell and Goldman 1994; Wen 1994). These may provide mechanistic explanations for reports that PR agonists block both ER transcriptional activity and ER-mediated growth (Vignon et al. 1983; Musgrove et al. 1998; Chen et al. 2011; Mohammed et al. 2015). Importantly, the actions of PR on ER appear to be context-dependent, i.e. influenced by the presence of E2 and progestogens (Vignon et al. 1983; Mohammed et al. 2015); the interplay between PR and ER will be discussed further in section 1.7.7. Similar interactions

between GR and ER have been described, with analysis of genome-wide binding profiles showing reprogramming of ER binding sites by activated GR (Miranda et al. 2013). Co-expression of AR and ER has also been reported, with AR even substituting for ER in molecular apocrine breast cancer, which is ER-negative but has similar gene expression profiles to ER+ breast cancer (Farmer et al. 2005; Doane et al. 2006; Peters et al. 2009). AR coordinates the expression of ER target genes in this subtype of breast cancer by being recruited to the enhancers by FOXA1 in place of ER. Consolidating the theory of AR replacing the function of ER, an AI resistance mechanism whereby the expression of ER is decreased and AR increased has also been proposed (Ni et al. 2011). More recently a role for AR in the treatment of ER+ breast cancer has been suggested, after AR agonists were shown to redistribute the genomic distribution of ER and ER coactivators, resulting in repression of ER-regulated cell cycle genes and overexpression of several AR target genes, many of which are known tumour suppressors (Hickey et al. 2021). This crosstalk raises the possibility that targeting other NRs and their signalling pathways may directly as well as indirectly modify the ER activity and have therapeutic utility in ER+ breast cancer.

Reports of cooperation between ER and non-sex hormone members of the NR superfamily also exist, including LRH-1 and retinoic acid receptor-α (RARα). In a similar manner to PR, RARα functions in a context dependent manner according to whether E2 is present/absent, but unlike PR it stimulates ER-mediated expression of target genes and promotes ER-induced cell growth (Ross-Innes et al. 2010). Through ChIP-reChIP studies (ER ChIP, release of ER-bound chromatin, then RARα ChIP), this is proposed to occur through co-occupancy (whereby RARα and ER simultaneously occupy the same binding region) and RARα is thought to play a critical

role in activating the ligand-bound ER complex by maintaining ER-coactivator interactions (Ross-Innes et al. 2010). Binding of LRH-1 has also been reported at many ER-binding sites and facilitates transcription of ER target genes through direct binding to EREs (Lai et al. 2013). Here, overexpression of LRH-1 also enhanced ER recruitment to ER binding sites. However, unlike RARα, reChIP studies failed to show co-occupancy of ER and LRH-1 and their interplay is therefore proposed to function through 'assisted loading', with sequential recruitment and dissociation of each NR at the same binding site (Lai et al. 2013). The mechanisms of crosstalk between ER and the NRs PR, RARα and LRH-1 are illustrated in Figure 1.6.

The NR superfamily has been divided into 6 subfamilies according to structural similarity of the DBD and LBD of the NRs and their function (Nuclear Receptors Nomenclature Committee 1999). The NR3C group has 4 members, including GR (NR3C1), MR (NR3C2), PR (NR3C3) and AR (NR3C4) and, as members of the same subfamily, by definition these NRs are more closely related to one another than other NRs. These 4 NRs all bind to the same DNA response elements, which comprises 2 hexameric half-sites (5'-AGAACA-3') as inverted repeats with 3bp of separating DNA (Beato et al. 1995). Therefore, there is potential for lack of DNA target specificity of these NRs and resultant competition between them (Shaffer et al. 2004). As discussed further in sections 1.6.2 and 1.8, members of the NR3C subfamily can bind endogenous and synthetic ligands that are primarily associated with another member of the group. For example, RU486, which is used predominantly to inhibit PR activity in clinical practice, also binds GR and AR (Whitaker et al. 2014). The roles of AR, GR and MR in breast cancer are discussed below; PR is discussed in section 1.7.

1.6.1 AR in breast cancer

AR is responsible for mediating the effects of testosterone and DHT and has critical functions in the development and normal physiology of the male reproductive system as well as playing a key role in prostate cancer, in an analogous fashion to ER in breast cancer (Heinlein and Chang 2004; Balk and Knudsen 2008; Watson et al. 2015). Androgens are involved in the regulation of breast development through cooperation with E2, although the two hormones have opposing actions; regardless of E2 concentrations, high circulating levels of androgens result in impaired morphogenesis of the breast, whilst low levels of androgen relative to E2 result in stimulation of breast development (Dimitrakakis and Bondy 2009). A role for AR in malignancies has also been proposed since it is expressed in 90% of primary and up to 75% of metastatic breast cancers, though the incidence varies according to intrinsic subtype, with almost all ER+ cases but only 10-35% of triple negative breast cancer (TNBC) expressing AR (Hickey et al. 2012; Proverbs-Singh et al. 2015). The activity of AR is context-dependent, varying with changes in the hormonal environment, ER expression and the AR:ER ratio (Sikora 2016; Peters et al. 2009). AR is an independent prognostic predictor in ER+ cancer, associated with better prognostic characteristics such as smaller tumour size, lower histological grade and lower Ki67 proliferation index (Aleskandarany et al. 2016). Most studies in ER+ disease suggest that ligand-induced AR signalling is protective, antagonising ER activity and thereby reducing ER-mediated cellular proliferation and ER target gene expression (Hickey et al. 2012; Peters et al. 2009; Castellano et al. 2010). The historical use of AR agonists (in combination with Tamoxifen) in breast cancer supports this proposed mode of action although controversially, both agonists and antagonists have been reported to be growth inhibitory in *in vitro* and *in vivo* models (Ingle et al. 1991; Peters et al. 2009;

Cochrane et al. 2014). Recently, Hickey et al. (2021) reviewed the optimal AR-targeting treatment strategies for ER+ breast cancer, after demonstrating tumour suppressor activity of AR in ER+ breast cancer cell lines and in PDX models (Hickey et al. 2021). Treatment of ZR-75-1 xenografts with both the selective AR modulator (SARM), Enobosarm, and the native AR agonist, DHT resulted in sustained inhibition of growth (Hickey et al. 2021). Unlike DHT, SARMs are an attractive treatment option as they possess AR agonism in breast cancer cells but lack unwanted virilizing side effects in other tissues (Narayanan et al. 2018; Hu et al. 2016). Phase II trials have demonstrated that Enobosarm is well-tolerated and has potential as a novel endocrine therapy for ER+/AR+ breast cancer (Palmieri et al. 2021; Overmoyer et al. 2015). A phase III trial, ARTEST is currently investigating the efficacy of Enobosarm vs standard endocrine therapy in heavily pre-treated patients with metastatic ER+/AR+ breast cancer who have progressed on a non-steroidal AI, Fulvestrant and a CDK4/6 inhibitor (ClinicalTrials.gov Identifier NCT04869943). Unlike its better prognostication in ER+ disease, AR expression is associated with poor outcomes in TNBC, particularly in the luminal androgen receptor subtype (Lehmann et al. 2011). These tumours are androgen-sensitive and anti-androgens such as bicalutamide and enzalutamide have shown promising clinical activity in phase II trials in patients with TNBC (Gucalp et al. 2013; Traina et al. 2018). As stated above, in this TNBC subtype, AR appears to substitute for ER, and directs transcriptional programmes similar to those directed by ER in ER+ breast cancer (Ni et al. 2011).

1.6.2 GR in breast cancer

Both endogenous glucocorticoids (e.g. cortisol) and myriad synthetic glucocorticoids (e.g. dexamethasone, prednisolone) exert their effects through GR, which is

ubiquitously expressed and facilitates diverse metabolic, immune-related and neurological functions (Dwyer et al. 2020). Like AR, the function of GR in the breast is context dependent and dependent on ER status (Truong and Lange 2018). High levels of GR confer a better prognosis in ER+ breast cancers but, conversely, carry a worse prognosis for ER-negative tumours (Pan et al. 2011). Crosstalk between liganded GR and ER occurs in ER+ disease, with both NRs regulating the other's recruitment to chromatin through assisted loading resulting in a shift towards tumour growth inhibition (similarly to LRH-1 and ER, as described in section 1.6) (Miranda et al. 2013; Voss et al. 2011; West et al. 2016). Patients with breast cancer are already routinely prescribed GR agonists to counteract the toxicities of systemic anti-cancer drugs including emesis and hypersensitivity, making GR an attractive and easily manipulated target. Clinical trials in breast cancer patients have shown modest response rates to single agent glucocorticoids and improvement in response but not survival rates when GR agonists are combined with endocrine therapy or chemotherapy (Keith 2008). However, *in vitro* studies using TNBC cells have shown that activated GR signalling inhibits chemotherapy-induced apoptosis and stimulates pro-proliferative genes (Chen et al. 2015; Skor et al. 2013). Both TNBC patient- and cell line-derived xenografts have also been used to demonstrate increased tumour heterogeneity and metastatic potential following activation of GR (Obradović et al. 2019). Since these discoveries, there have been concerns that the regular use of glucocorticoids as a pre-treatment may reduce the efficiency of chemotherapy-induced apoptosis and indeed, long-term, high dose glucocorticoids have been associated with a survival disadvantage (Keith 2008). The combination of RU486 (which is a GR and PR antagonist) with dexamethasone and Paclitaxel treatment has been found to mitigate this and increase cytotoxicity in TNBC cells in an *in vitro* study (Skor et al. 2013). As

well as RU486, GR is able to bind many other PR-modulating drugs at affinities similar to its own ligands and, conversely, PR is also modulated by glucocorticoids and able to bind to glucocorticoid response elements (GREs) (Truong and Lange 2018; Lippman et al. 2001). Therefore, selection of ligands for studying the effects of GR or PR signalling must be carefully considered.

1.6.3 MR in breast cancer

The primary function of MR is regulating electrolyte and fluid balances through activation by its cognate ligand, aldosterone. Despite being expressed in the majority of breast cancers, its role in this disease has not been studied to the same degree as other NRs discussed in this section (Kumar et al. 2021). One study has demonstrated that together, liganded MR and another NR, RAR, have a tumour suppressive relationship and increased expression of both is associated with improved survival in ER+ breast cancer (Doan et al. 2020). Co-treatment with a mineralocorticoid (aldosterone) and a retinoid (all-trans retinoic acid) but neither ligand alone, inhibited growth of MCF7 cells and this dual treatment may therefore represent a potential therapeutic strategy (Doan et al. 2020). Hence, although relatively little is known about MR's function in breast cancer currently, it may well involve interaction with other NRs.

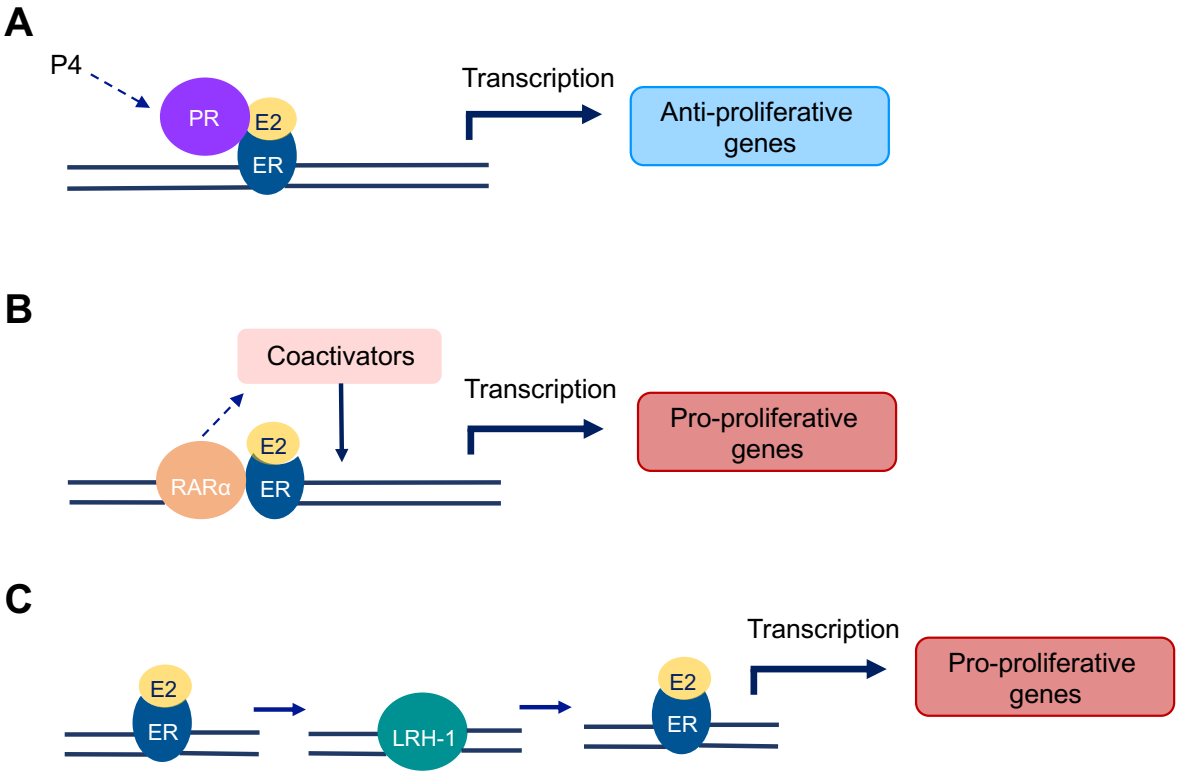


Figure 1.6 Nuclear Receptor Crosstalk

(**A**) Ligand-stimulated PR is recruited to the ER complex in the presence of E2 and alters the genomic binding profile of ER into a less proliferative gene expression pattern (**B**) RARα and ER 'cooperatively interact' through occupying the same binding region; RARα also maintains ER-coactivator interactions and results in transcription of ER target genes, thereby promoting ER-mediated cellular proliferation (**C**) LRH-1 facilitates transcription of ER-regulated genes and ER-mediated cell growth through 'sequential loading' with ER, where LRH-1 and ER are sequentially recruited to then dissociated from the same binding site.

1.7 Progesterone and breast cancer

Five years after E2 was reported as the first ovarian hormone, Allen and Corner described a ‘pro-gestational’, proliferative effect on the endometria of castrated female rabbits following treatment with corpus luteum extract but not E2-containing follicular fluid or placental extract (Corner and Allen 1929). After they subsequently proved that a component of this corpus luteum extract maintained implantation, multiple international groups raced to isolate, purify and determine the chemical formula of this substance, initially named ‘Progestin’ then subsequently ‘Progesterone’ (P4), which was finally accomplished in 1934 (Allen and Corner 1929; Butenandt and Westphal 1934; Slotta et al. 1934; Hartmann and Wettstein 1934; Wintersteiner and Allen 1934). P4’s cognate receptor, PR, was identified over 30 years later using the chick oviduct model and, once purified, 2 isoforms were found, PR-A and PR-B, the roles of which are still being fully delineated today (outlined in section 1.7.2) (O'Malley et al. 1970).

As discussed in section 1.6, there is clear evidence that the functions of ER and PR in breast cancer are intertwined. PR is expressed in approximately 75% of ER+ breast cancers and, as an ER target gene, it is rarely present without ER (McGuire and Clark 1986). For this reason, PR was viewed for many years as simply a surrogate marker of ER, which predicted response to endocrine therapy. However, PR is only a predictive marker of response in premenopausal women (who have much higher levels of circulating P4, as discussed in section 1.7.1) but not in postmenopausal patients. Historically, ER has therefore been the main candidate implicated in the pathogenesis of ER+/PR+ breast cancer and the key therapeutic target. More recently however, PR has been proposed to confer favourable treatment outcomes through directly modifying the ER transcriptome (discussed further in section 1.7.7). Synthetic

PR agonists have been used effectively in advanced ER+/PR+ breast cancer (discussed in section 1.8), and the recent findings of PR's ER-modulating behaviour has reignited research into targeting PR as a potential treatment strategy. The effects of both PR agonists and antagonists in breast cancer have been investigated (detailed in section 1.8). In terms of nomenclature, P4 is the only native progesterone, synthetic PR agonists are known as 'progestins' and any ligand that activates PR (including P4) is termed a 'progestogen' (Carroll et al. 2017). 'Anti-progestin' refers to PR antagonists.

A number of challenges have made deciphering the role of PR signalling in normal and malignant breast physiology more complex: (1) the existence of 2 PR isoforms with distinct and overlapping functions and a paucity of isoform-specific assays and ligands, (2) the presence of both genomic and non-genomic PR signalling pathways (discussed in sections 1.7.3 and 1.7.4), (3) the different effects of liganded and unliganded PR, (4) cross-talk with other steroid hormone NRs and, (5) the potential context-dependence of PR activity in the fluctuating hormone milieu resulting from menstrual cycles and menopause. In addition, PR ligands also carry a number of complexities and controversies: (1) are progestogens, anti-progestins or potentially both an effective therapeutic strategy depending on context (possibly reflecting the effects of AR modulation in breast cancer discussed in section 1.6.1, whereby anti-androgens are effective in ER-/AR+ breast cancer, whilst AR agonists have activity in ER+/AR+ breast cancer), (2) are these PR ligands tumorigenic, antiproliferative or potentially both, depending on context, (3) what are the implications of using synthetic progestins vs natural progestogens, (4) do different doses of progestins result in different effects on the breast, (5) what non-PR driven effects are conferred by the

receptor promiscuity of some of these ligands and (6) do progestogens have differential effects in early, pre-malignant lesions relative to established breast cancers? Hence, the field of PR signalling is relatively unknown compared to ER and, despite PR being routinely measured with immunohistochemistry in every single patient diagnosed with breast cancer, many fundamental questions about its role in breast cancer remain (Figure 1.7). This section focuses on the current evidence in some of these key areas.

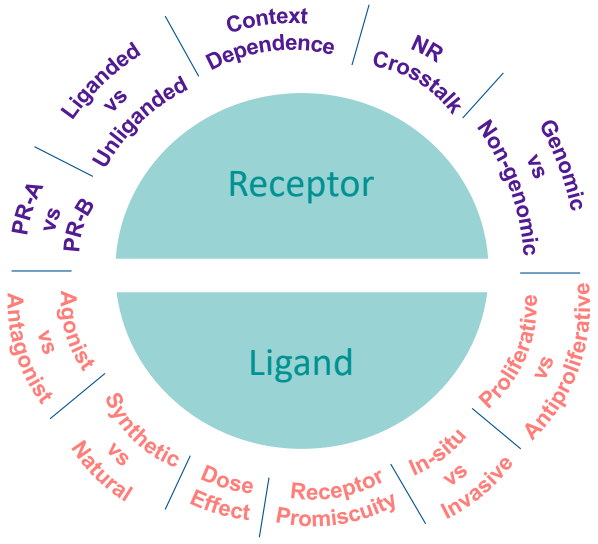


Figure 1.7 Challenges in delineating the function of PR signalling

Schematic summarising the PR-specific and PR ligand-specific challenges in deciphering the roles of this NR.

1.7.1 Progesterone biosynthesis and physiological actions

After the structures of the steroid hormones were resolved, each was found to be derived from cholesterol and they therefore share highly similar structures (Miller and Auchus 2011). Although the major supply of cholesterol is dietary (low-density-lipoproteins), the adrenal gland is capable of de novo synthesis of cholesterol (Gwynne and Strauss 1982; Mason and Rainey 1987). The conversion of cholesterol to intermediary metabolites and eventually steroid hormones, including P4, is catalysed by a series of steroidogenic enzymes, the activities of which are altered by regulatory cofactors (Figure 1.8). These enzymes are classified as either cytochrome P450 enzymes (subdivided as type 1, mitochondrial, or type 2, in the endoplasmic reticulum) or hydroxysteroid dehydrogenases (dehydrogenases or reductases) (Miller and Auchus 2011). Production of gonadal sex hormones results from the acute adrenal steroidogenic response, which is triggered by adrenocorticotropic hormone (ACTH) in 3 mechanisms, over 3 time frames; (1) via inducing adrenal hypertrophy, ACTH optimises the location of steroidogenesis over weeks or months, (2), through cAMP, ACTH stimulates the expression of genes encoding the steroidogenic enzymes over days and (3) ACTH stimulates the StAR (steroidogenic acute regulatory protein) to transport cholesterol from the outer to the inner mitochondrial membrane, where P450scc (side chain cleavage enzyme) catalyses the first step in steroidogenesis (the conversion of cholesterol to pregnanolone) over minutes (Miller 2017). P4 is converted from pregnanolone by 3-hydroxysteroid dehydrogenase, and then into 11-deoxycorticosterone and 17-hydroxyprogesterone by P450c21 and P450c17 respectively, before further enzymatic activity results in a cascade of downstream metabolites with the production of steroid hormones as the endpoint (Miller 2017). With deciphering the steroidogenesis pathway came the understanding that P4 is not

just a product of this pathway but an important intermediary, essential to the synthesis of aldosterone, cortisol, E2 and testosterone (Figure 1.8).

P4 primarily exerts its functions during the ovulatory phase of the menstrual cycle and during pregnancy (Trabert et al. 2019). In premenopausal women, LH release induces P4 production from the corpus luteum soon after ovulation has occurred; this production then increases through the follicular and luteal phases (Figure 1.9) (Trabert et al. 2019). During the follicular phase of the menstrual cycle, serum progesterone levels are less than 1ng/mL with roughly equal proportions produced by the ovaries and adrenal glands (Trabert et al. 2019). P4 then peaks in the mid-luteal phase as it is produced by the corpus luteum and reaches serum concentrations of up to 35ng/mL (Trabert et al. 2019). E2 peaks during the follicular phase, followed by a smaller peak in the luteal phase (Brisken 2013). Menopause, which occurs at an average age of 51.4 years, is heralded by a rise in FSH levels and a decrease in early follicular inhibin B and anti-Mullerian hormone (AMH) to almost undetectable levels 6 and 4-5 years before the final menstruation, respectively (Santoro and Randolph 2011; Randolph et al. 2011). P4 levels gradually fall with the progressive ovarian follicle loss associated with increasing age (urinary excretion of the P4 metabolite, pregnanediol glucuronide, falls by 7% per year during the 2-6 year menopausal transition phase) until they plateau at <0.2ng/mL in the postmenopausal period, when production is primarily taken over by the adrenal glands (Figure 1.9) (Trabert et al. 2019; Santoro et al. 2008; Santoro and Randolph 2011). In contrast, E2 levels remain relatively stable until 2 years prior to the final period and plateau 2 years after this (Santoro et al. 2008; Santoro and Randolph 2011). At the start of pregnancy, P4 levels are equivalent to the luteal phase but then increase dramatically towards the end of the first trimester

with placental P4 production peaking at 300ng/mL at term (Trabert et al. 2019). P4 is usually bound to either corticosteroid binding globulin (CBG) or albumin; in premenopausal women, approximately 20% of P4 is CBG-bound but in pregnancy, CBG increases and the proportion of CBG-bound P4 increases to 40% (Gardill et al. 2012; Trabert et al. 2019; Solano and Arck 2020). Given the rise in P4 with each menstrual cycle and the risk factors for breast cancer associated with a greater number of menstrual cycles (early menarche, late menopause), it may be that lifetime exposure to P4 contributes to this risk. Furthermore, the luteal phase is generally fixed at 14 days, whilst the follicular phase ranges from 10-21 days; the increased risk of breast cancer related to shorter menstrual cycles may therefore be related to a longer cumulative luteal period with the characteristic P4 surge (Brisken 2013).

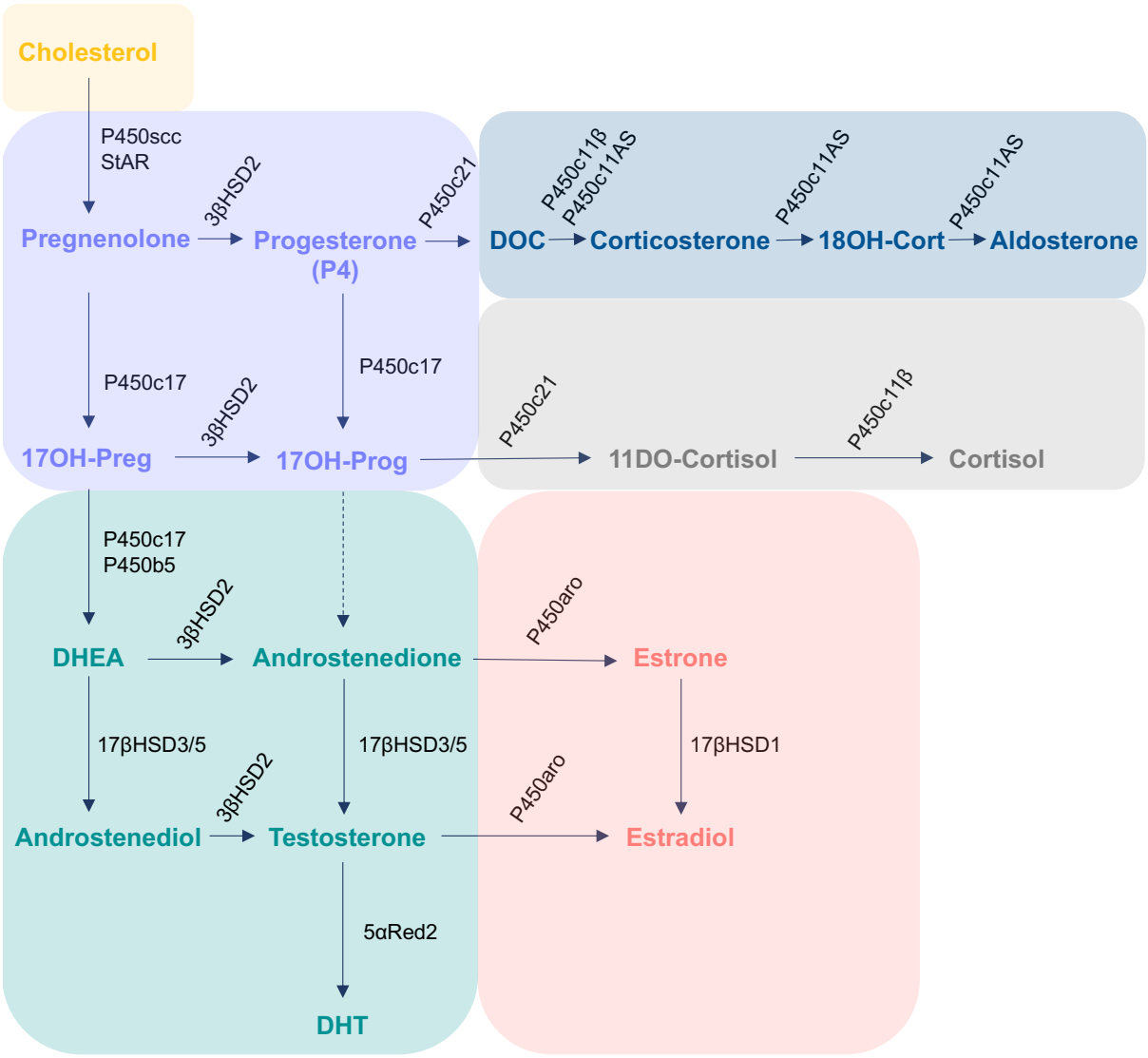


Figure 1.8 Steroid Biosynthesis Pathway

Hormones and enzymes involved in steroidogenesis. The abbreviations used are as follows: DOC: 11-deoxycorticosterone, 18OHCort: 18-hydroxycorticosterone, 17OH-Preg: 17-hydroxypregnenolone, 17OH-Prog: 17-hydroxyprogesterone, 11DO-Cortisol: 11-deoxycorticosterone, DHEA: dehydroepiandrosterone, DHT: dihydrotestosterone, P450scc: P450 side chain cleavage enzyme, 5α-reductase type 2 enzyme

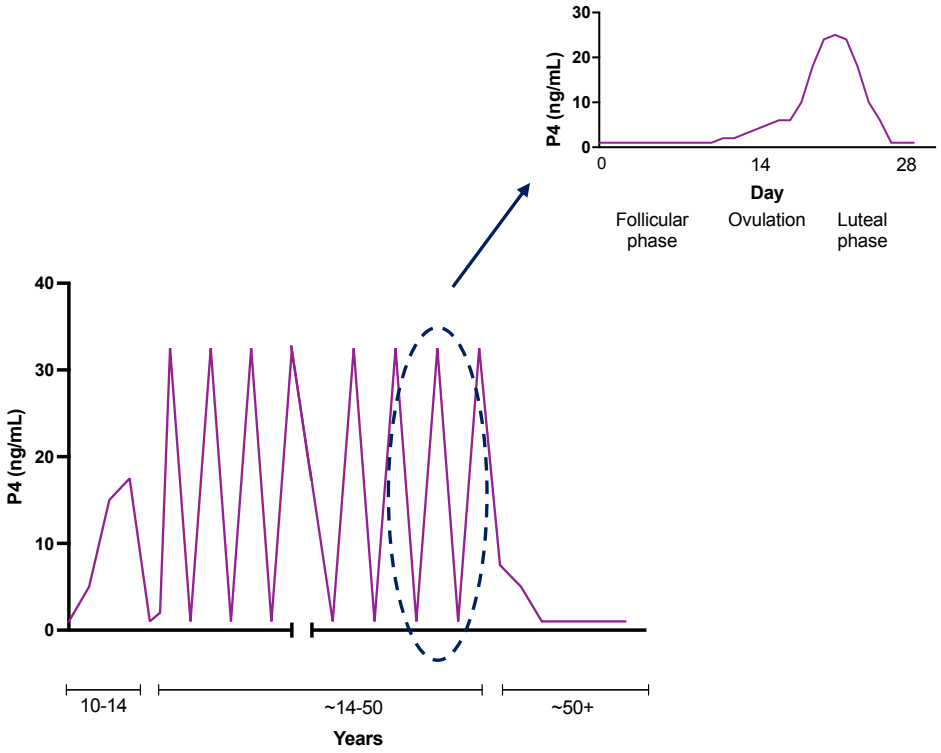


Figure 1.9 Physiological Progesterone levels

Pre-pubertal levels of P4 are maintained at <1ng/mL, then rise to 10-12ng/mL at purberty. During the reproductive years (highlighted in dashed circle and separate graph), follicular levels of P4 remain <1ng/mL and fluctuate between 3-35ng/mL during the luteal phase.

Figure adapted from Trabert et al. 2019

1.7.2 Progesterone receptor isoforms and structure

PR has 2 main isoforms, PR-A and PR-B, that are transcribed as 2 distinct mRNA from the same gene on chromosome 11 by two different promoters (Kastner et al. 1990; Lamb et al. 2018). Both isoforms are expressed in the breast. PR-A (769 amino acids long, 94kDa) and lacks the 164 amino acid N-terminus residues termed the 'B-upstream segment' (BUS), that comprises AF3 (activation function 3) in PR-B (933 amino acids, 116kDa) (Figure 1.10) (Sartorius et al. 1994; Jacobsen and Horwitz 2012). The BUS is responsible for the PR-B-unique transcription profile, as mutation

of specific amino acids within it, disrupts PR-B-dependent gene transcription (Tung et al. 2006). A third isoform, PR-C, is also transcribed from the same gene by a distinct promoter at an alternative translation site and is expressed in breast cells as well as fundal myometrial cells during pregnancy (Wei et al. 1990; Condon et al. 2006). PR-C is even smaller than PR-A, with a molecular mass of 60kDa and consisting of the LBD but no functional DBD (the first DBD zinc finger is absent) (Figure 1.10) (Condon et al. 2006). PR-C has been proposed to modify the transcriptional activity of PR-A and PR-B through either dimerising with them or by competing for ligand (Wei et al. 1996; Wei et al. 1997; Cork et al. 2008). Furthermore, PR antibodies detected a 78kDA protein in 25.7% (n=202) of PR+ breast tumour samples and other PR mRNA variants with various exon deletions have also been described (Graham et al. 1995; Cork et al. 2008). PR-C and the other potential PR transcripts are not well characterised or described in the context of breast physiology; discussion of PR isoforms from hereon will therefore focus on PR-A and PR-B.

Upon ligand stimulation, PR-A and PR-B can form homo- or heterodimers, which then bind to P4 response elements (PREs). Modes of activation other than dimerization have been proposed, including binding of PR monomers to PRE half-sites and tetramerization of PR in PR-B transfected cells (Jacobsen 2009; Presman et al. 2016). Following DNA binding, the 2 isoforms have distinct transcriptional actions as demonstrated through the generation and study of PR-negative, T47D-Y cells, inducibly expressing PR-A or PR-B (Jacobsen et al. 2002; Richer et al. 2002). PR-A and PR-B have differential gene expression patterns; ligand-stimulated PR-B regulates a greater number of genes than PR-A and, in the case of genes regulated by both isoforms, PR-B is the more potent transactivator (Richer et al. 2002; Tung et

al. 2006; Jacobsen et al. 2005). In the absence of P4, however, PR-A shows greater transcriptional activity than PR-B as well as greater inhibition of E2-dependent growth in tumour xenograft models (Jacobsen et al. 2005; Sartorius et al. 2003). Interestingly, ligand-bound PR-A blocks gene expression by PR-B and other nuclear receptors, including ER and MR, suggesting a repressive role for this isoform (Wen 1994; McDonnell et al. 1994). As well as separate transcriptional landscapes, the isoforms also have differing post-translational modification profiles (discussed in section 1.7.3) (Abdel-Hafiz and Horwitz 2014; Daniel et al. 2007; Diep et al. 2015). Finally, PR-B is thought to mediate the non-genomic actions of P4 (described in section 1.7.4), as unlike PR-A which is largely nuclear, PR-B is able to shuttle between the nucleus and the cytosol (Lamb et al. 2018).

Unsurprisingly, these isoforms have different roles in the development and physiology of the mammary gland and reproductive systems (Sartorius et al. 1994; Wen 1994). Knockout mice have been used to study the individual roles of the PR isoforms in breast development and established PR-B as essential for the development of side-branching and alveogenesis in the mammary gland (Mulac-Jericevic et al. 2000; Mulac-Jericevic et al. 2003). Conversely, PR-A is necessary for normal ovarian and uterine function (Mulac-Jericevic et al. 2003; Conneely et al. 2001). Levels of PR-A and PR-B are equivalent in normal human breast tissue but this ratio is commonly altered in the malignant breast, with a predominance of PR-A. Patients with PR-A enriched tumours have greater resistance to Tamoxifen and worse survival outcomes (Mote et al. 2002; Graham et al. 1995; Hopp et al. 2004; Mote et al. 2007). PR-A may therefore contribute to carcinogenesis, particularly when found in the cytoplasm (rather than just in the nucleus as it usually is) where it may interfere with normal PR

signalling (Lamb et al. 2018). Recently, PR-A has been implicated in metastasis of luminal breast cancer, with its expression correlating with lymph node involvement in treatment-naïve patients with primary disease (Rosati et al. 2020). In addition, cancer stem cell (CSC) populations that pose therapy resistance and recurrence risk (discussed further in section 1.7.6), expand in PR-A positive T47D tumorosphere models (malignant equivalents of mammospheres) through increased phosphorylation of PR-A at serine 294, with associated R5020-stimulated expression of CSC-related target gene sets (Truong et al. 2018).

Several challenges have complicated resolving the overlapping and distinct roles of PR-A and PR-B. Single isoform detection has been restricted by difficulties in accessing isoform-specific antibodies for immunohistochemistry, and indeed, clinically, only total PR is tested for (Mote et al. 2001). Both *in vitro* and *in vivo* experimental models have varying PR-A:PR-B ratios which, given that gene-regulation is isoform-specific, results in a wide range of potentially unique transcriptional landscapes being studied and compared, without full appreciation of the potential variation in PR-A:PR-B ratio (Lamb et al. 2018). Targeting the individual isoforms has also been limited by a lack of isoform-specific ligands and poor understanding of the isoform-specific actions of the agonists and antagonists that are available – differing isoform relative binding affinities (RBAs) have been shown for a wide range of synthetic agonists and antagonists but not for medroxyprogesterone acetate (MPA, a PR agonist) (Schoonen et al. 1998; Ghatge et al. 2005). Hence, PR-A and PR-B clearly have diverse transcriptomes, functions and phenotypes but their full roles are yet to be elucidated.

1.7.3 Genomic activation and post-translational modifications of PR

The classical pathway of PR-mediated gene transcription is well established. Upon binding P4, PR dissociates from the chaperone complex (including various heat shock proteins and immunophilins such as FK506 binding proteins 5 and 4 (FKBP51 and FKBP52) (Cenciarini and Proietti 2019). PR then translocates to the nucleus where it may bind directly to PREs of target genes via the DBD. Alternatively PR, like ER, may be recruited to DNA by tethering to other transcription factors (such as AP-1, SP-1 and signal transducer and activator of transcription 3 (STAT3)) and thereby regulate expression of genes lacking PREs (Lamb et al. 2018). Coregulators are recruited to DNA-bound PR and the transcriptional response modulated according to the coactivator:corepressor ratio (Scarpin et al. 2009). In human breast tissue, ligand-bound PR moves into nuclear aggregates or 'foci', which is also important for transcriptional activity. Within these nuclear aggregates, PR co-localizes with RNA polymerase II (Pol II), nascent RNA and the coactivator, p300, which all promote transcription (Arnett-Mansfield et al. 2007). Inhibition of coactivator recruitment prevents the movement of PR into these nuclear aggregates and represses transcriptional activity (Arnett-Mansfield et al. 2007; Scarpin et al. 2009).

Post-translational modifications of PR can further adjust target gene expression, through phosphorylation, SUMOylation, ubiquitination, acetylation or methylation. These modifications can alter the effects of PR through altered dimerization, nuclear localization, promotor selectivity, coregulator interactions, transcriptional activity, receptor degradation and sensitivity to P4 (Diep et al. 2015; Hagan 2014; Lamb et al. 2018; Cenciarini and Proietti 2019; Abdel-Hafiz and Horwitz 2014; Daniel et al. 2007). This results in PR exhibiting a diverse array of context-dependent actions. Kinases

with mitogenic activity (e.g. CDK2, CK2 and MAPK) phosphorylate PR, promoting a proliferative phenotype; in cancers with enhanced growth factor and cell-cycle dependent factors, overactive kinases may result in persistent phosphorylation of PR (Hagan 2014). Phosphorylated PR also interacts with cytoplasmic proteins and their downstream cascades, which is discussed further in section 1.7.4. More than 10 PR phosphorylation sites have been described, the majority of which are located within the N-terminal region and 5 of these are in the BUS of PR-B (Cenciarini and Proietti 2019). As a result, PR-B appears to be particularly strongly regulated by phosphorylation events. For example, MAPK activation results in phosphorylation of PR-B but not PR-A on ser294 (Diep et al. 2015). Phosphorylation of PR-B ser294 has wide ranging regulatory action on this isoform, including maintaining ligand-sensitivity, facilitating ligand-independent transcription, modulating promoter sensitivity, and increasing PR-B receptor turnover relative to PR-A (Diep et al. 2015; Daniel 2009; Knutson et al. 2012; Shen et al. 2001). SUMOylation, defined as, 'the covalent and reversible conjugation of small ubiquitin-related modifiers (SUMOs) to target proteins', has been reported on PR K388, although to different degrees in the two isoforms. PR is rapidly (within 15 minutes) SUMOylated after R5020 (a potent PR agonist) or Mifepristone (RU486, a PR antagonist) treatment but to a much greater extent in T47D-YA than T47D-YB cells (described in section 1.7.2) (Bossis and Melchior 2006; Abdel-Hafiz et al. 2002; Daniel et al. 2007). SUMOylation is a repressive, protein stabilising modification which is negatively regulated by phosphorylation of PR (Knutson et al. 2012; Daniel et al. 2007). Since PR-B ser294 is preferentially phosphorylated over PR-A, it is hypothesised that the greater stability enhanced SUMOylation confers to PR-A may explain, at least in part, its repressive role and its greater predominance in human breast cancer (Daniel et al. 2007). Acetylation of both

PR-A and PR-B have been reported in response to ligand-binding at Lys183 within the N-terminal region and at another Lysine at the acetylation consensus sequence, KXKK, in the hinge region (Chung et al. 2014a; Daniel et al. 2010). PR acetylation is implicated in a number of functions, since T47D cells engineered to be deficient in PR acetylation (through disruption of the lysines in the KXKK motif by mutation to alanine) exhibit reduced phosphorylation, impaired nuclear retention of PR and decreased progestin-induced transcriptional activity (Daniel et al. 2010). Finally, methylation at Lys464, which is situated within the AF1, has also been described and, through studies with mutation of this residue, has been implicated in altered ligand sensitivity and interaction with coregulators such as NCOR1 and SRC-1 (Chung et al. 2014b). The key residues that are involved in post-translational modification of PR are annotated in Figure 1.10.

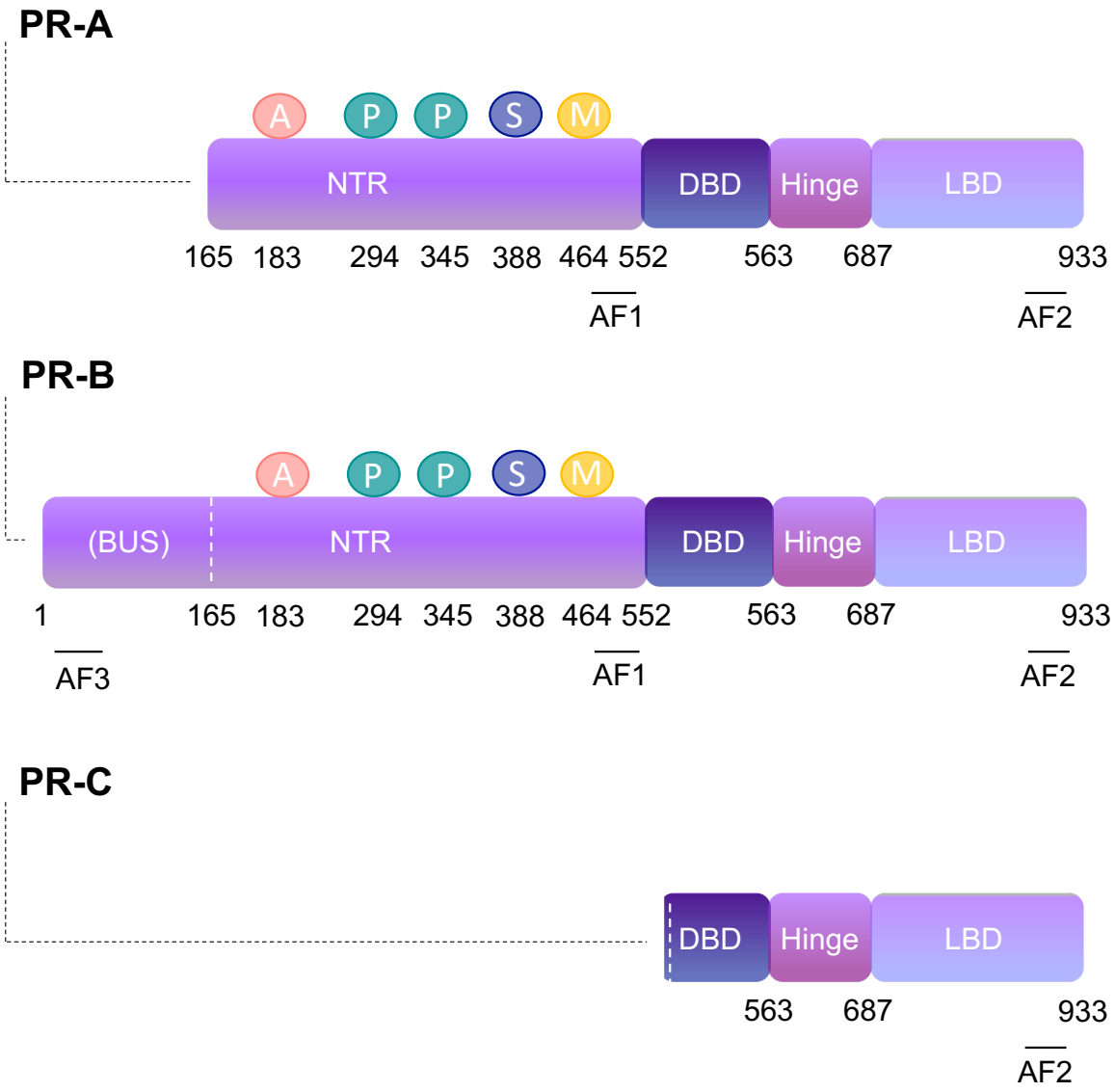


Figure 1.10 Structure of PR isoforms and sites of post-translational modifications

Structures of PR-A, PR-B and PR-C are shown. The abbreviations used are as follows: NTR: N-terminal region, DBD: DNA binding domain, LBD: ligand binding domain, AF1-3: activation functions 1-3, BUS: B-upstream segment. Sites of post-translational modification are also highlighted: acetylation (A) of Lys183, phosphorylation (P) of Ser294 and Ser345, SUMOylation (S) of Lys388 and methylation (M) of Lys464.

1.7.4 Non-genomic actions of Progesterone

In addition to its role as a ligand-activated transcription factor, PR is also able to bind to membrane-associated molecules and activate downstream cytoplasmic signalling pathways (Dressing et al. 2011). These so-called 'non-classical' effects can be mediated more rapidly than transcription and translation and involve pathways including protein kinases, ion channels and G-proteins (Dwyer et al. 2020; Trabert et al. 2019). The MAPK pathway is reported to be PR-regulated as, following treatment with a progestin, c-Src is directly activated within 3-15 minutes, which then induces p42/p44 MAPK phosphorylation and results in proliferation of T47D cells (Ballaré et al. 2003; Boonyaratanakornkit et al. 2001; Migliaccio et al. 1998). Progestin treatment also rapidly (within 10 minutes) induces EGFR autophosphorylation, which then activates MAPK, which in turn phosphorylates PR-B on the MAPK consensus site, ser345, in a feed-forward mechanism (Faivre et al. 2008). In addition, the PI3K/AKT pathway is rapidly stimulated by progestins, which results in increased growth of breast cancer cells and tumour xenografts, and modulation of secretory proteases urokinase-type plasminogen activator (uPA), MMP-2 and MMP-9 in breast cancer cells (Salatino et al. 2004; Carnevale et al. 2007). The N-terminal region of PR (and other NRs, including ER) contains proline-rich sites which may be phosphorylated through enhanced MAPK or CDK signalling; the most frequently phosphorylated PR sites as ser294, ser345 and ser400 (Dwyer et al. 2020). Feedforward mechanisms are therefore likely to regulate non-genomic PR signalling. Cytoplasmic signalling can also result in transcriptional changes through kinase activity of other molecules that interact with PR at target gene loci (Diep et al. 2015; Hagan 2014). For example, MPA-induced phosphorylation of STAT3 (through JAK and c-Src) facilitates formation of a PR-STAT3 complex, in which STAT3 functions as a PR coactivator, stimulating

expression of PR target genes such as bcl-x and p21 (Proietti et al. 2011). A further example is that phospho-PR-B ser345 (phosphorylated through progestin-stimulated EGFR, c-Src and MAPK signalling) is required for interaction with SP1 by regulating expression of growth (EGFR) and PR cell cycle (p21) target genes that have promoters lacking PREs (Faivre et al. 2008). Hence, through these ligand-independent post-translational modifications, ER+/PR+ cells may be altered to show different growth, motility and treatment response characteristics.

1.7.5 ER and PR in the normal breast

Breast tissue possesses unique plasticity in its ability to develop predominantly after birth (Brisken 2013). E2 and P4 are instrumental to the morphogenesis of the breast during puberty but their roles are difficult to fully distinguish due to their paracrine regulation (Trabert et al. 2019). Since maintaining hormone receptor positivity in human models of the normal breast is challenging (cells from mammoplasty samples rapidly lose their hormone receptor expression when cultured *in vitro*), studies have mostly been performed in rodent models, with rat mammary tissue having more similar morphology and physiology to the human breast than mouse (Huggins et al. 1959; Brisken 2013; Stampfer and Bartley 1985; Brisken and Scabia 2020). Importantly for studies of endocrine resistance, mammary tumours in mice tend to be ER-negative, whilst carcinogen-induced mammary tumours in rats express both ER and PR and show dependence on E2 (Huggins et al. 1959; Cheung et al. 2003). During the luteal phase, cellular proliferation of the mammary gland occurs in the terminal distal lobular units (TDLUs) with changes in the surrounding stoma (Masters et al. 1977; Longacre and Bartow 1986). Importantly, all breast cancers, regardless of histological site of origin (ductal, lobular), arise from TDLUs, implying that the luteal phase, and possibly

the P4 surge that occurs during the luteal phase, plays a role in the early stages of a malignancy (Wellings and Jensen 1973; Brisken 2013). The adult human breast comprises 10-25 ducts that extend from the nipple, form branches that develop into lobes and eventually become TDLUs, surrounded by a vascular stroma, formed of loose connective tissue (Brisken 2013). ER and PR expression occurs in both the epithelial and stromal areas of the murine mammary gland; 80% of PR receptors are found in the epithelial cells and 20% in stromal cells (Daniel et al. 1987; Haslam and Shyamala 1981; Haslam 1989; Wang et al. 1990).

Ovariectomy has been performed in mouse models with the resultant hormone ablation and then reintroduction of individual hormones enabling study of the independent effects of E2 and P4, albeit in non-physiological conditions (Daniel et al. 1987). In ovariectomized, young, virgin mice, E2 alone is enough to restore cellular proliferation in the mammary gland, resulting in ductal growth akin to that seen in hormonally intact mice (Daniel et al. 1987). However, in adult ovariectomized mice, E2 monotherapy was not sufficient to induce mammary epithelial proliferation (Beleut et al. 2010). This suggests that E2 stimulates the early stages of pubertal breast development but does not have a solo role in the proliferation of the mature mammary gland (Brisken 2013). The low PR expression and absence of progestin-induced proliferation at short time points (48 hours) in ovariectomized mice are not surprising, as *PGR* is an E2-regulated gene and will therefore be expressed at lower levels in the absence of E2 (Haslam and Shyamala 1979; Wang et al. 1990). However, cellular proliferation was observed in adult ovariectomized mice following treatment with P4 alone at longer timepoints (3, 5 and 10 days – although it should be noted that endogenous adrenal hormone production may occur during this time) and, when E2

and P4 or a progestin are administered concurrently, proliferative responses appear to be faster than P4 treatment alone (evident at 48 hours) and more extensive (Aupperlee and Haslam 2007; Wang et al. 1990). The implications of this are that P4 is the driver hormone for cellular proliferation in mature, adult breast tissue with E2 playing a permissive role (Beleut et al. 2010). Further supporting this theory, grafting experiments have been performed to investigate the actions of ER and PR in the epithelial and stromal components of the breast, in which ER-/- or PR-/- epithelium is engrafted to WT mouse mammary fat pads stripped of the endogenous epithelium, or ER-/- or PR-/- fad pads are transplanted with WT epithelium (Mallepell et al. 2006; Lydon et al. 1995; Brisken et al. 1998). E2 and P4 again appear to act sequentially - ER playing a supporting role for PR in these models, with ER-/- epithelium failing to proliferate or develop terminal end buds in young mice and PR-/- epithelium growing initially but then failing to develop side branches or alveoli (Mallepell et al. 2006; Brisken et al. 1998). Stromal ER and PR do not appear to be required for cellular proliferation in the mammary gland (Mallepell et al. 2006; Brisken et al. 1998).

Beleut et al. identified two P4-induced ‘waves’ of proliferation in the mammary gland; the first, smaller phase targeting PR+ cells directly in a cyclin D1-dependent manner and the second through paracrine receptor activator of NF-κB (RANKL)-mediated regulation of PR-negative cells (Beleut et al. 2010). A paracrine mode of action for P4 has long been postulated since only 15-40% of mammary epithelial cells express PR and, interestingly, these cells tend to be non-proliferative, suggesting that PR+ cells are P4 ‘sensors’ and PR-negative cells ‘responders’ (Grimm et al. 2002; Clarke et al. 1997; Russo et al. 1999; Brisken and Scabia 2020). ER and PR are co-expressed in the majority (96%) of hormone receptor positive epithelial mammary cells but are

absent in myoepithelial cells (Clarke et al. 1997; Brisken 2013). This co-expression is expected, given that PR is ER regulated, but again makes deciphering the individual roles of these NRs difficult. Data from mouse studies further supports a paracrine function; when mammary epithelial cells from either PR-/- or ER -/- mutant mice were mixed with WT cells and transplanted into cleared fat pads, mammary gland morphogenesis and growth is restored (Mallepell et al. 2006; Brisken et al. 1998). This is not achieved when PR-/- or ER-/- epithelial cells are transplanted without WT cells, or when intact sections of PR-/- or WT epithelial tissue are 'co-transplanted' into the same fat pad, confirming that both the presence and proximity of ER and PR positive cells are essential for paracrine signalling (Mallepell et al. 2006; Brisken et al. 1998). Secretory factors such as RANKL, WNT4 and EGF family members such as amphiregulin (AREG) are all PR-regulated and have been described as mediators of PR's paracrine actions (Brisken et al. 2002; Mulac-Jericevic et al. 2003; Brisken et al. 2000; Aupperlee et al. 2013).

RANKL, a member of the tumour necrosis factor-α family (TNF-α) has roles in osteoclast differentiation and formation of lymph nodes (Kong et al. 1999). Several studies have demonstrated that RANKL is implicated in breast morphogenesis in the following ways: (1) overexpression of RANKL's receptor, RANK, increases mammary epithelial proliferation, (2) RANKL stimulates development of the breast lactational network in pregnancy and when RANK/RANKL signalling is impaired through mutation of a downstream mediator (IKKα) lactation is defective, and (3) RANKL induction facilitates generation of ductal side branches and alveogenesis (P4-dependent processes) in ER+, PR-/- models, thereby restoring the PR+ phenotype (Gonzalez-Suarez et al. 2007; Mukherjee et al. 2010; Fata et al. 2000; Cao et al. 2001). Of note,

RANKL has also been associated with cyclin D1 expression in the breast which, as discussed in the previous paragraph, is instrumental to autocrine PR signalling, highlighting a possible link between the two systems (Cao et al. 2001; Beleut et al. 2010). RANKL is induced by P4 and its expression localised to PR+ epithelial cells. It is found at the cell membrane and it remains unclear whether it mediates its effects through interaction with adjacent cells or via secretion (Mulac-Jericevic et al. 2003; Brisken et al. 2002; Brisken 2013). RANKL is therefore a key effector of the actions of PR. Injection of osteoprotegerin (OPG), a RANKL decoy receptor, resulted in a 54% reduction in P4-stimulated proliferation (Beleut et al. 2010). Clinically, an anti-RANKL monoclonal antibody, Denosumab, is used in millions of patients with breast cancer to reduce the risk of pathological fractures and pain associated with bone metastases, as well as lowering the increased risk of osteoporosis associated with adjuvant AI treatment (Gennari et al. 2021). The ABCSG-18 trial, is investigating the effects of Denosumab on survival of postmenopausal, ER+/PR+ patients with early breast cancer who are taking adjuvant AIs. At 8 years of follow-up, the median DFS was 80.6% for patients receiving Denosumab and 77.5% for patients prescribed a placebo (Gnant et al. 2019).

The drosophila wingless gene (WNT) family are involved in embryogenesis of various vertebrates and invertebrates and 2 of its members, WNT1 and WNT4 are well-characterised mediators of PR signalling (Zhan et al. 2017; Brisken et al. 2000). WNT1 expression is strongly involved in mouse mammary gland development, with overexpression resulting in uncontrolled side branching and tumorigenesis (Tsukamoto et al. 1988). In PR-/- knockout mice, ectopic WNT1 expression restored the development of side branches (Tsukamoto et al. 1988; Brisken et al. 2000). WNT4

is the only family member directly induced by P4 (it is also induced by ER, albeit less potently) and when constitutively expressed in virgin mice, results in the extensive ductal branching characteristic of early pregnancy, suggesting a role for WNT4 in this setting (Brisken et al. 2000; Bradbury et al. 1995). Like WNT4, AREG expression is induced by P4 and, like RANKL, it colocalises with PR+ cells in the mammary gland (Kariagina et al. 2010; Aupperlee et al. 2013). On upregulation by ligand-stimulated PR, AREG facilitates proliferation and formation of terminal end buds (which is reversed by Gefitinib, an EGFR inhibitor) and is therefore thought to be active in the pubertal phase of breast development (Aupperlee et al. 2013; Ciarloni et al. 2007). In support of a paracrine role, when AREG -/- mammary epithelial cells are in the vicinity of WT cells in mouse models, the proliferation and morphogenesis associated with intact AREG are restored (Ciarloni et al. 2007). As outlined earlier in this section, ER is largely responsible for breast development in puberty; its effects have also been shown to be mediated through AREG, which is an ER as well as PR target gene (Howlin et al. 2006; Aupperlee et al. 2013).

A further paracrine role for WNT4, RANKL and amphiregulin, through mediating the effects of PR, is in the maintenance of mammary stem cell (MaSC) populations (Booth et al. 2010; Horwitz and Sartorius 2020). MaSCs may be defined on the basis of: (1) a Fluorescence-Activated Cell Sorting (FACS) profile with expression of integrin α6 (ITGA6) and integrin β1 (ITGB1), (2) single cells possessing outgrowth potential and giving rise to mammospheres and (3) their ability to repopulate cleared mammary fat pads (Dontu et al. 2003; Tosoni et al. 2012; Shackleton et al. 2006; Stingl et al. 2006; Brisken and Scabia 2020). Caution must be taken in interpreting results from studies using these parameters as both cell-surface markers and mammary fat pads are under

hormonal control and therefore changes may not be solely representative of the MaSC population (Brisken and Scabia 2020). ER-/PR- stem and progenitor cells are located in a niche in the basal epithelium (surrounded by luminal and myoepithelial cells) and are PR-regulated, as shown by an expansion in numbers with exogenous P4 and during the P4-rich luteal phase and pregnancy, and stasis of the population size with abrogation of the menstrual cycle (Joshi et al. 2010; Asselin-Labat et al. 2006; Asselin-Labat et al. 2010). In addition, use of organoid cultures derived from reduction mammoplasties, which represent the normal breast and contain both basal progenitor and differentiated luminal cells, have shown that P4 induces proliferation of these cultures, formation of mammospheres and aldehyde dehydrogenase (ALDH) activity, which are all markers of MaSCs (Graham et al. 2009a; Graham et al. 2009b; Dontu et al. 2003; Ginestier et al. 2007). The function of MaSCs is also modulated by P4; transplantation of MaSCs from ovariectomized mice into cleared mammary fat pads (with hormonally intact stroma) resulted in a 4.3-fold reduction in the total repopulating cell count relative to controls, suggesting that hormone-intact epithelial cells are required for maintenance of MaSC activity through paracrine signalling (Asselin-Labat et al. 2010). Ovariectomy did not result in a decrease in the total number of MaSCs and, in combination with P4, E2 is also required to increase the number of repopulating MaSCs in mouse models (Asselin-Labat et al. 2010). Treatment with letrozole but not RU486, results in a dramatic shift in the MaSC population with marked reduction in repopulating cells and outgrowth potential (Asselin-Labat et al. 2010). Together, these findings suggest that E2 may be required to ensure that levels of P4 are sufficiently high to stimulate secretion of paracrine factors such as WNT4 and RANKL from PR+ cells to maintain normal numbers and function of PR-negative MaSCs (Joshi et al. 2010; Asselin-Labat et al. 2010). Inhibition of RANKL with a monoclonal antibody in

mouse models, significantly reduced the clonogenicity of the MaSC population and another RANKL inhibitor, RANK-Fc, suppressed proliferation of normal mammary epithelium, development of pre-malignant hyperplasia and tumorigenesis (Asselin-Labat et al. 2010; Gonzalez-Suarez et al. 2007). However, WNT4 has been proposed to have a larger role in maintaining stem cell potency, as serial transplantation assays using mammary epithelium with various mutations revealed that WNT4 deletion has the greatest impact on the regenerative potential of MaSCs, relative to RANKL and even PR loss (Rajaram et al. 2015). The putative ligand-receptor pair CXCL12/CXCR4 is also implicated as a mediator of P4 in MaSC regulation (Shiah et al. 2015). Like RANKL and WNT4, CXCR4 is induced by P4, and CXCR4 inhibition using 2 different inhibitors (AMD3100 and AMD3465) decreased total, basal and luminal mammary clonogenicity by 20% following stimulation with E2 and P4 in WT mice; this effect was not seen in PR knockout mice, confirming that PR signalling is required for CXCR4 activity (Shiah et al. 2015).

Modification of the extracellular membrane (ECM) is required for the morphological changes in the breast necessary for lactation. Through P4 (and E2) paracrine regulation of WNT4 expression and signalling, the secretion of the protease Adamts18 is induced. Adamts18 function is linked to the basement membrane, since *in vitro* studies show that it cleaves fibronectin and, *in vivo*, Adamts18-/- pubertal mammary glands show greater collagen production and deposition than WT mice (Ataca et al. 2020). Deletion of Adamts18 in mice also resulted in a 43% decrease in the number of MaSCs and interaction between Adamts18 and the basement membrane proteoglycan, Coll18a1, has been reported, adding evidence to the basal membrane acting as the site of the stem cell niche (Ataca et al. 2020). Hence, as an indirect target

of PR, Adamts18 maintains the MaSC pool number, the site of the MaSC niche and remodelling of the ECM.

In summary, P4 has multiple actions in the normal development and physiology of the breast, including formation of ductal side branches and alveoli, epithelial cell proliferation, maintenance and expansion of the mammary stem cell population and ECM restructuring. At least some of these activities may become aberrant in the malignant breast, as discussed in the next section.

1.7.6 PR signalling in breast cancer

P4 has been proposed to be carcinogenic ever since it was linked with the increased risk of breast cancer in women taking MHT. Progestins were initially included in MHT to mitigate the unopposed, potentially tumorigenic effects of E2 on the endometrium but were subsequently associated with an increased incidence of breast cancer, a greater proportion of patients with abnormal mammography and a higher percentage of metastatic breast cancer at diagnosis (Chlebowski et al. 2003). Hence the Women's Health Initiative trial, investigating E2 and MPA combination therapy, was terminated early and the Million Women Study, published shortly afterwards, reported similar findings of increased incidence and mortality from breast cancer following combined E2 and progestin treatment (Beral 2003; Chlebowski et al. 2003; Chlebowski et al. 2009; Chlebowski et al. 2015). As MHT use dropped sharply after publication of these findings, the incidence of invasive breast cancer also subsequently fell (Chlebowski et al. 2009; Farhat et al. 2010).

The risk of malignancy associated with MHT is thought to be mediated through increased mammary epithelial proliferation and has been attributed to progestins, as MHT containing single agent E2 (given to women following hysterectomy) shows no or only a minimal increase in the risk of breast cancer and has even been shown to be protective in women without benign breast disease or a family history of breast cancer (Anderson et al. 2012; Brisken 2013; Hofseth et al. 1999). It is important to note that many of the progestins included in MHT target other NRs as well as PR (discussed in section 1.8), have longer half-lives than P4 and, when synthetic progestins are replaced with natural progestogens in MHT, there is no increase in breast cancer risk (Fournier et al. 2005; Fournier et al. 2008; Brisken 2013). However, since early menarche, late menopause and progestin-containing contraception are established risk factors for breast cancer, an alternative theory is that cumulative exposure to P4 (gained through recurrent menstrual cycles) contributes to the pathogenesis of breast cancer. Interestingly although the overall incidence of breast cancer is 12.5%, a much larger proportion (30%) of women in their mid 40s (who died of non-breast cancer causes) were found to have ductal carcinoma in situ (DCIS). It has been postulated that repeated exposure to P4 may result in the progression of some of these pre-malignant lesions (Brisken 2013; Nielsen et al. 1987). In keeping with this, multiple studies have shown that PR agonists induce tumour development in mice pre-treated with a carcinogen but not, critically when treated with a PR agonist alone (Chatterton et al. 2002; Jabara et al. 1979; Huggins et al. 1962; Huggins 1965; Jabara 1967).

Breast cancer stem cells (CSCs), defined as expressing $CD44^{+}CD24^{-/low}EpCAM^{+}$ (referred to as $CD44^{+}$ from hereon) and having increased ALDH activity, have self-

renewal properties that mimic MaSCs but also have tumorigenic potential and may contribute to treatment resistance (Al-Hajj et al. 2003; Ginestier et al. 2007; Reya et al. 2001). More recently, cytokeratin 5 (CK5) has also been discussed as a characteristic marker of breast CSCs (Axlund et al. 2013; Lim et al. 2009; Böcker et al. 2002). Several studies have demonstrated that both native P4 and synthetic progestins (including R5020 and MPA) increase the population size of breast CSCs and facilitate tumorosphere formation (Truong et al. 2018; Hilton et al. 2014; Cittelly et al. 2013; Finlay-Schultz et al. 2015). It has been postulated that different cohorts of breast CSCs may exist; CSCs enriched in triple negative breast cancer are predominantly $CD44^+$ and $ALDH^+$, whilst luminal tumours have very low levels of cells expressing these markers (Horwitz and Sartorius 2020). Treatment of ER+/PR+ T47D cells grown as tumours in ovariectomized mice with either P4 or MPA, resulted in increased expression of the basal cytokeratins CK5 and CK6, and reduced expression of luminal CK8, CK18 and CK19, raising the possibility that progestogen treatment induces a luminal to basal shift in these cells, which is in keeping with the poor prognosis associated with CK5 expression (Sartorius et al. 2005; Cheang et al. 2008). In the same ER+/PR+ T47D xenograft model, 3 distinct populations of $CD44^+$ tumour cells have been identified expressing either ER-/PR-/CK5+, ER-/PR-/CK5- or ER-/PR+/CK5- (and a very rare population of ER+/PR+/CK5+ cells that exists only in response to progestin treatment) (Horwitz et al. 2008). With progestin-specific induction of CK5 expression, ER and PR expression appears to be lost and a CK5+ CSC-associated phenotype conferring invasiveness, tumorigenicity and treatment resistance is acquired (Horwitz et al. 2008; Haughian et al. 2012; Axlund et al. 2013; Sato et al. 2014). The proportion of ER-/PR-/CK5+ cells is small (1%) and non-expanding but reportedly present in more than 50% of primary breast cancers

(Haughian et al. 2012; Horwitz et al. 2008). Hence, in ER+/PR+ tumours, PR may induce a subpopulation of ER-/PR-/CK5+ cells that persist through endocrine therapy and stimulate the maintenance and growth of a larger population of ER+/PR+/CK5- cells, potentially through paracrine signalling.

Proposed mechanisms of PR-regulation of CSC number and activity include upregulation of PR target genes, signalling pathways and non-coding regulatory RNAs, known as microRNAs (miRNAs). As mentioned in section 1.7.2, PR-A is thought to be the predominant isoform in CSC function since PR-A+ tumorospheres have higher proportions of ALDH+ and CD44+/CD24- cells relative to PR-B+ models and there is more rapid phosphorylation of PR-A ser294 than PR-B in response to R5020 treatment. Furthermore, PR-A ser294 is required for transcription of CSC-related genes such as *FOXO1, KLF4* and *NOTCH2*; mutant PR-A ser294 (PR-A S294A) results in impaired CSC function (Truong et al. 2018). Hence, quantification of phosphorylated PR may be a useful measure of breast CSC activity (Knutson et al. 2017). The RANK pathway is implicated in CSC as well as MaSC activity; overexpression of RANK increases the CD44+ population and promotes tumour formation, invasion and metastasis in normal and malignancy human mammary cells (Palafox et al. 2012). Finally, several miRNAs have been shown to be progestin-regulated including miR-29 and miR-141, which when downregulated, increase expression of KLF4 and STAT5A respectively, resulting in expansion of the CD44+/CK5+ population and promotion of the associated CSC phenotype of invasion and tumorigenicity (Cochrane et al. 2012; Cittelly et al. 2013; Finlay-Schultz et al. 2015).

Secreted proteases that are components of or interact with the ECM have also been implicated in P4-mediated carcinogenesis (Brisken and Scabia 2020). Increased breast density (detected by mammography) is strongly associated with breast cancer risk and has been linked to progestin exposure (Greendale et al. 2003; Boyd et al. 2007). The Komen Tissue Bank has collected matched blood samples, breast biopsies and questionnaires including information on breast cancer risk factors from over 1,000 healthy participants; by identifying menstrual cycle phases through serum hormone measurements and performing RNA sequencing (RNA-seq) on 20 paired breast tissue samples, transcription profiles specific to the luteal phase and the follicular phase have been revealed (Pardo et al. 2014). The luteal phase, with its P4 peak, was associated with upregulation of paracrine signalling pathways including RANKL and WNT4, but also an increase in MMP3 and ADAMTS9 expression, which, may provide a mechanism for progestin-related mammographic density and increased risk of cancer.

Unlike the expansion of CSCs which occurs with and without the addition of E2 to P4/progestin, the effect of P4 on proliferation appears to be context dependent (Finlay-Schultz et al. 2015; Sartorius et al. 2005). In the absence of E2, P4 or R5020-activated PR has a proliferative effect on MCF7 cells and T47D cells and mammospheres (Faivre and Lange 2007; Goodman et al. 2016; Finlay-Schultz et al. 2015). In contrast, when ER+/PR+ PDX models were exposed to both E2 and P4 long-term, progestogen treatment exhibited an ER-independent means of regulating RNA polymerase III (Pol III), the enzyme responsible for transcription of tRNA genes, which conversely confers an antiproliferative phenotype (Finlay-Schultz et al. 2017). Finlay-Schultz et al. confirmed the Pol III modulating behaviour of PR through revealing that: (1) unliganded PR was localized at Pol III transcribed tRNA genes in chromatin occupancy analysis,

(2) that PR physically interacts with Pol III in rapid IP-mass spectrometry studies and, (3) on stimulation by either P4 or MPA, Pol III and therefore transcription of tRNA genes and mRNA translation is repressed (Finlay-Schultz et al. 2017). Pol III is a key player in quiescence, an established mechanism of treatment resistance, and through inhibiting it, in contrast to the other data discussed in this section, PR may actually reduce growth of ER+ tumours in an ER-independent manner.

Other soluble factors involved in paracrine, PR-mediated development of the normal breast have also been reported as critical in the early stages of breast cancer development. RANKL is predominantly expressed in areas of DCIS rather than invasive cancer and inhibition of RANKL is effective in preventing tumorigenesis but not treating a pre-formed tumour (Tanos et al. 2013; Gonzalez-Suarez et al. 2010). WNT signalling is also implicated in the pathogenesis of breast cancer, as ectopic overexpression of WNT1 resulted initially in pre-malignant hyperplasia before transformation into invasive disease (Tsukamoto et al. 1988). This adds weight to the theory, outlined at the beginning of the section, that P4 is an accessory, alongside other carcinogenic factors or susceptibilities, in facilitating tumorigenesis in its earliest stages. The proportion of proliferating ER+/PR+ cells is much higher in malignant mammary cells than in the normal breast, representing up to 60% of PR+ cells and 85% of ER+ cells in a tumour (Anderson 2002; Lee et al. 2005). This suggests that the usual paracrine signalling associated with PR may be deregulated and succeeded by autocrine pathways including EGFR, WNT-1 and cyclin D1 (Faivre and Lange 2007). The differing transcriptome of progestin-treated normal mammary epithelial cells vs T47D cells further reinforces that an alternative mechanism of signalling exists in malignant breast tissue (Graham et al. 2009b). Hence, through a variety of

mechanisms detailed above, PR activity is implicated in the early development and progression of breast cancer.

1.7.7 Modulation of ER activity by PR

ER has long been known to regulate PR but, more recently, PR has been implicated in modifying ER activity. Several studies have used immunoprecipitation to show a physical interaction between ER and PR, suggesting that they may cooperate in a transcriptional complex (Ballaré et al. 2003; Giulianelli et al. 2012; Mohammed et al. 2015; Daniel et al. 2015). Unliganded PR has been found at ER target genes and functions as a coregulator; however, on stimulation by R5020, PR redirects ER to new loci resulting in an altered transcription profile conferring reduced proliferation and tumorigenicity (Mohammed et al. 2015). Singhal et al. also demonstrated that treatment of T47D xenografts with P4 or 2 other progestins (R5020 and MPA), shifted gene expression to a novel, less oncogenic pattern (Singhal et al. 2018). However, in addition they showed that treatment with PR antagonists (EC3131 and CDB4124 (telepristone acetate)) resulted in this same transcriptome and furthermore, CDB4124 also blocked E2-mediated tumour growth. Other pre-clinical studies have also shown that single agent RU486 and Onapristone (another PR antagonist) inhibit tumour growth in mice and, in addition, combination therapy with Onapristone and Tamoxifen achieved 80% partial and 20% complete remission in rats with mammary tumours (Schneider et al. 1992; Michna et al. 1989; Esber et al. 2016; Nishino et al. 2009). This suggests that the actions of PR may be dependent on being ligand bound but not necessarily on the agonist/antagonist status of the binding ligand; this provides an explanation for the anti-proliferative effects seen with both PR agonists and antagonists (discussed further in section 1.8) and implies that both may have

therapeutic potential (Carroll et al. 2017; Horwitz and Sartorius 2020). As discussed in section 1.7.6, PR localizes to Pol III and progestogen treatment of ER+ PDX models inhibits Pol III activity and therefore represses transcription of tRNA genes and mRNA translation; PR may therefore modulate the actions of ER through reducing the availability of translational molecules required for protein synthesis and hence, cell growth (Finlay-Schultz et al. 2017). Another potential mechanism has been proposed whereby ER, PR-B, insulin-like growth factor 1 receptor (IGF1R) and the coactivator, proline, glutamate and leucine rich protein 1 (PELP-1) form a constitutive complex in the absence of exogenous progestogen, which results in increased cell growth, reduced sensitivity to Tamoxifen and PR-B dependent expression of ER-regulated genes (Daniel et al. 2015). IGF1R inhibition, *PGR* knock down and a PR antagonist (Onapristone) abrogated ER target gene (CTSD) transcription, which may suggest that PR modifies ER signalling in conjunction with other receptors and scaffolding proteins (Daniel et al. 2015). Although the exact mechanisms of action are not fully clear, the body of evidence supporting the modulation of ER by PR has expanded in recent years and further highlighted the potential for PR in the treatment of ER+/PR+ breast cancer.

1.8 PR ligands

Given the extensive role of P4 in the female reproductive system and in breast cancer, many synthetic PR ligands have been developed and studied. PR's cognate ligand is the only naturally occurring agonist, P4, a 21-carbon steroid (Stanczyk et al. 2013). P4 undergoes significant first pass metabolism by reductase and hydroxysteroid dehydrogenase enzymes in the liver and is transformed into the metabolites dihydroprogesterone (2 isomers), pregnanolone (4 isomers) and pregnanediol (8

isomers) (Stanczyk 2003). P4 can also be hydroxylated by CYP450 enzymes before being reduced. Over 100 P4 metabolites exist, which may be sulphated and glucuronidated before the majority are removed through urinary or faecal excretion. Other available forms of P4 include dydrogesterone, an isomer of P4, and a micronized version of P4 (oral micronized progesterone (OMP), which has improved the bioavailability of P4 and enabled oral administration (Carroll et al. 2017; Hargrove et al. 1989). Importantly, when dydrogesterone or OMP are included in combination MHT, which is commonly done in France, there appears to be no increase or even a decrease in breast cancer risk (Fournier et al. 2014; Cordina-Duverger et al. 2013; Gadducci et al. 2009; Mueck et al. 2009; Asi et al. 2016). In keeping with this, a crossover trial involving ovariectomized monkeys investigated the effects of micronized P4 vs MPA, in combination with E2; mammary epithelial proliferation and Ki67 expression were significantly higher in the E2 + MPA group but not in the monkeys receiving E2 + micronized P4 (Wood et al. 2007).

1.8.1 Progestins

Since oral P4 is poorly absorbed (even when micronized) and has a short half-life, synthetic PR agonists (progestins) have been developed, which have a greater binding affinity for PR, are better absorbed and are more stable than P4 (Brisken 2013). Many progestins are prodrugs, which are subsequently converted to active metabolites following oral ingestion (Stanczyk et al. 2013). These drugs are generally well-tolerated and have numerous indications, including inclusion in MHT, contraception, infertility, dysfunctional uterine bleeding and even renal cancers. The utility of these drugs is balanced against the increased breast cancer risk, as discussed previously in section 1.7.6, although paradoxically, progestins are also

efficacious in the treatment of advanced breast cancer at higher doses (>100 fold for MPA) than those used in MHT (Gadducci et al. 2009; L'Hermite et al. 2008; Carroll et al. 2017). However, several studies have shown that megestrol acetate (also known as megace – discussed more later in this section) is inferior to AIs in the treatment of metastatic ER+ breast cancer, and hence progestins are not used as first line treatment (Buzdar et al. 2001; Buzdar et al. 1998; Kaufmann et al. 2000).

The first progestin formulated, norethindrone, was created in the 1950s and the number of drugs in the class has rapidly expanded ever since (Djerassi 1966). Synthetic progestogens can be classified according to whether their structure mimics P4, so called 'true progestins', or testosterone, termed 'androgenic progestins' (Africander et al. 2011). Progestins structurally related to P4 can then be subdivided according to whether they possess a methyl group at carbon 10 (pregnanes) or not (19-norpregnanes) and then whether they are acetylated or not (Stanczyk et al. 2013). Similarly, progestins related to testosterone are categorised according to the presence of an ethinyl group at carbon 17 and whether these ethinylated progestins have an estrane or a 13-ethylgonane structure (Stanczyk et al. 2013). The classification of progestins and examples of the drugs in each category is summarised in Figure 1.11.

Two of the most potent and commonly used progestins in breast cancer are MPA and megestrol acetate which are structurally identical aside from the presence of a double bond linking carbons 6 and 7 in megace (Stanczyk et al. 2013). MPA has a wide range of other indications including menstrual disorders (e.g. menorrhagia, secondary amenorrhea and endometriosis), contraception, endometrial cancer and is the most commonly used progestin in combination MHT in many countries (Horwitz and

Sartorius 2020; Carroll et al. 2017). Historically, MPA and megace have both been used to treat ER+ metastatic breast cancer with several studies showing increased PFS and equivalent efficacy of megace to Tamoxifen in the first-line setting (Alexieva-Figusch et al. 1980; Izuo et al. 1981; Becher et al. 1989; Mattsson 1983; Espie 1994; Morgan 1985; Ingle et al. 1991; Muss et al. 1988). Megace has even been shown to have efficacy in disease resistant to non-steroidal AIs, with a clinical benefit rate of 40% and a median PFS benefit of 3.9 months (Bines et al. 2014). However, the evidence from some of the randomized clinical trials in metastatic breast cancer patients were less clear, with good response rates seen with MPA treatment but no PFS or overall survival benefits (Muss et al. 1994). R5020 is a potent, stable and relatively PR-specific progestin, which revolutionised the study of PR signalling as, unlike radiolabelled P4, [^{3}H] R5020 could be used to detect PR in human tissue samples (Horwitz and McGuire 1975; Philibert and Raynaud 1974). It is not used clinically in the UK but is used extensively in cell and animal model studies of PR signalling, replacing P4 as the reference ligand in binding affinity assays (Stanczyk et al. 2013).

The activity of progestins can be measured by a number of parameters such as bioavailability, half-life, potency (the concentration required to elicit 50% of the maximal response), efficacy (the maximal effect induced by a ligand) and RBA (the concentration of ligand that competes for 50% of the total receptor binding, often calculated as a percentage of the IC_{50} of the test ligand relative to that of a radiolabelled reference agonist) (Africander et al. 2011; Stanczyk et al. 2013). The data for these measures is summarised for some key progestins in Table 1.2. Although assessment of RBA can differ according to different assay methods and test tissue, it

is a particularly valuable parameter for progestins, since many of them bind to other structurally homologous NRs including AR, GR and MR, which results in potential cross-reactivity and off-target effects (Moore et al. 2012; Sitruk-Ware 2004). The relative binding affinities for AR, GR and MR vary widely between progestins. MPA, levonorgestrol and norethindrone bind strongly to AR and act as agonists/partial AR agonists. Drospirenone and progesterone bind weakly to AR and antagonise DHT-induced activation of AR, while nestorone has no androgenic activity (Teulings et al. 1980; Bentel et al. 1999; Schoonen et al. 2000; Bergink et al. 1983; Kemppainen et al. 1999). Low doses of progestins that exert androgenic effects have been implicated in the breast cancer risk associated with MHT, through altered AR genomic signalling which may abrogate the protective effects of physiological AR signalling in the breast (Birrell et al. 2007). Progestin-induced AR signalling has also been reported to contribute to the cardiovascular effects of these ligands (Stanczyk et al. 2013). In terms of GR activation, MPA acts as a potent agonist or partial agonist through the recruitment of GR to a glucocorticoid response element (GRE)-containing promoter, gestodene has weaker partial agonism, and most other progestins have little or no activity on the receptor (Africander et al. 2011). The immunosuppression, decreased bone density, cardiovascular events, neurological effects and some of the increases in breast cancer risk associated with MPA have been attributed to GR-induced changes in gene expression (Courtin et al. 2012; Stanczyk et al. 2013). With respect to MR, trimegestone exerts weak, partial agonistic activity, drospirenone and P4 exhibit strong antagonism, mimicking aldosterone antagonists, and MPA and norethindrone acetate have no mineralocorticoid activity (Africander et al. 2011; Fuhrmann et al. 1996; Quinkler and Diederich 2002; Wambach et al. 1979). Unlike other progestins, drospirenone has antihypertensive effects; P4 only reduces blood

pressure in hypertensive women but this may be related to its short half-life and its rapid conversion to intermediates that lack MR activity (Oelkers 2005; Quinkler et al. 2002; Rylance et al. 1985). Hence, the differences in relative binding affinities for PR, AR, GR and MR may account for the differential actions and side effect profiles of different progestins.

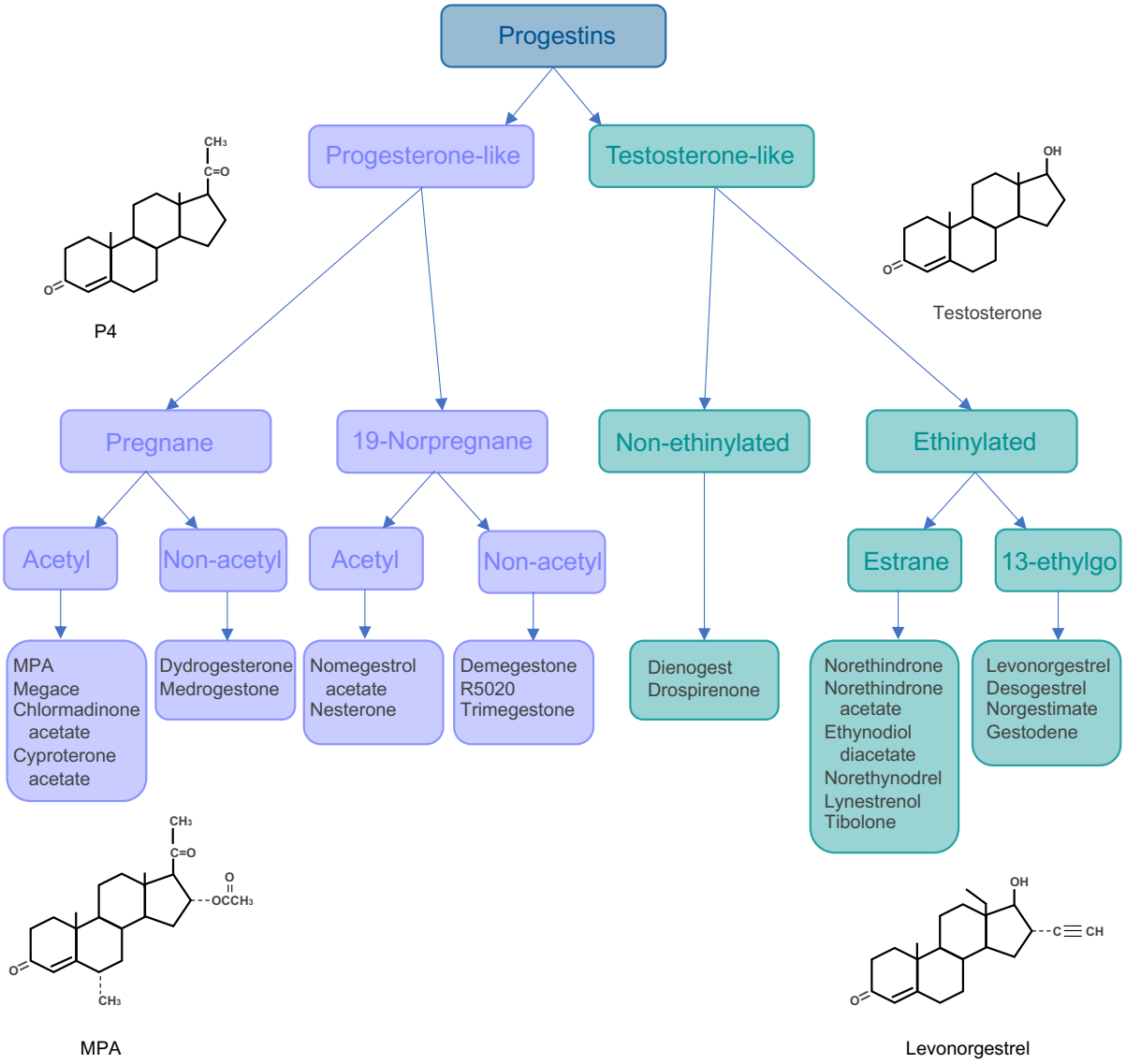


Figure 1.11 Classification of Progestins

Progestins are categorized according to whether their structure mimics Progesterone or Testosterone. Progesterone-like ligands are then subdivided by the presence/absence of a methyl group (Pregnanes and 19-Norpregnanes respectively), and by acetylation status. Testosterone-like ligands are classified according to the presence/absence of a 17-carbon ethinyl group and then whether ethinylated ligands have an estrange or 13-ethylgonane (13-ethlgo) structure. Example ligands are listed for each group.

Table 1.2 Bioavailability, Half-life and Relative Binding Affinity (RBA) of key Progestogens

Progestogen	Bioavailability (%)	Half-life (hours)	RBA			
			PR	AR	GR	MR
P4	<5	16.2-18.3	50	0 (wk +)	10	100 (-)
R5020	/	/	100	/	5 (+)	53
Cyproterone acetate	/	54-78.6	90	6 (+)	6 (+)	8
Chlormadinone acetate	~100	80.1	67	5 (+)	8 (+)	0
Dienogest	96.2	10.8/11.6	5	10 (-)	1	0
Drospirenone	66	31.1-32.5	35	65 (-)	6	230 (-)
Gestodene	87/99	12-14	90	85	27	290
Levonorgestrel	89/99	9.9/13.2	150	45 (+)	1	75
MPA	>90	24	115	5	29 (+)	160
Nomegestrol acetate	60	50	125	42 (-)	6	0
Norethindrone	64	8	75	15 (+)	0	0
Trimegestone	~100	15	330	1	9	120

Adapted from the review by Stancyzk et al. 2013. RBAs were determined by competitive binding assays using the following reference ligands: R5020 for PR, metribolone or R1881 for AR, dexamethasone for GR and aldosterone for MR. All the ligands in this table exhibit PR agonism. (/) denotes data not available, (+) denotes agonistic effect, (-) denotes antagonistic effect.

1.8.2 PR antagonists

After the effects of inhibiting both ER and PR were investigated in the 1960s, RU486 was the first anti-progestin developed (Kovacs et al. 1984; Lanari et al. 2012). The use of PR antagonists was initially limited due to side effects including hepatotoxicity. Tamoxifen was discovered a decade later and the development of anti-progestins for breast cancer treatment was paused (Brisken 2013). RU486 and ulipristal acetate are the only anti-progestins used in clinical practice; the former for the termination of early pregnancies and Cushing's disease and the latter for uterine leiomyomata (Li et al. 2017; Sartor and Cutler 1996; Whitaker et al. 2014). There are 3 classes of anti-progestins. Type I include complete antagonists, such as Onapristone (also known as

ZK98299), which disrupt the PR transcriptional complex and inhibit expression of PR target genes through prevention of PR dimerization (and therefore PR-PRE binding), reduce ligand-induced PR phosphorylation and impair PR-coactivator interactions (Klein-Hitpass et al. 1991; Beck et al. 1996; Afhüppe et al. 2009). Onapristone possesses 10-30 times greater anti-progestogenic activity than type II anti-progestins (Nishino et al. 2009; Cottu et al. 2018). Type II anti-progestins, or selective PR modulators (SPRMs), can exhibit both agonistic and antagonistic actions and include RU486 and telepristone acetate (Wagenfeld et al. 2016; Lee et al. 2020). For example, RU486 functions as a partial agonist in the absence of P4, by inducing phosphorylation of ser294 PR-B by MAPK and CDK2 (Knutson et al. 2012). In contrast, when P4 is present, RU486 functions as an antagonist by promoting PR-PRE binding but then facilitating recruitment of corepressors, stabilisation of the PR transcriptional complex and inhibition of PR-mediated gene expression (Lanari et al. 2012). Although less potent than Onapristone, RU486 binds to PR with twice the RBA of P4 (Kamaraju et al. 2021). Finally, type III anti-progestins, including Lonaprisan (also known as ZK230211), are ‘pure’ antagonists which promote PR-DNA binding and recruitment of corepressors (Afhüppe et al. 2010).

Like progestins, PR antagonists have varying activity on other NRs, primarily GR and AR. RU486 is the most promiscuous ligand, with strong anti-glucocorticoid activity and weak AR antagonism (Whitaker et al. 2014). The newer progestins are more selective for PR; Onapristone has low levels of anti-GR and minimal anti-AR activity and Lonaprisan exerts only weak anti-glucocorticoid effects (Afhüppe et al. 2010; Kamaraju et al. 2021). As mentioned in section 1.7.7, anti-progestins have been shown to inhibit growth of *in vitro* and *in vivo* models of ER+ tumours. Following on

from this, clinical trials have been undertaken but these are sparse and generally limited by small sample sizes. Onapristone was investigated as first line treatment for metastatic disease in 18 patients (89% of tumours expressed ER and 67% PR); 56% showed a partial response and 11% stable disease, but the hepatotoxicity rate of >30% was concerning (Robertson et al. 1999). Extended release Onapristone resulted in less dose-limiting hepatotoxicity with deranged liver function found only with liver metastases; 3/20 patients with PR+ breast cancer had clinical benefit with this formulation (Cottu et al. 2018). RU486 has been investigated in 3 trials as first-, second- or third-line treatment for metastatic breast cancer. In the first-line setting, an objective response rate of 11% and stable disease in 39% of patients (n=28) was observed in a phase II study (Perrault et al. 1996). In the trials studying its efficacy in second-line (n=11, 4 with unknown ER/PR status, 3 with ER+/PR+ tumours and 4 with ER+/PR- tumours) and third-line treatments (n=22 ER+/PR+ patients), no complete responses were seen, partial response rates of 9% and 14% respectively were reported, and stable disease observed in 55% and 41% of cases respectively (Klijn et al. 1989; Romieu et al. 1987). Lonaprisan was studied in the second line setting for metastatic, PR-/HER-2-negative breast cancer but in the cohort of 68 patients, there were no complete or partial responses (Jonat et al. 2013). Therefore, although there is a body of evidence suggesting that anti-progestins have potency in breast cancer, the volume of data is limited and issues remain with respect to heterogeneity of the study population and toxicity of drugs.

1.9 Study Aims

As discussed in section 1.5.1, *ESR1* mutations have been implicated as a mechanism of endocrine resistance in approximately 20-30% of ER+ breast cancers. Multiple breast cancer cell lines have been generated to model these mutations using CRISPR-Cas9 gene-editing (Harrod et al. 2017; Bahreini et al. 2017; Martin et al. 2017), including novel MCF7 and T47D cell lines specifically carrying the Y537S mutation, which were previously created within my host laboratory (Harrod et al. 2017). *PGR* is upregulated in MCF7-Y537S cells relative to WT-ER cells and is expressed in an E2-independent manner (Harrod et al. 2017).

To extend the studies to an independent breast cancer cell line, I also evaluated *PGR* expression in T47D cells in which we had used the same CRISPR-Cas9 approach for generating the Y537S mutation. T47D cells are a particularly useful model for studying PR signalling in luminal A breast cancer due to their E2-independent, expression of high levels of *PGR* (which exceed those of MCF7 cells) (Nordeen et al. 1993; Horwitz et al. 1982; Read et al. 1988). Hence, they have become the key cell line for studying the effects of PR ligands in breast cancer and, to my knowledge, the only cell line in which PR isoform-specific or -inducible models have been created (as discussed in chapter 1, section 7.2) (Sartorius et al. 1994; Jacobsen et al. 2002). Studies in T47D cells and xenografts have shown that both agonist and antagonist-stimulated PR is a potent transcriptional activator (Sartorius et al. 1993; Beck et al. 1993; Mohammed et al. 2015; Singhal et al. 2018). T47D models have also been used to demonstrate the growth effects of progestogens and anti-progestins and decipher the role of PR in expansion of the CSC population in breast cancer (as discussed in chapter 1, section 7.6) (Singhal et al. 2018; Finlay-Schultz et al. 2015).

A growing body of evidence suggests that activated PR reprogrammes the binding events and transcriptomic landscape of ER into a less oncogenic profile. Hence, the hypothesis to be tested was whether PR ligands have utility in the treatment of *ESR1* mutant, metastatic breast cancer.

The aims of this study are to:

- Confirm the upregulation of *PGR* in MCF7-Y537S cells,
- Investigate whether *PGR* is upregulated in other *ESR1* mutant cells, including T47D-Y537S cells,
- Investigate whether modulation of PR provides treatment strategies for endocrine-resistant metastatic breast cancer with *ESR1* mutations,
- Determine the mechanisms of action of PR in endocrine resistant breast cancer through transcriptomic studies in cell line models of both WT and mutant ER.

2. Materials and Methods

2.1 Materials

2.1.1 Reagents and Materials

Chemicals and reagents were purchased from Sigma Aldrich (Gillingham, UK), Fisher Scientific (Loughborough, UK) and VWR Ltd (Lutterworth, UK) unless otherwise specified. DNA and protein markers, cDNA synthesis reagents, PCR reagents and other molecular biology reagents were obtained from Thermo Scientific (Life Technologies, Paisley, UK) and New England Biolabs (Hitchin, UK). RNA preparation kits were purchased from QIAGEN Ltd (Crawley, UK) and DNA preparation kits from Invitrogen (Life Technologies, Paisley, UK). Taqman and SYBR Green real-time PCR reagents were purchased from Applied Biosystems (Life Technologies, Paisley, UK). Protease inhibitor tablets were supplied by Roche Diagnostics Ltd (Sussex, UK) and Femto and SuperSignal West Pico substrates were obtained from Thermo Scientific. Promega (Southampton, UK) supplied the FuGENE HD transfection reagent and Dual-Glo Luciferase Assay System. Lipofectamine RNAiMAX transfection reagent was purchased from Invitrogen (Paisley, UK). Small interfering RNAs (siRNA) were purchased from Dharmacon™ (Horizon Discovery Biosciences Ltd, Cambridge, UK).

2.1.2 Sundries

Corning Incorporated tissue culture and microbiology grade plastics and stripette pipettes were purchased from Appleton Woods (Birmingham, UK). Fast 96-well and 384-well reaction plates were obtained from Applied Biosystems (Life Technologies). Microcentrifuge tubes (1.5ml and 2ml) and pipette tips were supplied by STARLAB Ltd (Milton Keynes, UK). Thermo-PCR tubes (0.2ml) were purchased from Thermo Fisher

Scientific (Life Technologies). Nitrocellulose membrane (0.45µm, 30cm x 3.5m) was supplied by Bio-Rad Laboratories Ltd (Hemel Hempstead, UK).

2.1.3 Cell culture equipment and reagents

RS Biotech Galaxy R+ incubators (New Brunswick, Eppendorf, Cambridge, UK) were used to maintain cells at 37°C with 5% CO_2. All tissue culture experiments were carried out in BIOMAT 2 Microbiological Safety Cabinets (Contained Air Solutions Ltd, Manchester, UK). Dulbecco's Modified Eagle Medium (DMEM) was purchased from Sigma-Aldrich. Phenol red-free DMEM and Opti-MEM reduced serum medium were obtained from Gibco (Life Technologies). Fetal Calf Serum (FCS) and dextran-coated, charcoal-treated FCS (DSS) were supplied by First Link Ltd (Birmingham, UK). L-Glutamine-Penicillin-Streptomycin solutions (200mM L-glutamine, 10,000 units/ml penicillin and 10mg/ml streptomycin in 0.9% saline) (PSG), 0.02% ethylenediaminetetraacetic acid (EDTA) solution and 10X trypsin solution were obtained from Sigma-Aldrich.

2.1.4 Chemicals

Table 2.1 Estrogen and Progesterone Agonists and Antagonists

Chemical	Supplier
17ß-Estradiol (E2) E2758	Sigma Aldrich
4-Hydroxytamoxifen (OHT) H7904	Sigma Aldrich
Fulvestrant (ICI) I4409	Sigma Aldrich
Progesterone (P4) P8783	Sigma Aldrich
Promegestone (R5020) NLP00400	Perkin Elmer
Medroxyprogesterone acetate (MPA) M1629	Sigma Aldrich
Mifepristone (RU486) M8046	Sigma Aldrich
Onapristone	Kind gift of Context Therapeutics

The estrogen and progesterone agonists and antagonists were dissolved in either ethanol or dimethyl sulfoxide (DMSO) to a final concentration of 10mM and then these stock solutions stored at -20°C.

2.1.5 General Equipment

A Sorvall RC6 Plus centrifuge with Fiberlite™ F21-8 x 50y and Fiberlite™ F14-6 x 250y fixed angle rotors (Thermo Scientific) was used for centrifuging large volumes (>2ml). Small volume (<2ml) centrifugation was carried out in Sorvall Pico™ (Sorvall, Leicester, UK) or Heraeus™ Biofuge Pico™ bench top microcentrifuges. Incubations were performed in a water bath (Grant SUB Aqua Pro, Grant Instruments Ltd, Shepreth, UK) or a block heater (Grant-bio, Wolf Laboratories, York, UK). An Applied Biosystems Veriti™ 96-well thermal cycler (Life Technologies) was used to perform PCR and either an Applied Biosystems 7900HT Fast Real-Time PCR System (Life Technologies) or a QuantStudio™ 7 Flex Real-Time PCR System (Applied Biosystems™) were used for real-time quantitative PCR (RT-qPCR).

Horizontal agarose gel electrophoresis tanks were obtained from Thistle Scientific (Glasgow, UK) and Western blotting electrophoresis tanks and transfer apparatus from Hoeffer (GE Healthcare Life Science, Buckinghamshire, UK) and Bio-Rad. Bio-Rad also supplied power packs.

Spectrophotometric measurements for RNA quantification were performed using a Nanodrop™ ND-1000 (Labtech International, UK). Absorbance readings were performed using a Tecan Sunrise™ absorbance microplate reader (Tecan UK Ltd, Reading, UK). A Vortex-Genie 2 (Scientific Industries, London, UK) was used to mix

samples and an Agilent 2100 Bioanalyser (Agilent Technologies UK) for determining RNA and DNA quality. Luminescence measurements were carried out using a VICTOR Light Luminescence Counter (Perkin Elmer, Cambridgeshire, UK) and chemiluminescence imaging using the Fusion Solo system (Vilder Lourmat, Collégien, France).

Next generation RNA sequencing was performed by BGI Tech Solutions (Hong Kong), using the Illumina NovaSeq system.

2.2 Methods

2.2.1 Cell Culture

MCF7-Luc cells, which stably express the firefly luciferase gene, were obtained from Cambridge Bioscience, UK. T47D-GFP cells were purchased from Cell Biolabs, Inc., USA and stably express the GFP gene. MCF7-Luc and T47D-GFP cells are referred to as MCF7 and T47D respectively hereafter. These cell lines had previously been used for the introduction of the Y537S mutation into the endogenous *ESR1* gene, using the gene-editing system CRISP-Cas9, generating the MCF7-Y537S (Harrod et al. 2017) and T47D-Y537S lines (performed by Ms Paula Jiminez Gomez and Professor Laki Buluwela). Professor S. Oesterreich (University of Pittsburgh) kindly gifted us additional T47D cells, which had also been engineered using CRISPR-Cas9 to carry *ESR1* mutations. Five of these cell lines were used in this study including the parental line (T47D-WT.SO), 2 Y537S mutant clones (T47D-Y537S#1 and T47D-Y537S#2) and 2 D538G clones (T47D-D538G#49 and T47D-D538G#60). Details about the generation of these cell lines and studies performed using them have been published (Bahreini et al. 2017; Li et al. 2018). Cells were routinely tested every 3-6

months to exclude mycoplasma infection and genotyped annually for authenticity. Details of the cell lines used and their source are listed in Table 2.2.

Cell lines were kept in a humidified incubator maintained at 37ºC with 5% CO_2, maintained in a logarithmic phase of growth in 75cm^2 or 150cm^2 cell culture flasks (unless otherwise specified) and passaged when confluency was around 70-80%. This was performed by aspirating the cell culture medium, washing the cells twice with warm (37ºC) 0.02% EDTA solution (Sigma), then detaching the cells using 1-5ml of 1X Trypsin solution (in 0.02% EDTA) for 3-5 minutes at 37ºC. 5-10ml of warm (37ºC) culture medium was added to the cells to neutralise the trypsin, the cell suspension was transferred to a 15ml falcon tube and then centrifuged at 1200rpm for 3 minutes. The cells were then gently resuspended in fresh media and transferred to new flasks. Cells were routinely passaged at a dilution ratio of 1:5 or 1:10. The culture medium for both MCF7 and T47D cells was DMEM, supplemented with 10% FCS and PSG.

For long term storage, cells were frozen and maintained in liquid nitrogen. This was performed by trypsinising the cells as described above, centrifuging the cell suspension in a 15ml falcon tube for 5 minutes at 1200rpm and then resuspending in freezing medium (90% FCS and 10% DMSO). 1ml aliquots were transferred into 1.5ml cryovials and kept in a Mr Frosty^{TM} cell freezing tub (Nalgene Thermo Fisher Scientific) at -80ºC for a minimum of 24 hours before being transported on dry ice to the liquid nitrogen cell store. Frozen cells were thawed by warming for 5 minutes at 37ºC before being pipetted into a 75cm^2 culture flask with 20ml media.

For experiments where E2 was to be added, cells were washed and trypsinised as per routine passaging but the trypsin inactivated using phenol red-free DMEM supplemented with double charcoal stripped FCS (DSS). Cell suspensions were then centrifuged twice and resuspended in this estrogen-free media before being transferred to T75 or T150 cell flasks. Cells were then maintained as usual (at 37ºC) for 72 hours prior to further treatment and experimentation.

When cells were treated with drugs, the medium was supplemented with stock solutions at a dilution of 1 in 1000. Vehicle controls contained an equal volume of ethanol or DMSO according to the diluent of the relevant drug. In order to ensure that only the effect of the relevant test progestogen or anti-progestin was being studied, the sex steroid hormone content of both phenol-red containing and double charcoal-stripped (E2-depleted) culture media was tested in the Pathology department of Imperial College Healthcare NHS Trust by Liquid Chromatography-Mass Spectrometry (Table 2.3). This confirmed that although E2 levels were much higher in full media as expected (107pmol/L v <37pmol/L), P4 levels were low and at the same level in full medium as in E2-depleted medium (<0.3nmol/L).

In order to seed cells in culture plates, cell counting was performed using the Countess™ II FL Automated Cell Counter (Thermo Fisher Scientific) and a disposable cell counting slide. Immediately after trypsinisation, an equal volume of 0.4% trypan blue solution (Thermo Fisher Scientific) was mixed with the cell suspension. 10µl of this cell/trypan blue suspension was loaded on a Countess™ counting slide and inserted into the Countess™ II FL Automated Cell Counter. The Countess™ II FL

Automated Cell Counter automatically calculates the cell concentration/ml, live and dead cell counts and an image of the cells.

Table 2.2 Cell Lines and their Source

Cell line	Source
MCF7-Luc	Cambridge Bioscience
MCF7-Y537S	Harrod et al. 2017
T47D-GFP	Cell Biolabs, Inc.
T47D-Y537S	Jiminez Gomez et al. unpublished
T47D-WT.SO	Prof S. Oesterreich
T47D-Y537S#1	Prof S. Oesterreich
T47D-Y437S#2	Prof S. Oesterreich
T47D-D538G#49	Prof S. Oesterreich
T47D-D538G#60	Prof S. Oesterreich

Table 2.3 Steroid hormone content of full and estrogen-depleted media

Hormone (units)	Full media	E2-depleted media
Aldosterone (pmol/L)	<60	<60
Androstenedione (nmol/L)	<0.4	<0.4
Cortisol (nmol/L)	<28	<28
DHEAS (nmol/L)	<0.41	<0.41
DHT (nmol/L)	0.54	<0.15
E2 (pmol/L)	107	<37
17OH-Prog (nmol/L)	<2.0	<2.0
P4 (nmol/L)	<0.3	<0.3
Testosterone (nmol/L)	<0.45	<0.45

Abbreviations; DHEAS: dehydroepiandrosterone sulphate, DHT: 5α-dihydrotestosterone, 17OH-Prog: 17α-hydroxyprogesterone.

2.2.2 Total RNA extraction and complementary DNA synthesis

Medium was aspirated from plated cells using a pipette. Cells were then scraped into 350µl/well (for 6 well plates) RLT buffer (QIAGEN) supplemented with 1% (v/v) ß-mercaptoethanol. Homogenisation was performed by centrifugation through a QIAShredder spin column (QIAGEN) at 13,000rpm for 2 minutes. The RNeasy Mini

Preparation kit (QIAGEN) was used for RNA extraction as per the kit protocol. RNA was eluted in 30µl of RNase-free water. The NanoDrop™ ND-1000 spectrophotometer was used to assess RNA concentration and quality by measuring absorbance at 260 and 280nm.

Complementary DNA (cDNA) prepared by reverse transcription was performed using reagents from Thermo Scientific and reactions carried out in thin-walled PCR tubes. Reactions were prepared using:

- 4µl 5x Reaction buffer,
- 2µl dNTP mix (10mM),
- 1µl Random hexamer primer (0.2µg/µl),
- 2µg RNA,
- made up to 12µl with RNase free water
- 1µl RevertAid Reverse Transcriptase

An Applied Biosystem Veriti™ 96 well thermal cycler (Life Technologies) was used to perform the reaction at 42ºC for 1 hour then 95ºC for 5 minutes to inactivate the reverse transcriptase and denature template DNA-RNA hybrids. The cDNA was then diluted 1:10 for quantitative RT-PCR (RT-qPCR) in individual wells of 96 well plates or 1:20 for 384 well plates, with DNase-free sterile water. Two microlitres of diluted cDNA was used per PCR reaction.

2.2.3 Polymerase Chain Reaction (PCR) and Reverse Transcriptase-Quantitative Polymerase Chain Reaction (RTqPCR)

REDTaq® Readymix™ PCR Reaction Mix (Sigma Aldrich) was used to perform PCR reactions; a master mix of 400µl of REDTaq® Readymix™ PCR Reaction Mix, 8µl of the forward primer and 8µl of reverse primer was prepared. Each reaction mix contained 10µl of this master mix, 4µl cDNA and 6µl DNase/RNase free water. The following thermocycling protocol was used:

- 95ºC for 5 minutes,
- 32 cycles of 95ºC for 1 minute, 55ºC for 1 minute, 72ºC for 2 minutes,
- 72ºC for 5 minutes.

CleanSweep™ PCR purification reagent (Applied Biosystems) was used to remove excess primer and unincorporated nucleotides. 4µl of CleanSweep™ was added to 10µl of PCR product and thermal cycling performed as per the manufacturer's recommendations.

RT-qPCR was carried out on either a 7900HT fast real-time PCR machine or a QuantStudio™ 7 Flex Real-Time PCR System. Taqman® gene expression assays (Applied Biosystems, UK) or SYBR™ Green assays (Invitrogen) were used; Taqman® assay numbers and SYBR™ Green primer sequences are listed in tables 2.5 and 2.6, respectively. MicroAmp® fast optical 96-well and 384-well reaction plates (Applied Biosystems) were used, sealed with MicroAmp® Optical Adhesive Film (Applied Biosystems). Each Taqman® gene expression assay reaction mixture comprised:

- 10µl Taqman® fast universal PCR master mix,
- 1µl Taqman® assay probe,
- 2µl diluted cDNA (1:10 for 96-well plate, 1:20 for 384-well plate)

- 7µl DNase/RNase free water.

Each SYBR green assay mixture contained:

- 10µl PowerUp™ SYBR™ Green Master Mix,
- 1µl forward primer (10µM),
- 1µl reverse primer (10µM),
- 2µl diluted cDNA (1:10 for 96-well plate, 1:20 for 384-well plate)
- 6µl DNase/RNase free water.

The thermal cycling protocol used was:

- Stage 1 - 95ºC for 20 seconds,
- Stage 2 (40 cycles) - 95ºC for 3 seconds, 60ºC for 30 seconds.

The housekeeping genes TBP and GAPDH were used to normalise the expression of genes of interest and made relative to the appropriate control as required using the $2^{-\Delta\Delta CT}$ method.

Table 2.4 Primers for PCR

Primer	Sequence
ESR1 Exon 5 (Forward)	5′-CCAGGGAAGCTACTGTTTGC-3′
Mutation specific (Reverse)	5′-TAGTGGGCGCGTGAAGTCTA-3′
ESR1 Exon 8 (Reverse)	5′-GATGCATGCCGGAGTGTATG-3′

Table 2.5 Taqman® Gene Expression Assays

Gene	Reference
GAPDH	Hs99999905
ESR1	Hs00174860
TFF1	Hs00170216
PGR	Hs00172183
AR	Hs00171172
NR3C1	Hs00353740
NR5A2	Hs00187067
NR3C2	Hs01031809
RORC	Hs01076122

Table 2.6 SYBR™ Green Primer Sequences

Primer	Lab Primer Cat. No.	Sequence
TBP	SA4701TBPpd-f	5′-GTTTGCCAAGAAGAAAGTGAAC-3′
	SA4702TBPpd-r	5′-GGGTCAGTCCAGTGCCAT-3′
ESR1	SA4703ESR1pd-f	5′-AAGAAAGAACAACATCAGCAGTAAA-3′
	SA4704ESR1pd-r	5′-TCTTTGGATGACCTAGCCTCTC-3′
PGR	SA4707PGRpd-f	5′-GAGTCACCTTGCCCCTTCA-3′
	SA4708PGRpd-r	5′-GCCTTTTATGCTTGCCTGTAAA-3′
TFF1	SA4709TFF1pd-f	5′-CCCCCGTGAAAGACACAATT-3′
	SA4710TFF1pd-r	5′-ACGTCGATGGTATTAGGATAGAAG-3′
GREB1	SA4705GREB1pd-f	5′-ATAAGAGAATCCACAATAGAGACCTT-3′
	SA4706GREB1pd-r	5′-CTCTCATCAGTTTCAGTGCCATTT-3′
PDZK1	SA5084PDZK1318037206c2f	5′-GAACTGCCCAATGGCTCTGT-3′
	SA5085PDZK1318037206c2r	5′-CCCCGAATCGCATTTAAGTGAA-3′
EGR3	SA5086EGR331317227c1f	5′-GACATCGGTCTGACCAACGAG-3′
	SA5087EGR331317227c1r	5′-GGCGAACTTTCCCAAGTAGGT-3′
BCL6	SA4699BCL6pd-f	5′-GGACTGTGAAGCAAGGCATT -3′
	SA4700BCL6-pd-r	5′-GGAGACGATTAAGGTTGAGAAGA-3′
FAM105A	SA4677FAM105Af	5′-GTGACCAAGTTCACTCCTGGA-3′
	SA4678FAM105Ar	5′-CCAACATCACAAAGCCTTTTGC-3′
HES2	SA4681HES2f	5′-CCAACTGCTCGAAGCTAGAGA-3′
	SA4682HES2r	5′-AGCGCACGGTCATTTCCAG-3′
MAFB	SA4637MAFBf2	5′-GACGCAGCTCATTCAGCAG-3′
	SA4638MAFBr2	5′-CTCGCACTTGACCTTGTAGGC-3′
NEDD9	SA4683NEDD9f1	5′-ATGGCAAGGGCCTTATATGACA-3′
	SA4684NEDD9r1	5′-TTCTGCTCTATGACGGTCAGG-3′
SGK1	SA4695SGKf2	5′-GCAGAAGAAGTGTTCTATGCAGT-3′
	SA4696SGKr2	5′-CCGCTCCGACATAATATGCTT-3′
FKBP5	SA5044FKBP5f	5′-CTCCCTAAAATTCCCTCGAATGC-3′
	SA5045FKBP5r	5′-CCCTCTCCTTTCCGTTTGGTT-3′
S100P	SA5046S100Pf	5′-AAGGATGCCGTGGATAAATTGC-3′
	SA5047S100Pr	5′-ACACGATGAACTCACTGAAGTC-3′
STAT5A	SA5054STAT5af	5′-GCAGAGTCCGTGACAGAGG-3′
	SA5055STAT5ar	5′-CCACAGGTAGGGACAGAGTCT-3′

2.2.4 Agarose Gel Electropheresis and DNA sequencing

PCR products were visualised with agarose gel electrophoresis. Agarose (Fisher Scientific, Life Technologies) gels were made at 1.2-1.5%, prepared in 1x Tris-Borate-EDTA (TBE) buffer (Sigma Aldrich). Prior to the gel setting, 10µl of GelRed™ Nucleic

Acid Stain (Biotium, California, USA) was added. Once set, the gel was run in TBE buffer for 1 hour at 100V in a horizontal gel electrophoresis apparatus, 24cm x 24cm gel HU13 (Thistle Scientific). PCR product sizes were estimated using the MassRuler^{TM} Low Range DNA Ladder (Thermo Fisher Scientific). Visualisation of the DNA was carried out using the UVIpro Platinum Gel Doc System ultraviolet transilluminator (UVItec, Cambridge, UK).

The GENEWIZ Sanger DNA sequencing service (GENEWIZ from Azenta Life Sciences, Takeley, UK) was used to sequence PCR products. Templates and sequencing primers were supplied by the user. Sequencing was performed using ABI 3730xl DNA Analyzers. SnapGene Viewer (GSL Biotech LLC, Chicago, USA) was used to analyse the sequencing chromatograms returned by the GENEWIZ Sanger DNA sequencing service.

2.2.5 Nuclear localised Green Fluorescent Protein Gene Transduction

To enable automated cell counting on the IncuCyte ZOOM (Essen Bioscience, Welwyn Garden City, UK), cells were transduced with a nuclear green fluorescent protein (GFP) lentiviral construct (pTRIP-SFFV-EGFP-NLS, addgene#86677). At 18-24 hours prior to transfection, HEK293T cells were seeded at a density of $1.5x10^6$ cells/15mL in full media on a 10cm dish.

These cells were then co-transfected with:

- 0.6pmol of pTRIP-SFFV-EGFP-NLS
- 0.47pmol of the lentiviral packaging plasmid (psPAX2) (addgene #12260)
- 0.26pmol of the envelope plasmid (pDM2.G) (addgene#12259) using FuGENE HD transfection reagent (Promega).

Culture media was replaced 24 hours after transfection. Lentiviral media was collected from the transfected HEK293T cells using a 10mL syringe following 48 hours incubation at 32°C. The media was then filtered to remove cell debris using a 0.45μM filter (Millipore) and polybrene (Millipore) was added at a final concentration of 8μg/mL. T47D cells were transduced with lentivirus for 24 hours, before the lentiviral media was replaced with fresh full media. Dr Chun Fui Lai performed transduction with the nuclear GFP lentiviral construct in T47D-WT.SO, T47D-Y537S#1, T47D-Y537S#2, T47D-D538G#49 and T47D-D538G#60 cells, as described above.

2.2.6 Cell Growth Assays

Sulforhodamine B (SRB) growth assays were performed as follows. Cells were seeded (2000 cells/well for experiments in full media, 3000 cells/well for charcoal-stripped media and 5000 cells/well for siRNA transfections) in 96 well plates with 6 technical replicates. Culture medium was replaced with fresh medium and the appropriate ligands every 3 days and cells fixed on days 0, 3, 6, 9, 12 and 15, as required for the duration of the experiment, using 100μl 40% w/v trichloroacetic acid (TCA) in distilled and deionised water (ddH_2O) at 4ºC for a minimum of 1 hour. Cell plates were then washed five times with ddH_2O, before being stained with 0.4% w/v SRB (Sigma) in 1% v/v acetic acid in ddH_2O at room temperature for 1 hour. Five washes with 1% acetic acid were performed to remove the excess dye and then the plates were left to dry at room temperature for at least 24 hours. The dye was resuspended by adding 100μl of 10mM Tris-base to each well and performing a 10-minute incubation with shaking. The Tecan Sunrise™ absorbance microplate reader was used to calculate absorbance measurements at 492nm. Each experiment was performed at least three independent times. The average growth was plotted with the standard error of the mean (SEM) used for error bars.

50% Growth Inhibition (GI_{50}) values for compounds were determined by preparing the test compounds in culture medium in four-fold serial dilutions. 4000 cells/well were seeded in 100µl medium in 96 well plates for 48 hours, at which point the medium was replaced with fresh medium containing the drug of interest. After 5 days from the addition of the compounds, cell growth was measured using the SRB assay. The equation below was used to calculate the percentage cell growth and the curve-fitting method (Graphpad Prism software v9) to calculate GI_{50} values.

% Cell Growth = (Mean OD_{sample} – Mean OD_{day0})/(Mean $OD_{DMSO\ control}$ – Mean $OD_{day\ 0}$) X 100%

Growth assays were also performed using the IncuCyte ZOOM (Essen Bioscience, Welwyn Garden City, UK). 3000 cells/well were seeded in 96 well plates in phenol red-free DMEM, supplemented with 5% DSS for 3 days before being treated with E2 in 3-fold serial dilutions (highest concentration 100nM, lowest concentration 0.015nM) or an equivalent volume of ethanol (vehicle). Culture media were replaced with fresh medium containing every 3 days. The IncuCyte ZOOM software package (Essen Bioscience) was used to calculate percentage confluency (for T47D-WT and T47D-Y537S cells) or count cells that had been labelled with nuclear localised GFP (T47D-WT.SO, T47D-Y537S#1, T47D-Y537S#2, T47D-D538G#49 and T47D-D538G#60 cells).

2.2.7 Scratch Wound Migration Assays

T47D-WT and T47D-Y537S cells were seeded at a density of 20,000 cells/well on a 96-well plate and incubated for 48 hours. The WoundMaker™ (Essen Bioscience,

Welwyn Garden City, UK) was used to simultaneously create wounds in all wells. Cells were then immediately washed twice with culture media and treated with the appropriate ligand. Images were taken every 3 hours for 4 days using the IncuCyte ZOOM (Essen Bioscience, Welwyn Garden City, UK). Relative wound density (%) was calculated using the IncuCyte ZOOM software package (Essen Bioscience) and used to assess the effect of test ligands on migration.

2.2.8 Reporter Gene Assays

HEK293T cells were washed and then incubated in phenol red-free DMEM, supplemented with 5% DSS for 48 hours in T150 culture flasks. Following this, cells were seeded in 24 well plates (50,000 cells/well) and incubated for 24 hours. Cells were transfected with 100ng TAT-GRE-Luc Firefly luciferase reporter plasmid, 10ng pSG5-PR or pSG5 (vector control) and 10ng pRL-CMV Renilla luciferase control plasmid (Promega) using FuGENE HD reagent (Promega). The total amount of DNA in each well was made to 0.4µg using Bluescribe DNA (BSM) (Promega). Opti-MEM was used to further dilute the DNA mix resulting in a final concentration of 0.02µg/µl. The FuGENE HD: DNA ratio used was 5:2 and once mixed, 20µl of this was added to each well and incubated for 5 hours. Medium was then replaced with fresh medium and cells incubated for a further 24 hours. Cell lysates were then prepared using x1 passive lysis buffer (Promega). These lysates were transferred to 96 well opti-plates (Perkin Elmer) and firefly and renilla luciferase activity assessed using the DualGlo luciferase assay kit (Promega). 50µl DualGlo reagent was added to each well, incubated for 10 minutes and then firefly luciferase activity determined using the TopCount NXT microplate scintillation and luminescence counter (Perkin Elmer). Following this, 50µl of Stop and Glo reagent was added to each well and incubated

for 10 minutes before the renilla luciferase activity assessed. Firefly luciferase measurements were normalized to renilla luciferase measurements to enable renilla luciferase to act as a transfection control.

2.2.9 Small interfering RNA (siRNA) Transfection

ON-TARGETplus SMARTpool and deconvoluted siRNAs (Dharmacon) (details in Table 2.7) were resuspended in siRNA dilution buffer (Invitrogen) to a concentration of 10μM. Transfections were performed using the Lipofectamine RNAiMax reverse transfection system (Invitrogen). Experiments in 6 well plates were performed by diluting 5μl of 10μM siRNA stock in 250μl of warmed Opti-MEM along with 5μl of lipofectamine RNAiMAX. After mixing and incubating for 20 minutes at room temperature, 250μl of the siRNA/RNAiMAX mix was added to each well along with a suspension of 300,000 cells in 2ml full medium (antibiotic-free), resulting in a final siRNA concentration of 20nM. After incubating for 24 hours, the medium was replaced with fresh medium containing antibiotics and cells incubated for a further 48 hours before being harvested. Experiments performed in 96 well plates were carried out by adding 10μl of siRNA/RNAiMAX mix (prepared as detailed above) to each well (with 5000 cells in 100μl full medium). Transfection was again performed for 24 hours in antibiotic-free medium before being changed for medium containing antibiotics.

Table 2.7 SMARTPool and Deconvoluted siRNAs (Dharmacon)

siRNA	Sequence
ON-TARGETplus Non-targeting deconvoluted #2	5′-UGGUUUACAUGUUGUGUGA-3′
ON-TARGETplus Human ESR1 (2099)	SMARTpool
ON-TARGETplus Human ESR1 (2099) deconvoluted #1	5′-GAUCAAACGCUCUAAGAAG-3′
ON-TARGETplus Human ESR1 (2099) deconvoluted #2	5′-GAAUGUGCCUGGCUAGAGA-3′
ON-TARGETplus Human ESR1 (2099) deconvoluted #3	5′-GAUGAAAGGUGGGAUACGA-3′
ON-TARGETplus Human ESR1 (2099) deconvoluted #4	5′-GCCAGCAGGUGCCCUACUA-3′
ON-TARGETplus Human PGR (5241)	SMARTpool
ON-TARGETplus Human PGR (5241) deconvoluted #1	5′-GGACGUGGAGGGCGCAUAU-3′
ON-TARGETplus Human PGR (5241) deconvoluted #2	5′-GAGAUGAGGUCAAGCUACA-3′
ON-TARGETplus Human PGR (5241) deconvoluted #3	5′-ACAUAUUGAUGACCAGAUA-3′
ON-TARGETplus Human PGR (5241) deconvoluted #4	5′-GCACCUGAUCUAAUACUAA-3′
ON-TARGETplus Human NR3C1 (2908)	SMARTpool
ON-TARGETplus Human AR (367)	SMARTpool
ON-TARGETplus Human NR3C2 (4306)	SMARTpool

2.2.10 Protein Lysate preparation and Western blotting

150,000 cells/well for 6 well plates and 2 million cells/10 cm dish were seeded. Protein lysates were either prepared using Hot Lysis Buffer (HLB) extraction or RadioImmune Precipitation (RIPA) buffer extraction.

HLB (0.12M Tris-HCl pH6.8, 4% w/v SDS, 20% v/v glycerol, 0.2M DTT, 0.008% w/v bromophenol blue) extraction was performed by washing cells twice with PBS then adding pre-heated hot lysis buffer (100ºC) in volumes of 200µl per well of 6 well plates and 400µl per 10cm dish. The lysed cells were scraped, transferred to 1.5ml Eppendorf tubes and then heated at 100ºC for 10 minutes before being stored at -80ºC.

RIPA extraction was carried out by again washing cells twice in PBS then, for each well of a 6 well plate, 200µl of ice-cold RIPA buffer (50nM Tris-HCl pH8.0, 150mM

NaCl, 1% Igepal CA-630 (NP-40), 0.5% sodium deoxycholate, 0.1% SDS), (Sigma Aldrich), along with protease and phosphatase inhibitor cocktail tablets (Roche), was added. Lysed cells were scraped on ice, moved to 1.5 ml eppendorf tubes, then incubated on ice for 30 minutes with vortexing at 5-minute intervals. The lysates were centrifuged at 13,000rpm for 20 minutes at 4ºC, then the supernatant transferred to new eppendorf tubes and stored at -80ºC.

Lysates prepared by RIPA extraction had the protein content calculated using the Pierce™ BCA Protein Assay Kit (Thermo Fisher Scientific) as per the manufacturer's instructions. Lysates and bovine serum albumin (BSA) standards were diluted in ddH_2O to a volume of 10µl and plated in triplicate in 96 well plates. BCA reagents A and B were mixed 50:1 and 200µl added to each sample and standard. After mixing on the plate shaker for 30 seconds, plates were incubated for 30 minutes at 37ºC. After cooling plates to room temperature, the Tecan Sunrise™ microplate reader was used to measure optical density of the samples at 562nm absorbance. The protein concentration of the lysates was calculated from the standard curve of the known amounts of BSA.

Protein lysates were thawed, heated at 100ºC for 7 minutes then cooled on ice. 5-20µl of protein lysate (20µg of lysate prepared with RIPA extraction) was loaded onto an SDS-polyacrylamide gel electrophoresis (PAGE) resolving gel (8-12%) with a 5% stacking gel. 5µl of PageRuler™ Plus Pre-stained Protein Ladder (Thermo Fisher Scientific) was also loaded onto the gel to aid protein size estimation. Electrophoresis was performed using a SE250 mini-gel system (Hoefer, GE Healthcare) at 60V for 1 hour until proteins reached the stack, then 100V for 1-2 hours until the bromophenol

dye front reached the bottom of the gel. Gel transfer was performed onto Hybond ECL Nitrocellulose membrane (Amersham Biosciences) with 1x transfer buffer for 90 minutes at 100V using a TE-22 transfer unit (Hoefer, GE Healthcare). Non-specific binding of the primary antibody was minimised by incubating the membrane in blocking buffer for 1 hour at room temperature. Incubation with the primary antibody, diluted in blocking buffer was then carried out on a rocking platform at 4ºC overnight. Three washes in PBST were then performed (for 15 minutes each on the rocking platform) and then incubation with the HRP-conjugated secondary antibody (diluted in blocking buffer) for 1 hour. After another three washes in PBST, the SuperSignal West Pico Chemiluminescent Substrate and SuperSignal West Femto Maximum Sensitivity Substrate (Thermo Fisher Scientific) were added to the membrane as required and the Fusion Solo chemiluminescence imager (Vilber Lourmat) used for visualisation.

Table 2.8 SDS-PAGE buffers

Solution	Recipe
Upper Buffer	1.25M Tris-HCl (pH 6.8), 1% w/v SDS
Lower Buffer	1.5M Tris-HCl (pH 8.8), 0.4% w/v SDS
Running Buffer	0.25M Tris, 1.9M glycine, 1% (w/v) SDS, pH 8.3
Transfer Buffer	0.25M Tris. 1.9M glycine, 20% (v/v) methanol
PBST Buffer	0.1% (v/v) Tween 20 in PBS
Blocking Buffer	5% (w/v) dry skimmed milk powder in PBST

Table 2.9 SDS-PAGE acrylamide gel solutions

Name	Supplier
8% Resolving Gel	8ml lower buffer, 8.5ml 30% acrylamide: bisacrylamide, 62.5µl TEMED, 250µl 10% APS, 15.3ml ddH2O
10% Resolving Gel	8ml lower buffer, 10.6ml 30% acrylamide: bisacrylamide, 50µl TEMED, 200µl 10% APS, 13.4ml ddH2O
12% Resolving Gel	8ml lower buffer, 12.7ml 30% acrylamide: bisacrylamide, 41.7µl TEMED, 166.7µl 10% APS, 11.2ml ddH2O
5% Stacking Gel	2.5ml upper buffer, 1.5ml 30% acrylamide: bisacrylamide, 20µl TEMED, 5µl 10% APS, 6ml ddH2O

Table 2.10 Antibodies for Western Blotting

Name	Supplier
β-actin (ab6276)	Abcam
ER (VP-E613)	Vector Laboratories
PGR (sc-538)	Santa Cruz Biotechnology

2.2.11 RNA-sequencing (RNA-seq)

T47D-WT and T47D-Y537S cells were seeded at densities of 100,000 cells in 5ml full media or 150,000 cells in 5ml hormone-deplete media. Cells seeded in full media were grown for 4 days before RNA was extracted. Cells seeded in hormone-deplete media were grown for 4 days then treated with either 10nM E2 or vehicle control for 8 hours prior to RNA harvesting. For RNA-seq using P4 or R5020-treated cells, cells were seeded for 3 days and 8 hours, then treated with vehicle (ethanol) control or 10nM E2 for 16 hours before being treated with either vehicle control, 10nM E2 or 1nM P4 or 1nM R5020 for 3 hours. Total RNA was extracted (as described in chapter 2.2.2) from 6 biological replicates for each condition and samples sent to BGI Tech Solutions (Hong Kong) for quality assessment, non-stranded mRNA library preparation and generation of paired end 150bp reads on an Illumina NovaSeq S4 (Illumina). The

FastQC tool was used to perform quality control, which all samples passing (Babraham Bioinformatics).

2.2.12 Bioinformatic analysis of RNASeq data

HISAT2 version 2.1.0 (https://daehwankimlab.github.io/hisat2/) was used to align Fastq files containing the sequence reads to the University of California at Santa Cruz (UCSC) human reference genome (hg38 assembly). Mapped, sorted and indexed bam files (obtained using samtools version 1.10, http://www.htslib.org) were then quantified using HTSeq-count version 0.11.1 (https://htseq.readthedocs.io/en/release_0.11.1/index.html). Counts were normalized using a regularized log transformation (rlog) ((Love et al. 2014). Differential expression analysis, through calculating shrunken log2 fold changes, was performed using R package, DESeq2 version 1.26.0. Genes with an adjusted p value <0.05 and a log2 fold change of ≤-0.632 or ≥0.632 (which equates to a linear fold change of ≤-1.55 or ≥1.55) were considered differentially expressed.

R was used for statistical analyses and for generation of principle component analysis (PCA) (DESeq2) and heatmaps (gplots). Venn diagrams were recreated using the web applications BioVenn (Hulsen et al. 2008) and InteractiVenn (Heberle et al. 2015)

Genes were ranked according to log2 fold change following P4 or R5020 treatment, and GSEA analyses performed using the pre-ranked function of GSEA version 4.1.0. Molecular Signatures Database version 7.2 *(http://www.gsea-msigdb.org/gsea/msigdb/index.jsp)* (Subramanian et al. 2005), 'Hallmarks' (Liberzon et al. 2015), 'Gene Ontology' ('The Gene Ontology resource: enriching a GOld mine' 2021;

Ashburner et al. 2000) ‘Curated’ and ‘Reactome’ (Fabregat et al. 2018) collections were used.

The RNA-seq data presented in this thesis and that published by Bahreini et al. 2017 and Mohammed et al. 2015 was compared. This was performed by accessing the deposited data from the National Center for Biotechnology Information (NCBI) Gene Expression Omnibus (GEO) (https://www.ncbi.nlm.nih.gov/geo/ Bahreini et al. 2017 GEO:GSE89888, Mohammed et al 2015 GEO:GSE68359) (Edgar et al. 2002). Genes with an adjusted p value <0.05 and a log2 fold change of ≤-0.632 or ≥0.632 (which equates to a linear fold change of ≤-1.55 or ≥1.55) were considered differentially expressed and compared to the genes identified as differentially expressed in the dataset presented in this thesis. Gene enrichment scores and plots were generated using GSEA version 4.1.0. Molecular Signatures Database version 7.2 *(http://www.gsea-msigdb.org/gsea/msigdb/index.jsp)* (Subramanian et al. 2005)

3. Results

3.1 Characterisation of MCF7-Y537S and T47D-Y537S cell lines

3.1.1 Confirmation of E2-independent expression of ER target genes in MCF7-Y537S cells

Firstly, I confirmed the previous findings from the laboratory, in which the MCF7-Y537S cells showed elevated *PGR* expression in E2-free culture media, with further increase in *PGR* levels in the presence of E2 (Harrod et al. 2017). RT-qPCR was carried out in MCF7 and MCF7-Y537S cells cultured in full medium, which confirmed higher expression of *PGR* and a second ER-regulated gene, *TFF1*, in the mutant cells (Figure 3.1A). Much greater increase in *PGR* as well as *TFF1* was observed in the MCF7-Y537S line when cells were cultured in E2-free conditions, in agreement with the previous work (Figure 3.1B). Western blotting using lysates from MCF7 and MCF7-Y537S cells seeded in full media confirmed that the levels of both PR isoforms were increased in MCF7-Y537S cells relative to the WT MCF7 cells (Figure 3.1C).

3.1.2 Generation and confirmation of Y537S knock-in mutation in T47D-Y537S cells

Prior to the commencement of my studies, our laboratory used CRISPR-Cas9 mediated homology directed DNA repair (HDR) to create T47D cells with a genetically encoded Y537S mutation in *ESR1* (Jiminez, Buluwela et al. unpublished). Details of the generation of this cell line are included in Appendix I.

As part of the studies for this thesis, the T47D-Y537S line was further evaluated to confirm the presence of the Y537S mutation, investigate the effect of the indel mutation and ultimately establish whether these cells have utility for further studies of

ER and PR signalling. Total RNA was prepared from both the T47D-WT and T47D-Y537S cells and RT-PCR of *ESR1* exons 5-8 was performed, using three different primers (sequence details in Table 2.4). Firstly, a mutation-specific PCR was performed using a primer in exon 5 and the mutation specific primer (primers x and y (Figure 3.2B) were used to selectively amplify mutant *ESR1* and confirm expression of the mutant ER in the T47D-Y537S line. Secondly, primer x was used together with primer z. The latter maps 3' to CRISPR19, so will amplify mutant and WT ER. RT-PCR with the exon 5 and mutation-specific primer gave a PCR product of the expected size (466bp) for the T47D-Y537S clone but not the T47D-WT, confirming expression of Y537S only in the mutant clone (Figure 3.2A). Primers x and z provided the expected 700bp product in both T47D WT and Y537S cells as expected, which was of a similar intensity in both lines. A product of 516 bp, consistent with a described ER splice variant lacking sequences from exon 7 (ERΔ7) was also apparent for primers x and z (Herynk and Fuqua 2004), with the relative levels of full-length and smaller PCR products being similar in the T47D-WT and T47D-Y537S cells. The 284bp product seen only with the mutant-specific PCR primers is also consistent with ER mRNA lacking exon 7. The presence of ERΔ7 and the relative levels of full-length and ERΔ7 products suggests that the CRISPR-Cas9 knockin mutagenesis does not affect appropriate ER expression and regulation in T47D-Y537S cells (Harrod et al. 2017). To support this further, RT-qPCR also showed that *ESR1* mRNA levels are similar in T47D-WT and T47D-Y537S cells cultured in full media (Figure 3.2B). Sequencing of the total *ESR1* RT-PCR products showed both WT and Y537S mutant sequences for the T47D-Y537S cell line, confirming that it is heterozygous for the Y537S mutation (Figure 3.2C). The deletion-derived frameshift was also evident, but at lower levels, with this allele being WT up to the CRISPR19 recognition site, then

mutated by the indel, which corresponded to an 89 bp deletion of *ESR1* Exon 8 sequences. Once ER was found to be of full length and functional in T47D-Y537S cells, this line was considered suitable for further studies.

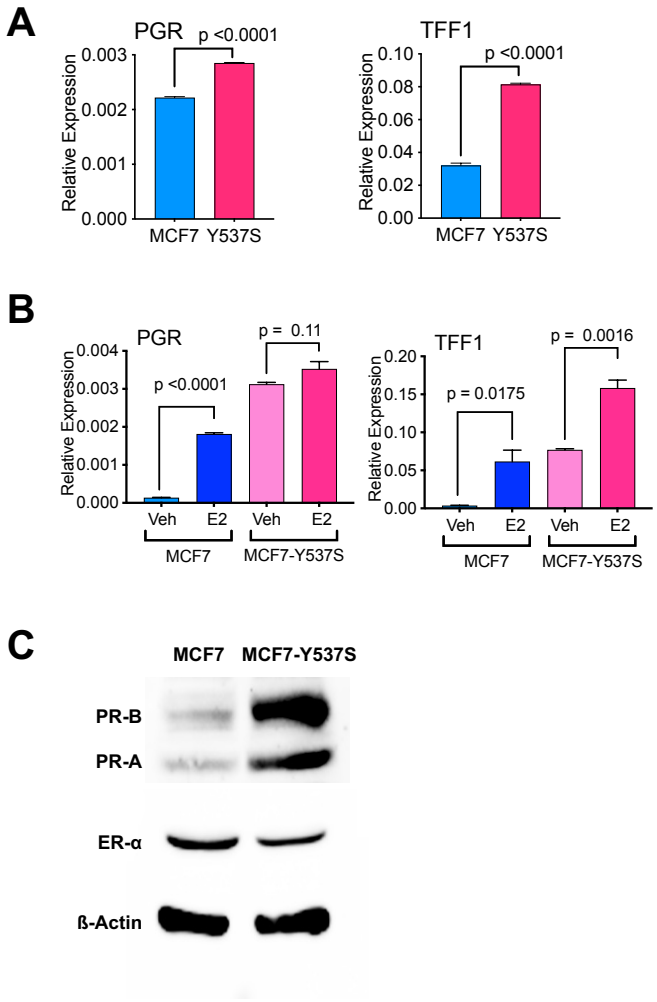


Figure 3.1 ER target genes upregulated in MCF7-Y537S cells

(**A**) RNA was prepared from MCF7 and MCF7-Y537S cells seeded in full media for 72 hours. (**B**) MCF7 and MCF7-Y537S cells were cultured in hormone-depleted medium for 72 hours then treated for 16 hours with 10nM 17β-Estradiol or vehicle prior to RNA extraction. (**A-B**) Shown are the RT-qPCR results for 3 biological replicate RNA preps. Gene expression is shown relative to levels of GAPDH expression. The bars show mean expression; error bars represent the standard errors of the mean (SEM). (**C**) Protein lysates were harvested from MCF7 and MCF7-Y537S cells seeded in full media for 72 hours and Western blotting performed using antibodies for the proteins as labelled.

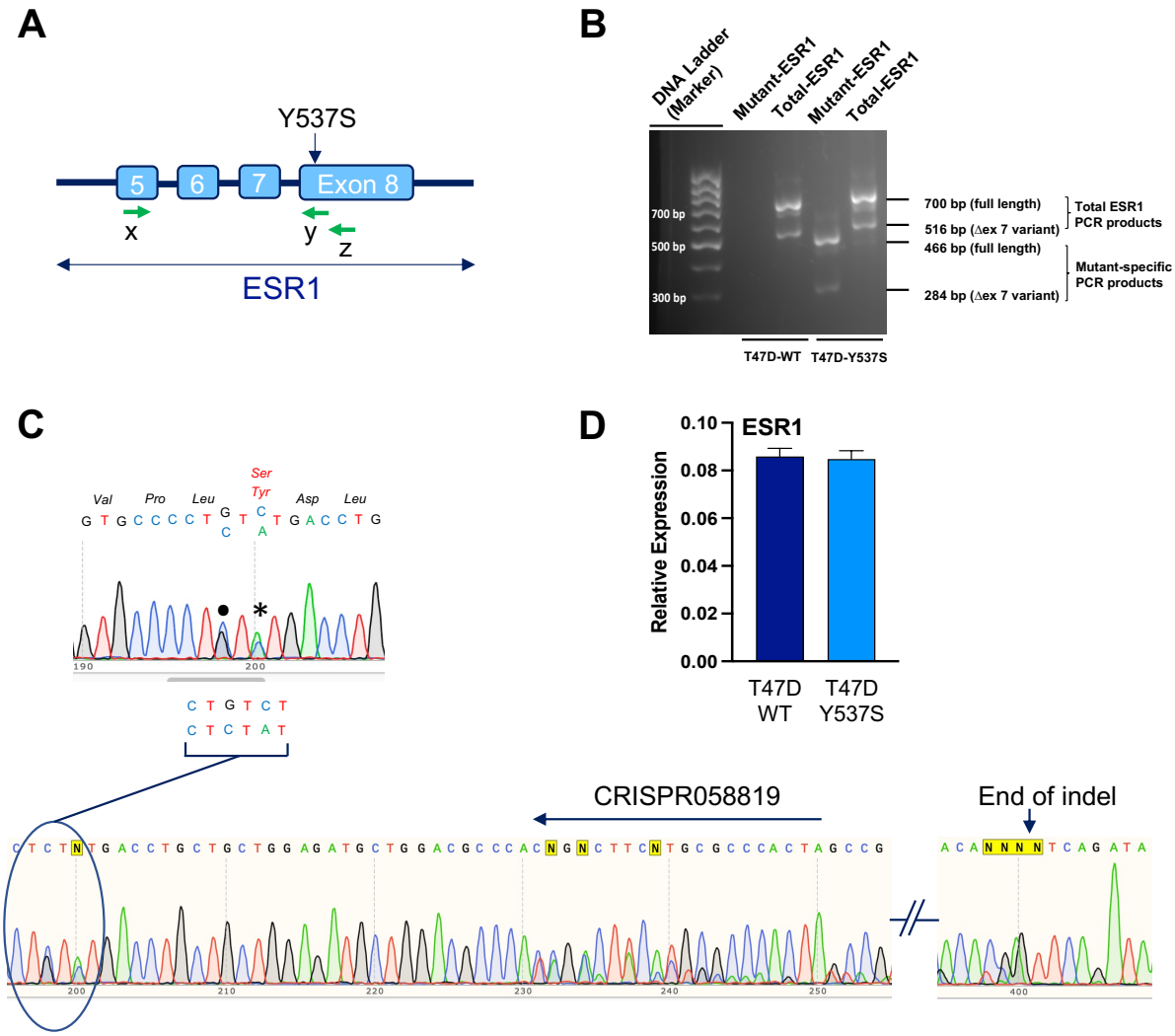


Figure 3.2 Characterisation of CRISPR-Cas9 generated ER Y537S mutation in the endogenous ESR1 gene in T47D-Y537S cells

(**A**) Position of primers used for RT-PCR analysis on ESR1 exons 5-8; x: primer in ESR1 exon 5, y: Y537S mutation-specific primer, z: primer in ESR1 exon 8. Primer sequences are detailed in Table 2.2 (**B**) RT-PCR of T47D-WT and T47D-Y537S cells using PCR primers that amplify mutant and WT ER mRNA and a primer set that amplify mutant ER cDNA, but not WT ER. (**C**) Sequencing chromatogram generated by Sanger sequencing of the PCR product amplified with primers that amplify the region around ER amino acid Y537 for T47D-Y537S cells. The encircled area highlights the targeted mutations at L536 and Y537: (•) denotes a silent single base mutation with cytosine replacing guanine at L536. (*) highlights the Y537S mutation with substitution of adenine for cytosine, which converts the tyrosine at position 537 to serine. Indel is noted from the CRISPR058819 recognition site (annotated) and the end of the indel mutation is also visualised. (**D**) RT-qPCR was performed using RNA prepared from cells cultured in full medium. ESR1 gene expression is plotted relative to expression of TBP (n=3 bioreplicates; error bars = SEM.

3.1.3 T47D-Y537S cells show estrogen-independent growth and expression of ER-regulated genes

Given the E2-independence shown in the MCF7-Y537S and other MCF7- and T47D-derived *ESR1* mutant cell lines (Harrod et al. 2017; Bahreini et al. 2017; Mao et al. 2016), I investigated whether this was also a feature of our T47D-Y537S clone. In E2-depleted culture conditions, immunoblotting showed that levels of ER protein are higher in T47D-Y537S cells, relative to the parental T47D-WT, suggestive of greater stability of the mutant ER (Figure 3.3A). E2 treatment of WT ER has been shown to increase the stability of ER protein, so the active conformation of the mutant ER in the absence of E2 may provide an explanation for this difference (Bai and Giguère 2003; Tecalco-Cruz and Ramírez-Jarquín 2017). However, ER mRNA expression was also greater in E2-depleted T47D-Y537S cells relative to T47D-WT and was stimulated by E2 treatment in both these lines (Figure 3.3B).

ER target gene expression has also been shown to be E2-independent in cell lines carrying *ESR1* mutations (Bahreini et al. 2017; Martin et al. 2017; Harrod et al. 2017). Cells cultured in E2-free medium were treated with 10nM estrogen for 8 hours. E2 stimulated expression of the ER target genes *PGR, GREB1, PDZK1* and *EGR3* (Figure 3.3B). The expression for all of these genes, except *PDZK1*, was greater in the vehicle-treated T47D-Y537S cells than in T47D-WT. *EGR3* showed particularly good upregulation with a 28-fold increase in expression between the T47D WT and mutant cells and a 5-fold increase for the E2-treated samples in both lines. Levels of *EGR3* expression were similar between the vehicle-treated T47D-Y537S cells and the E2-treated T47D-WT cells ($p=0.81$). *PGR* appeared to be expressed to a greater

degree in the vehicle-treated T47D mutant line relative to T47D-WT, although this was non-significant (p=0.26).

In order to investigate the effects of E2-depletion on growth, T47D-WT and T47D-Y537S cells were treated with either 10nM E2 or with vehicle control (ethanol). SRB assays were undertaken with absorbance measured at days 0 and 15, and the mean growth at day 15 relative to day 0 calculated. T47D-Y537S cells demonstrated a 2-fold increase in growth in the absence of E2, in comparison to the T47D-WT cells (Figure 3.3C).

3.1.4 Effect of anti-estrogens on ER target gene expression in T47D-Y537S cells

Partial insensitivity to anti-estrogens and reduced affinity of mutant ER to some anti-estrogens has been demonstrated previously in the MCF7-Y537S line and other breast cancer cell lines expressing *ESR1* mutations (Harrod et al. 2017; Bahreini et al. 2017; Martin et al. 2017; Toy et al. 2013; Fanning et al. 2016; Merenbakh-Lamin et al. 2013). Hence, anti-estrogens such as the SERM, Tamoxifen, or the SERD, Fulvestrant, result in greater expression levels of ER target genes in mutant expressing cells than in WT cells (e.g. see (Harrod et al. 2017)). RT-qPCR was performed to confirm whether this was also the case in the T47D-Y537S cells, using RNA harvested from T47D-WT and T47D-Y537S cells treated with 10-fold increasing concentrations (1-1000nM) of either Fulvestrant or Tamoxifen (Figures 3.4B and 3.4C). Both Tamoxifen and Fulvestrant reduce expression of the ER target gene, *EGR3*. e.g. 100nM of Tamoxifen or Fulvestrant reduced *EGR3* mRNA levels by 6.3-fold (p-value = 0.0372) and 24.2-fold (p-value = 0.0015) respectively in the T47D-WT

cell line. However, at a dose of 1nM of both anti-estrogens, the reduction in *EGR3* expression is not as great for the T47D-Y537S cells as for the T47D-WT cells (1.2-fold vs 3.0-fold decease in *EGR3* expression for Tamoxifen and 1.9-fold vs 8.2-fold for Fulvestrant), suggesting reduced sensitivity to anti-estrogens in the T47D-Y537S line. In keeping with this, for all tested concentrations of Fulvestrant, expression of ER regulated genes (*PGR, PDZK1* and *EGR3*) was higher in the mutant line relative to the T47D-WT (e.g. following treatment with 1nM of Fulvestrant the expression levels of *PGR* were 1.4-fold higher in the T47D-Y537S line than the T47D-WT (p-value = 0.0034). Similarly, levels of *PGR, PDZK1* and *EGR3* expression were also higher in the T47D-Y537S line relative to the T47D-WT with all tested concentrations of Tamoxifen (e.g. treatment with 1nM Tamoxifen resulted in *PGR* mRNA levels that were 2.3-fold higher in the T47D-Y537S line than the WT (p-value = 0.0002). *PDZK1* did not show sensitivity to Fulvestrant in the T47D-Y537S line or to Tamoxifen in either cell line. *PGR* showed reduced anti-estrogen sensitivity in comparison to *EGR3* (e.g. 1nM Fulvestrant resulted in 8.2-fold decrease in *EGR3* expression (p-value = 0.022) but only a 1.5-fold decrease in PGR expression levels (p-value = 0.004) in T47D-WT cells. In conclusion, expression of ER target genes is higher in the T47D-Y537S line and this persists after treatment with Fulvestrant or Tamoxifen.

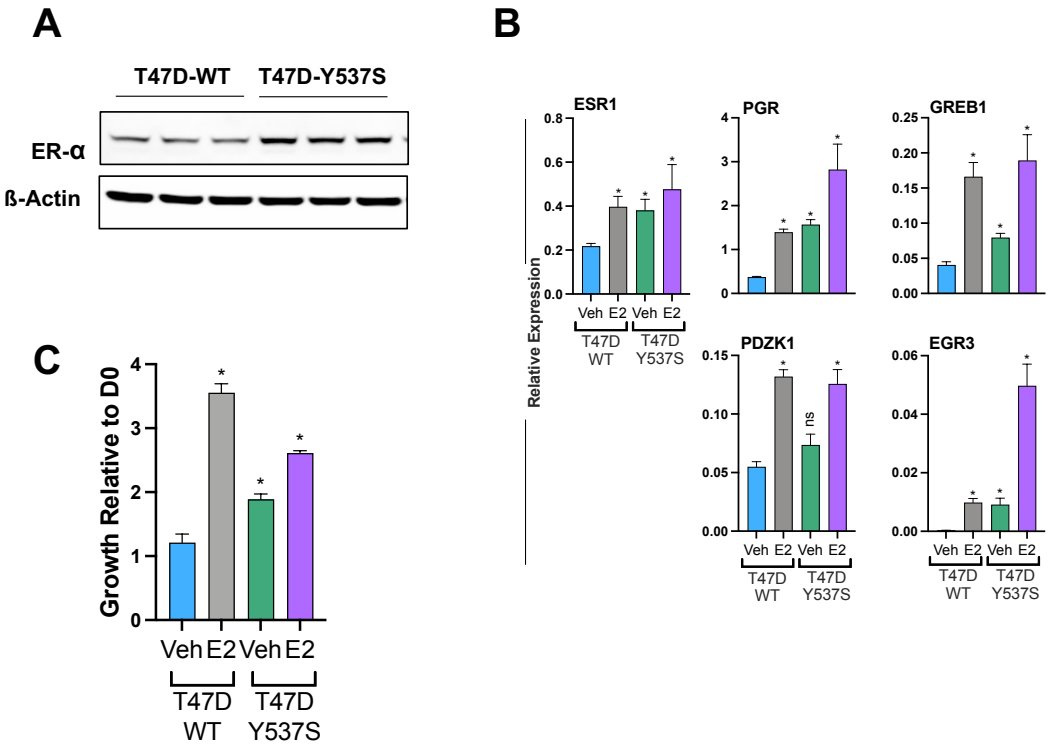


Figure 3.3 T47D-Y537S cells show increased levels of ER protein, estrogen-independent cell growth and increased expression of ER target genes

(**A**) Western blotting was performed using protein lysates prepared from cells cultured in hormone depleted medium for 2 days. (**B**) RT-qPCR results from RNA extracted from T47D-WT or T47D-Y537S cells treated with 10nM 17β-Estradiol or vehicle control for 8 hours. RNA was harvested from 3 independent biological replicates. Expression shown is relative to TBP and error bars show the SEM. * $p < 0.05$ relative to Vehicle-treated T47D-WT samples. (**C**) Data represents the mean growth at day 15 relative to day 0, following treatment of T47D-WT or T47D-Y537S cells with either vehicle or 10nM E2. Error bars show the SEM (n=6, data representative of 3 independent experiments), * $p < 0.05$ relative to vehicle-treated samples for each cell line (vehicle-treated T47D-Y537S is shown relative to vehicle-treated T47D-WT).

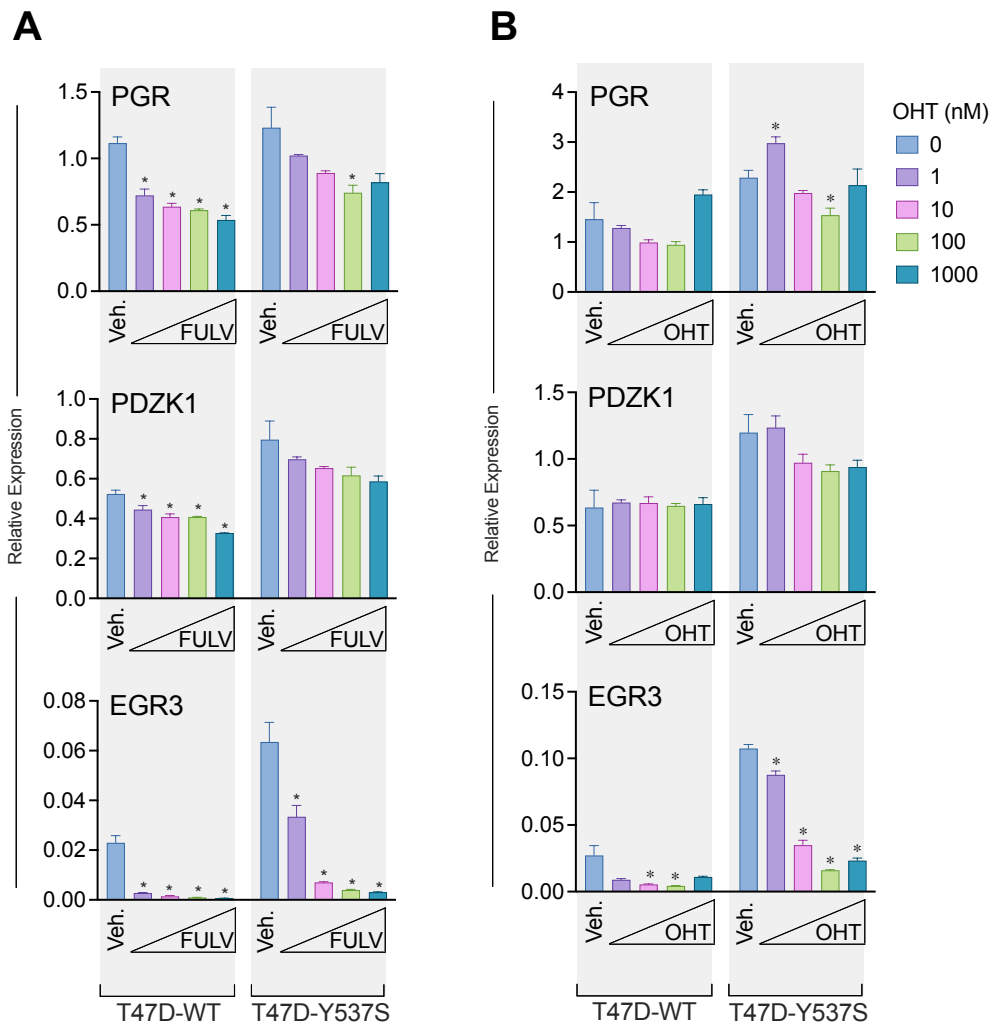


Figure 3.4 ER target gene expression in the T47D-Y537S line is less sensitive to anti-estrogens than in T47D-WT cells

(**A**-**B**) RT-qPCR using RNA extracted from T47D-WT and T47D-Y537S cells treated with 1-1000nM Fulvestrant (**A**) or Tamoxifen (**B**) for 8 hours. Gene expression was normalized to expression of TBP. n=3 bioreplicates; error bars = SEM. * $p < 0.05$ relative to the vehicle control sample for each cell line. Abbreviations – FULV: Fulvestrant, OHT: Tamoxifen

3.2 Effect of modulating PR on the growth of *ESR1* mutant cells

3.2.1 PR modulating drugs used in this thesis

As discussed in chapter 1, section 8, a wide range of PR-modulating small molecules have been described, including the natural PR ligand, P4, as well as synthetic PR agonists and antagonists. R5020 (Promegestone), a progestin, is not generally used in clinical practice in the UK but has been used extensively in *in vitro* and animal studies of PR signalling in breast cancer (Mohammed et al. 2015; Vignon et al. 1983; Horwitz and McGuire 1975). R5020 has great utility in studying PR as, unlike many other PR ligands, it shows excellent potency and good specificity for PR (Stanczyk et al. 2013; Vignon et al. 1983). MPA, on the other hand, activates AR and GR as well as PR, but is in frequent clinical use and therefore relevant to this study (Stanczyk et al. 2013; Kuhl 2005). P4, R5020 and MPA all function as agonists, activating PR. RU486 is a commonly used PR antagonist, although, like MPA, also targets AR and GR (Zhang et al. 2006; Hayes et al. 2006).

The activities of these 4 PR ligands for PR was confirmed in reporter gene assays, to assess their suitability for further studies. HEK293 cells were transfected with a PR-responsive firefly luciferase gene along with a renilla luciferase reporter gene. The latter served as a control for transfection efficiency. Transfected cells were treated with P4, R5020 or MPA at 10-fold increasing concentrations, ranging from 0.01-1000nM, and reporter gene activity assessed 24 hours later (Figure 3.5A-C). As expected, the PR agonists increased reporter gene activity, generally in a dose-dependent manner. Near maximal activity was obtained with 1nM P4 or R5020 and 10nM MPA. The same gene reporter assay was repeated with the antagonist, RU486, using the same treatment concentrations (Figure 3.5D). This was performed in the presence of 1nM

P4 to ensure activation of PR and, therefore, PR inhibitory activity of RU486 could be determined. PR activity was reduced >50% with 0.1nM RU486, with reporter stimulation by P4 being completely absent for RU486 at concentrations of 1nM or greater.

3.2.2 Effect of PR ligands on growth of MCF7-Y537S cells

The effect of PR-modulating drugs on MCF7-Y537S cells was studied. MCF7 and MCF7-Y537S cells were seeded in full media in 96-well plates and treated with 10-fold increasing concentrations (1-10,000nM) of either P4, R5020 or MPA (Figure 3.6A). Growth was assessed using the SRB assay. There was little or no impact of P4 or R5020 on MCF7 cell growth. A small, 11% reduction in growth of the MCF7-Y537S cells was observed with 10,000nM P4, but a similar reduction in growth was not seen for R5020. MCF7-Y537S cells were also sensitive to MPA, but to a similar extent as MCF7-WT cells. Most studies investigating the effects of progestins in breast cancer cell lines use concentrations between 10-100nM; the impact on growth only at the high dose of 10,000nM suggests this growth inhibition is likely to be due to off-target effects (Zaurin et al. 2021). The inhibitory effect of 10,000nM MPA on the T47D-WT line may reflect this, given the well-described binding to and activation of other nuclear receptors, specifically AR and GR by MPA (Kuhl 2005; Africander et al. 2011; Stanczyk et al. 2013). A growth assay was also performed with the anti-progestin RU486, using the same cell lines and drug concentrations; cells were seeded in E2-depleted media with the addition of 1nM E2 (Figure 3.6B). Unexpectedly, given the growth inhibition with the PR agonists, albeit only at high ligand concentrations, significant growth inhibition ($p<0.05$) by RU486 was only seen in the MCF7-Y537S line, although again this growth inhibition was only observed for 10,000nM RU486.

Given that RU486 acts on receptors other than PR and the high dose at which growth inhibition was observed, this growth inhibition likely also reflects off-target effects of RU486 (Zhang et al. 2006; Hayes et al. 2006). Altogether, this data suggests that the PR ligands have no clear inhibitory or stimulatory effect on either MCF7 or MCF7-Y537S cells.

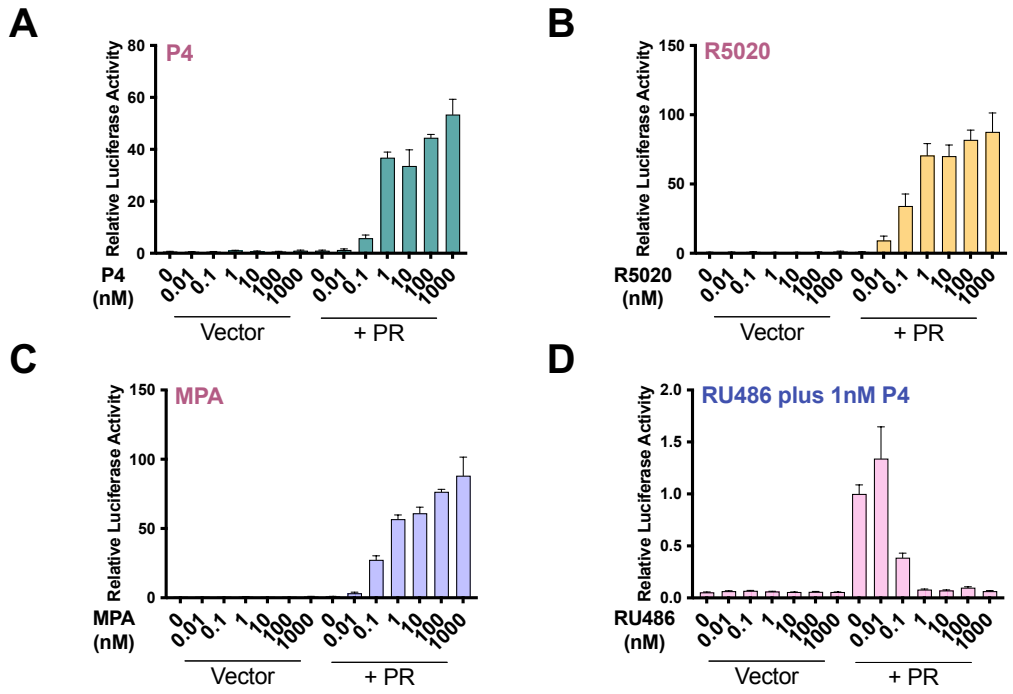


Figure 3.5 Reporter gene assay demonstrating the agonist (PR activating) and antagonist (PR inhibiting) activities of the drugs used in this thesis

(**A-C**) HEK293 cells were transfected with PR, a PR-responsive firefly luciferase reporter gene, together with a control renilla luciferase reporter gene. PR agonists P4, R5020 and MPA were added 5 hours following transfection and reporter gene activities were determined after a further 24 hours. Firefly luciferase activities are shown relative to the renilla luciferase activity, with PR reporter activity in vector-transfected cells in the absence of ligand, taken as 1. All other reporter activities are shown relative to this. The results are the means of two independent experiments, each with three bioreplicates. Error bars represent SEM. (D) HEK293 cells were transfected and processed exactly as above, except that 1nM P4 was present in all transfections. The PR antagonist, RU486 was added at the concentrations indicated.

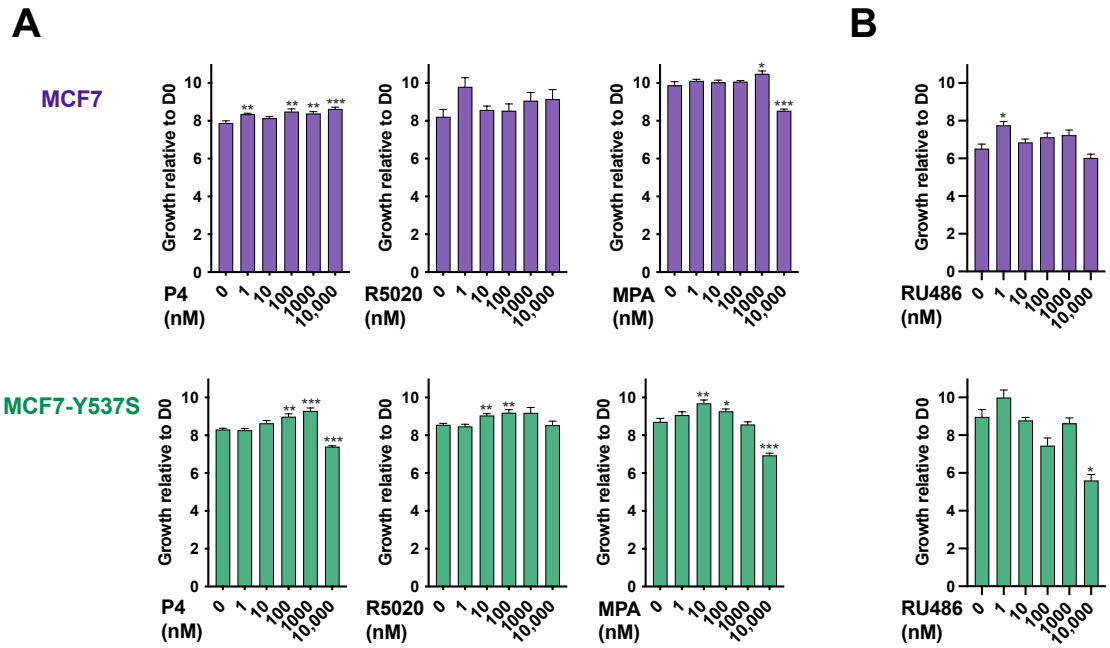


Figure 3.6 Effect of PR ligands on growth of MCF7 cells carrying ESR1 mutations

(**A**) Mean growth is shown at day 9 relative to day 0 following treatment with 1-10,000nM (10-fold serial dilutions) of P4, R5020 or MPA in full media (n=6, 1 experiment) and (**B**) at day 15 relative to day 0 for 1-10,000nM RU486 in stripped media supplemented with 1nM 17β-Estradiol (n=12, 2 independent experiments). (**A-B**) Error bars show the SEM, * P < 0.05, ** P < 0.001, *** P < 0.0001.

3.2.3 R5020 inhibits the growth of T47D-Y537S cells

In order to extend the studies performed in chapter 3, section 2.1 to another ER+ breast cancer cell line, I explored the effects of P4 and R5020 on the growth of T47D-WT and T47D-Y537S lines. As discussed in chapter 1, section 1.9, T47D is the ER+ breast cancer cell line of choice for investigating the effects of PR signalling due to its high level of *PGR* expression and was therefore essential to include in this study. Indeed, the RT-qPCR data for *PGR* expression in the MCF7-WT and T47D-WT lines in E2-depleted medium (Figures 3.1B and 3.3B) show *PGR* is expressed >2,700-fold higher in the T47D-WT line than the MCF7-WT. Therefore, growth assays were

undertaken using P4 (1-1000nM) and R5020 (1-10,000nM) in the T47D-WT and T47D-Y537S lines, with absorbance calculated at day 6 relative to day 0 (Figure 3.7A). There was no effect on growth of either cell line with any concentration of P4. By contrast, R5020 inhibited growth of T47D-Y537S cells in a dose-dependent manner. The growth inhibition was greater in the T47D-Y537S cells than in T47D-WT cells. The higher expression of *PGR* in the T47D-Y537S line compared to the T47D-WT (Figure 3.3C) and the greater RBA of R5020 for PR in comparison to P4 (discussed in chapter 1, section 8) may explain why growth inhibition was only seen in the T47D-Y537S line and with R5020 treatment but not P4 (Stanczyk et al. 2013; Kuhl 2005).

In keeping with the data from the MCF7 cells, MPA and RU486 also had no appreciable effect on growth of either the T47D-WT or mutant T47D line, aside from at a concentration of 10,000nM (Figure 3.7B). As a PR ligand that demonstrates complete antagonism and good PR affinity, Onapristone (0.01-10,000nM) was selected to investigate its effect on growth of T47D-Y537D cells (Chabbert-Buffet et al. 2005; Diep et al. 2015) (Figure 3.7C). Aside from at the highest treating concentration of 10,000nM, no significant effect on growth was evident in either cell line with Onapristone. Again, an off-target effect is the likely explanation for the growth inhibition at this high dose. Growth data using MPA, RU486 and Onapristone was kindly provided by C.F.Lai.

The effect of R5020 on PR protein level was assessed through Western blotting. Lysates were prepared from T47D-WT and T47D-Y537S cells that were treated with 1nM and 10nM R5020 and western blotting performed using PR antibody (Figure 3.7D). In keeping with previous reports in the literature, R5020 appeared to decrease

PR protein levels in the T47D-WT line representing a reduction in PR protein synthesis and an increase in the degradation rate (Nardulli and Katzenellenbogen 1988; Daniel 2009; Read et al. 1988). This phenomenon was not seen in the T47D-Y537S cells, where PR protein was present at much higher levels than the T47D-WT even in the absence of R5020, reflecting the higher PR mRNA levels in the T47D-Y537S line (Figure 3.3B) as well as the findings in the MCF7-Y537S clone (Harrod et al. 2017).

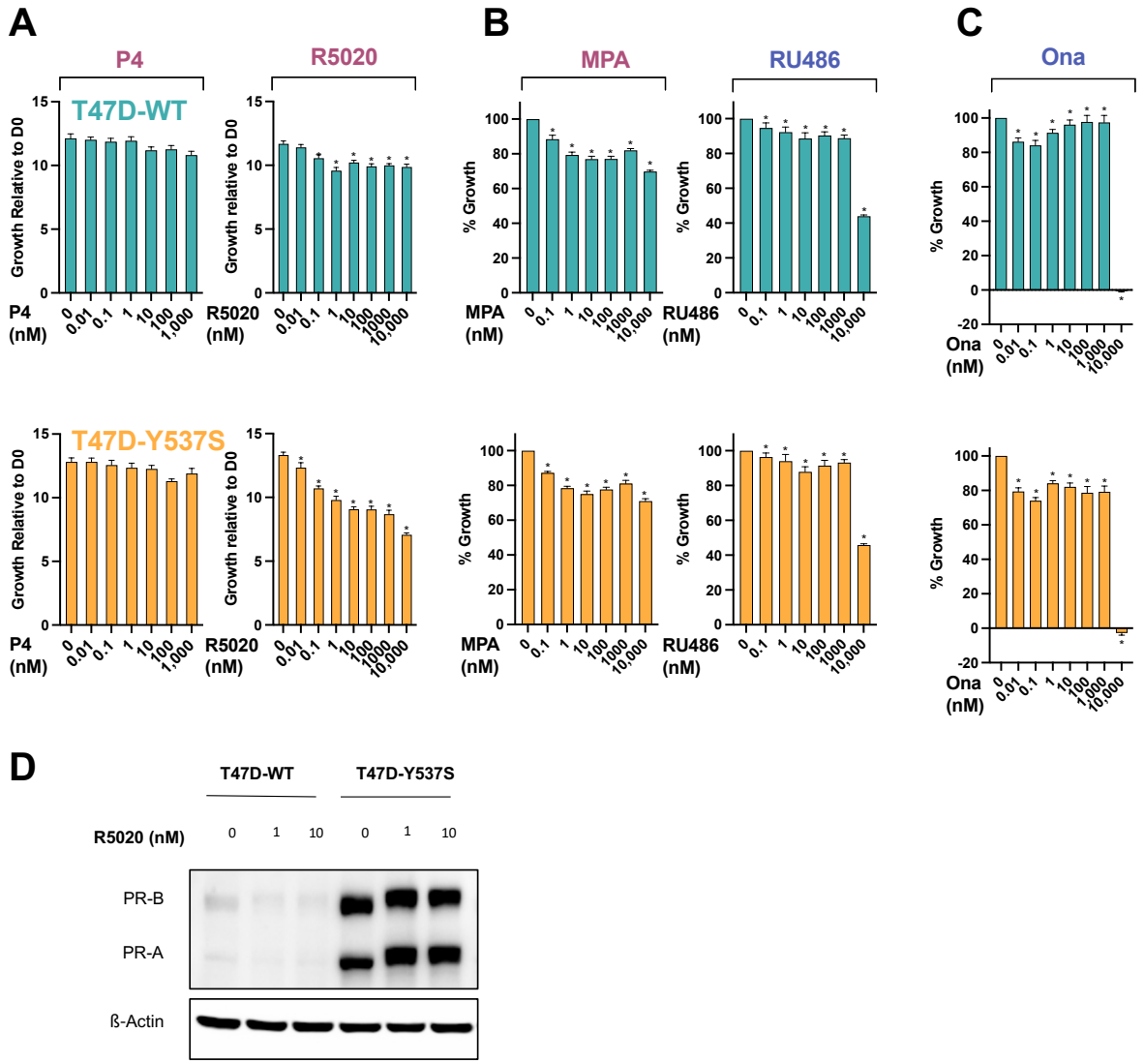


Figure 3.7 T47D-Y537S cells are sensitive to R5020

(**A**) Data represents the mean growth at day 6 relative to D0, in the presence of 0.01-1000nM P4 or 0.01-10,000nM R5020 (10-fold serial dilutions) of T47D-WT and T47D-Y537S cells in full media. Error bars represent the SEM, * P < 0.05. The results are the means of 3 independent experiments, each with 6 replicates. (**B-C**) Percentage growth of T47D-WT and T47D-Y537S cells is shown at 6 days following 0.01-10,000nM (10-fold serial dilutions) MPA or RU486 treatment (**B**) and Onapristone treatment combined with 1nM R5020 and 10nM 17β-Estradiol (**C**). Error bars show the SEM, n=6, 1 experiment. MPA, RU486 and Onapristone growth data courtesy of Dr C.F. Lai. (**D**) Protein lysates were harvested from T47D-WT and T47D-Y537S cells cultured in hormone deplete media for 2 days and then treated for 1 hour with either 1nM R5020, 10nM R5020 or vehicle control; Western blotting was performed using antibodies for the proteins as labelled.

3.2.4 Effect of siRNA-mediated *ESR1* and *PGR* knock-down on MCF7 and T47D cells

In order to further investigate whether modulating PR has any effect on growth of ER+ breast cancer cells, *PGR* knockdown was performed, using siRNA. PR ligands showed no obvious effect on the growth of MCF7 and MCF7-Y537S cells (Figure 3.6), but ER-dependence of these cells is demonstrated by the fact that they were sensitive to anti-estrogens, albeit at higher concentrations (Harrod et al. 2017) . Therefore, MCF7-WT and MCF7-Y537S cells were transfected with siESR1 and siPGR pools, 4 deconvoluted siPGRs (comprising the individual siPGRs that, together, make up the siPGR pool), and a non-targeting control siRNA (Figure 3.8A). As expected, siESR1 inhibited growth to 22.5% of that observed in the siNegative control-transfected cells. There was also a significant effect on growth with the siESR1 pool in the MCF7-Y537S line (growth inhibited to 28.3% of that seen with siNegative control).

Given that neither the anti-progestin, RU486, nor 3 different PR agonists (P4, R5020 and MPA) greatly inhibited the growth of MCF7 cells, it was surprising to observe that *PGR* knockdown using the siPGR pool reduced the growth of MCF7-WT cells to a similar extent to that seen with the siESR*1* pool (Figure 3.8A). Using each of the 4 *PGR* siRNAs separately showed that siPGR #2 was likely to be responsible for the growth inhibition in MCF7 cells. Similar results for *ESR1* and *PGR* dependency were observed for MCF7-Y537S cells. RT-qPCR showed that all of the *PGR* siRNAs, except siPGR #1, strongly reduced *PGR* expression (Figure 3.8B). As expected, *PGR* expression was also strongly reduced upon *ESR1* knockdown. Surprisingly, siPGR #2 almost completely abrogated *ESR1* expression in MCF7-WT and MCF7-Y537S cells, whereas the other *PGR* siRNA did not affect *ESR1* levels. Although regulation of ER

by PR has previously been reported (Verde et al. 2018), my findings demonstrate that the reduction in *ESR1* expression only by siPGR #2 represents an off-target effect. Moreover, these results indicate that *PGR* knockdown has little or no effect on the growth of MCF7-WT and MCF7-Y537S cells.

As expected, given the E2-sensitivity of the T47D-WT cells, all 4 *ESR1* siRNAs inhibited their growth (Figure 3.8C). This growth inhibition was accompanied by a reduction in ER and PR mRNA (Figure 3.8D). In keeping with the lack of efficacy of anti-progestins in the T47D cells and reflecting the findings following *PGR* knockdown in the MCF7 lines, there was little or no effect on growth of T47D-WT and T47D-Y537S cells (Figure 3.8C), despite efficient *PGR* knockdown (Figure 3.8D). siPGR#2 and the siPGR pool were excluded.

It was observed that siPGR1 showed the least efficient *PGR* knockdown in comparison with siPGRs 3 and 4 (Figure 3.8C-D). As introduced previously (chapter 1, section 7.2), there are 2 PR isoforms (PR-A and PR-B), which are transcribed as 2 distinct mRNA from the same gene and possess different functions (Kastner et al. 1990; Lamb et al. 2018). Analysis of the sequences of siRNA sequences showed that si*PGR*1 would target the PR-B but not the PR-A mRNA (Figure 3.9). In contrast, siPGRs 3 and 4 target both isoforms, explaining their superior *PGR* knockdown efficiency relative to siPGR1. Similar results were obtained in independent T47D cells (see below and Figure 3.33D).

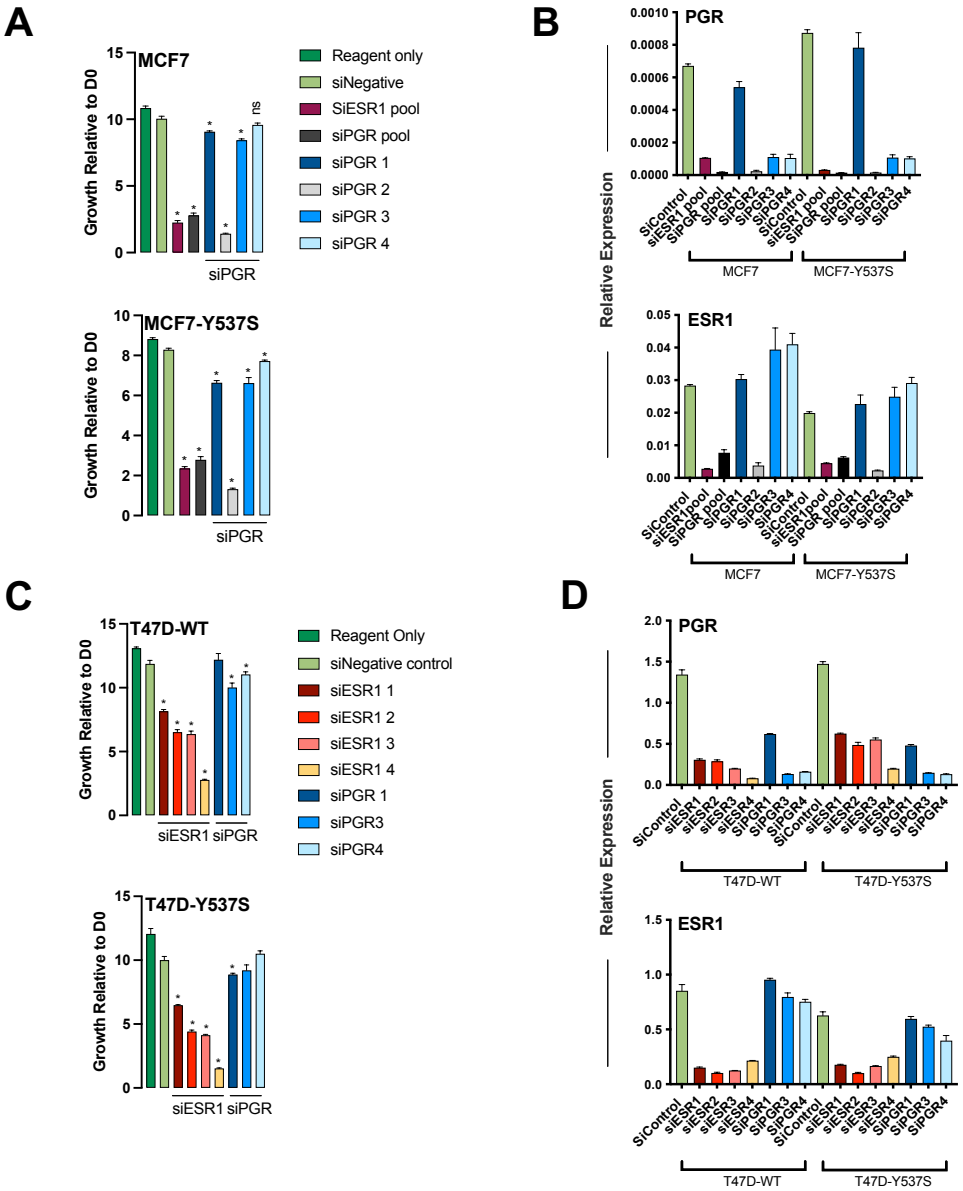


Figure 3.8 PGR knockdown has only a small effect on growth of MCF7, MCF7-Y537S, T47D-WT and T47D-Y537S cells

siRNA mediated knockdown of ESR1 and PGR in MCF7, MCF7-Y537S (**A-B**), T47D-WT and T47D-Y537S (**C-D**) cells. This was performed using siESR1 and siPGR pools (**A**), deconvoluted ESR1 siRNA (**C**) and deconvoluted siRNA targeting PGR (**A,C**). Mean growth is shown at day 6 relative to D0, error bars show the SEM. (n=6, 1 experiment each for **A** and **C**). (**B,D**) RT-qPCR using RNA extracted from MCF7 and MCF7-Y537S cells transfected with either siControl, siPGR pool and deconvoluted siPGRs 1-4 (**B**) and with RNA from T47D-WT and T47D-Y537S cells transfected with either siControl, deconvoluted siESR1s 1-4 or siPGRs 1,3, and 4 (**D**) . Error bars show the SEM, expression is shown relative to GAPDH (**B**) or TBP (**D**). RNA was harvested from 3 biological replicates.

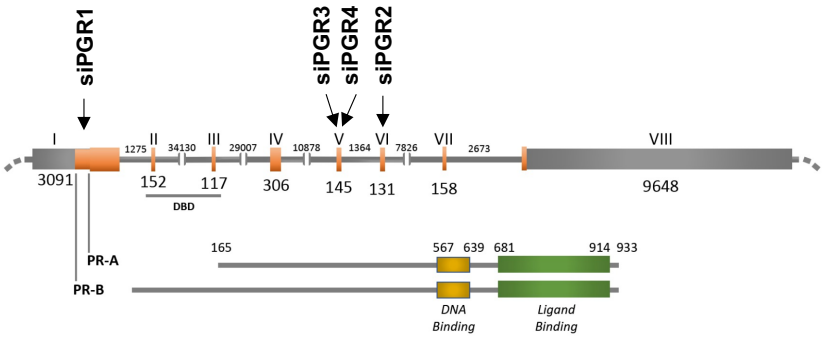


Figure 3.9 Human PGR gene and position of siPGR 1-4

Schematic of the human PGR gene with the position of the 4 deconvoluted siPGRs (1-4) used in this study.

3.3 PR target gene expression in ESR1 mutant cells

3.3.1 Effect of PR modulating drugs on PR target gene expression in MCF7 and T47D cells

Since *PGR* is expressed at higher levels in both the MCF7-Y537S (Figure 3.1A-B) and T47D-Y537S (Figure 3.3B) cells relative to their parental, WT cell lines, I investigated whether this resulted in differential expression of PR target genes following treatment with a progestogen. In order to do this, I searched the literature for genes reported to be regulated by PR in MCF7 and T47D cells. Through RNA-seq and PR ChIP-seq, Mohammed et al. 2015 defined a set of PR-regulated genes in both MCF7 and T47D cell lines (Mohammed et al. 2015). They performed this after treating cells with either 100nM P4 or 10nM R5020 for 3 hours in E2-containing media. They reported that 543 genes were P4-regulated, 718 R5020-regulated and 470 regulated by both P4 and R5020 in MCF7 and T47D cells (Figure 3.10A) (Mohammed et al. 2015). Mohammed et al. 2015 also generated a progestogen-regulated 'gene signature' through integration of the RNA-seq and ChIP-seq data; all genes that were differentially regulated by P4/R5020 and also had an ER binding event within 10kb of the

transcription start site were included, which resulted in a group of 38 genes (Figure 3.10B) (Mohammed et al. 2015). Six genes from this list (*BCL6, FAM105A, HES2, MAFB, NEDD9* and *SGK1*) that have also been described as PR targets elsewhere in the literature were selected to investigate the effect of PR ligands on the transcriptome of the WT and *ESR1*-mutant MCF7 and T47D cells used in this study (Godbole et al. 2018; Richer et al. 2002; Clare et al. 2016).

I first studied the effect of PR ligands (0.001 – 10μM (10-fold increasing concentrations) of either the PR agonists P4, R5020, MPA or the antagonist RU486)) on expression of the 6 chosen PR target genes in MCF7-WT and MCF7-Y537S cells (Figure 3.10C). To ensure that PR was activated in the MCF7 cells, this was performed in E2-depleted media supplemented with 1nM E2. None of the genes showed an increase in basal expression (vehicle treatment) in MCF7-Y537S compared with MCF7-WT cells, indicating that the increased *PGR* levels do not reflect increased expression of PR target genes, at least in the absence of PR ligand. On the contrary, expression of 3 of the selected PR target genes (*SGK1, MAFB* and *HES2*) was lower in the MCF7-Y537S cells relative to the MCF7-WT and was not much altered by progestogen or anti-progestin treatment. Given that *PGR* is upregulated in the mutant line and *SGK1, MAFB* and *HES2* are PR regulated, the reduced expression of these genes in the MCF7-Y537S cells was unexpected, although this was not observed in the T47D-Y537S cells (Figures 3.11A and 3.13A-B). Note that RNAs for the different progestogen/anti-progestin treatments were prepared at different times, which may reflect the difference in expression that is sometimes evident for the vehicle controls (Figure 3.10C). For example, *BCL6* expression is evidently lower in the MPA treatment control than the P4 or R5020 treatment control. None of the six genes showed clear

regulation by P4, R5020 or RU486 in either the MCF7-WT or MCF7-Y537S cells. With MPA treatment however, at concentrations as low as 0.1μM, increased expression of *FAM105A, BCL6* and *MAFB* was seen in MCF7-WT cells. *FAM105A* expression was also stimulated by MPA in MCF7-Y537S cells and to a greater degree than in MCF7-WT cells, which is consistent with direct PR regulation of *FAM105A* by MPA since *PGR* is upregulated in the MCF7-Y537S line. In contrast, the MPA-stimulated increase in *BCL6* expression was not greater in the MCF7-Y537S cell line than in the MCF7-WT. Stimulation of *MAFB* expression, was actually greater in the MCF7-WT line than the MCF7-Y537S cells. Unlike, *FAM105A*, the trends in MPA-regulated expression of *BCL6* and *MAFB* are therefore not consistent with the higher *PGR* levels found in MCF7-Y537S cells. As described previously, AR, GR, MR and PR bind to identical response elements and often regulate expression of the same sets of genes. Although AR mRNA levels are similar in the MCF7-WT and MCF7-Y537S cells, expression of GR and MR mRNA is lower in the mutant cells, raising the possibility that the lower expression of *BCL6* and *MAFB* in MCF7-Y537S cells is a reflection of their regulation by GR and/or MR.

The effects of 2 progestogens (P4 and R5020) on 3 of the selected PR-regulated genes (*HES2, FAM105A* and *SGK1*) were then investigated in T47D and T47D-Y537S cells (Figure 3.11A). Although PR has been reported to be constitutively active in T47D cells (as mentioned in chapter 3, section 1.1), E2-depleted media supplemented with 10nM E2 was used to ensure *PGR* was expressed. In contrast with MCF7 cells, expression of each of these genes was stimulated even in the presence of 0.001μM P4 in both T47D-WT and T47D-Y537S lines. P4 did not stimulate expression of these genes in MCF7 cells more than about 2-fold even at the highest concentration of P4

(Figure 3.10C). There were no obvious differences in the P4 response for these genes in T47D-WT compared with T47D-Y537S cells. Thus, SGK1 expression was stimulated 3.5-fold with 0.001μM P4 in T47D-WT and in T47D-Y537S cells. Expression of three other PR target genes were also studied in T47D-WT and T47D-Y537S cells, *FBKP5* which featured in the 38 gene progestogen-regulated 'gene signature', as well as *S100P* and *STAT5A* which have both been identified as PR targets in other studies (Mohammed et al. 2015; Richer et al. 2002) (Figure 3.11B). Expression of all 3 genes was stimulated at all doses of P4 and R5020. Near maximal stimulation was reached with 0.001μM of each ligand, except for *S100P*, which showed a further increase in expression with 10μM R5020 in both cell lines. As seen for *HES2, FAM105A* and *SGK1*, the stimulation in expression of these genes was not different between the T47D-WT and T47D-Y537S cells. These data suggest that the MCF7 line has low PR activity in comparison to T47D cells, as the latter demonstrate good responsiveness to PR ligands. The difference between the MCF7 and T47D cells is likely to be due to the substantially lower *PGR* expression in MCF7 cells. Furthermore, in T47D cells, the Y537S mutation, despite the considerable increase in PR mRNA and protein, does not lead to increased expression of the PR target genes examined here.

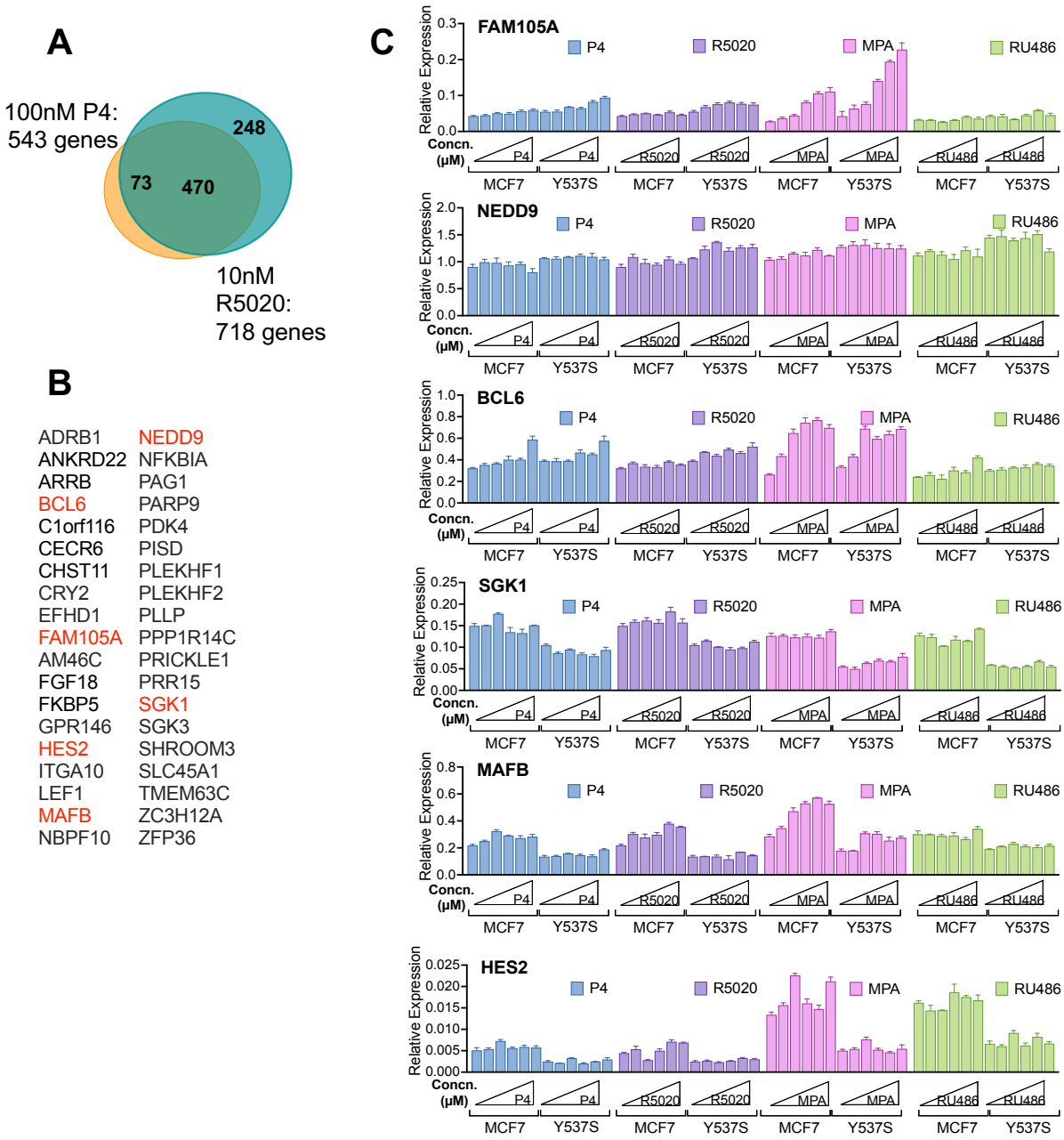


Figure 3.10 Low PR activity in MCF7 cells suggested by PR target gene expression

(**A-B**) PR target genes as defined by Mohammed et al. 2015 (figures amended from Mohammed et al. 2015); (**A**) the overlap of genes regulated by 100nM P4 and 10nM R5020 (as determined by RNA-seq) in both T47D and MCF7 cell lines. (**B**) 38 genes were identified by Mohammed et al. as being differentially regulated by R5020/P4 and having a differentially regulated ER binding event within 10kb of the transcription start site. Genes in red were included in further studies for this thesis. (**C**) RT-qPCR using RNA extracted from MCF7 and MCF7-Y537S cells seeded in stripped media supplemented with 1nM 17β-Estradiol and treated with 0.001-10μM of PR ligand (using 10-fold increasing concentrations) for 16 hours. Error bars show the SEM and expression is shown relative to TBP. (n=3 biological RNA replicates)

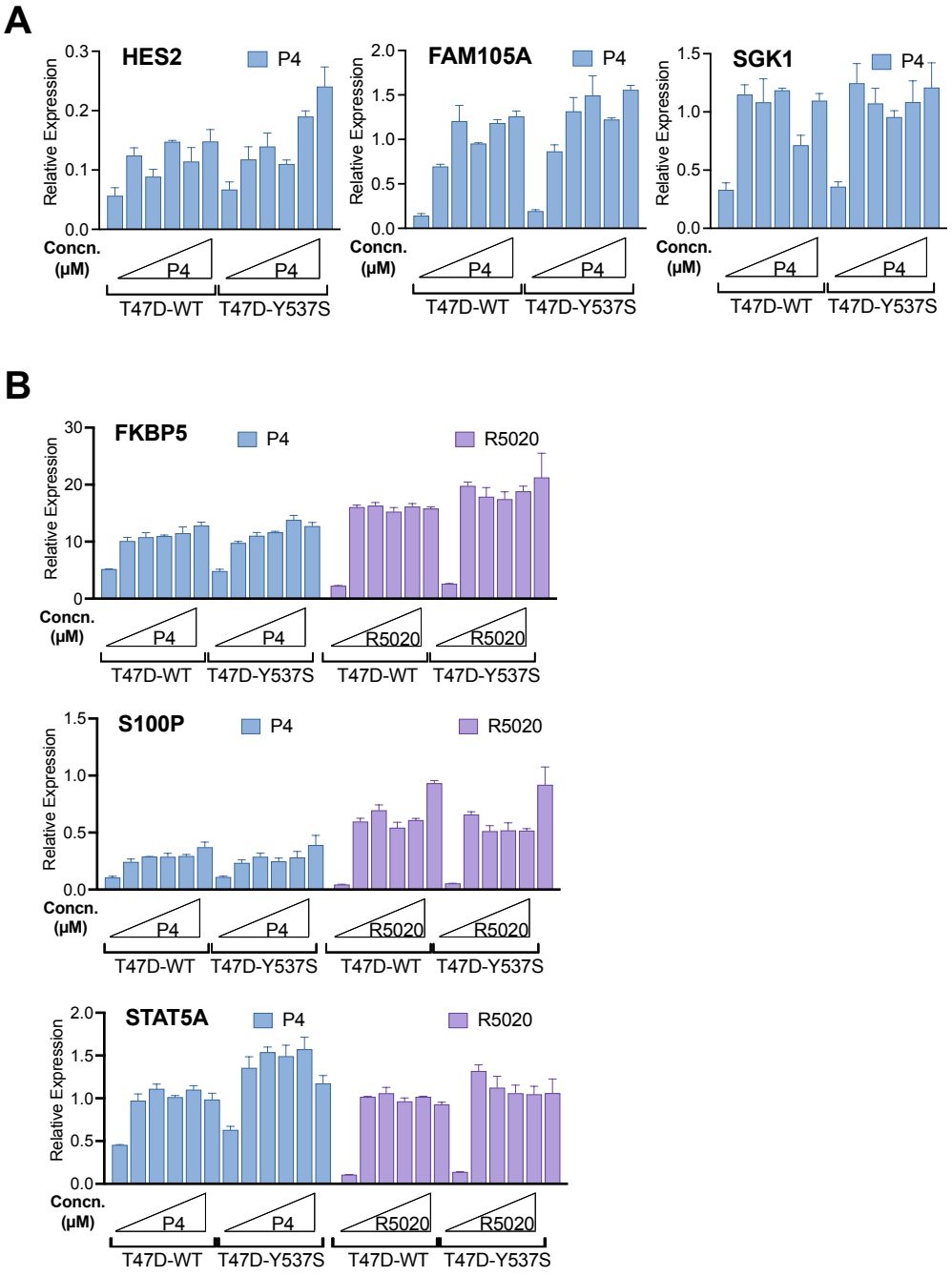


Figure 3.11 Expression of PR regulated genes suggests T47D-WT and T47D-Y537S cells are responsive to Progestin treatment

RT-qPCR using 3 biological RNA replicate preparations from T47D-WT or T47D-Y537S cells treated with vehicle control, or 0.001 - 10μM (with 10-fold increasing concentrations) P4 (**A-B**) or R5020 (**B**) for 8 hours in phenol red-free media supplemented with 10nM 17β-Estradiol. Expression shown is relative to TBP, error bars show the SEM.

3.3.2 Optimisation of conditions for RNA-seq to identify PR regulated gene expression in T47D-Y537S cells

As expected, the T47D-Y537S cells show E2-independent growth (Figure 3.3), but despite the large increase in *PGR* levels in T47D-Y537S cells, there is only a very limited effect of PR agonists and antagonists on cell growth or expression of well-known PR target genes. RNA-sequencing (RNA-seq) provides the opportunity to determine gene expression differences between breast cancer cells expressing WT and mutant *ESR1*. Indeed, previous work from the laboratory has shown that E2-regulated gene expression is elevated in the absence of E2 in MCF7 cells expressing Y537S (Harrod et al. 2017). To determine if Y537S expression in T47D cells similarly impacts ER-regulated gene expression, I undertook RNA-seq analysis using the T47D and T47D-Y537S cells with and without 10nM E2. As *PGR* is greatly upregulated in T47D-Y537S cells, and even though the over-expression appears to have only a small effect on cell growth, I investigated the effect of treatment with the PR ligands P4 and R5020. Finally, I performed RNA-seq using cells grown in full medium, wherein stable gene expression profiles can be established.

After testing a range of different seeding densities (100,000, 200,000, 300,000 and 400,000 cells/well) a seeding density of 100,000 cells/well was selected for the experiment performed in full media and 150,000 cells/well for the experiments conducted in E2-depleted media (data not shown). A time-course RT-qPCR experiment was used to determine the optimal treatment time with E2. For this, T47D-WT and T47D-Y537S cells were treated with 10nM E2 or vehicle control for 4, 8 or 24 hours (Figure 3.12A). Maximal induction of the ER target genes, *PGR* and *GREB1*,

was seen for the 8-hour treatment with E2, so this was selected as the duration of E2 treatment for the RNA-seq.

Optimisation of the concentration and duration of progestogen treatment was also carried out, where P4 or R5020 were added, in the presence or absence of E2. As *PGR* is an E2-regulated gene, treatment with E2 (prior to the addition of progestogen) was performed to ensure that expression levels of *PGR* were sufficient for progestogen-responsiveness of the cells, especially in the T47D-WT line with its lower *PGR* levels. Therefore, T47D-WT and T47D-Y537S cells were seeded in 6-well plates either with charcoal-stripped FCS containing media for 80 hours, before 10nM E2 was added for a further 16 hours (Figure 3.13A) or with E2-depleted media supplemented with 10nM E2 for 96 hours (Figure 3.13B). Given that in previous experiments, maximal PR target gene expression was seen following 1nM P4 or R5020 treatment (chapter 3.3.3), cells were treated with either 0.01, 0.1 or 1nM P4 or R5020 for either 3 or 8 hours (Figures 3.13A-B) before RNA was prepared for RT-qPCR. *SGK1* expression was observed to be maximal with 1nM P4 or 1nM R5020 with either 16 or 96 hours of E2 pre-treatment for both T47D-WT and T47D-Y537S cell lines. 3 hours of progestogen treatment appeared just as sufficient as 8 hours in stimulating *SGK1* expression. Therefore, pre-treatment with 10nM E2 for 16 hours and a dose of 1nM P4/R5020 treatment for 3 hours were selected as timepoints and doses for the planned RNA-seq. 1nM of both PR ligands was selected as the treatment dose, as the lowest dose that produced the greatest stimulation of target gene expression based on the data from Figures 3.11 and 3.13.

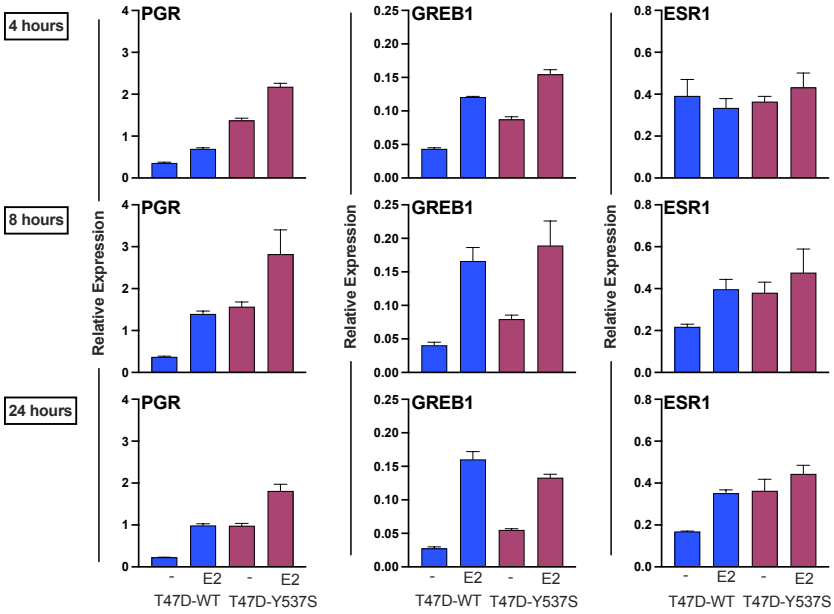


Figure 3.12 Optimisation of treatment conditions for RNA-seq experiment using 10nM 17β-Estradiol

RT-qPCR with RNA extracted from T47D-WT or T47D-Y537S cells deprived of estrogen for 72 hours, then treated with vehicle control or 10nM 17β-Estradiol for 4, 8 or 24 hours. Expression shown is relative to TBP, error bars show the SEM. RNA was harvested from 3 biological replicates.

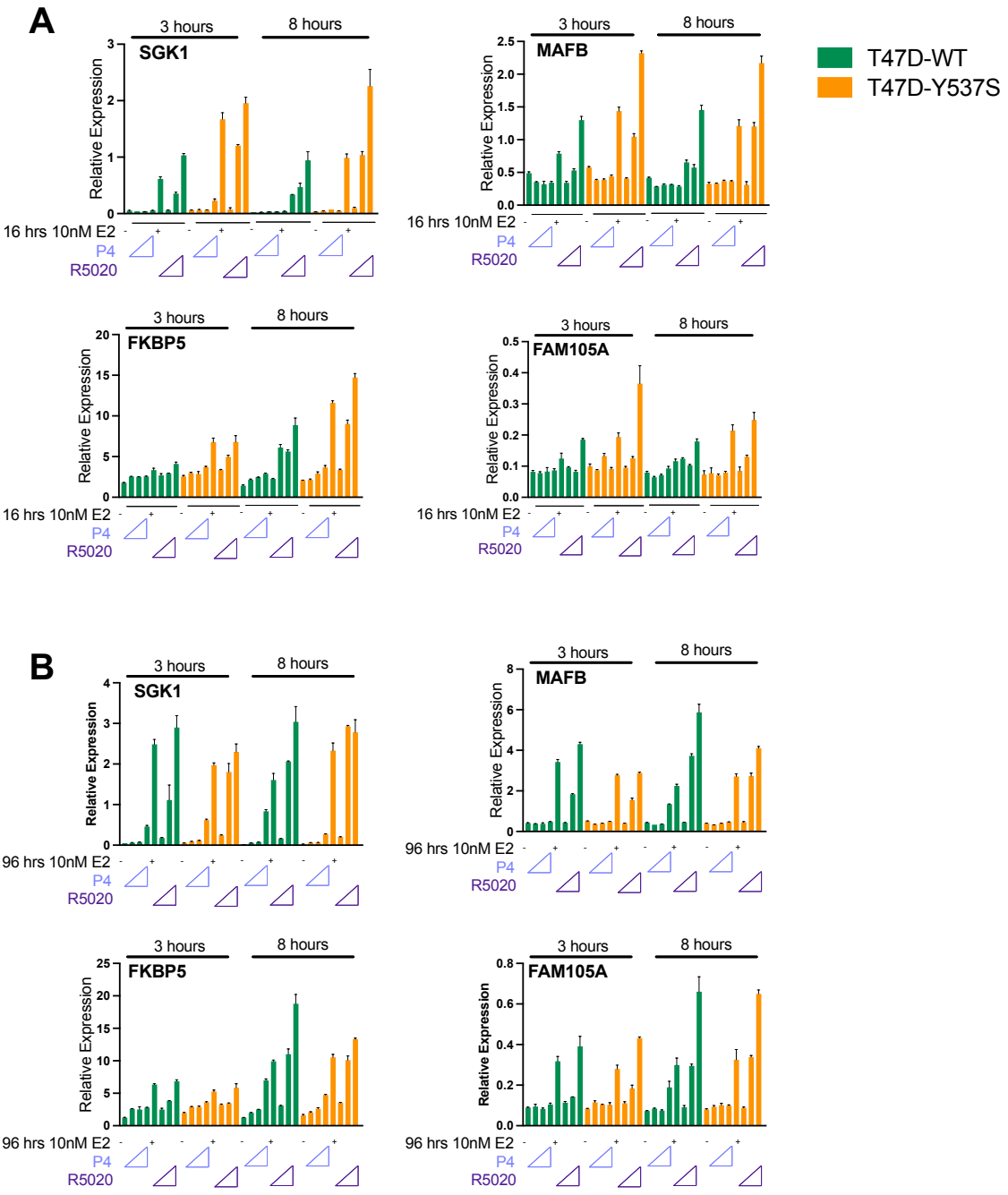


Figure 3.13 Optimisation of treatment conditions for RNA-seq experiment using P4 and R5020

(**A-B**) RT-qPCR with RNA extracted from T47D-WT or T47D-Y537S cells that were treated with 0.01, 0.1 or 1nM P4 or R5020 for either 3 or 8 hours. Cells were either E2 depleted for 80 hours then treated with 10nM 17β-Estradiol for 16 hours (**A**) or treated with 10nM 17β-Estradiol for 96 hours (**B**) prior to treatment with P4 or R5020. Expression shown is relative to TBP, error bars show the SEM. (n=1 biological replicate)

3.3.3 T47D-Y537S cells show ligand-independent expression of E2-regulated genes

RNA-seq using RNAs prepared from cells cultured in full medium was used to compare global gene expression patterns in T47D-WT and T47D-Y537S cells. For identifying E2 and progestogen responsive genes, cells grown in E2-free medium were treated with E2 for 8 hours, as described in chapter 3, section 3.4. Once RNA was extracted and quantified using the Nanodrop^{TM} ND-1000, RT-qPCR for ER target genes (*PGR* and *GREB1*) was performed to confirm the suitability of these RNAs for RNA-seq. Analysis of RNA-seq bioinformatics methods to determine the appropriate number of biological replicates required for robust identification of gene expression differences recommends the use of six biological replicates per condition, employing DEseq2 with fold change cut-off (Schurch et al. 2016). The minimum number of biological replicates rises to 12 for detection of all differential genes (no fold change cut-off). In line with this, I undertook RNA-seq using six independent RNA replicates, following the pipeline in Figure 3.14. The number of read counts obtained from each sample and their alignment (%) to the reference genome is detailed in Appendix II. Analysis was undertaken using the R package DESeq2. Genes with a log2 fold change ≥0.632 or ≤-0.632 (which equates to a fold change ≥1.55 or ≤-1.55) with an adjusted p-value of <0.05 were defined as differentially regulated.

<u>RNA-seq with T47D-WT and T47D-Y537S cells in Full Media</u>

The Principal Component Analysis (PCA) was calculated for the T47D-WT and T47D-Y537S samples in full media using DESeq2 (Figure 3.15A). Clustering was evident for the replicates within each line but not between the two lines, indicating that there are differential gene expression patterns between the T47D WT and mutant cells. Three

thousand, four hundred and seventy-two genes were differentially regulated between the two lines in full media, with 207 genes meeting the threshold for upregulation (log2 fold change ≥0.632 (linear FC ≥1.5), padj <0.05) and 115 for downregulation (log2 fold change ≤-0.632 (linear FC ≤-1.5), padj <0.05) (Figure 3.15B). Gene set enrichment analysis (GSEA) showed a strong enrichment in E2 responsive genes, with 'Estrogen Response Early' and 'Estrogen Response Late' identified as the two most significant and strongly enriched Hallmark pathways (Figure 3.15C). The 3,417 genes differentially regulated in the T47D-Y537S line compared to the T47D-WT in full media (padj <0.05) are enriched in the genes from the 'Hallmark Estrogen response Early' and 'Hallmark Estrogen response Late' pathways (299 in total) (Figure 3.15D, Appendix III). Some of the genes found to be the most significantly differentially expressed in the T47D-Y537S cells have previously been reported in the literature as being E2-downregulated (*CLU* and *EPAS1*) and E2-upregulated (*OLMFL3*) (Harvell et al. 2006; Korkmaz et al. 2019; Fuady et al. 2016; Buterin et al. 2006), in keeping with the findings of this study (Figure 3.15B). Altogether it is clear that expression of the ER-Y537S mutation leads to considerable alteration in E2-responsive gene expression (Figure 3.12).

RNA-seq with E2-treated T47D-WT and T47D-Y537S cells

PCA of the T47D-WT and T47D-Y537S samples treated either with vehicle or 10nM E2 showed tight clustering of all replicates, showing that the different biological replicates are very similar (Figure 3.16A). Cells grown in full media clearly clustered away from cells grown in E2-depleted media. There was also evidence of segregation of the T47D-Y537S cells away from the T47D-WT. Furthermore, samples clustered according to treatment type, with vehicle- and E2-treated samples segregating away

from each other. Indeed, it is evident that E2 treatment brings the T47D-WT line closer to the T47D-Y537S cells, which, by virtue of the Y537S mutation, possess ER activity in the absence of E2.

Two thousand, seven hundred and seventy-three genes were differentially regulated by E2 in the T47D-WT line compared to just 1,504 in the T47D-Y537S, likely due to the elevated expression of many E2-regulated genes in T47D-Y537S cells. Seventy-five percent of the genes regulated by E2 in the T47D-Y537S line were also E2-regulated in the T47D-WT line (Figure 3.16B). Conversely, only 40% of the E2-regulated genes in T47D-WT cells were also E2-responsive in the T47D-Y537S line. This may reflect the E2 independence of the T47D-Y537S cells. Genes that were differentially regulated by E2 in each cell line, and genes that were vehicle- or E2-regulated in the T47D-Y537S cells relative to the T47D-WT were analysed. Several *bona fide* ER target genes (e.g. *CXCL12, EPAS1, CLDN1, PGR* and *GREB1*) are among the most significantly differentially regulated between vehicle-treated T47D-WT and T47D-Y537S cell lines (Figure 3.16C). Using *CXCL12, PGR, GREB1* and *CDC20B* as specific examples, the significance and magnitude of differential expression was considerably reduced between the T47D WT and Y537S lines after both were treated with E2 (Figure 3.16D). This is in keeping with the PCA results, where E2 treatment of T47D-WT cells reduces the variance (PC2) between these and the vehicle-treated T47D-Y537S samples (Figure 3.16A). Of note, however, the numbers of genes up- and down-regulated between the T47D-WT and T47D-Y537S cells were similar following both vehicle and E2 treatment. In vehicle conditions, 395 genes were downregulated and 299 upregulated, while in E2 treated cells 353 were downregulated and 226 upregulated. Although E2 treatment brings the expression

levels of some E2-regulated genes in the T47D-WT line closer to those seen in T47D-Y537S cells, it appears that other genes may be differentially regulated between the two lines by the addition of E2. In keeping with the greater E2-responsiveness of the T47D-WT cells, a larger number of genes were regulated by E2 than in the T47D-Y537S cells. In T47D-WT E2 treatment resulted in 80 genes downregulated and 185 upregulated, whereas only 44 genes were downregulated and 101 genes upregulated in T47D-Y537S cells (Figure 3.16E-F). Moreover, the E2 induction of many ER target genes (e.g. *CXCL12, PGR, GREB1*) was greater in T47D-WT cells than in the T47D-Y537S cells, while these genes were upregulated in vehicle-treated T47D-Y537S cells, compared with T47D-WT cells (Figures 3.16E-F). Altogether, many E2-responsive genes were upregulated in T47D-Y537S cells in the absence of E2, with lower E2 stimulation in T47D-Y537S cells than in T47D-WT cells. Hence, the E2-independence conferred by the Y537S mutation results in reduced E2-responsiveness in comparison to the T47D-WT cells.

The majority of the genes differentially expressed following the addition of E2 in both the T47D-WT and T47D-Y537S lines were up- rather than downregulated (70% of differentially expressed genes were upregulated in each line). Comparing the up-regulated genes showed that 92 genes were upregulated solely in the T47D-WT line, compared to just 8 up-regulated only in the T47D-Y537S (log2 fold change ≥0.632, padj <0.05) (Figure 3.17A). In total, 93 genes were upregulated by E2 in both T47D-WT and T47D-Y537S cells. This group included genes that are well-documented as being E2-regulated, including *CXCL12, PGR, GREB1* and *PDZK1*. GSEA was performed for these 93 genes using the Hallmark, Curated MsigDB and Gene Ontology Molecular Function datasets (Pathways enriched can be found in Appendix

III). E2 response and steroid hormone/NR activity pathways were strongly enriched in these datasets, confirming that E2 responsiveness is predominant in this set of 93 genes (Figure 3.17B).

Two hundred and ninety-five genes that were up- or downregulated (log2 fold change ≥0.632 or ≤-0.632, padj <0.05) by E2 in both T47D WT and Y537S cell lines were identified. Of these, 150 were E2-regulated in the T47D-WT cells only, 30 in the T47D-Y537S clone only and 115 in both cell lines (Figure 3.18A). All 295 genes were studied through hierarchical cluster analysis (Figure 3.18B). Four separate clusters were formed from these 295 genes (genes in each cluster are listed in Appendix IV). Cluster 1 contained 36 genes that were downregulated by E2, to a greater extent in the T47D-WT line than in the T47D-Y537S. Cluster 4 was small, containing just 10 genes which exhibited increased expression following E2 treatment, more notably in the T47D-WT line. The 66 genes in cluster 3 were downregulated by E2. *CITED2* is inhibited by E2 in the T47D-WT line but was already downregulated in the absence of E2 in T47D-Y537S cells relative to T47D-WT. The addition of E2, further inhibited the expression of *CITED2* in the T47D-Y537S cells. The largest cluster, cluster 2, contained 183 genes with the highest and most significant increase in expression levels following E2 treatment. Cluster 2 featured classical ER target genes such as *PGR, CXCL12* and *EGR3*. As in the case of cluster 4, the T47D-Y537S cells exhibited reduced E2-sensitivity, demonstrated by a smaller increase in expression of these genes with E2 treatment (demonstrated clearly by *PGR*) relative to the T47D-WT line. However, unlike *SYBU* in cluster 4, PGR expression was greater in full media than in E2-depleted media for both T47D-WT and T47D-Y537S cells.

The effects of E2 on global gene expression in T47D WT and in a pool of 2 different T47D-Y537S mutant clones have been published (Bahreini et al. 2017). Although Bahreini et al. 2017 performed RNA-seq using RNA derived from cells treated with a lower dose of E2 (1nM vs 10nM) and used a longer treatment duration (24 vs 8 hours) than opted for in this study, this still provides a valuable resource for validation of the findings presented in this chapter. A comparison of these datasets was therefore performed. Here I have distinguished these cells from our cells by the addition of the suffix “SO” (Prof Steffi Oesterreich lab). Overall, 3,153 genes were differentially expressed (padj <0.05) by E2 treatment in both T47D-WT and T47D-Y537S cells in my study (Figure 3.19A). A much larger number of genes (9,271) were E2-regulated (padj <0.05) in both the T47D-WT.SO and T47D-Y537S.SO cells (Figure 3.19B). This was unexpected, especially given that Bahreini et al. used a 10-fold lower dose of E2, but it may reflect the clonal nature of these cell lines and the fact that fewer replicates were used (4 vs 8). It may also reflect the longer treatment time with E2 (24 vs 8 hours) as, when comparing samples from my own data treated with 10nM E2 for either 8 hours (Figure 3.14) or, as detailed in section 3.3.6, 16 hours (Figure 3.20), a greater number of genes are E2-regulated at 16 hours. For example, in the T47D-WT line, 756 genes were differentially regulated by 16 hours of E2 treatment but only 265 by 8 hours of E2 treatment. The majority of genes regulated by E2 (padj <0.05) in the T47D-Y537S and T47D-Y537S.SO lines were differentially regulated in the parental T47D lines (T47D-WT and T47D-WT.SO) in both studies (74.8% in this study and 86.7% in the findings of Bahreini et al. 2017) (Figures 3.19A-B). 74.8% of genes regulated by E2 (padj <0.05) in the T47D-WT line were also E2-regulated in the T47D-WT.SO line (Figure 3.19C). A smaller proportion (56.2%) of genes differentially expressed by E2 (padj <0.05) in the T47D-Y537S line were also E2-induced in the T47D-Y537S.SO line

(Figure 3.19D). The clonal nature of the T47D-Y537S and T47D-Y537S.SO lines (both generated using CRISPR genome-editing) and therefore potential differences between them, may explain the reduction in overlap of differentially expressed genes relative to the T47D-WT and T47D-WT.SO cells. Bahreini et al. 2017's data revealed 8,338 genes that were differentially expressed (padj <0.05) between vehicle-treated T47D-WT.SO and vehicle-treated T47D-Y537S.SO cells. Two hundred and ninety-nine genes were upregulated (log2 fold change ≥0.632, padj <0.05) in vehicle-treated T47D-Y537S cells relative to vehicle-treated T47D-WT in this study. Enrichment analysis was performed for these 299 upregulated genes in the 8,338 genes identified to be differentially expressed in the vehicle-treated T47D-Y537S.SO cells by Bahreini et al. 2017 (Figure 3.19E). This revealed very strong enrichment of these genes, with a normalised enrichment score (NES) of 3.97. Enrichment analysis was also undertaken for the 395 genes downregulated (log2 fold change ≤-0.632, padj <0.05) in vehicle-treated T47D-Y537S cells relative to vehicle-treated T47D-WT using the same 8,338 gene set from Bahreini et al. 2017 (Figure 3.19F). Again, enrichment was very clear for these genes repressed in the T47D-Y537S line relative to the T47D-WT, with a NES of -3.78.

Therefore, in keeping with the data from the MCF7 and MCF7-Y537S cells performed by Harrod et al. 2017, E2-independent expression of many ER target genes is observed in the T47D-Y537S line. The patterns of gene expression seen here in E2-treated T47D-WT and T47D-Y537S cells also reflects those previously published in other clones of these cell lines (Bahreini et al. 2017).

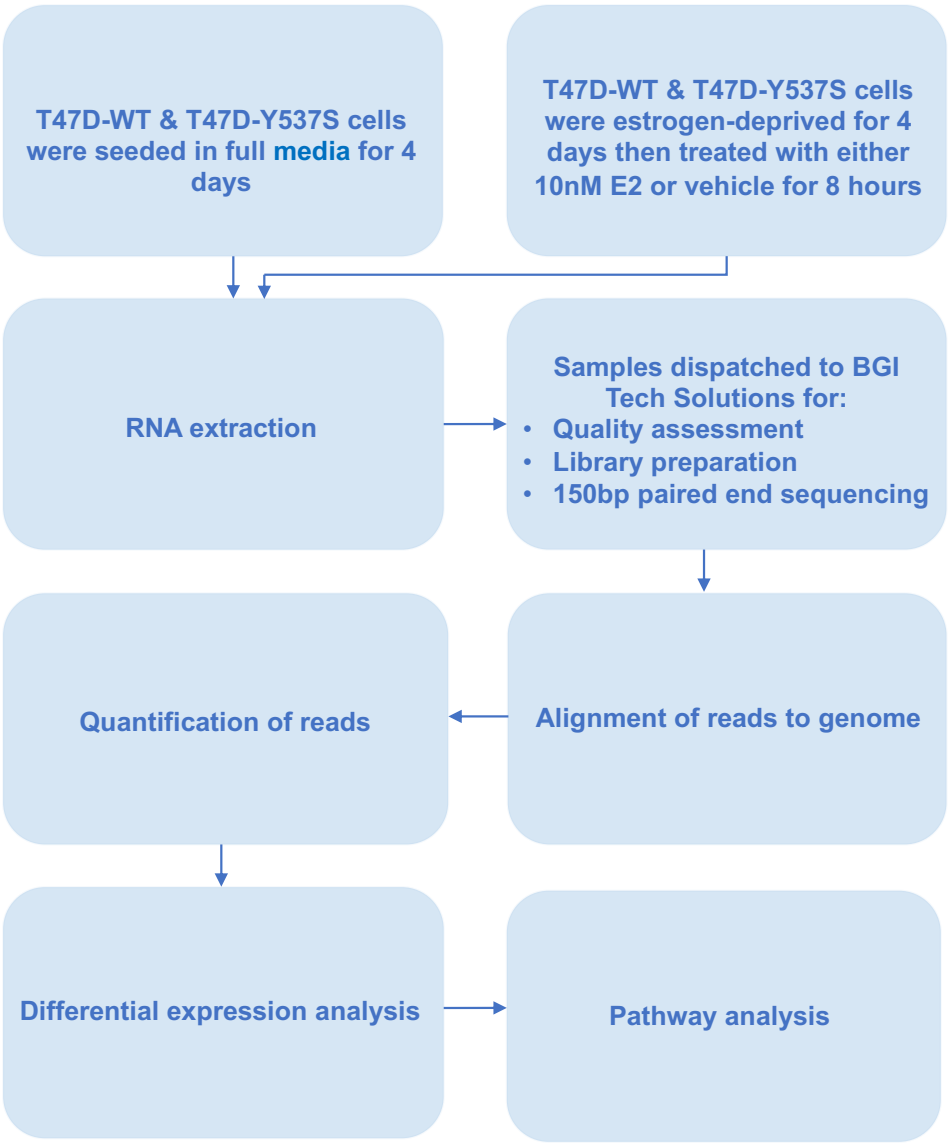


Figure 3.14 Flowchart detailing RNA-seq pipeline

RNA-seq was performed using RNA harvested from T47D-WT and T47D-Y537S cells grown either in full media or in hormone-deplete media treated with 10nM 17β-Estradiol or vehicle control for 8 hours.

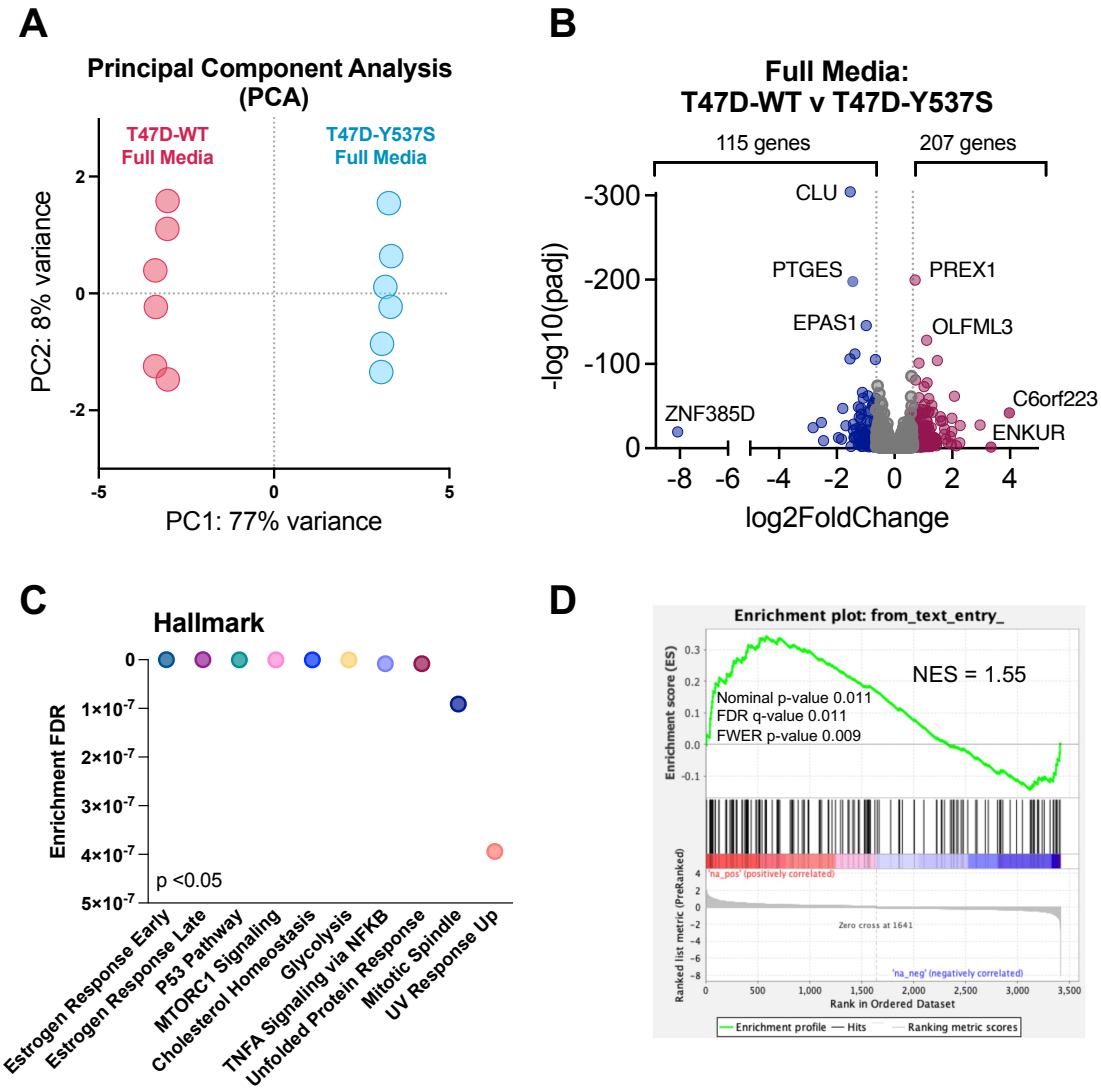


Figure 3.15 Estrogen response pathways are enriched in T47D-Y537S cells in full media RNA-seq was carried out on estrogen-deprived T47D-WT and T47D-Y537S cells cultured in full media using 6 independent biological replicate RNA samples. (**A**) Principal component analysis (PCA) plot generated using calculations from DESeq2 and showing clustering of T47D-WT and T47D-Y537S replicates based on normalized read counts. (**B**) Volcano plot showing the differential gene expression between the T47D-WT and T47D-Y537S lines in full media (padj <0.05). (**C**) Gene set enrichment analysis (GSEA) showing the 10 most significantly enriched Hallmark pathways for all 3417 genes differentially expressed between the wildtype and mutant lines in full media (p<0.05). (**D**) Enrichment of the 3417 genes differentially expressed between the T47D-WT and T47D-Y537S cells in full media (p<0.05) in the 299 genes in the 'Hallmark Estrogen Response Early' and 'Hallmark Estrogen Response Late' pathways.

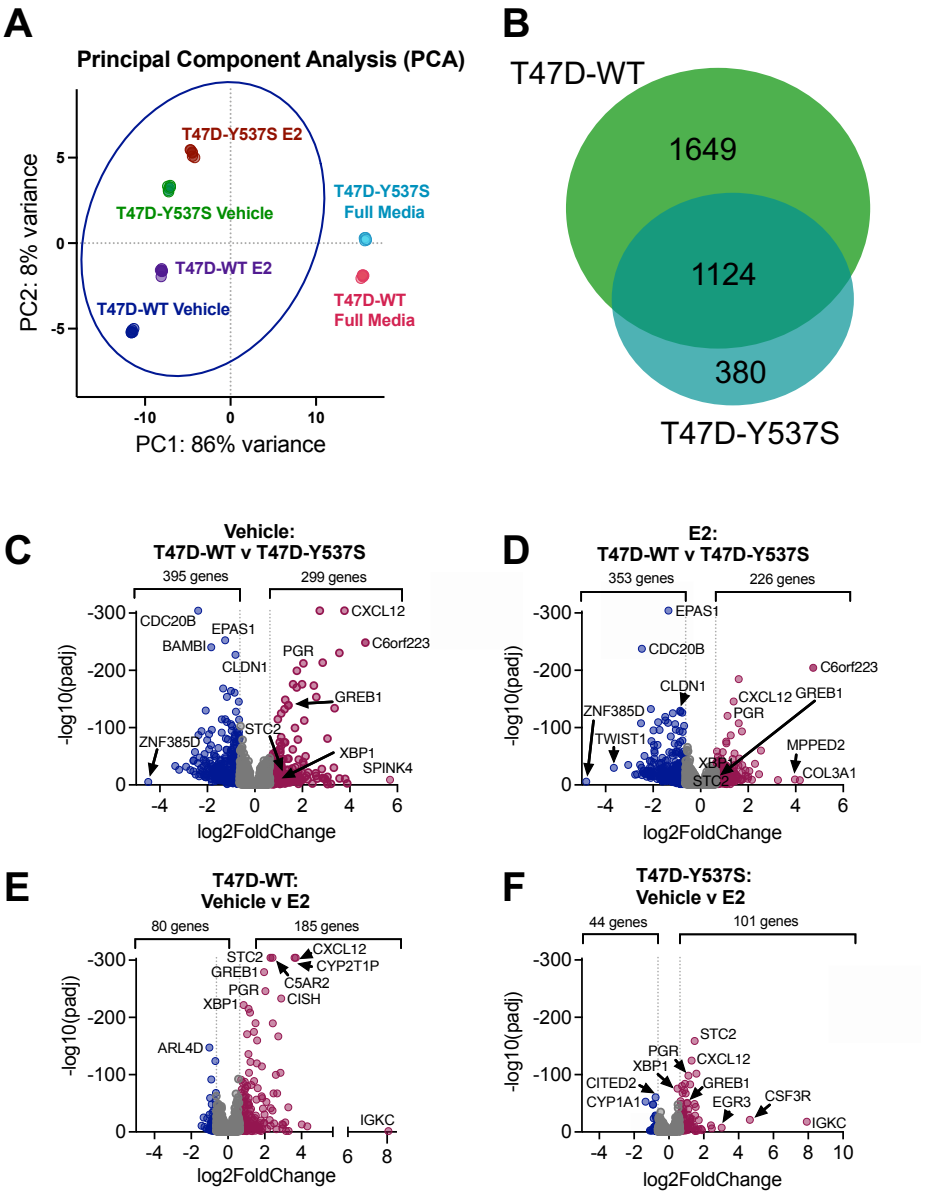


Figure 3.16 ER target genes are differentially expressed in T47D-Y537S cells in hormone deplete conditions

RNA-seq was carried out on estrogen-deprived T47D-WT and T47D-Y537S cells treated with either vehicle control or 10nM 17β-Estradiol for 8 hours (n= 6 independent replicates). (**A**) Principal Component Analysis representing clustering of these samples (encircled), alongside samples from the same lines cultured in full media. (**B**) Venn diagram displaying all differentially expressed genes (padj <0.05) following 10nM 17β-Estradiol treatment in both cell lines. (**C-F**) Volcano plots showing the differential gene expression with 17β-Estradiol in T47D-WT cells (**C**) and T47D-Y537S cells (**D**) and between the T47D-WT and T47D-Y537S lines following vehicle (**E**) and 17β-Estradiol treatments (**F**) (padj <0.05).

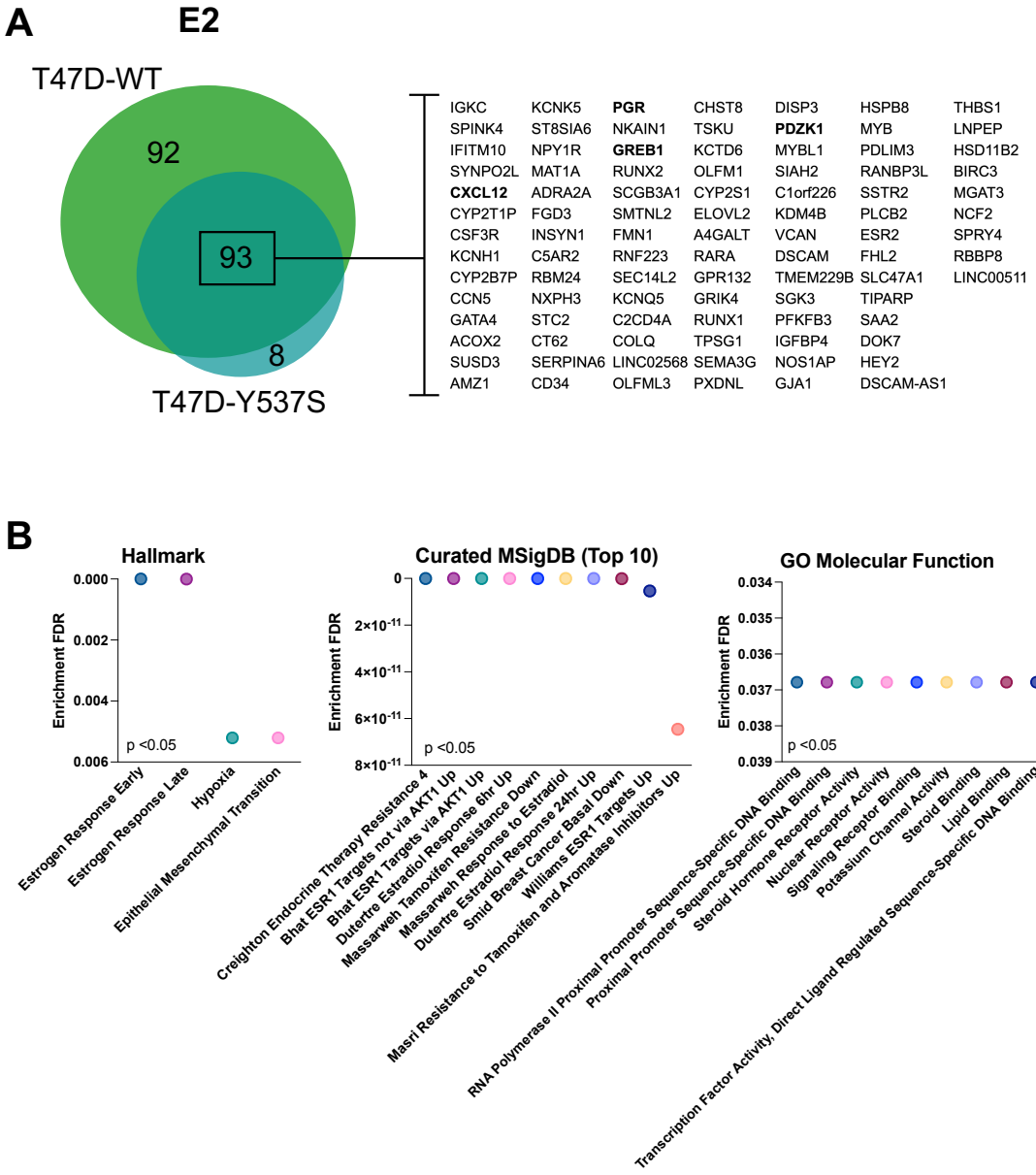


Figure 3.17 Estrogen pathways are enriched in both T47D-WT and T47D-Y537S 17β-Estradiol treated cells

(**A**) Venn diagram illustrating the genes that are upregulated by 17β-Estradiol treatment in T47D-WT and T47D-Y537S cells. Genes with a log2 fold change ≥0.632 and padj <0.05 are included. 93 genes are upregulated in both lines following 17β-Estradiol treatment. Genes shown in bold are *bone fide* ER target genes (**B**) GSEA pathways (Hallmark, Curated MSigDB (10 most significant pathways shown) and GO Molecular Function) that are significantly enriched for these 93 genes (p<0.05) are shown.

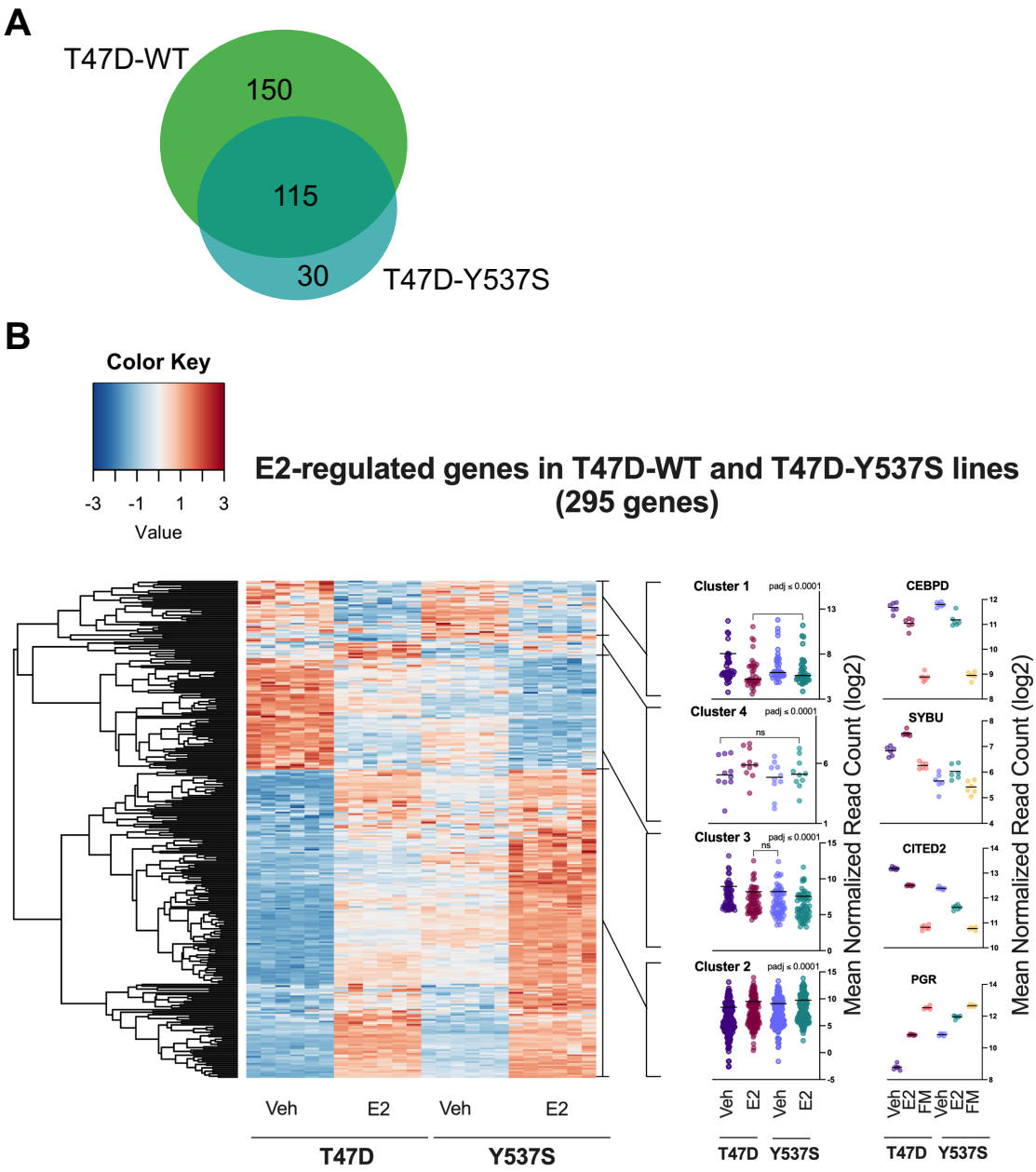


Figure 3.18 Cluster analysis of the 295 differentially expressed genes in T47D-WT and T47D-Y537S cells treated with 17β-Estradiol

(**A**) Venn diagram illustrating the genes that are differentially expressed by 17β-Estradiol treatment in T47D-WT and T47D-Y537S cells. Genes with a log2 fold change ≥0.632 and ≤-0.632 with padj <0.05 are included. (**B**) Heatmap illustrating hierarchical cluster analysis of these 295 genes. Cluster charts show the mean normalised read count of the genes within each cluster, with an example gene illustrated adjacent to each cluster. RNA-seq performed with independent biological RNA samples. Abbreviations – Veh: vehicle, E2: estrogen, FM: full media.

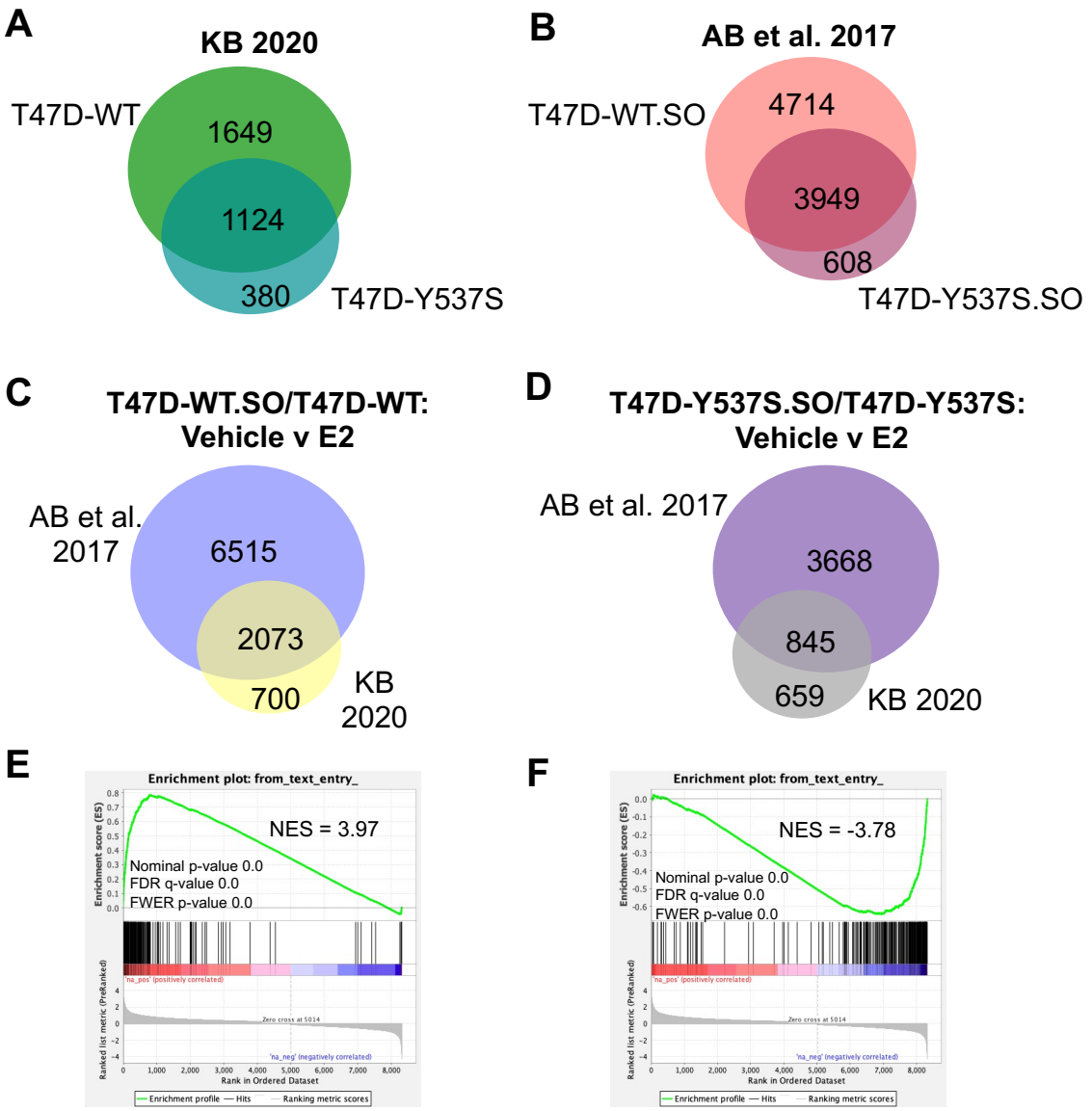


Figure 3.19 The patterns of gene expression in T47D-WT and T47D-Y537S cells are in keeping with previously published data

(**A-D**) Venn diagrams illustrate the genes that are differentially expressed in T47D-WT and T47D-Y537S cells by 10nM 17β-Estradiol treatment in this study (KB 2020) (**A**) and in T47D-WT.SO and T47D-Y537S.SO cells by 1nM 17β-Estradiol as performed by Bahreini et al. 2017 (AB ett al. 2017) (**B**). The overlap in the genes regulated by 17β-Estradiol in the T47D-WT and T47D-WT.SO lines (**C**) and T47D-Y537S and T47D-Y537S.SO lines (**D**) in both studies are shown. All genes with padj <0.05 are included. (**E-F**) Enrichment of the 299 genes upregulated (**E**) and 395 genes downregulated (**F**) in vehicle-treated T47D-Y537S v vehicle-treated T47D-WT cells in this study (log2 fold change ≥0.632 or ≤-0.632, padj <0.05), in the 8,338 geneset identified as differentially regulated in the T47D-Y537S.SO v T47D-WT.SO cells by Bahreini et al. 2017 (padj <0.05).

3.3.4 The Y537S mutation confers greater sensitivity to PR ligands

The effect of progestogens on the transcriptome of T47D-WT and T47D-Y537S cells was analysed through RNA-seq, following the pipeline in Figure 3.20. Cells were seeded in E2-depleted media for 80 hours then treated with 10nM E2 or vehicle for 16 hours. Either 1nM P4, 1nM R5020 or vehicle was then added for a further 3 hours. As per the previous RNA-seq experiment (chapter 3, section 3.5) RNA was harvested from 6 independent replicates for each treatment condition, and RT-qPCR performed for genes confirmed to be PR-regulated in chapter 3, section 3.3 (MAFB, SGK1) to ensure samples were suitable for sequencing. The number of reads for each sample and alignment (%) of these reads to the reference genome can be found in Appendix II. DESeq2 was again used to identify differentially expressed genes between the treatment conditions and cell lines, and genes were considered differentially expressed with log2 fold change ≥0.632 or ≤-0.632 and adjusted p-value <0.05.

Reassuringly, PCA, performed using DESeq2, showed tight clustering of replicates confirming the similarity of the biological replicates (Figure 3.21A). The E2-treated samples for both the T47D-WT and T47D-Y537S cells cluster away from the vehicle, progestogen- and (E2 + progestogen)-treated samples. Within each cell line, the samples treated with P4 and R5020 (in the absence of E2) clustered together and cells treated with P4 and R5020 (in combination with E2) also clustered together. However, the progestogen-treated and (progestogen+E2)-treated samples clustered away from each other for both cell lines. As seen in the PCAs previously described (Figures 3.15 and 3.16), T47D-WT and T47D-Y537S cells cluster apart from each other, with the exception of the vehicle-treated T47D-Y537S, (E2+P4)-treated T47D-WT and (E2+R5020)-treated T47D-WT cells which interestingly cluster very closely

together. Indeed, the vehicle-treated T47D-Y537S samples cluster directly in the middle of the (E2+P4)- and (E2+R5020)-treated T47D-WT samples. This indicates there are strong similarities in the gene expression patterns for these samples.

Genes that were up- or down-regulated (log2 fold change ≥0.632 or ≤-0.632, padj <0.05) in each cell line by P4 (Figure 3.21B), R5020 (Figure 3.21C), (P4+E2) (Figure 3.21D) and (R5020+E2) (Figure 3.21E) were identified. For each progestogen, with or without the addition of E2, a greater number of genes was regulated in the T47D-Y537S clone than in the T47D-WT cells. For example, in vehicle-treated cells 357 genes were R5020 regulated in the T47D-Y537S line but only 99 in the T47D-WT cells (Figure 3.21C). The majority of P4 and R5020 regulated genes in T47D-WT cells were also regulated by these progestogens in T47D-Y537S cells. The E2-independence and elevated *PGR* levels in T47D-Y537S cells is likely responsible for greater numbers of progestogen-regulated genes in T47D-Y537S cells. This differs from the effect seen with E2 treatment only, where less genes were differentially regulated in the T47D-Y537S line, which demonstrates E2-independence relative to the T47D-WT (Figure 3.16B). The inclusion of E2 further increased the number of P4 and R5020 regulated genes in the T47D-WT line. There was a 2.4-fold increase in the number of genes regulated in the T47D-WT line by (P4+E2) compared to P4 alone and a 2.0-fold increase in the genes regulated by (E2+R5020) compared to R5020 alone (Figure 3.21B-E). This effect was observed to a lesser extent in the T47D-Y537S cells where the number of genes regulated in this line by P4 was 1.3-fold lower than those regulated by (E2+P4). The difference observed between the T47D WT and Y537S mutant lines is likely due to the constitutive activity of ER in T47D-Y537S cells and the subsequent upregulation of *PGR* even in the absence of E2. This results in a T47D-

Y537S line that is already responsive to progestogens without E2 and the addition of E2 does not really increase sensitivity to P4/R5020 any further. In contrast, the T47D-WT line is dependent on E2 for ER target expression (including *PGR*) and therefore sensitivity to progestogens. The majority (75.0%) of genes regulated by P4 alone in T47D-WT cells were also P4-regulated in T47D-Y537S cells. 70.7% of the genes regulated by (E2+P4) in T47D-WT cells were also regulated by this treatment in T47D-Y537S. Similarly, the majority of genes (85.9%) regulated by R5020 in the T47D-WT line were also differentially expressed by R5020 in the -Y537S cells. 84.2% of the genes regulated by (E2+R5020) in the T47D-WT line were also differentially expressed by the same treatment in T47D-Y537S cells. Therefore, a greater number of genes are progestogen-regulated in the T47D-Y537S line than in T47D-WT cells and the majority of those that are P4 or R5020 regulated in the T47D-WT line, are also regulated by progestogens in T47D-Y537S cells. However, there are a substantial number of progestogen-regulated genes in T47D-Y537S cells that are not progestogen regulated in T47D-WT cells. For example, 142 and 156 genes were P4-regulated in T47D-Y537S cells, but not in T47D-WT cells.

Many well-known PR target genes are amongst those regulated by P4 and R5020 in both cell lines in this dataset. These include *FKBP5, KLF4, MAFB, NDRG1, PLK2, SGK1, STAT5A* and *SYBU*. The total number of genes regulated (both up- and down-regulated, log2 fold change ≥0.632 or ≤-0.632, padj <0.05) by R5020 in each line is greater than those regulated by P4. In the T47D-WT cells, 1,056 genes are R5020-regulated compared to 923 that are P4-regulated, and in the T47D-Y537S line 3,390 are R5020-regulated vs just 1,997 that are P4-regulated). When taking into account the log2 fold change cut-offs, this translates to 52 P4 regulated genes and 99 R5020

regulated genes (Figure 3.22A-B and C-D). In agreement with these findings, PR target genes such as *STAT5A, SGK1* and *NDRG1* are more strongly regulated by R5020 treatment compared to P4 in both the T47D-WT and T47D-Y537S cell lines (Figure 3.22A-B and C-D). This reflects the increased RBA for PR and potency of R5020 compared to P4 (section 1.8.1, Table 1.2) (Stanczyk et al. 2013). In the T47D-Y537S line, however, the levels of significance of some PR regulated genes such as *MAFB, FKBP5* and *KLF4*, which are already very significantly regulated by P4, does not increase further with R5020 treatment. This in contrast to the T47D-WT cells, where the level of significance these genes are differentially expressed with, increases with R5020 treatment compared to P4. This observed difference between the cell lines is most likely due to the upregulation of *PGR* in T47D-Y537S cells, rendering them more sensitive to P4 than T47D-WT cells. When the differential gene expression patterns following progestogen treatment are compared between the two lines (Figures 3.22A-C and 3.22B-D), more genes are regulated in the T47D-Y537S clone compared to the T47D-WT cells. P4 results in 52 genes being differentially expressed in T47D-WT cells vs 181 in the T47D-Y537S and R5020 regulates 99 genes in the T47D-WT line vs 357 in the T47D-Y537S. The level of significance that many PR target genes (e.g. *MAFB, KLF4, SGK1, NDRG1*) are differentially regulated at is also greater in the T47D-Y537S line than the T47D-WT with both P4 or R5020. Again, this observation is explained by the higher levels of *PGR* in the T47D-Y537S line and, therefore, its increased responsiveness to progestogens.

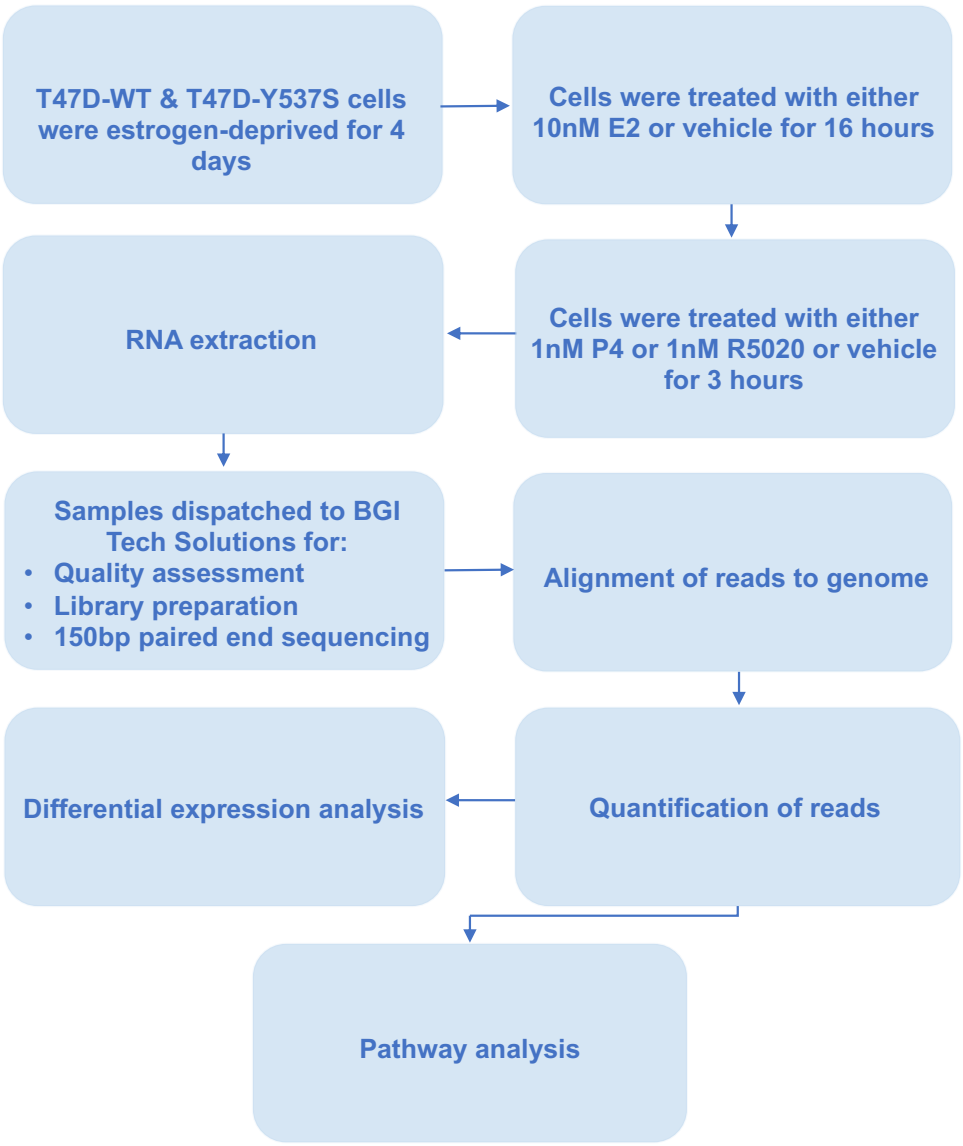


Figure 3.20 Flowchart detailing RNA-seq pipeline

RNA-seq was performed using RNA harvested from T47D-WT and T47D-Y537S cells treated with either 10nM E2 or vehicle for 16 hours and then either 1nM P4, 1nM R5020 or vehicle for 16 hours.

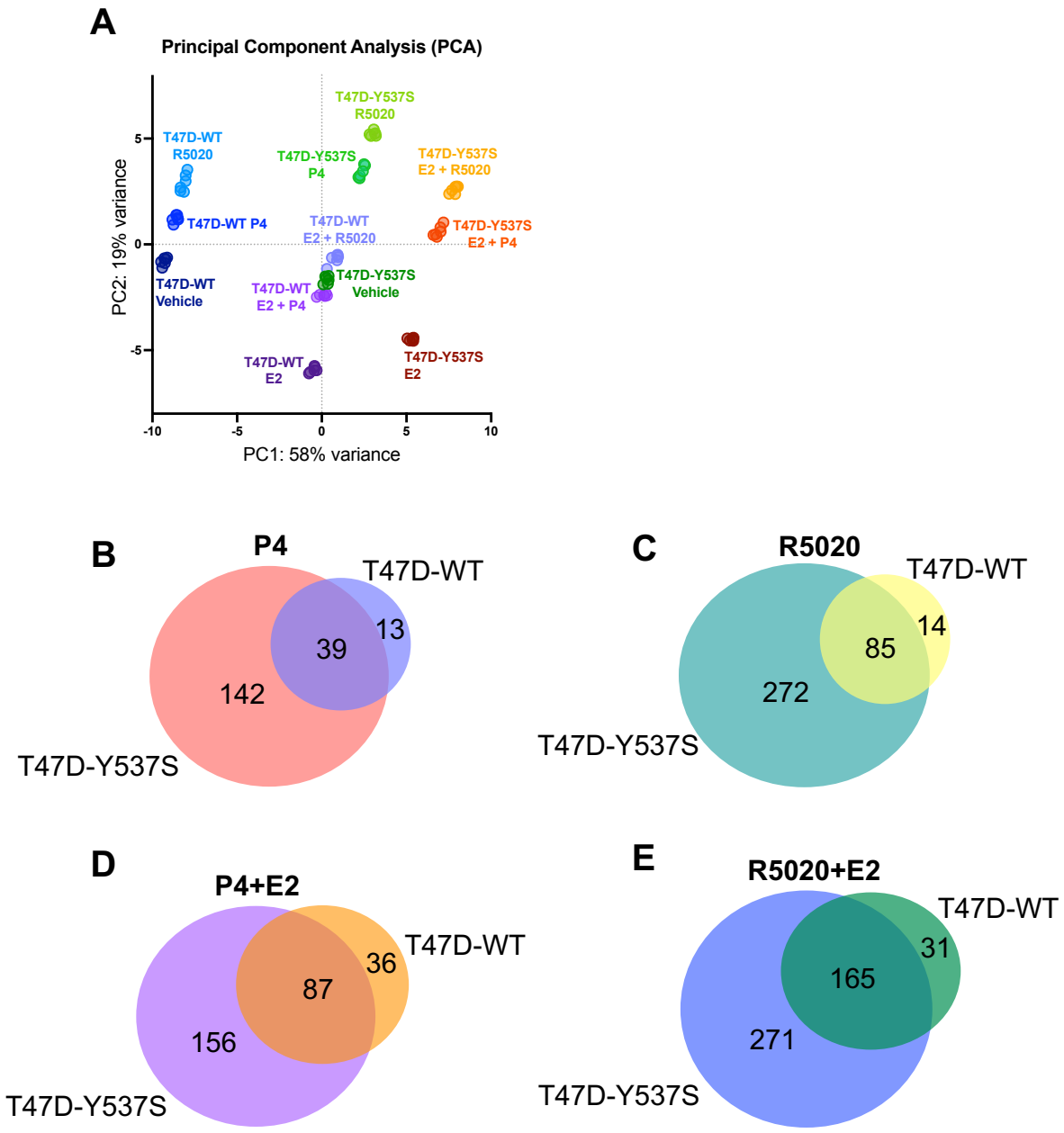


Figure 3.21 The majority of genes regulated by PR in the T47D-WT line are also regulated in the T47D-Y537S line

(**A-E**) RNA-seq was carried out on estrogen-deprived T47D-WT and T47D-Y537S cells treated with either vehicle, 1nM P4 or 1nM R5020 with or without 10nM 17β-Estradiol (n= 6 independent bioreplicates). (**A**) Principal component analysis. (**B-E**) Venn diagrams showing the number of genes differentially expressed in each line (log2 fold change ≥0.632 or ≤-0.632, padj <0.05) following treatment with 1nM P4 (**B**), 1nM R5020 (**C**), 1nM P4 and 10nM 17β-Estradiol (**D**) and 1nM R5020 and 10nM 17β-Estradiol (**E**).

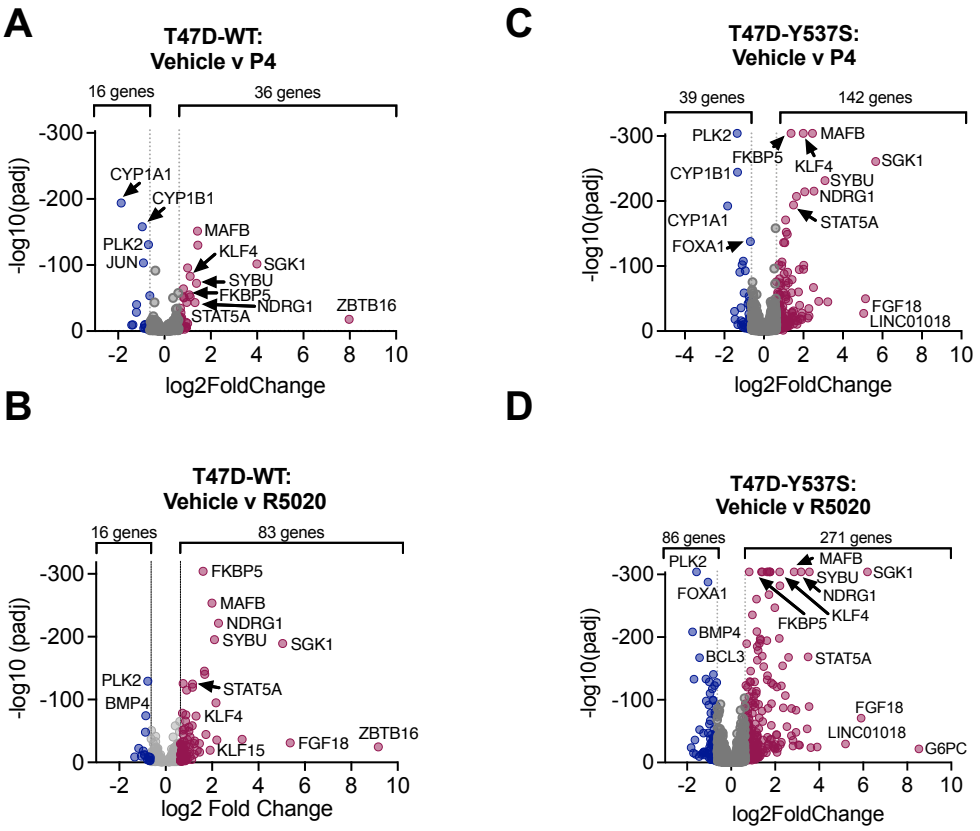


Figure 3.22 The magnitude and significance of PR target gene expression is greater with R5020 treatment relative to P4 and in the T47D-Y537S line relative to the T47D-WT

Volcano plots showing the differential gene expression in the T47D-WT line with 1nM P4 (**A**) and 1nM R5020 (**B**), and in the T47D-Y537S line with 1nM P4 (**C**) and 1nM R5020 (**D**). padj <0.05 for all genes plotted.

3.3.5 Most P4-regulated genes are also R5020-regulated

To focus my studies, I wanted to select one progestogen (either P4 or R5020) for further, extended investigation of the PR transcriptome. As discussed in section 3.3.6, most genes regulated by P4 or R5020 in the T47D-WT line were also regulated in T47D-Y537S cells and so the mutant line alone was used to select the best progestogen for use in further analysis. In the absence of E2, 92.8% of the genes regulated by P4 were also regulated by R5020 in T47D-Y537S cells (Figure 3.23A). The findings were similar for the progestogens in combination with E2; 90.5% of genes induced by (P4+E2) were also differentially expressed by (R5020+E2) in the T47D-Y537S line (Figure 3.23B). Therefore, analysis hereafter focuses on the effects of R5020 only.

Although RNA-seq with progestogen-treated ESR1 mutant cells has not been reported, Mohammed et al. (2015) have defined genes regulated by P4 and R5020 in T47D cells, which provides an opportunity for validation of the RNA-seq findings in the T47D-WT line in this thesis (Mohammed et al. 2015). In total, 3,163 genes were regulated by 1nM P4 or 1nM R5020 in combination with 10nM E2 in T47D-WT cells in this thesis (padj <0.05); 49.9% of which were regulated by both ligands (Figure 3.24A). Mohammed at al. 2015 showed that a larger number of genes (6,385) were regulated, albeit at higher doses of P4 (100nM) or R5020 (10nM) than used in the current study in 'estrogenic' media (padj <0.05). A much greater proportion of these genes (78.9%) were responsive to both ligands (Figure 3.24B). The higher doses of P4 and R5020 may be responsible for the greater number of progestogen-regulated genes the Mohammed et al. dataset. The larger dose of P4 (100nM) compared to R5020 (10nM) may explain the better overlap Mohammed at al. observed in the genes regulated by

both the progestogens, as the lower potency of P4 is somewhat compensated for by its dose being 10-fold higher than that of R5020. The genes differentially expressed by P4 in this study and those reported to be P4-regulated by Mohammed at al. 2015 were studied (Figure 3.24C); 55.7% of the genes regulated by 1nM P4 in this thesis were commonly regulated by 100nM P4. The overlap for R5020 was similar, with 60.7% of the genes regulated by 1nM R5020, also regulated by 10nM R5020 in the published study (Figure 3.24D). The different doses of progestogen used and differences in the clones of T47D cells may limit the overlap in the gene expression stimulated by P4 and R5020 in the two different studies. Enrichment analyses were performed using the 5,872 genes identified as significantly regulated by R5020 by Mohammed et al. 2015 (padj <0.05) and the genes up- and down-regulated by (R5020+E2) (log2 fold change ≥0.632 or ≤-0.632, padj <0.05) in this study (Figure 3.24E-F). This revealed very strong enrichment of the genes identified in this study as (R5020+E2)-regulated, in the 5,872 genes identified as R5020-regulated by Mohammed et al. 2015 with normalised enrichment scores of 3.14 for R5020-stimulated genes and -3.18 for R5020-repressed genes.

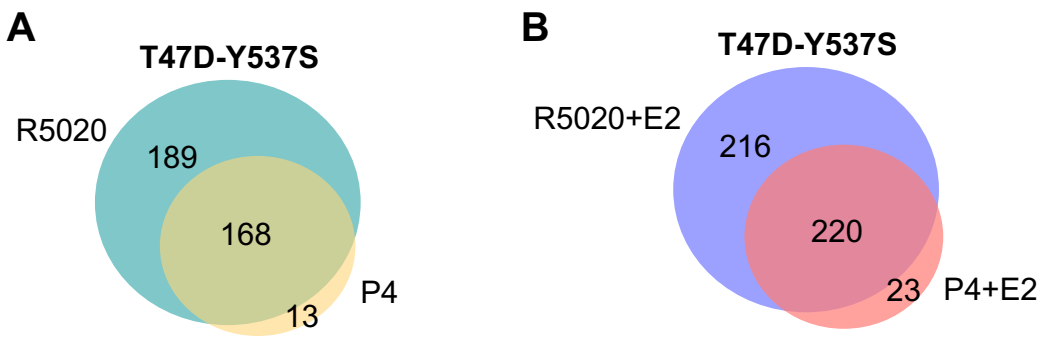


Figure 3.23 The majority of genes regulated by R5020 in the T47D-Y537S line are also regulated by P4

Venn diagrams illustrating the genes that are differentially expressed in T47D-Y537S cells by 1nM P4 and 1nM R5020 treatment (**A**) and by (1nM P4 and 10nM 17β-Estradiol) and (1nM R5020 and 10nM 17β-Estradiol) (**B**). Genes with a log2 fold change ≥0.632 or ≤-0.632, padj <0.05 were included.

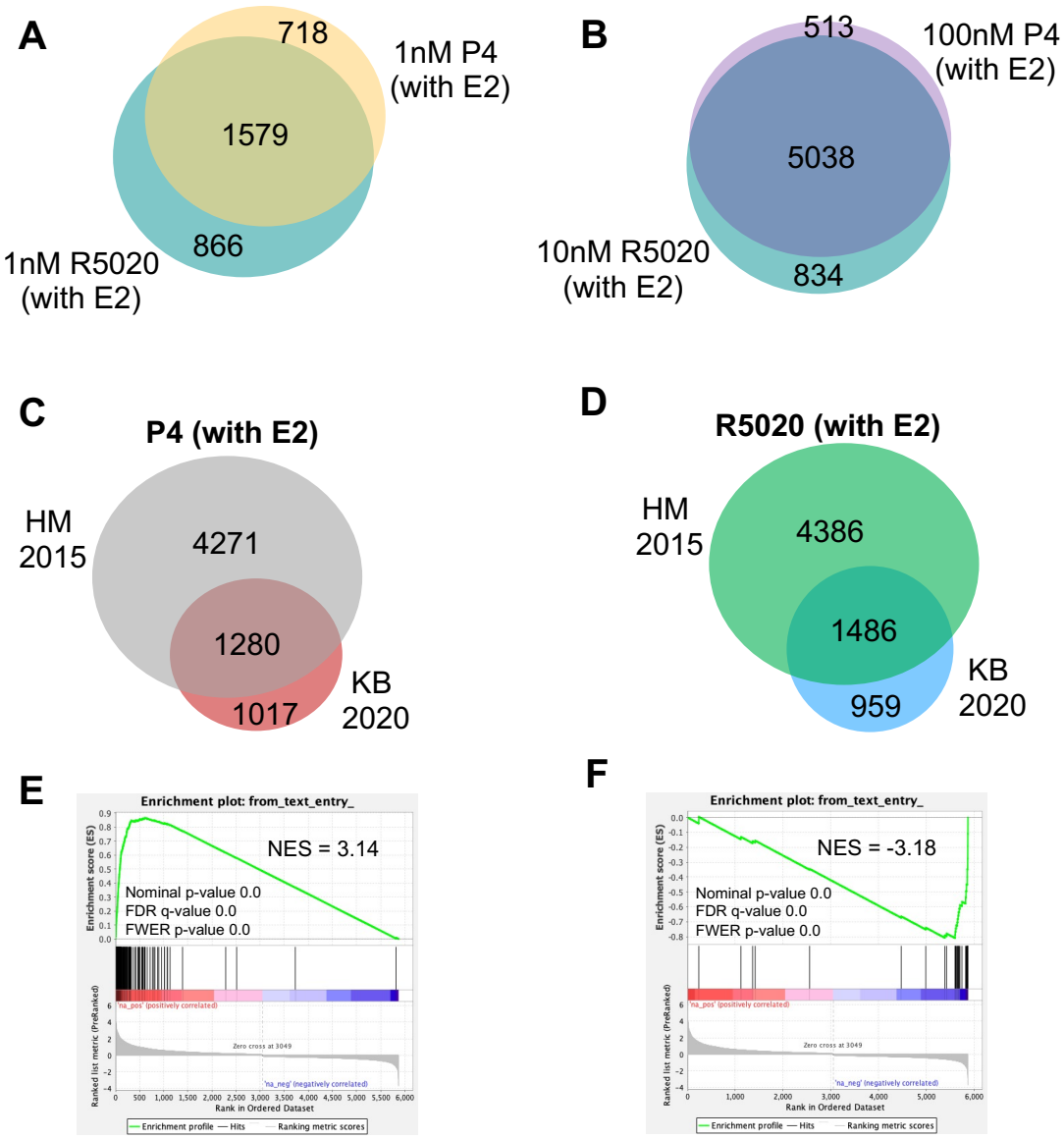


Figure 3.24 Patterns of PR-regulated gene expression in T47D-WT cells are in keeping with published data

(**A-D**) Venn diagrams illustrate the genes that are differentially expressed in T47D-WT cells by 1nM P4 and 1nM R5020 (in combination with estrogen) treatment in this study (KB 2020) (**A**) and by 100nM P4 and 10nM R5020 in full media as performed by Mohammed et al. 2015 (HM 2015) (**B**). The genes regulated in the T47D-WT lines by P4 (**C**) and by R5020 (**D**) in the presence of E2 in both studies are shown. All genes with padj <0.05 are included. (**E-F**) Enrichment of the 160 genes upregulated (**E**) and 36 genes downregulated (**F**) by (R5020+E2) in this study (log2 fold change ≥0.632 or ≤-0.632, padj <0.05) , in the 5,872 geneset identified as R5020-regulated by Mohammed et al. 2015 (padj <0.05).

3.3.6 Expression of PR-regulated genes is further stimulated by the presence of E2

Given the previously reported context-dependence of PR signalling, with altered activity according to the presence or absence of E2 (chapter 1, section 7), the effect of the addition of E2 to R5020 on gene expression in T47D-WT and T47D-Y537S cells was studied. The number of genes that were differentially expressed following R5020 treatment in the T47D-WT line was 2.3-fold higher in combination with E2 than with R5020 alone (2,445 vs 1,056) (Figure 3.25A-B). In the T47D-Y537S line, the addition of E2 to R5020 also induced expression of a greater number of genes than R5020 alone but the difference was much smaller (3,795 vs 3,390 genes, which equates to 1.1-fold) (Figure 3.25C-D). This reduction in the magnitude of the effect of E2 in the T47D-Y537S line again reflects the increased activity of mutant ER (and therefore higher *PGR* expression levels, since *PGR* is an ER target) in the absence of E2, relative to the T47D-WT cells. The number of genes differentially expressed following (R5020+E2) is 2.2-fold (436 v 196 genes) greater in the T47D-Y537S line in comparison to the T47D-WT (Figure 3.25B and 3.25D). However, this is lower than the 3.6-fold rise observed in the number of genes induced by R5020 alone in T47D-Y537S cells relative to T47D-WT (357 genes v 99 genes) (Figures 3.25A and 3.25C). The greater dependence of the T47D-WT line on E2 for expression of *PGR* (as an ER target gene) and therefore for responsiveness to R5020, explains the greater disparity between the magnitude of R5020-induced gene expression in the T47D-WT and T47D-Y537S lines in the absence of E2.

The genes regulated by R5020 alone in both the T47D-WT and T47D-Y537S cells were then analysed. In total, 371 genes were up- or down-regulated (log2 fold change

≥0.632 or ≤-0.632, padj <0.05) by R5020 treatment (without E2) in the T47D WT and mutant cells (Figure 3.26A). Hierarchical cluster analysis (Figure 3.26B) generated 4 individual clusters (genes in each cluster are listed in Appendix IV). Cluster 4 contained 59 R5020-regulated genes, which had lower expression levels with the addition of E2 in both cell lines. There was no statistical difference in the expression of the genes in cluster 4 between the T47D-WT and T47D-Y537S lines treated with R5020 alone. *NDRG1* was one of the genes in cluster 4; it appears repressed by E2 (and is downregulated in the T47D-Y537S line relative to the T47D-WT) but stimulated by P4 and, to an even greater extent, by R5020. The regulation of *NDRG1* by P4 or R5020 was more pronounced in the T47D-Y537S line than the T47D-WT and, particularly for T47D-WT cells, enhanced with the addition of E2. The expression of the 94 R5020-regulated genes in Cluster 1, also decreased with the addition of E2 treatment but the difference in expression levels between the cell lines treated with R5020 alone was statistically significant. *PLK2* is an example of a gene from cluster 1 and, like *NDRG1*, its expression is also inhibited by E2. However, it is repressed by both P4 and R5020 (R5020>P4). The progestogen-mediated reduction in *PLK2* expression was enhanced by E2 and was also more dramatic in the T47D-Y537S cell line than the T47D-WT. Cluster 3, the smallest, contained just 24 genes, the expression of which was increased with (R5020+E2) treatment relative to R5020 alone. Interestingly, *RARA*, a well-known ER target gene, was one of the genes found in this cluster and showed upregulation with E2 as expected (Ross-Innes et al. 2010). *RARA* was downregulated by R5020 in both cell lines but its expression was only inhibited by P4 in the T47D-Y537S line; this suggests that the lower *PGR* levels of T47D-WT cells are insufficient for P4-stimulation of *RARA*. The largest cluster, cluster 2, contained 194 R5020-regulated genes which showed further stimulation in

expression when E2 was combined with R5020. This cluster included classical PR target genes including *BCL6, FKBP5, MAFB, SGK1* and *STAT5A*. An example from this cluster, *FKBP5*, is upregulated in the mutant line relative to the WT. *FKBP5* expression is stimulated by both P4 and, to a greater extent, R5020, again demonstrating the increased potency of R5020. Expression of *FKBP5* was also increased by E2, more so in the T47D-WT line than the T47D-Y537S.

Next, the genes regulated by (R5020+E2) (log2 fold change ≥0.632 or ≤-0.632, padj <0.05) in both the T47D WT and Y537S cells were analysed. Four hundred and sixty-seven genes were regulated by (R5020+E2) in both cell lines (Figure 3.27A) and these were also studied using hierarchical cluster analysis (Figure 3.27B). Genes formed 4 clusters (genes in each cluster are listed in Appendix IV) with 45 in cluster 2, 47 in cluster 3, 147 in cluster 4 and 228 in cluster 1. Cluster 2 included genes that had lower expression levels following (R5020+E2) treatment relative to R5020 alone in both lines (padj value ≤0.05) and reduced expression in T47D-Y537S cells compared to T47D-WT, regardless of treatment (padj value ≤0.0001). A gene from cluster 2, *FAM107B*, is repressed by E2 but is stimulated by both P4 and R5020 (R5020>P4); this effect is greatest in T47D-Y537S cells likely due to their increased levels of *PGR*. In contrast to cluster 2, the genes in cluster 3 were expressed more highly in T47D-Y537S cells than in T47D-WT with both R5020 and (R5020+E2) treatment. Expression of *ATP1A1* is also decreased by E2 but increased by P4 and stimulated further by R5020; like *FAM107B*, progestogen-regulation of *ATP1A1* is greater in T47D-Y537S cells than in T47D-WT. *EGFR* was also present in cluster 3 of the 467 (R5020+E2)-regulated genes (and in cluster 4 of the 371 R5020-regulated genes (Figure 3.26B); its expression was regulated by both progestogens (R5020>P4) but not by E2 and was

equivalent in both the T47D-WT and T47D-Y537S cell lines (data not shown). Cluster 4 included genes that were downregulated by the addition of E2 to R5020 treatment, more notably in the T47D WT line than the mutant. Interestingly, the ER pioneer factor, *FOXA1*, is present in this cluster and exhibits strong progestogen-induced repression (R5020 is more potent inhibitor of its expression than P4), which again is much more pronounced in the T47D-Y537S line. The P4- and R5020- regulation of *FOXA1* is particularly interesting since, as a pioneer factor, this may provide a potential mechanism for how PR modulates the activity of ER, with progestogen-mediated overexpression of *FOXA1* resulting in enhanced chromatin accessibility and promotion of E2-induced transcription of ER target genes. The further enhanced upregulation of *FOXA1* with P4 and R5020 treatment in the T47D-Y537S line also raises the possibility that, through overexpression of *PGR*, T47D-Y537S cells may be even more susceptible to the progestogen-induced modulatory effects on ER than the WT cells. Finally, cluster 1, like cluster 2 of the hierarchical cluster analysis of genes differentially regulated by R5020 alone (Figure 3.27B), contained key PR target genes including *BCL6, FKBP5, HES2, MAFB* and *SGK1*; *FKBP5* showed additional stimulation when E2 was combined with R5020 treatment and greater expression levels and progestogen-responsiveness (R5020>P4) in T47D-Y537S cells compared to T47D-WT.

R5020 treatment alone upregulated 197 genes in the T47D-Y537S line, just 9 genes in T47D-WT cells and 74 genes in both lines (Figure 3.28A). GSEA was carried out for the 74 genes upregulated by R5020 alone in both T47D-WT and T47D-Y537S cells (Figure 3.28C, Appendix III); interestingly, the most significantly enriched Hallmark pathway was ‘TNFA Signaling via NFKB’ which, given the role of RANKL (a member

of the TNF-α family) as key secretory mediator of autocrine PR signalling and PR-mediated breast morphogenesis, MaSC population maintenance, CSC expansion and tumorigenesis (discussed in chapter 1, sections 7.5 and 7.6), is potentially highly relevant. Eight genes (from the 74 upregulated by R5020 in both cell lines) were common to the 'TNFA Signaling via NFKB' pathway, including some of those observed to be the most strongly and significantly progestogen-regulated in this dataset (Figure 3.25), including *SGK1, KLF4*, and *STAT5A*. 'WNT Beta Catenin Signaling' was also identified as an enriched Hallmark pathway which is important given the roles of WNT family members such as WNT1 and WNT4 in PR signalling (discussed in chapter 1, sections 7.5 and 7.6). Analysis of enriched Gene Ontology Molecular function pathways for the 74 R5020-regulated genes, included several pathways involved in DNA binding/RNA pol II activity and potassium/cation channel activity. Potassium ion channels play an important role in cell motility and may therefore be implicated in metastatic potential; activation of the Kv11.1 channel has been shown to reduce the metastatic phenotype in triple negative breast cancer (Breuer et al. 2019).

The genes regulated in the T47D-WT and T47D-Y537S cells by (R5020+E2) were then identified and analysed. One hundred and seventy-three genes were (R5020+E2)-regulated in the T47D-Y537S line, 20 in the T47D-WT and 140 genes in both cell lines (Figure 3.28B). GSEA was undertaken for the 140 genes upregulated by (R5020+E2) in both the T47D WT and mutant cell lines (Figure 3.28D, Appendix III). The Hallmark pathways enriched for these 140 (R5020+E2)-regulated genes were similar to those enriched for the 74 R5020-regulated genes (Figure 3.28C), including 'TNFA Signaling via NFKB' as the most significantly enriched, 'WNT Beta Catenin Signaling' (enriched with greater significance than for the 74 R5020-regulated genes),

‘Estrogen Response Early/Late’ and ‘Androgen Response’. However, ‘NOTCH signalling’ was also enriched in the (R5020+E2)-regulated genes, which is of interest since, as discussed in chapter 1, section 7.6, PR-A ser294 regulates expression of NOTCH2, which is involved in CSC function. Enriched Gene Ontology Molecular function pathways included 2 relevant to WNT activity, several relating to DNA binding and 1 to potassium channel activity. Therefore, GSEA of R5020- and (R5020+E2)-regulated genes in T47D-WT and T47D-Y537S cells reveal enrichment of similar pathways, including several related to established mediators of PR (e.g. RANKL, WNT).

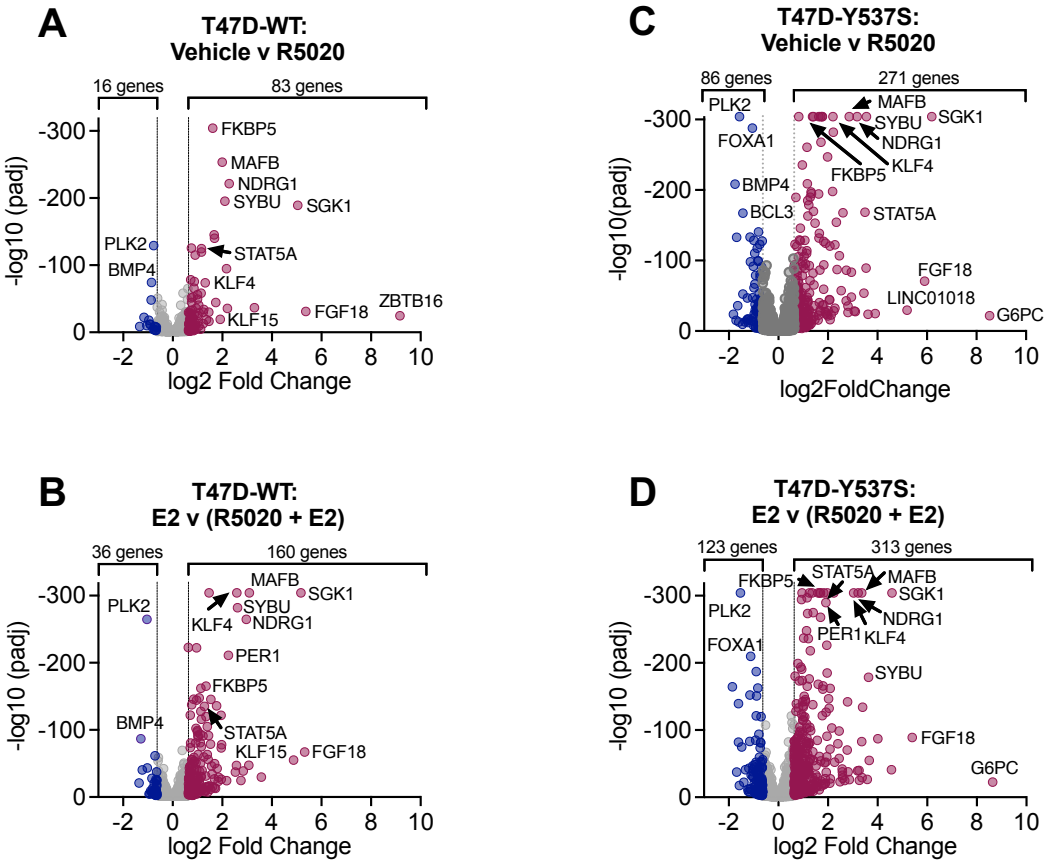


Figure 3.25 The addition of E2 further increases the expression of PR-regulated genes

Volcano plots showing the differential gene expression in the T47D-WT line following 1nM R5020 (**A**) and (1nM R5020 and 10nM 17β-Estradiol) (**B**), and in the T47D-Y537S line with 1nM R5020 (**C**) and (1nM R5020 and 10nM 17β-Estradiol) (**D**). padj <0.05 for all genes plotted.

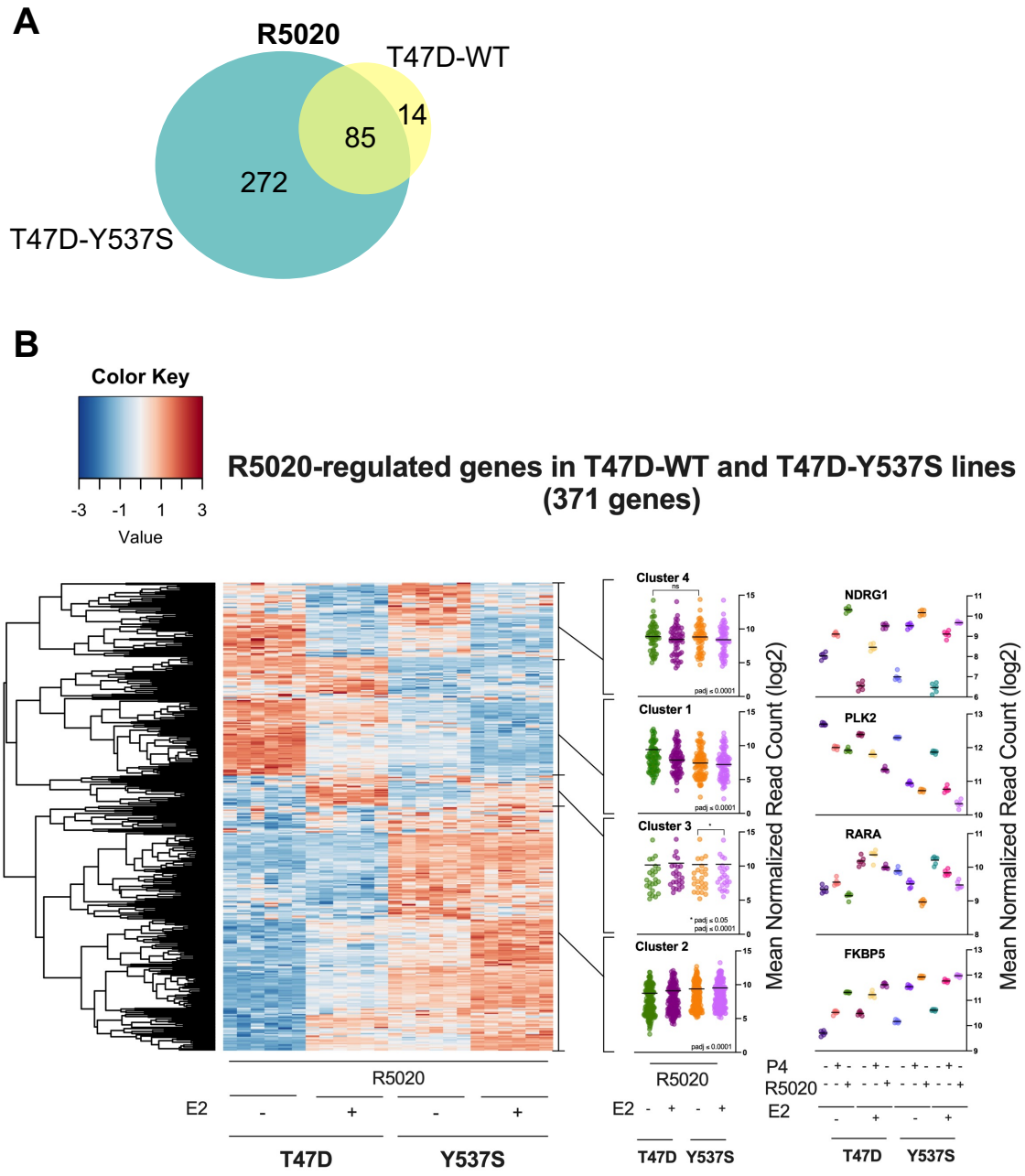


Figure 3.26 Cluster analysis of the 371 differentially expressed genes in T47D-WT and T47D-Y537S cells treated with R5020

(**A**) Venn diagram illustrating the genes that are differentially expressed by 1nM R5020 treatment, relative to vehicle treatment, in T47D-WT and T47D-Y537S cells (log2 fold change ≥0.632 or ≤-0.632, padj <0.05) (**B**) Heatmap illustrating hierarchical cluster analysis of these 371 genes. Cluster charts show the mean normalised read count of the genes within each cluster, with an example gene illustrated adjacent to each cluster (n= 6 independent RNA replicates)

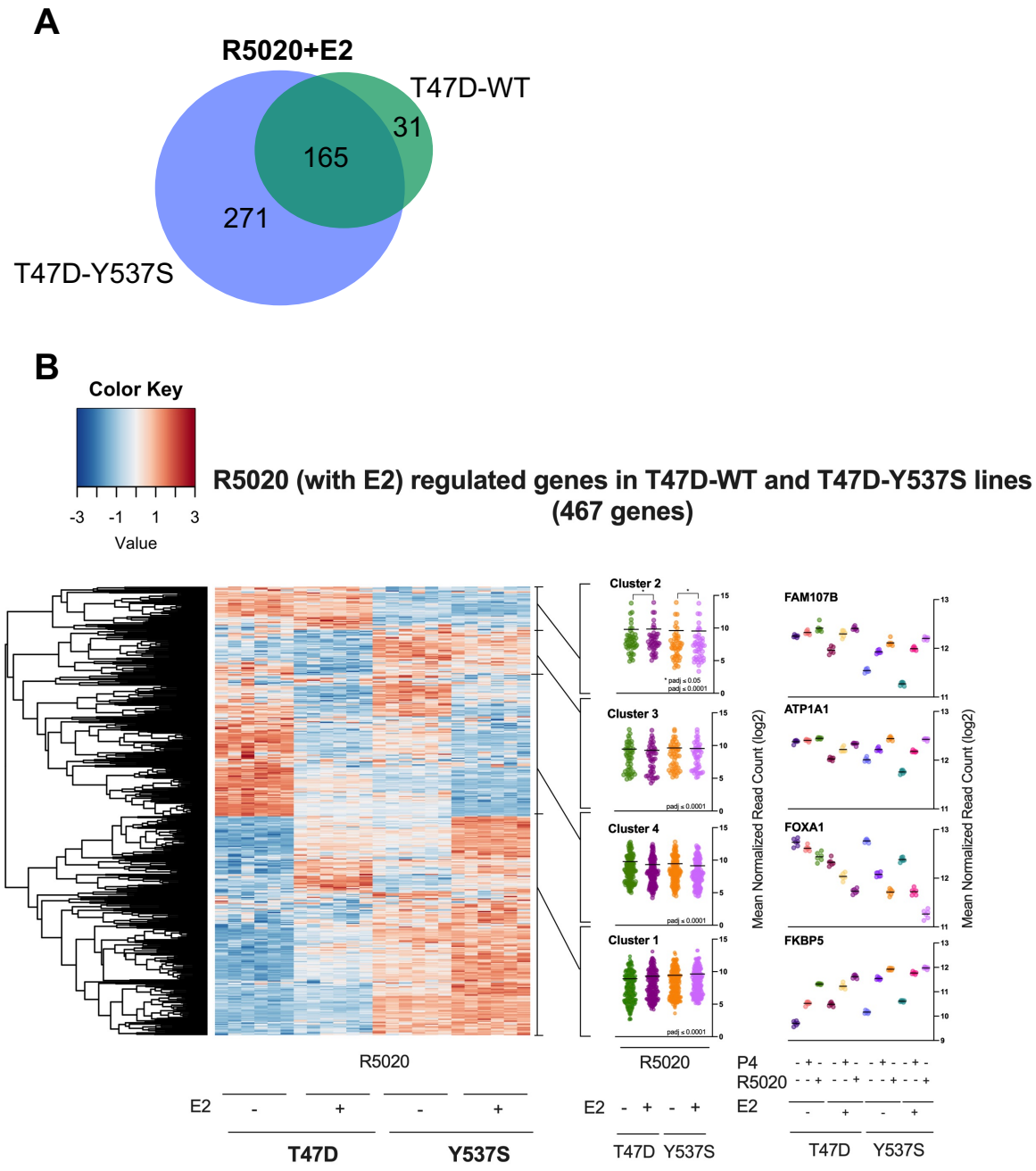


Figure 3.27 Cluster analysis of the 467 differentially expressed genes in T47D-WT and T47D-Y537S cells treated with the combination of R5020 and E2

(**A**) Venn diagram illustrating the genes that are differentially expressed by (1nM R5020 and 10nM 17β-Estradiol treatment) in T47D-WT and T47D-Y537S cells (log2 fold change ≥0.632 or ≤-0.632, padj <0.05) (**B**) Heatmap illustrating hierarchical cluster analysis of these 467 genes. Cluster charts show the mean normalised read count of the genes within each cluster, with an example gene illustrated adjacent to each cluster (n= 6 independent biological replicates)

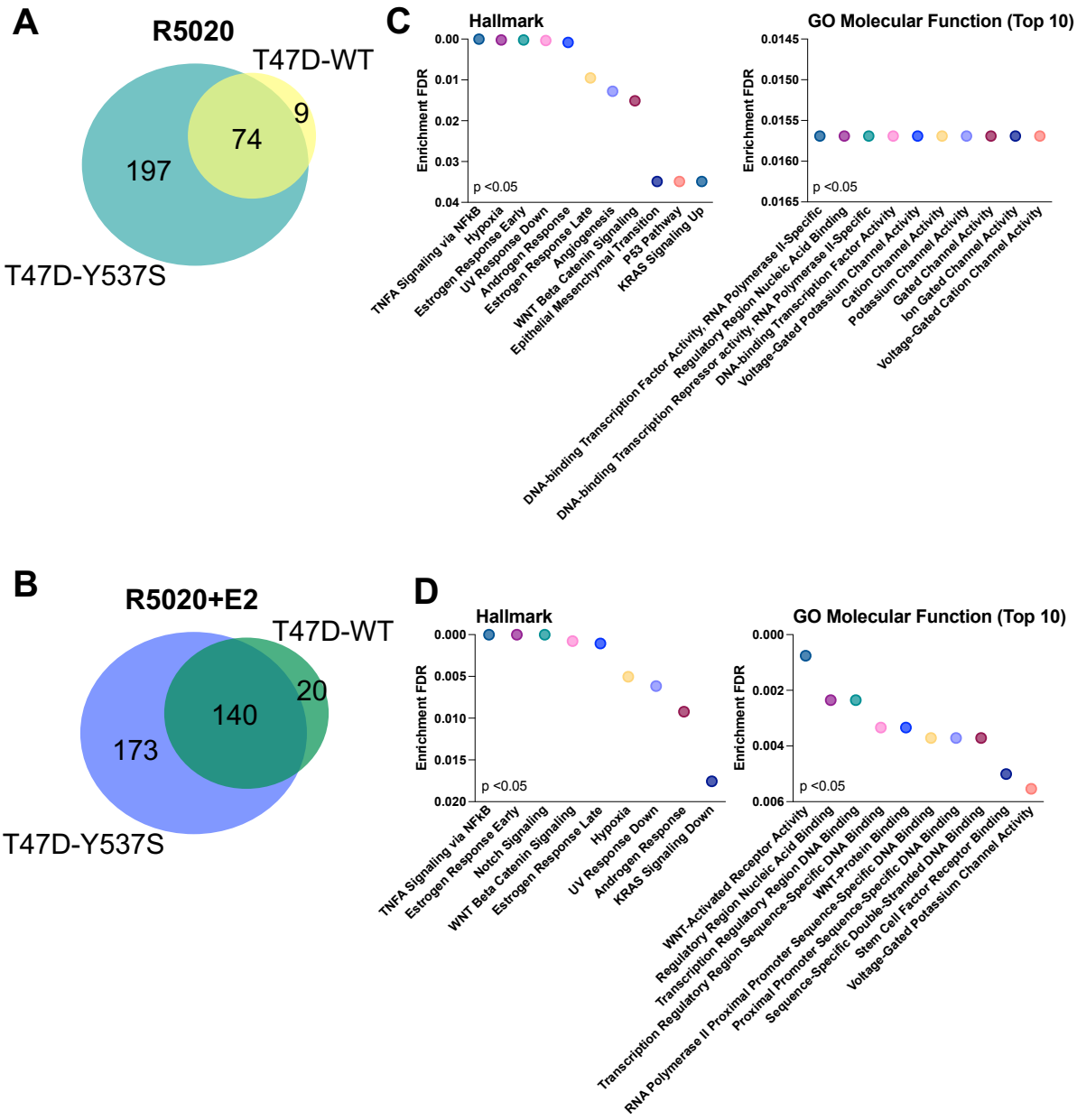


Figure 3.28 Pathway Enrichment resulting from R5020-upregulated genes in both T47D-WT and Y537S cells

(**A-B**) Venn diagrams showing the number of genes upregulated (log2 fold change ≥0.632, padj <0.05) in T47D-WT and T47D-Y537S lines following treatment with 1nM R5020 (**A**) and (1nM R5020 and 10nM 17β-Estradiol treatment) (**B**). (**C-D**) GSEA revealing Hallmark and Gene Ontology Molecular Function (top 10 most significant) pathways enriched for the 74 genes upregulated by 1nM R5020 (**C**) and for the 140 genes upregulated by (1nM R5020 and 10nM 17β-Estradiol treatment) (**D**) in both T47D-WT and T47D-Y537S lines (p<0.05).

3.3.7 Genes regulated by R5020 uniquely in the Y537S line

In order to establish whether the T47D WT and mutant lines respond differently to progestogen treatment, differential expression between T47D-WT and T47D-Y537S cells was studied following treatment with R5020 and (R5020+E2). A greater number of genes were differentially expressed between the 2 lines with R5020 treatment compared to (R5020+E2); in the T47D-WT line, 546 genes were downregulated by R5020 compared to just 383 by (R5020+E2) and in T47D-Y537S cells, 363 genes were upregulated by R5020 and 288 by (R5020+E2) (Figures 3.29A-B). The E2-independent activity of ER in the T47D-Y537S cells is likely responsible for this phenomenon, with E2 treatment bringing the levels of ER and therefore ER-mediated gene expression patterns of the E2-sensitive T47D-WT cells closer to the T47D-Y537S. This is demonstrated by the PCA showing closer clustering of E2-treated T47D-WT cells with T47D-Y537S (Figure 3.16A). Following 1nM R5020 treatment, many of the most differentially expressed genes between the lines were ER target genes, including *CXCL12, PGR, EPAS1* and *GREB1* (Figure 3.29A). This suggests that, regardless of progestogen treatment, the upregulation of ER in the T47D-Y537S cells is a predominant difference between the T47D WT and mutant cells. In keeping with the increased E2-responsiveness of the T47D line, these ER-regulated genes were regulated with much lower significance levels between the lines when R5020 treatment was combined with E2 (Figure 3.29B). PR-regulated genes, such as *MAFB, SGK1* and *PLK2*, were also amongst those significantly differentially regulated with 1nM R5020 between both cell lines (Figure 3.29A). These were also differentially regulated between the 2 lines with (R5020+E2) treatment but with lower log2 fold changes and significance levels compared to R5020. The increased E2-sensitivity of T47D-WT cells is again likely responsible for this, with E2 treatment resulting in

upregulation of ER target genes, including *PGR*, and therefore improved progestogen-responsiveness in the WT line – minimising the degree of differential expression of PR-regulated genes between the T47D WT and Y537S cell lines.

Genes that are differentially expressed by R5020 exclusively in the T47D-Y537S line were then analysed to identify any specific patterns of gene expression that are unique to the Y537S mutation. Two hundred and seventy-two genes were identified as being differentially expressed solely in T47D-Y537S cells by R5020 alone (Figure 3.29C) and 271 by (R5020+E2) (Figure 3.29D). These two groups of genes were then overlapped to define 3 distinct gene sets regulated only in the T47D-Y537S line; (1) 145 genes regulated by R5020 alone, (2) 144 genes regulated by (R5020+E2) only and (3) 127 genes regulated by both R5020 and (R5020+E2) (Figure 3.29E). When the 3 gene sets were combined, a total of 416 genes resulted and GSEA was performed for these genes (Figure 3.29F, Appendix III). The 10 most significantly enriched Gene Ontology Molecular function pathways exclusively featured RNA pol II and DNA-binding pathways. GSEA was also carried out for each of the defined 3 gene sets individually (Figure 3.30A-C, Appendix III). For the 145 genes regulated by R5020 alone in the T47D-Y537S line, enriched Hallmark pathways included those seen previously with R5020 regulated genes in both T47D WT and Y537S cell lines (Figure 3.28C), including 'TNFA Signaling via NFKB', 'WNT Beta Catenin Signaling' and 'Estrogen Response Early/Late' (Figure 3.30A). However, the most significantly enriched Hallmark pathway was, 'NOTCH signalling', which was only previously seen in (R5020+E2)-regulated genes in both the T47D-WT and T47D-Y537S cells (Figure 3.28D). The 10 most significantly enriched Gene Ontology Biological Process pathways for these 145 R5020-regulated genes were all related to motility or migration

(Figure 3.30A). For the 144 genes regulated by (R5020+E2) in the T47D-Y537S line, the top 10 most enriched Gene Ontology Molecular Function and Biological Process pathways were almost exclusively related to RNA polymerase II and DNA-binding (Figure 3.30B). Finally, for the 127 genes regulated by both R5020 and (R5020+E2) in the T47D-Y537S line, Hallmark pathways again featured 'TNFA Signaling via NFKB' and 'Estrogen response Early' and the top 10 Gene Ontology Molecular Function pathways were predominantly transcription and DNA-binding focused.

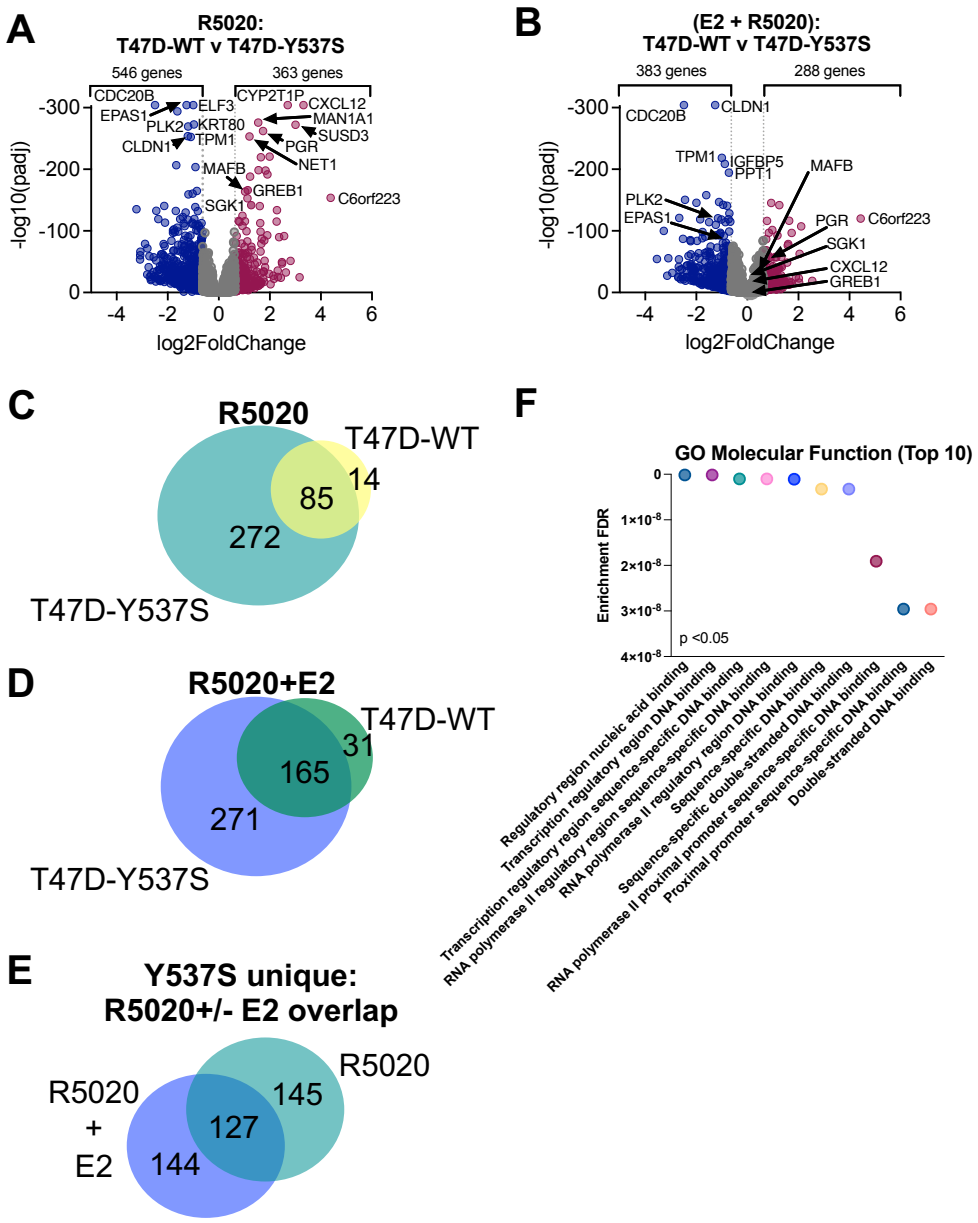


Figure 3.29 Differential gene expression between the T47D-WT and T47D-Y537S lines following R5020 treatment

(**A-B**) Volcano plots showing the differential gene expression between the T47D-WT and T47D-Y537S lines following 1nM R5020 (**A**) and (1nM R5020 + 10nM 17β-Estradiol) treatment (**B**). padj <0.05 for all genes plotted. (**C-E**) Venn diagrams showing the genes regulated in both lines by 1nM R5020 alone (**C**), 1nM R5020 in combination with 10nM 17β-Estradiol (**D**) and the genes regulated uniquely in the Y537S line by R5020 and (R5020 +E2) (**E**). Genes with a log2 fold change ≥0.632 or ≤-0.632, padj <0.05 were included. (**F**) GSEA pathways (Gene Ontology Molecular function - 10 most significant pathways shown) enriched for all 416 genes shown in (**E**) (p<0.05).

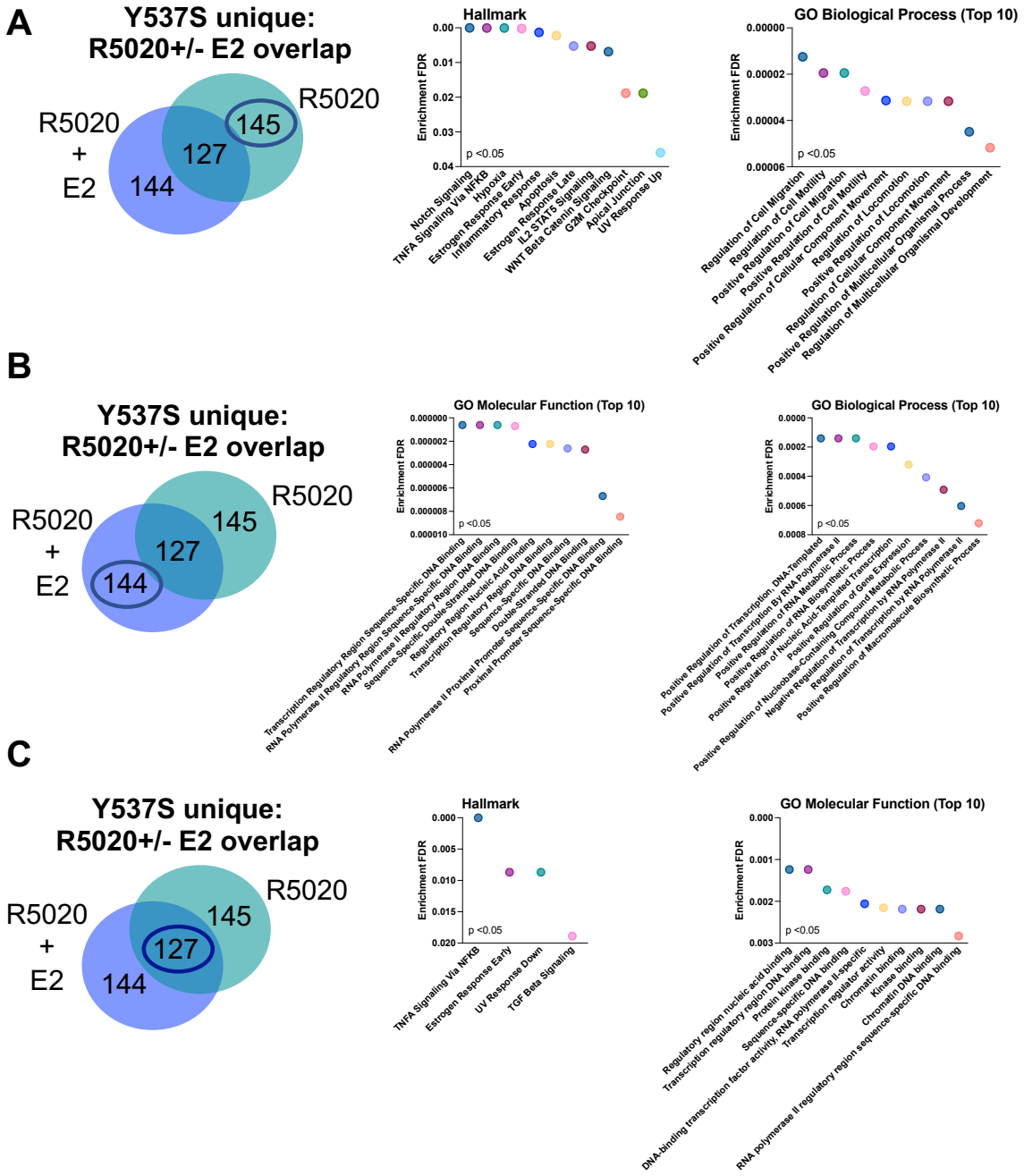


Figure 3.30 Genes uniquely R5020-regulated in the T47D-Y537S line, with or without E2

(**A-C**) GSEA identified pathways for the 145 genes differentially regulated by 1nM R5020 only in the T47D-Y537S line (Hallmark and top 10 GO Biological process) (**A**) the 144 genes regulated by (1nM R5020 + 10nM 17β-Estradiol) treatment only in T47D-Y537S cells (top 10 GO Molecular function and Biological process) (**B**) and the 127 genes differentially regulated by both 1nM R5020 and (1nM R5020 + 10nM 17β-Estradiol) treatment in T47D-Y537S cells (Hallmark and top 10 GO Molecular function) (**C**). Genes included in all Venn diagrams have a log2 fold change ≥0.632 or ≤-0.632, padj <0.05

3.4 Validation of RNA-seq findings

3.4.1 Additional models of the Y537S and D538G mutation modelled in another T47D line

In order to validate the findings of RNA-seq carried out with R5020 treatment (section 3.6-3.9), additional models of ESR1 mutations were sought. As mentioned in section 3.5, other T47D cell lines have been engineered to carry the Y537S and D538G mutations using CRISPR-Cas9 gene-editing and these were kindly provided to us by Prof S. Oesterreich (University of Pittsburgh). In total, five lines gifted to us were used for further studies; the parental WT line (T47D-WT.SO), 2 Y537S mutant clones (T47D-Y537S#1 and T47D-Y537S#2) and 2 D538G mutant clones (T47D-D538G#49 and T47D-D538G#60). These cells have already been used to investigate the effects of ESR1 mutations and details of the generation of these lines and studies including them have previously been published (Bahreini et al. 2017; Li et al. 2018).

As previously performed using the T47D-WT and T47D-Y537S lines (chapter 3.1.2), the mutational status of the new cell lines was first confirmed before any studies were undertaken. cDNA was prepared from T47D-WT.SO, T47D-Y537S#1, T47D-Y537S#2, T47D-D538G#49 and T47D-D538G#60 cells and ESR1 RT-PCR products were sequenced (Figure 3.31A-B). The presence of both WT and mutant sequences were evident in the sequencing of the PCR products from the T47D-Y537S#1 clone, whilst only a mutant sequence was seen in the T47D-Y537S#2 clone (Figure 3.31A). Sequencing of the T47D-D538G#49 and T47D-D538G#60 clones also showed that both WT and D538G mutant alleles were present; similar WT:mutant levels were observed between the two D538G clones (Figure 3.31B). Data kindly provided by Dr C.F. Lai.

RT-qPCR was carried out using RNA prepared from T47D-WT.SO, T47D-Y537S#1, T47D-Y537S#2, T47D-D538G#49 and T47D-D538G#60 cells which were E2-deprived then treated with either vehicle or 10nM E2 for 16 hours, then vehicle or 1nM R5020 for a further 3 hours (Figure 3.31C) as undertaken with the previous RNA-seq experiment using the T47D-WT and T47D-Y537S cells (Figure 3.20). ESR1 expression was confirmed in all 5 vehicle-treated lines, at higher levels in all the mutant cell lines relative to the T47D-WT.SO, except T47D-Y537S#2 cells. ESR1 was expressed at a higher level in the vehicle-treated D538G#49 and D538G#49 cells than in the T47D-Y537S#1. Two classical ER target genes, *PGR* and *TFF1* were upregulated in all the vehicle-treated mutant lines relative to the T47D-WT.SO but to a greater extent in the 2 Y537S lines (T47D-Y537S#1 > T47D-Y537S#2) than in the 2 D538G cell lines. The E2-responsiveness of these lines was also assessed and the greatest increases in *PGR* and *TFF1* expression following E2 treatment were seen in both D538G clones, reflecting their increased *ESR1* mRNA levels. There was some upregulation of *PGR* and *TFF1* with E2 in the T47D-Y537S#2 clone but not in the T47D-Y537S#1 clone. *GREB1* was defined as both E2- and R5020-regulated in T47D-WT and T47D-Y537S cells through RNA-seq (sections 3.6-3.9). This was validated in the T47D-WT.SO, T47D-Y537S#1, T47D-Y537S#2, T47D-D538G#49 and T47D-D538G#60 cells, which all exhibited regulation of *GREB1* with both E2 and R5020. The D538G#49 clone appears to be the most sensitive of all the 4 mutant lines to both E2 and R5020 and Y537S#2 cells, the least. Of the remaining 2 mutant clones, T47D-Y537S#1 was more R5020-sensitive and D538G#60 was more responsive to E2. As 2 of the most significantly R5020-induced genes established through RNA-seq (sections 3.6-3.9), *SGK1* and *MAFB* were selected to evaluate the effects of R5020

on the newly available T47D cell lines. Both genes were upregulated by R5020 with and without E2 in the T47D-WT.SO line, and to a far greater degree, in all 4 mutant clones. *SGK1* expression was upregulated more in both D538G cell lines than in either Y537S#1 or Y537S#2. In contrast, R5020-stimulation of *MAFB* was greatest in the Y537S#1 clone. Therefore, with the exception perhaps of T47D-Y537S#2 cells, these mutant clones exhibit E2-independent expression of ER and ER target genes and both the T47D-WT.SO and the 4 mutant clones are R5020-responsive. These cells were therefore considered suitable for further validation studies. Data kindly supplied by Dr C.F. Lai.

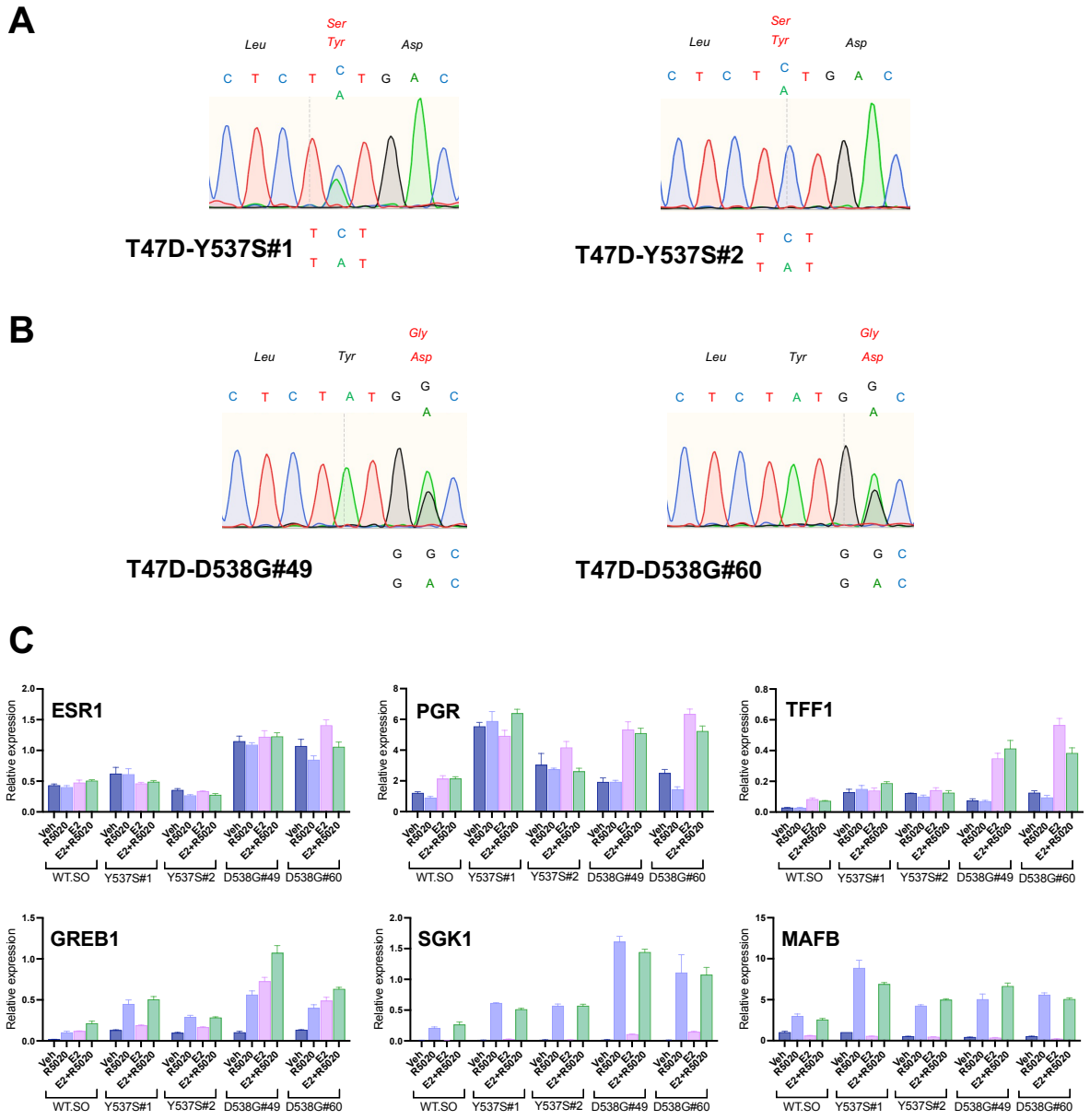


Figure 3.31 Validation of RNA-seq results using T47D-WT.SO, T47D-Y537S#1, T47D-Y537S#2 T47D-D538G#49 and T47D-D538G#60 cell lines

(**A-B**) Sequencing chromatogram generated by Sanger sequencing of PCR product amplified with primers that amplify WT and Y537S mutant ER (**A**) and D538G mutant ER (**B**). (**C**) RT-qPCR was performed using RNA harvested from T47D-WT.SO, T47D-Y537S#1, T47D-Y537S#2, T47D-D538G#49 and T47D-D538G#60 cells treated with either vehicle or 10nM E2 for 16 hours, then vehicle or 1nM R5020 for a further 3 hours. Gene expression is plotted relative to TBP (n=3 biological replicates, error bars=SEM). Data courtesy of Dr C.F. Lai.

3.4.2 R5020 inhibits growth of T47D-WT cells, T47D-Y537S clones #1 and #2 and T47D-D538G clones #49 and #60

As already undertaken for the MCF7-WT, MCF7-Y537S (Figure 3.6), T47D-WT and T47D-Y537S cells (Figure 3.7), the effects of 3 PR agonists (P4, R5020 and MPA) and 1 PR antagonist (RU486) at concentrations of 0.01nM-10μM (with 5 10-fold serial dilutions) on growth of the T47D-WT.SO, T47D-Y537S#1, T47D-Y537S#2, T47D-D538G#49 and T47D-D538G#60 cells was investigated (Figure 3.32). These cells were transfected with nuclear localised green fluorescence protein (GFP) to enable cell counting to be used as the measure of growth with the Incucyte Zoom. Data for this was kindly obtained by Dr C.F. Lai.

Unlike the MCF7-WT and T47D-WT lines (Figures 3.6A and 3.7A), growth of T47D-WT.SO cells was inhibited by P4 at concentrations ≥10nM. T47D-Y537S#2 cells were also inhibited by ≥10nM P4 but the T47D-Y537S#1 clone appeared more sensitive to P4, with growth inhibition seen at concentrations ≥1nM. This effect was less pronounced in the 2 D538G clones. Although there was some limited reduction in growth with ≥10nM P4 in T47D-D538G#60 cells, only 10μM P4 clearly inhibited growth in the T47D-D538G#49 cells. As discussed in section 2.5, growth inhibition seen with doses as high as this are likely to represent off-target effects.

In keeping with the data from the T47D-Y537S line (Figure 3.7A), R5020 reduced growth of both T47D-Y537S#1 and T47D-Y537S#2 cells in a dose-dependent manner, with concentrations ≥0.01nM. The T47D-D538G#49 and T47D-D538G#60 cells again appeared less progestogen-responsive than the Y537S lines, with concentrations ≥10nM R5020 resulting in some reduced growth. Interestingly, unlike our T47D-WT

cells (Figure 3.7A), R5020 also inhibited growth of the T47D-WT.SO line at concentrations ≥0.01nM, though to a lesser extent than in the T47D-Y537S#1 and T47D-Y537S#2. The dose-dependent growth inhibition of R5020 was much more evident in the T47D-WT.SO cells, however, than in either of the D538G lines.

There was no appreciable effect seen on growth with MPA in our MCF7-WT, MCF7-Y537S (Figure 3.6A), T47D-WT and T47D-Y537S lines (Figure 3.7B). In contrast, MPA restricted growth at concentrations ≥0.01nM in the T47D-WT.SO, T47D-Y537S#1 and T47D-Y537S#2 cells. Growth of the T47D-D538G#49 and T47D-D538G#60 clones was only inhibited by the highest dose of 10μM MPA, which may not be PR-mediated, especially given the described activity of MPA on MR and GR.

The PR antagonist, RU486 was also evaluated for its effect on growth. In keeping with the results from the MCF7-WT, MCF7-Y537S (Figure 3.6B), T47D-WT and T47D-Y537S lines (Figure 3.7B), there was no apparent effect, with clear inhibition only seen with a concentration of 10μM in the T47D-WT.SO, T47D-Y537S#1, T47D-Y537S#2, T47D-D538G #49 and T47D-D538G #60 cells.

The increased number of E2-regulated genes identified with RNA-seq of the T47D-WT.SO, T47D-Y537S#1 and T47D-Y537S#2 (pooled as T47D-Y537S.SO) cells relative to the T47D-WT and T47D-Y537S cells (Figure 3.19A-B) reflects the enhanced sensitivity of these cells to E2 and it appears that these cells are also more responsive to progestogens, even less potent progestogens such as P4. It may be, due to the clonal origins of all these cell lines, that they have differing receptor expression levels and therefore responses to corresponding ligands. Neither of the

D538G lines appear as sensitive to any of the PR ligands tested as T47D-Y537S#1 and T47D-Y537S#2 cells.

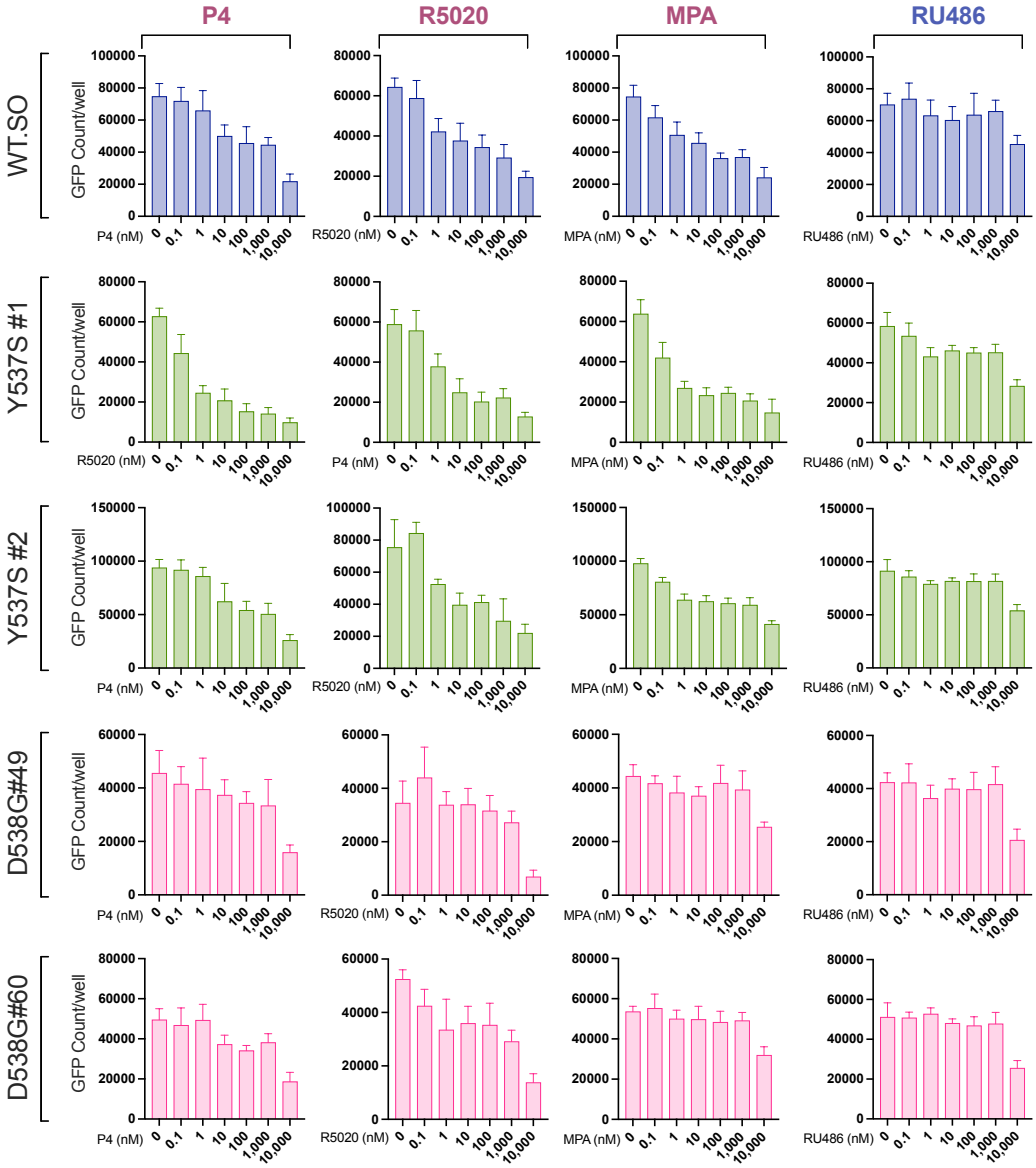


Figure 3.32 R5020 inhibits growth of T47D-WT.SO, T47D-Y537S#1/#2 and T47D-D538G#49/60 cells in a dose-dependent manner

Growth assays were undertaken using RNA prepared from T47D-WT.SO, T47D-Y537S#1, T47D-Y537S#2, T47D-D538G#49 and T47D-D538G#60 cells treated with media only, vehicle or 0.01nM–10,000nM of P4, R5020, MPA or RU486. The Incucyte Zoom was used to calculate the cell count at day 9, by measuring cells that exhibited green fluorescence (cells had previously been transfected with green fluorescent protein (GFP)). Data displayed is the cell count per well. (n=6 replicates from 1 experiment, error bars=SEM). Data courtesy of Dr C.F Lai.

3.4.3 The effects of R5020 are mediated through PR

Given the crosstalk that occurs between members of the nuclear receptor superfamily, confirming that R5020 mediates its effects through PR was investigated next. Given that the D538G mutant cell lines did not appear to be as responsive to PR ligands as the T47D-Y537S#1 and T47D-Y537S#2 cells, these have not been included in studies from hereon. T47D-WT.SO, T47D-Y537S#1 and T47D-Y537S#2 cells were transfected with the same non-targeting, deconvoluted siNegative control siRNA and 3 deconvoluted individual siPGRs (siPGR1, siPGR3 and siPGR4) used previously in the MCF7-WT, MCF7-Y537S, T47D-WT and T47D-Y537S lines (Figure 3.8A-D). Once transfected with the relevant siRNA, these cells were treated with either vehicle or 1nM R5020 and growth assays were performed with cell counts measured at day 9 using the Incucyte Zoom (Figure 3.33A).

With vehicle treatment, there was no clear effect of *PGR* knockdown on growth of any of the 3 cell lines tested, reflecting the findings of previous *PGR* knockdown experiments in the T47D-WT and T47D-Y537S cells (Figure 3.8C). With R5020 treatment, growth of the T47D-WT.SO, T47D-Y537S#1 and T47D-Y537S#2 cells transfected with siControl was inhibited, in agreement with the growth assays performed with R5020 in these cell lines (Figure 3.32). The inhibition was greater in the T47D-Y537S#1 and T47D-Y537S#2 cells than in the T47D-WT.SO, likely reflecting the higher levels of PR mRNA in the mutant lines. *PGR* knockdown rescued the inhibition associated with R5020 treatment, restoring growth of all 3 cell lines. This suggests that PR is required for the R5020-mediated growth inhibition of the T47D-Y537S clones. The restoration of growth was particularly strong for siPGRs 3 and 4 and likely reflects the knockdown of PR-B but continued expression of PR-A (Figure

3.9). The effect of siRNA-mediated *PGR* knockdown in T47D-WT and T47D-Y537S cells treated with 1nM R5020 was also evaluated; this time confluency was measured at day 6 using the Incucyte Zoom (Figure 3.33B). Except for vehicle-treated T47D-Y537S cells, there was no evident growth inhibition resulting from *PGR* knockdown. Data kindly provided by Dr C.F. Lai.

RT-qPCR was performed with T47D-WT.SO, T47D-Y537S#1 and T47D-Y537S#2 cells transfected with siNegative control or siPGRs 1, 3 and 4 and treated with either vehicle or 1nM R5020 for 3 hours (Figure 3.33C). All 3 siPGRs effectively reduced the expression of ligand-activated *SGK1* and *MAFB*, confirming that their R5020-stimulated expression was mediated through PR. Data kindly supplied by Dr C.F. Lai.

Western blotting was carried out using lysates prepared from T47D-WT.SO, T47D-Y537S#1 and T47D-Y537S#2 cells transfected with siNegative control or siPGRs 1, 3 and 4 and treated with either vehicle or 1nM R5020 for 3 hours (Figure 3.33D). In vehicle conditions, all 3 cell lines transfected with siPGRs 1, 3 and 4 had reduced levels of both PR isoforms compared to those transfected with siNegative control, with no appreciable difference between the T47D-WT.SO and T47D-Y537S#1 and T47D-Y537S#2 cells. Levels of both PR isoforms was reduced in all 3 lines transfected with siPGRs 1, 3 and 4 and treated with R5020, relative to the siControl, although siPGR1 seemed to result in lower levels of levels of PR-B than PR-A, likely due to its position only on PR-B, as already discussed in section 2.6. In R5020-treated samples, PGR levels were similar in the siControl-transfected T47D-WT.SO and T47D-Y537S#1 samples but slightly reduced in the T47D-Y537S#2 sample. In T47D-WT.SO cells transfected with siNegative control, PGR levels were similar with both vehicle and

R5020 treatments. In summary, the effects of R5020 on growth, gene expression and protein levels are reversed through *PGR* knockdown. It can therefore be concluded that R5020 acts through PR. Data kindly provided by Dr C.F. Lai.

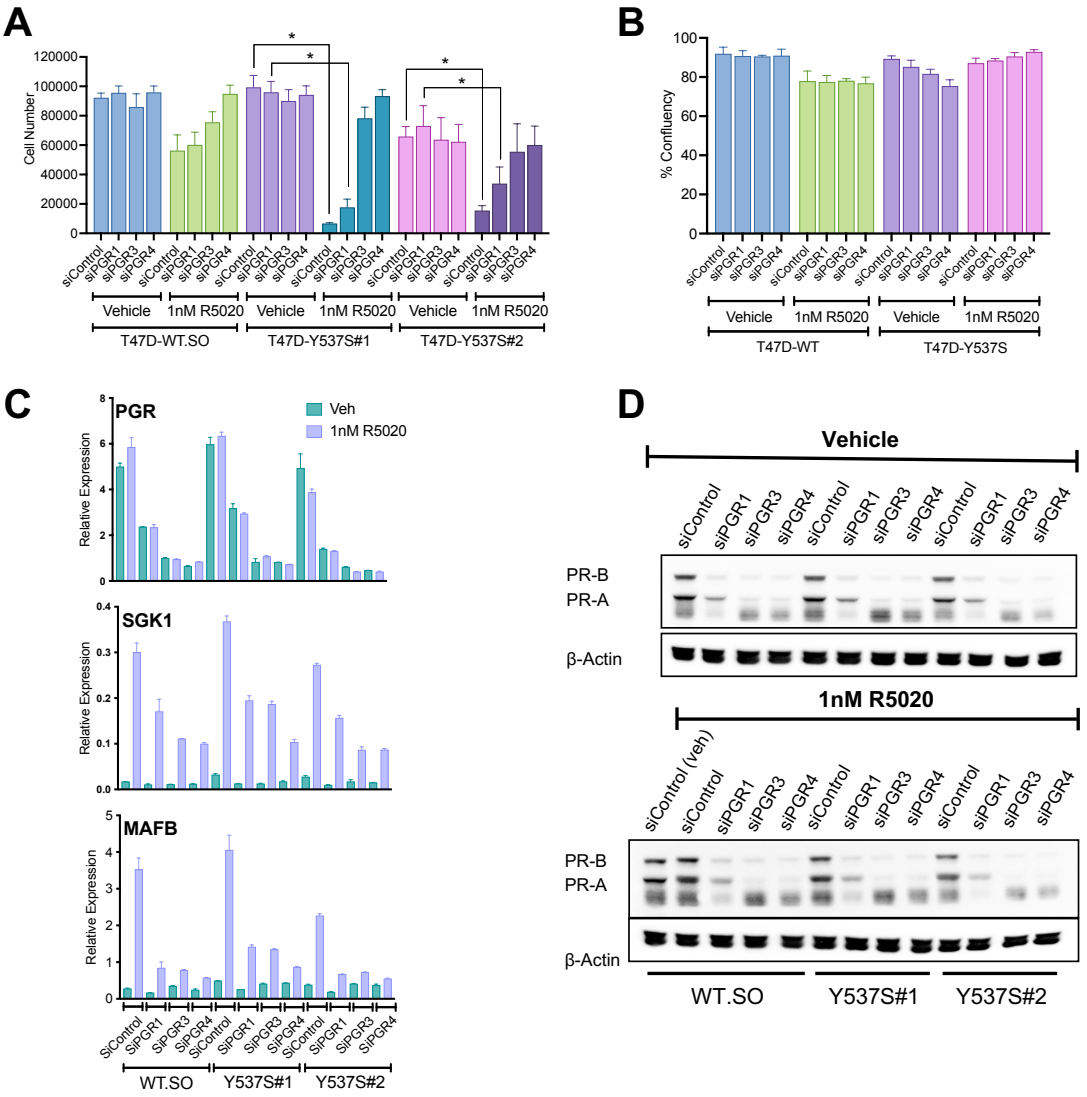


Figure 3.33 The effects of R5020 are mediated through PR in T47D-WT.SO, T47D-Y537S#1 and T47D-Y537S#2 cells

(**A-B**) siRNA mediated knockdown of PR was performed in the T47D-WT.SO, T47D-Y537S#1 and T47D-Y537#2 cells (growth is represented by the cell count at day 9 calculated using the Incucyte Zoom) (**A**) and in the T47D-Y537S and parental T47D-WT line (confluency at day 6 measured using the Incucyte Zoom) (**B**). (n=6, 1 experiment for **A** and **B**). (**C**) RT-qPCR using RNA prepared from T47D-WT.SO, T47D-Y537S#1 and T47D-Y537#2 cells grown in full media, transfected with siControl or deconvoluted siPGR and treated with either vehicle or 1nM R5020 for 3 hours. Expression is shown relative to TBP, error bars represent the mean. (n=3 independent biological replicates). (**D**) Protein lysates were harvested from cells cultured in full media, transfected with siControl or deconvoluted siPGR and then treated for 3 hours with either vehicle or 1nM R5020; Western blotting was performed using antibodies as labelled. Data courtesy of Dr C.F Lai.

3.4.4 R5020 reduces migration of T47D and T47D-Y537S cells

Once the activity of R5020 had been confirmed as mediated through PR, other potential effects of R5020 were considered. Given the strong enrichment of migration and motility pathways seen following RNA-seq with R5020 treatment in T47D-Y537S cells (Figure 3.30A) and the enrichment of potassium ion channels pathways (which have also been implicated in cell motility (as discussed in section 3.8) in R5020-regulated genes in both T47D-WT and T47D-Y537S cells (Figure 3.28A), the effect of R5020 on migration of T47D-WT and T47D-Y537S cells was evaluated. Wound healing assays were performed by seeding either T47D-WT or T47D-Y537S cells in 96-well plates for 48 hours before creating a wound. Cells were then treated with either vehicle, 10nM E2, 1nM R5020, 1μM R5020, (10nM E2 + 1nM R5020) or (10nM E2 + 1μM R5020). Using the Incucyte Zoom, wound density was determined every 3 hours for 4 days (Figure 3.34). Reduced wound density, indicative of restricted migration, was observed in both T47D-WT and T47D-Y537S lines treated with both doses of R5020, both alone and in combination with E2. The difference in effect of R5020 on migration between the T47D WT and Y537S mutant cell lines was minimal. Performing wound healing assays using the T47D-WT, T47D-Y537S#1, T47D-Y537S#2, T47D-D538G#49 and T47D-D538G#60 cells treated with R5020 would enable further study of this; given the increased sensitivity of these lines to Progestogens, the effects on migration may be greater. Data kindly produced by Dr C.F. Lai.

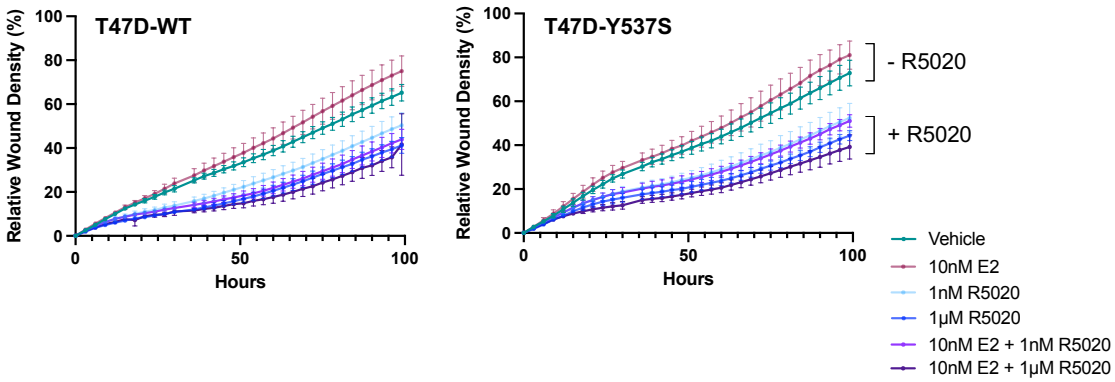


Figure 3.34 R5020 inhibits migration of T47D-WT and T47D-Y537S cells

T47D-WT and T47D-Y537S cells were seeded and hormone depleted in 96-well plates for 48 hours before a scratch was created. Cells were washed twice in media and then treated with either vehicle, 10nM E2, 1nM R5020, 1µM R5020, (10nM E2+1nM R5020) or (10nM E2+ 1µM R5020). Percentage wound density, as cells migrated into the wound area, was calculated every 3 hours for 4 days, using the Incucyte Zoom. (n=8, error bars represent the SEM). Data courtesy of Dr C.F Lai.

4. Discussion

In this thesis, I confirmed the constitutive activity of Y537S ER in the MCF7-Y537S cell line and then characterised the T47D-Y537S line, establishing that T47D-Y537S cells also exhibit E2-independent growth and ER target gene expression (including upregulation of PR). I therefore utilised T47D-Y537S cells to study PR signalling in an *ESR1* Y537S mutant setting, investigating the effects of PR ligands on growth and motility, the effect of PR knockdown and, through RNA-seq with P4 and R5020 treatment, the expression patterns of PR-regulated genes in this cell line compared to the T47D-WT. Defining the transcriptomic profile of ER+ breast cancer cells treated with progestogens or anti-progestins has been published previously but, to my knowledge, this is the first dataset of RNA-seq performed using progestogen-treated, *ESR1* mutant cells.

4.1 The Y537S mutation confers E2-independence in MCF7 and T47D cells

At the start of this study, two ER+ breast cancer cell line models were used to assess their suitability for studying the effects of PR signalling in *ESR1* mutant breast cancer. The MCF7-Y537S line has already been well-characterised and E2-independent growth, E2-independent ER target gene expression and partial resistance to anti-estrogens has been reported (Harrod et al. 2017). In keeping with these findings, I have demonstrated that the CRISPR-Cas9-generated MCF7-Y537S cells have higher levels of ER target gene expression (e.g. *PGR, TFF1*) in both full and E2-depleted media. Furthermore, I studied the T47D-Y537S line, which was also created within our laboratory using CRISPR-Cas9 to target *ESR1* exon 8 and create a knockin Y537S mutation in T47D cells (Jiminez, Buluwela at al. unpublished). I have demonstrated that the T47D-Y537S line, like the MCF7-Y537S, is heterozygous for *ESR1* Y537S,

encoding both WT and mutant alleles. This is likely to be representative of breast cancer cells in patients, with co-expression of WT and mutant ER (Andreano et al. 2020). However, through sequencing of the RT-PCR product of mRNA and the PCR product of genomic DNA (gDNA) from the T47D-Y537S clone, it became apparent that they also carry a deletion-derived frameshift mutation around the CRISPR19 targeting sequence (Figure 3.2C). In support of the presence of the indel mutation, a PCR product that was 89bp smaller than that expected was seen on *ESR1* exon 8 PCR (Figure 3.2B). Sequencing of cDNA and gDNA from the parental T47D-WT and T47D-WT.SO cell lines did not show the deletion-derived frameshift mutation seen in the T47D-Y537S line. Hence the indel is not present in endogenous *ESR1* in T47D WT cells and, as the deletion starts near the CRISPR19 targeting sequence in T47D-Y537S cells, the indel is very likely to be the result of CRISPR-Cas9 in the mutant line. Three different sequences are visible in the sequencing chromatogram using the PCR product of T47D-Y537S (Figure 3.2C). This suggests there are at least 3 *ESR1* alleles in T47D *ESR1* mutant cell lines, which is compatible with the g-banded karyotype of T47D cells reported previously, showing 3 copies of chromosome 6, where *ESR1* is located (Rondón-Lagos et al. 2014). I hypothesised that in the T47D-Y537S cell line there are at least 3 *ESR1* alleles, including: (1) WT, (2) Y537S and (3) an indel. PCR cloning and sequencing of ER would confirm the number of *ESR1* alleles, by performing PCR of *ESR1* using gDNA from T47D-Y537S cells, cloning this into a cloning vector, before transforming it into bacteria, extracting the plasmid from multiple independent bacterial colonies and sequencing it. This could also be performed with RT-PCR products. In addition, digital droplet PCR (ddPCR) of T47D-Y537S cells would also provide information on mutation allele frequency and enable calculation of the number of *ESR1* alleles in this mutant line.

As sequencing using the RT-PCR product from T47D-Y537S cells detected the indel, evidently mRNA with the deletion is being produced. However, this does not appear to affect T47D-Y537S *ESR1* mRNA levels, as RT-qPCR established that *ESR1* expression is equivalent in both cell lines cultured in full media (Figure 3.2D). Furthermore, *ESR1* mRNA levels are greater in T47D-Y537S cells relative to T47D-WT in E2-depleted media and are further stimulated by the addition of E2. ER protein is present at higher levels in lysates prepared from T47D-Y537S cells in E2-depleted media, implying greater stability of ER, in keeping with that seen with E2-treated T47D-WT cells (Bai and Giguère 2003; Tecalco-Cruz and Ramírez-Jarquín 2017). Western blotting was performed using lysates from the T47D-Y537S cell line with an ER antibody that recognises the N-terminal region of ER and would detect a smaller than expected ER protein. There was no evidence of a polypeptide smaller in size than full-length ER, suggesting that the *ESR1* mRNA from the indel does not result in production of a truncated ER (Figure 3.3A). Hence, it was concluded that, despite the presence of indel on one of the *ESR1* alleles, full-length and functional ER was present within T47D-Y537S cells. These were therefore considered to be a suitable model for further studies of the Y537S mutation.

In full media conditions, genes expressed differentially in the mutant cell line are evident (Figure 3.15). The genes differentially regulated in the T47D-Y537S line may be novel ER targets or genes that have altered expression in the presence of mutant ER. Unlike the T47D-WT cells, the T47D-Y537S line is clonal and some of these differentially expressed genes may be the result of the clone rather than the Y537S mutation. For example, *C6orf223* and *ZNF385D* are strongly up- and down-regulated

In the T47D-Y537S line with log2 fold changes of 3.98 and -8.10 respectively in full media conditions, and 4.65 and -4.49 respectively with vehicle treatment. However, in the pool of the T47D-Y537S#1 and T47D-Y537S#2 cells (termed T47D-Y537S.SO) that Bahreini et al. 2017 performed RNA-seq with, *C6orf223* and *ZNF385D* were not differentially expressed at all. Therefore, *C6orf223*, *ZNF385D* may well be differentially regulated in the T47D-Y537S cells by virtue of the clonal nature of the cell line, rather than by mutant ER. It would be valuable to distinguish true mutant-specific genes that result from Y537S ER from those that have altered expression merely due to clonal effects of the cell line. This could be done by comparing the mutant-specific genes from the T47D-Y537S cells with other published datasets that have used other ER mutant cell lines, including that published by Bahreini et al. 2017.

The possible mechanisms for a mutant-specific pattern of gene expression are as follows: (1) the constant activity of mutant ER results in different transcriptional regulation compared to that of WT (2) *ESR1* mutations confer properties that directly alter ER's target gene profile, (3) *ESR1* mutations indirectly alter ER-mediated gene expression through regulation of other transcription factors or epigenetic modifications (Arnesen et al. 2021). Through RNA-seq with prior long-term E2 treatment, Arnesen et al. 2021 report that half the genes uniquely expressed by mutant *ESR1* are the result of constant ER activity. *TBCD* is one of the genes reported to be overexpressed in T47D cells with Y537S and D538G ER due to the constant activity of ER associated with these mutants (Arnesen et al. 2021). However, *TBCD* did not meet the log2 fold change threshold for upregulation in the T47D-Y537S line in either full media or vehicle conditions (log2 fold change 0.17 and 0.38 respectively). Analysing Arnesen et al. 2021's data to identify the genes they report as being differentially regulated by the

constant activity of ER, and comparing this gene set to the mutant-specific genes found in T47D-Y537S cells would be useful to see how many genes overlap and are therefore also likely to have altered expression due to constantly active ER. Performing ER ChIP-seq and comparing data from long-term E2-treated T47D-WT cells and vehicle-treated T47D-Y537S cells would further confirm the impact of constant ER activity on genomic binding. Arnesen et al. 2021's findings suggest that the remaining mutant-specific genes are differentially regulated through alteration of ER genomic binding sites (10% for Y537S), increased chromatin accessibility (15%) (discussed further in section 4.4) and they postulate that post-translational modifications, differential interaction with cofactors and alterations in the genome structure may account for the remaining mutant ER gene regulation mechanisms (Arnesen et al. 2021). Performing ChIP-seq and ATAC-seq using vehicle- and E2-treated T47D-WT and -Y537S cells and comparing the data with the mutant-specific genes already determined through RNA-seq would be useful in determining whether the same genes have altered expression through differential binding sites or enhanced chromatin accessibility in the T47D-Y537S cells as reported by Arnesen et al. 2021.

To investigate the actions of the Y537S mutation in T47D cells, the E2-responsiveness of T47D-Y537S cells was investigated with a combination of growth and gene expression analysis, the latter using RT-qPCR and immunoblotting for classic E2-regulated genes, and globally using RNA-seq. E2-independent growth was observed in the T47D-Y537S line, relative to the T47D-WT cells, which is in keeping with published reports about the ligand-independence of MCF7 and T47D cells carrying Y537S and D538G mutations (Harrod et al. 2017; Martin et al. 2017; Bahreini et al. 2017; Mao et al. 2016). ER target gene expression has also been shown to be ligand-

independent in both MCF7 and T47D cells carrying *ESR1* mutations, including Y537S and D538G (Harrod et al. 2017; Martin et al. 2017; Bahreini et al. 2017; Mao et al. 2016). In line with these reports, RNA-seq revealed E2-independent expression of E2 response pathways in T47D-Y537S cells. Several classical ER target genes were differentially expressed in the absence of E2 in the T47D-Y537S cells, including *CXCL12* (log2 fold change 3.77), *GREB1* (log2 fold change 1.41) and *EPAS1* (log2 fold change -1.25). The log2 fold changes reported by Bahreini et al. 2017 for the same genes in the T47D-Y537S.SO cells are very similar (*CXCL12* 3.10, *GREB1* 1.71, *EPAS1* -1.39). There was also strong enrichment of all the genes differentially regulated in vehicle-treated T47D-Y537S cells relative to the T47D-WT, in the geneset reported to be differentially expressed in the T47D-Y537S.SO cells (relative to WT), which further confirmed the similarity between the dataset reported here and that published by Bahreini et al. 2017. Therefore, the findings shown here of E2-independent growth and expression of ER target genes in the T47D-Y537S line are consistent with previous reports in T47D *ESR1* mutant cells (Bahreini et al. 2017; Mao et al. 2016). Importantly for this thesis, one of the genes found to be most significantly overexpressed in T47D-Y537S cells in an E2-independent manner was *PGR (*log2 fold change 2.04*)*, which confirmed the utility of this line for studying PR signalling.

4.2 T47D-Y537S cells show greater progestogen-responsiveness than MCF7-Y537S

As discussed in chapter 1, section 8, a wide range of PR ligands are available which are used widely in clinical practice and in *in vitro/in vivo* studies of PR signalling. A number of these were selected for use in this thesis based on their clinical use (MPA, RU486), and their potency and relative specificity for PR (R5020, Onapristone). There

was no growth effect seen following treatment with any of the PR ligands tested in MCF7 WT and Y537S mutant cells, nor was there clear evidence of these ligands stimulating expression of PR target genes (e.g. *FAM105A, HES2, SGK1, BCL6, MAFB, NEDD9*). In contrast, growth of T47D-Y537S cells was inhibited by R5020 in a dose-dependent manner. R5020 also reduced proliferation of T47D-Y537S#1, T47D-Y537S#2 as well as T47D-WT.SO and, to a lesser extent, T47D-D538G#49 and T47D-D538G#60 cells. Two other progestogens, P4 and MPA, also had growth inhibitory effects on the T47D-WT.SO, T47D-Y537S#1 and T47D-Y537S#2 cell lines. P4 induced expression of PR-regulated genes in T47D-WT cells and, to a greater extent, in T47D-Y537S cells, reflecting the upregulation of PR in this cell line. R5020 treatment stimulated expression of a greater number of genes and with higher significance levels than P4 in both the T47D-WT and T47D-Y537S cells, in keeping with the increased RBA R5020 has for PR relative to P4 (Stanczyk et al. 2013). As expected, given that PR is upregulated by E2, the addition of E2 to either progestogen further enhanced PR target gene expression in both T47D-WT and T47D-Y537S cells (McGuire and Clark 1986). Hence, the T47D lines (both WT and mutant) display responsiveness to progestogens that is far greater than the MCF7-derived lines.

Both MCF7 and T47D cells are E2-responsive but there are several reports in the literature that the T47D line is more sensitive to P4 due to its higher expression of PR (Horwitz et al. 1982; Read et al. 1988; Nordeen et al. 1993; Mota et al. 2017). Mohammed at al. 2015 performed RNA-seq and ChIP-seq for ER, PR and p300 cultured in either (1) estrogenic conditions, (2) estrogenic conditions with P4 treatment, or (3) estrogenic conditions with R5020 treatment in MCF7 and T47D cells and reported findings on the combined results from both lines (Mohammed et al.

2015). Comparison between the dataset published by Mohammed et al. 2015 and that presented in this thesis is shown in Figure 3.24 and discussed in section 4.3. Yu et al. 2017 later analysed the differences between MCF7 and T47D cells for this dataset; a much greater magnitude of responsiveness to P4 was noted in the T47D line with changes in PR target genes (e.g. *STAT5A*) noted in T47D but not MCF7 cells (Yu et al. 2017). P4 treatment stimulated binding of ER, PR and p300 to PREs near the ESR1 and PR genes in T47D cells; there was no change in binding of ER, PR and p300 near these genes following P4 treatment in MCF7 cells (Yu et al. 2017). This reinforces the importance of selecting the most appropriate cell line for studying the effects of PR activity in *ESR1* mutant breast cancer and T47D cells appear superior to MCF7 for this purpose (Carroll et al. 2017; Yu et al. 2017).

Even within the same cell line, differences in progestogen-responsiveness may be seen between different clones; for example, growth of the T47D-WT.SO but not the T47D-WT line was inhibited by R5020. Similarly, P4 reduced the proliferation of T47D-WT.SO, T47D-Y537S#1 and T47D-Y537S#2 cells, an effect which was not evident in the T47D-WT or T47D-Y537S cells. The greater expression of PR mRNA in the T47D-WT.SO line (3.23-fold higher in vehicle-treated T47D-WT.SO than in vehicle-treated T47D-WT) and T47D-WT.SO-derived ESR1 mutant lines is likely responsible for this. As a further illustration of clonal differences, 3 different datasets of RNA-seq performed in E2-treated MCF7 cells with Y537S and D538G mutations were recently compared (Arnesen et al. 2021; Bahreini et al. 2017; Jeselsohn et al. 2018). Although multivariate analysis (to mitigate variation between the studies) revealed over 1900 differentially expressed genes commonly regulated by *ESR1* mutations across all 3 datasets, importantly the PCA showed that samples clustered according to the lab in

which they were studied, rather than by ER mutational status (Arnesen et al. 2021). There are many potential reasons for this, including different hormone deprivation and E2 treatment times, different modes of introducing *ESR1* mutations into cells and different sequencing techniques. However, this highlights that potential clonal effects must be considered when interpreting findings from studies which have used clones to model these mutations. Although using cells with high expression of PR (e.g. T47D), and therefore greater responsiveness to PR ligands, makes discovery of the importance of the actions of PR easier, these cells are not necessarily representative of the full spectrum of breast cancers, which will have a range of low, medium and high PR levels. Studying PR signalling in other ER+ cell lines (e.g. SUM-44, ZR-75), PDX-derived cell lines and *in vivo* models harbouring mutant ESR1 with varying levels of PR expression is required to fully elucidate the effects of modulating PR in WT and mutant ER breast cancer.

The context-dependence of PR can also complicate cell culture experiments. The estrogenic content of media can affect whether progestogens are pro- or anti-proliferative; in E2-depleted conditions, R5020 treatment can induce moderate growth of T47D cells but with combined (E2+progestogen) treatment, progestogens consistently abrogate the E2-stimulated growth of breast cancer cells, PDX models and primary human tumour explants (Hissom and Moore 1987; Mohammed et al. 2015; Kabos et al. 2012). The proliferative effects of R5020 in the absence of E2 is potentially of limited clinical relevance, since breast cancers are rarely PR+ and ER-negative (Carroll et al. 2017), but has significant implications for *in vitro* and *in vivo* work. Unlike T47D cells, MCF7 cells (with their lower levels of PR) require E2 treatment to induce detectable levels of PR, which is therefore a prerequisite for all

studies with PR ligands in MCF7 cells (Read et al. 1988). E2 supplementation is also required to support subcutaneous or mammary fat pad ER+/PR+ xenografts but methods have now been developed, which, when breast cancer cell lines or PDXs are engrafted directly into mouse milk ducts (intraductally), maintain ER and PR positivity without the need for E2 (Kabos et al. 2012; Sflomos et al. 2016). Several PDX models of mutant *ESR1* have been created and studied including one intraductal PDX-derived cell line that possesses a naturally occurring, homozygous *ESR1* D538G mutation (Li et al. 2013; Gu et al. 2021; Finlay-Schultz et al. 2020). Such PDX models may be particularly valuable experimental models, as they lack any potential off-target effects associated with CRISPR-Cas9, such as mutations at sites other than those intended (Finlay-Schultz et al. 2020). Arguably, PDXs are more representative of tumours than CRISPR-derived cells since they are not clonal. However, cell lines are isogenic, enabling clearer comparisons with the parental, WT line and therefore study of the effects conferred by *ESR1* mutations. This is more difficult for PDX models, since 'pre-mutation', WT tumours are not often available. PDX models are also derived from patients who may often have had multiple lines of treatment including chemotherapy, AIs and anti-estrogens, which may also potentially confound findings from these models. Therefore both cell line and PDX models have different advantages and extending the studies of PR signalling in *ESR1* mutant breast cancer from cell lines to PDXs carrying these mutations will be important.

4.3 Investigating the PR transcriptome in ER+ Breast Cancer cells

Within this thesis, I have used RNA-seq to define P4- and R5020-regulated genes in T47D-WT and T47D-Y537S cells. Most other studies that have explored the progestogen/PR transcriptome in ER+/PR+ breast cancer cells, have used either

microarray or RNA-seq in T47D cells treated with progestogens like P4 and R5020 and anti-progestins such as RU486 and telepristone acetate. The cell lines, PR ligands, treatment times and estrogenic conditions used in relevant studies published up to November 2021 are summarised in Table 4.1.

The RNA-seq data presented within this thesis supports the findings of other studies in confirming that ligand-activated PR is a key transactivator. The addition of E2 to R5020 increased the number of genes differentially regulated, to a greater degree in the T47D-WT line than the T47D-Y537S, reflecting the relative E2-independence of the mutant line (Figure 3.25A-D). Several classical PR target genes (e.g. *FKBP5, SGK1, MAFB, STAT5A*) were found to be progestogen-regulated within this geneset, with some of the greatest log2 fold changes and significance levels observed. Reassuringly, the log2 fold changes were similar for many *bona fide* PR target genes in this dataset and in that reported by Mohammed et al. 2015. For example, in this thesis, treatment of T47D-WT cells with (R5020+E2) resulted in a log2 fold change of 3.09 for *MAFB*, 2.58 for *KLF4* and 1.13 for *FKBP5* (padj value <0.05 for all 3 genes). The log2 fold change for these genes in T47D cells treated with R5020 in estrogenic media reported by Mohammed et al. 2015 was 3.90 for *MAFB*, 2.82 for *KLF4* and 1.85 for *FKBP5* (padj value <0.05 for all 3 genes). Comparison with all the genes reported to be P4- and R5020-regulated in T47D cells in estrogenic conditions by Mohammed et al. 2015, revealed that around 60% of the genes regulated with 1nM P4 or R5020 (in combination with 10nM E2) in T47D-WT cells in this study were commonly regulated by 100nM P4 or 10nM R5020 in T47D cells in the published study (Figure 3.24). The similarities between the genes found to be progestogen-regulated in this study and those described by Mohammed et al. 2015 was further confirmed by strong

enrichment of the up- (NES 3.14) and down-regulated genes (NES -3.18) regulated by (R5020+E2) in T47D-WT cells in the published set of R5020-regulated genes. In addition, some of the strongest PR targets (e.g. *SGK1, MAFB*) were also R5020 regulated in T47D-WT.SO, T47D-Y537S#1, T47D-Y537S#2, T47D-D538G#49 and T47D-D538G#60 cells (Figure 3.31). Therefore, I have a defined a set of robustly PR-regulated genes in T47D cells.

It would be interesting to explore whether these genes are also PR targets in other ER+ cell lines (e.g. ZR-75, SUM44) and PDX models. An important consideration for some of these PR targets is that they are regulated by other NRs in addition to PR. For example, both *NDRG1* and *GREB1* are ER-regulated and *NDRG1* and *FKBP5* are also well-known AR targets (Fotovati et al. 2006; Ghosh et al. 2000; Ulrix et al. 1999; Segawa et al. 2002; Magee et al. 2006). This is particularly relevant when selecting PR ligands for studying the effects of PR modulation, since many progestins and anti-progestins target multiple NRs (discussed in chapter 1, section 8). Nonetheless, I have identified a group of genes that are clearly PR-regulated in T47D cells, have been validated in other T47D lines, and have utility for studying the effects of PR signalling in ER+ cells, and particularly in identifying differences in this between WT and mutant ER cells. Cross referencing PR ChIP-seq data published by Mohammed et al. 2015, with the genes found to be PR-regulated through the RNA-seq data presented here, was performed to confirm whether any of these genes are direct PR targets. We studied one PR ChIP-seq replicate of T47D cells treated with 10nM R5020 in full media; 19,976 genes associated with the PR binding sites were found. Dr Van Nguyen kindly accessed this ChIP-seq data. 83.13% (133/160) of the genes upregulated (log2FC ≥-0.632, padj <0.05) by (R5020+E2) and 86.75% (72/83) of the genes

upregulated by R5020 alone in the T47D-WT cell line are direct PR targets. The proportion of genes downregulated (log2 fold change ≤-0.632, padj <0.05) in T47D-WT cells by (R5020+E2) or R5020 alone that are direct PR targets is much lower (61.11% (22/36) and 43.75% (7/16) respectively). Therefore, the majority of R5020-stimulated genes have PR binding sites but relatively fewer R5020-repressed genes are direct PR targets. This suggests that ~ 15% of R5020-upregulated genes and ~40-55% of R5020-downregulated genes are regulated by the involvement of other transcription factors or signalling pathways. Analysing the genes that are regulated by R5020 but not directly through PR binding, and performing GSEA on this geneset may provide insights on other factors or events that alter the expression of these genes following progestogen treatment,

Given the reports of ligand-activated PR redistributing ER genomic binding sites, it would also be interesting to explore the effect, if any, of progestogen treatment on the expression of ER target genes. Three classical ER target genes, *RARA, ELF3, CXCL12* were found to be downregulated by P4 and R5020 treatment in T47D-WT (and mutant) cells in this study and by the same PR ligands in T47D cells in the data published by Mohamed et al. 2015 (data not shown). In contrast, *GREB1* was upregulated by P4 and R5020 in both studies (data not shown). Since *GREB1* expression correlates with proliferation of breast cancer cells, this is not in keeping with the less tumorigenic profile of ER binding that progestogens are reported to induce (Rae et al. 2005; Mohammed et al. 2015; Singhal et al. 2018). Therefore, on the basis of these 4 genes, progestogens do appear to alter the expression of ER targets, although not necessarily in the same direction. Studying a larger number of

ER target genes and analysing the effect of progestogen treatment on their expression (using RNA-seq data from this study and others) may provide further insights.

One of the limitations of this thesis, particularly the RNA-seq study, is the use of only one *ESR1* mutant cell line (T47D-Y537S). This is important as in addition to the mutant-specific transcriptome, several reports have described mutant variant-specific gene expression profiles, phenotypes and responses to endocrine therapy (Arnesen et al. 2021; Li et al. 2022; Toy et al. 2013; Toy et al. 2017; Jeselsohn et al. 2018; Fanning et al. 2018b; Bahreini et al. 2017). Although validation experiments were performed with T47D cells carrying D538G mutations, (T47D-D538G#49 and T47D-D538G#60), RNA-seq using these and other *ESR1* mutant cell lines treated with progestogens would be valuable. Investigating the PR transcriptome in cells with ER mutations other than Y537S, particularly D538G, will be essential to extending the studies within this thesis, especially since differing responses of ER mutant variants to anti-estrogens and progestogens may result in patients with *ESR1* patients requiring mutant allele-specific treatments.

Table 4.1 Summary of studies that have defined PR-regulated genesets in ER+PR+ breast cancer cells

Cell Line	Ligand	Treatment time	Estrogen content	Method	No. DEGs (cut off threshold)	Ref
T47D-Y, T47D-YA, T47D-YB	10nM P4	6 hours	E2-depleted	Microarray	94 in total; 4 uniquely in T47D-YA, 65 uniquely in T47D-YB, 25 in both T47D-YA and T47D-YB (FC 1.8)	1
T47D-MTVL	10nM R5020	1, 6 hours	E2-depleted	Microarray	3,835 FC ≥1.5, p <0.05	2
T47D, T47D-wt PR-B, T47D-mCD PR-B	10nM R5020	6 hours	E2-depleted	Microarray	N/R (FC 1.5, p <0.05)	3
T47D	10nM R5020	3 hours	E2-depleted	RNA-seq	711 (FC 1.5, p <0.05)	4
T47D-MMTVluc	10nM R5020	6 hours	E2-depleted	RNA-seq	239 (ΔPSI >0.15, p <0.01)	5
T47D, MCF7	10nM R5020, 100nM P4	3 hours	Estrogenic	RNA-seq	P4: 543, R5020: 718 (FDR <0.01)	6
T47D	10nM R5020, 1μM TPA, (10nM R5020 + 1μM TPA)	24 hours	E2-depleted	Microarray	R5020 v control: 686, TPA v R5020: 790, (FC >+/-1.5, padj <0.001)	7
T47D-MTVL	10nM R5020	6 hours	E2-depleted	Microarray & RNA-seq	1,773 (FC ≥1.4)	8
T47D	10nM P4, 100nM RU486, 100nM Ona, 100nM Agl, (P4 + each antagonist)	6 hours	E2-depleted	Microarray	251, multiple sample comparisons (log2 FC ≥2, p ≤0.01)	9
T47D, MCF7, BT474, ZR-75-1,	10nM P4, (10nM P4 + 100nM RU486)	P4, RU486: 6 hours (P4+RU486): 2 hours RU486 then 6 hours P4	E2-depleted	Microarray	T47D: 623, MCF7: 553, BT474: 1873, ZR-75-1: 532 (Log FC 0.5, multiple sample comparisons)	10
T47D, T47Dco, ZR-75-1	10nM R5020	2, 4, 8, 12 hours	+/- 10nM E2	RNA-seq	N/R	11
T47D (siControl)	10nM R5020	6 hours	E2-depleted	RNA-seq	2,006 (FC >2, padj <0.01)	12
T47D	10nM R5020	6 hours	Estrogenic	RNA-seq	1,072 (log2 FC ≥1, p <0.05)	13
T47D (siControl)	10nM R5020	6 hours	E2-depleted	RNA-seq	795 (FC 2, p <0.01)	14
T47D-MTVL	50pM R5020, 10nM R5020	6 hours	E2-depleted	RNA-seq	50pM R5020: 1,700, 10nM R5020: 4,389, (FC 1.5, p <0.05)	15

Abbreviations – TPA: telepristone acetate, Ona: onapristone, Agl: aglepristone, FC: fold change, PSI; percent spliced in index, N/R: not reported. Cell lines – T47D-Y: PR negative, T47D-YA: stable expression of PR-A, T47D-YB: stable expression of PR-B, T47D-MTVL: carry a stably integrated copy of the luciferase reporter gene driven by the MMTV promoter, T47D-wt PRB: T47D-Y cells transfected with pSG5-wild type PR-B, T47D-mCD PR-B: T47D-Y cells transfected with pSG5-mCD PR-B (mutated common docking domain of PR-B) and pSV-neo, T47Dco: T47D variant that is the parental line for the T47D-Y, T47D-YA and T47D-YB lines, described in (Sartorius et al. 1994). Studies using ER+PR+ cells transfected with siRNA (except for those transfected with sicontrol, non-targeting siRNA) were excluded. References – 1 (Richer et al. 2002), 2 (Ballaré et al. 2013), 3 (Hagan et al. 2013), 4 (Kougioumtzi et al. 2014), 5 (Iannone et al. 2015), 6 (Mohammed et al. 2015), 7 (Clare et al. 2016), 8

(Nacht et al. 2016), 9 (Knutson et al. 2017), 10 (Godbole et al. 2018), 11 (Singhal et al. 2018), 12 (Nacht et al. 2019), 13 (Holloran et al. 2020), 14 (Malbeteau et al. 2020), 15 (Zaurin et al. 2021).

4.4 PR signalling in T47D-Y537S cells

This study represents the first study of the PR transcriptome in the setting of mutant ER. The number of progestogen-induced genes was far greater in the mutant line, with 357 genes differentially regulated in T47D-Y537S cells by R5020 treatment (without E2), compared to just 99 genes in the T47D-WT line (Figure 3.25). The magnitude of expression was also greater in the mutant line for many of these genes. For example, *KLF4* was differentially expressed following R5020 treatment in the T47D-WT line with a log2 fold change of 1.31, padj value 2.09x10^-74. In the R5020-treated mutant line, *KLF4* was more strongly regulated, with a log2 fold change of 2.20 and a padj value of <2.13x10^-288. The greater number of PR-regulated genes in the mutant line may simply be the result of the constitutive activity of ER (in the absence of E2), upregulation of PR and subsequent increased progestogen-sensitivity in the T47D-Y537S line. However, it is also possible that potential neomorphic effects conferred by the Y537S mutation alter regulation of gene expression patterns.

Many of the genes that were differentially regulated in the T47D-Y537S line relative to the T47D-WT by R5020 (without E2) with the highest significance level are well-known ER target genes (e.g. *CXCL12, ELF3, PGR, EPAS1*) (Figure 3.29A). A number of classical PR target genes were also differentially regulated in the mutant line relative to the WT with R5020 treatment alone (e.g. *MAFB, SGK1*) but, in general, these were regulated with lower significance levels than the ER-regulated genes (Figure 3.29A). This suggests that even with progestogen treatment, in the absence of E2 the predominant difference in gene expression patterns between the T47D-WT and T47D-

Y537S cells results from the E2-independence of the mutant line. The relative absence of these classical ER target genes from the genes most significantly regulated in the T47D-Y537S cells relative to the WT by R5020 in the presence of E2, further supports this (Figure 3.29B).

Genes regulated uniquely in the T47D-Y537S cell line by R5020 and/or (R5020+E2) were identified and studied to assess potential novel targets or expression patterns (Figure 3.29C-E and Figure 3.30). Interestingly, for the 145 genes regulated by R5020 in the absence of E2 exclusively in the T47D-Y537S line, 8 of the 10 most significantly enriched Gene Ontology Biological Process pathways were all related to cell motility or migration (Figure 3.30A). This is particularly relevant since ESR1 mutant cells exhibit greater motility, anchorage-independence and invasiveness relative to WT ER cells, and have therefore been implicated in the development of metastases in breast cancer (Merenbakh-Lamin et al. 2013; Martin et al. 2017; Li et al. 2022; Williams et al. 2021; Yu et al. 2019). Progestogens have been shown to reduce breast cancer cell migration and invasion in a WT ER setting but not, to my knowledge in ESR1 mutant cells (Fu et al. 2010; McFall et al. 2018). Other studies have shown that distinct mutant ER transcriptomes are also enriched for many migratory and metastatic pathways (Li et al. 2022; Arnesen et al. 2021; Bahreini et al. 2017). Li et al. 2022 have proposed potential mechanisms for the increased metastatic potential of *ESR1* mutant cells, including (1) enhanced cell-cell adhesion (via upregulation of desmosome and gap junction networks) and CTC clustering, (2) acquisition of pro-invasive properties through alteration of the TIMP3-MMP axis and, (3) greater migration of D538G mutant cells through FOXA1-regulated WNT pathway stimulation (discussed in more detail later in this section) (Li et al. 2022).

The enrichment of migration pathways for genes regulated by R5020 uniquely in the T47D-Y537S line in this study, together with the inhibition of motility observed in T47D-Y537S (and WT) cells (Figure 3.34), suggests that R5020 may have utility in decreasing the invasive phenotype of these cells. Performing *PGR* knockdown in T47D-WT and T47D-Y537S cells and then undertaking scratch wound assays with these cells treated with R5020 would confirm whether the anti-migratory effects of R5020 seen in these cell lines (Figure 3.34) are mediated through PR. Assessing the effect of R5020 (and other PR ligands) on motility and migration of T47D-WT, T47D-Y537S and other *ESR1* mutant cells should then be extended beyond scratch wound assays to include transwell migration assays and other *in vitro* motility assays. Beyond this, assessing the development (and sites) of metastases in *ESR1* mutant cell or PDXs treated with R5020 would also be important. Differences in the metastatic phenotype of *ESR1* mutant variants have been described; D538G ER is associated with greater metastatic potential and predilection for liver metastases than Y537S, although the latter are associated with a higher incidence of lung metastases (Merenbakh-Lamin et al. 2013; Jeselsohn et al. 2018; Li et al. 2022; Yu et al. 2019). The enhanced migratory potential of D538G ER relative to Y537S has also been reported by Li et al. 2022 so extending the studies of the effect of R5020 on migration, motility and ultimately metastasis to D538G and other ER mutant cells will be essential.

Interestingly, despite the relative E2-independence of T47D-Y537S cells, a distinct subset of genes were regulated in this line by (R5020+E2) but not R5020 alone (Figure 3.30B). The addition of E2 to R5020 increased the number of genes expressed in the

T47D-Y537S line (Figure 3.25C-D), and it may be that the 144 genes regulated just by (R5020+E2) in the mutant line (Figure 3.30B) are weaker PR targets that are only differentially expressed once the expression of PR is increased further by E2. This seems to be the case for some of these genes as 20/144 (13.89%) were also found to be regulated by the higher dose of 10nM R5020 (in the presence of E2) in WT T47D cells by Mohammed et al. 2015. The remaining ~86% of these 144 (R5020+E2) regulated genes may be even weaker PR targets (requiring higher doses of progestogen for induction) or may genuinely be novel, mutant-specific targets stimulated by the combination of R5020 and E2, but not by R5020 alone. For the 144 genes regulated by (R5020+E2) in the T47D-Y537S cell line only, the top 10 most enriched Gene Ontology Molecular Function and Biological Process were all related to the regulation of transcription or DNA binding (Figure 3.30B). This may reflect the transcriptional activity that is stimulated by the combination of R5020 and E2 treatment.

One of the 127 genes regulated by both R5020 and (R5020+E2) in the T47D-Y537S line (Figure 3.30C) is *FOXA1*, and the addition of E2 further increases its log2 fold change (log2FC -1.05 vs -1.12 respectively). In the T47D-WT line, FOXA1 did not meet the log2 fold change cut off of ≤-0.632 for R5020 regulation and only just met it for (R5020+E2) regulation (log2FC -0.71). However, it was found to be more strongly downregulated (log2FC -1.60) by 10nM R5020 (in the presence of E2) in T47D cells by Mohammed et al. 2015. Confirming the downregulation of *FOXA1* and log2 fold change of this in other ESR1 mutant cell lines and xenografts will be important. As discussed in chapter 1, section 3.2, FOXA1 is an essential ER pioneer factor, which improves chromatin accessibility and facilitates transcription of ER target genes.

Through rapid immunoprecipitation with tandem mass spectrometry of endogenous proteins (RIME) and coimmunoprecipitation of SUM44-WT and SUM44-LTED cells harbouring a naturally occurring Y537S mutation, Y537S ER has been observed to associate with FOXA1 at an increased level to WT ER (Martin et al. 2017). Arnesen et al. 2021 used ATAC-seq in T47D WT, Y537S and D538G cells from 2 different studies and showed that ER mutant cells have differential chromatin accessibility in thousands of different loci, the majority of which did not have ER binding (Arnesen et al. 2021; Bahreini et al. 2017). Mutant-specific genes were twice as likely to be found in close proximity to these differential sites of chromatin accessibility, compared to differential ER binding sites, and around 15% of the differentially expressed genes could be explained by the differential accessibility regions (Arnesen et al. 2021). Motif analysis of mutant-specific ATAC-seq sites revealed strongest enrichment of the FOX motif in D538G cells, with FOXA1 having the highest expression levels of all FOX members (Arnesen et al. 2021). ChiP-seq for T47D WT, Y537S and D538G cells was also performed and found enrichment of FOXA1 at transcription start site (TSS)-distal accessible chromatin sites in both ER mutant lines (Arnesen et al. 2021). In keeping with its role as an important ER pioneer factor, FOXA1 was enriched at ER+ binding sites more than ER-negative. Therefore, unlike a previous report suggesting that FOXA1 does not bind to mutant ER, Arnesen et al. 2021 demonstrate FOXA1-mediated chromatin remodelling in ER mutant cells and propose that this may contribute to mutant-specific transcriptome (Jeselsohn et al. 2018; Arnesen et al. 2021). Hence the downregulation of *FOXA1* (albeit modest) in the T47D-Y537S line following R5020 and (R5020+E2) treatment is certainly of interest. Given the reported enrichment of FOX motifs in D538G cells relative to Y537S, measuring *FOXA1* expression levels in the T47D-D538G#49 and T47D-D538G#60 cells following R5020

treatment would be interesting to see if the log2 fold change is greater than observed in the T47D-Y537S cells.

As part of their studies on the enhanced metastatic properties of mutant ER, Li et al. 2022 investigated the effect of *FOXA1* knockdown and found that this completely abrogated the enhanced motility of T47D-D538G cells (Li et al. 2022). Since R5020 inhibits the migration of T47D-Y537S (and WT cells), it would be interesting to see whether the R5020-induced downregulation of *FOXA1* contributes to this. Assessing whether overexpression of *FOXA1* restores the migratory phenotype of R5020-treated T47D-Y537S cells may help establish this. Furthermore, if R5020 inhibits migration in a FOXA1-independent manner, it would be useful to establish whether R5020 treatment in addition to *FOXA1* knockdown in T47D-Y537S (and D538G) cells impairs motility to a greater extent than either R5020 or *FOXA1* knockdown alone.

To determine how FOXA1 mediates this anti-migratory effect, Li et al. 2022 performed FOXA1 ChIP-seq, which revealed around a 1.6-fold increase in bindings sites in T47D Y537S and D538G cells than in WT (Li et al. 2022). Despite these additional ER mutant FOXA1 binding sites, the overlap between FOXA1 and ER binding sites was significantly lower for Y537S and D538G cells compared to E2-treated WT. In contrast to Arnesen et al. 2021's hypothesis that FOXA1 exhibits an enhanced pioneer function in ER mutant cells, Li et al. 2022 therefore propose that FOXA1 has reduced pioneer function and may contribute to D538G-specific gene expression profiles through novel binding sites (Arnesen et al. 2021; Li et al. 2022). 25 targets were identified through overlap of the gained FOXA1- and ATAC- sites in T47D-D538G cells; one of these, *TCF4* was also identified as a D538G-specific WNT regulator, a pathway which was

shown to be hyperactivated in the D538G line and associated with its migratory phenotype (Li et al. 2022). As discussed in chapter 1, sections 7.5 and 7.6, several WNT members including WNT1 and WNT4 have key roles in PR signalling. Furthermore, strong enrichment was seen for Hallmark and Gene Ontology Molecular Function WNT signalling pathways for the genes that were regulated by R5020 and (R5020+E2) in both T47D-WT and T47D-Y537S cells (Figure 3.28C-D). Performing FOXA1 ChIP-seq in T47D-Y537S (and other *ESR1* mutant) cells treated with R5020 would establish the effect of R5020 on the genomic binding patterns of FOXA1 and provide insights into how progestogens modulate FOXA1 activity in a mutant ER setting. It would be interesting to see whether additional WNT regulators are identified in gained FOXA1 sites following R5020 treatment and whether this differs between Y537S ER and D538G ER.

Li et al. 2022 hypothesise that mutant-specific redistribution of FOXA1 binding sites results in altered chromatin remodelling and then increased expression of genes, such as *TCF4*, which stimulate the WNT-induced enhanced motility of T47D-D538G cells. They base this hypothesis on 3 observations: (1) *FOXA1* knockdown reverses the increased expression of *TCF4* seen in D538G cells, (2) FOXA1 is strongly recruited to the *TCF4* gene locus and, (3) overexpression of *TCF4* inhibits migration of T47D-D538G cells relative to WT (Li et al. 2022). *TCF4* is not differentially expressed in progestogen-treated (1nM P4 or R5020 either with or without E2) T47D-Y537S or -WT cells in this thesis. However, *TCF4* is modestly downregulated following treatment with 10nM R5020 (log2FC -0.84, padj 9.13x10^-07) and with 100nM P4 (log2FC -0.98, padj 2.54x10^-10) in T47D cells in the presence of E2 in Mohammed et al. 2015's data. It would be interesting to establish whether *TCF4* is downregulated by R5020

treatment via FOXA1 (through *FOXA1* knockdown studies to see if *TCF4* expression is restored to vehicle-treated levels) in *ESR1* mutant cells. Utilising the T47D-Y537S#1, T47D-Y537S#2, T47D-D538G#49 and T47D-D538G#60 cells (along with the parental -WT.SO) for this would enable testing in 2 different *ESR1* mutant settings and these lines have also been shown to be more progestogen-responsive than the T47D-WT and -Y537S.

FOXA1 is clearly an important ER pioneer factor, playing a key role in recruiting ER and in the transcription of ER target genes. However, as described above, there are conflicting reports about how FOXA1 contributes to the ER mutant-specific transcriptome in terms of whether it facilitates enhanced ER-chromatin interactions or alters the ER genomic binding profile. I have shown that *FOXA1* expression is decreased by R5020 with and without E2 in T47D-Y537S cells and by (R5020+E2) in T47D-WT cells. The progestogen-mediated inhibition of *FOXA1* expression may provide a mechanism of action for the PR-mediated modulation of ER activity. This may be especially important for *ESR1* mutant cells, given the reported importance of FOXA1 in mutant-specific migration and gene expression patterns. Therefore, although the fold changes for *FOXA1* expression following R5020 treatment were relatively modest in this study, its progestogen-regulation and role in *ESR1* mutant breast cancer warrants further investigation. Finally, *FOXA1* is reported to have differential effects on WNT signalling and *FOXA1* activity in D538G cells but not Y537S mutant cells – ensuring future studies are performed in a range of mutant ER variants will be essential (Li et al. 2022).

4.5 Potential therapeutic strategies for patients with ESR1 mutations

As outlined in chapter 1, section 5.2, *ESR1* mutations impair the response to many ER-targeting therapies that are currently the backbone of treatment for patients with metastatic ER+ breast cancer. The ability to recognise patients with *ESR1* mutations through detection of ctDNA and cfDNA means that patients who may be resistant to standard treatment but benefit from specific treatments for mutant ER disease can easily be identified. There is still uncertainty about optimal treatment/timing of treatment on detection of *ESR1* mutant disease. The PADA-1 trial, the first to serially monitor patients for ESR1 mutations using ctDNA and then, once detected, incorporate a change of treatment (from (Palbociclib + AI) to (Palbociclib + Fulvestrant), should provide guidance on this (Bidard et al. 2019). In the future, it may be valuable to detect *ESR1* mutations before/as they are emerging, through measurement of biomarkers that have yet to be identified, enabling more prompt treatment. As several genes are differentially expressed in *ESR1* mutant cells relative to WT (both within this study and others), changes in the expression levels of some of these genes or those in their downstream pathways, may be discovered to be biomarkers for the emergence of *ESR1* mutations (Harrod et al. 2017; Martin et al. 2017; Bahreini et al. 2017; Arnesen et al. 2021; Li et al. 2022). As more information about the mutant variant-specific responses to various therapies emerges, particularly in the clinical setting, it may also be necessary to offer different treatments according to ER mutant variant. Historically, treatment of ER+ breast cancer has largely been focused on targeting ER regardless of PR status but, as the next section outlines, PR and its downstream targets may have a role here too.

4.5.1 PR-targeting therapies for ER+ and *ESR1* mutant breast cancer

As discussed in chapter 1, section 8, many PR drugs are available and, after the discovery that PR is able to alter the ER binding profile and reprogramme the ER transcriptome to a less tumorigenic state, the effects of PR agonists and antagonists in ER+ breast cancer have been investigated (Mohammed et al. 2015; Singhal et al. 2018). As a result, a number of clinical trials testing progestogens and anti-progestins in ER+ breast cancer are currently being undertaken and are summarised in Table 4.2. Despite the renewed interest in PR as a therapeutic target, there are still far fewer trials investigating the effects of PR modulating drugs compared to ER. None of the trials in Table 4.2 have specifically recruited patients with *ESR1* mutations but sub-analysis of the results may yield insights into the response of mutant ER to progestogens and anti-progestins.

The debate between whether PR agonists, antagonists or both (and if both, which have greater potency) are effective in ER+ breast cancer is ongoing. Historically, trials with PR antagonists were halted due to a lack of reproducibility and issues with hepatotoxicity but recent, unpublished work by Lange et al. has again raised a potential role for anti-progestins in endocrine resistance, since PR knockdown abrogated growth and mammosphere formation in several *ESR1* mutant models of breast cancer (Jonat et al. 2013; Robertson et al. 1999; Perrault et al. 1996; Kamaraju et al. 2021). However, the findings from this thesis do not support a role for anti-progestins in the treatment of *ESR1* WT or mutant breast cancer. Firstly, RU486 had no clear effect on the growth of either T47D-WT, T47D-Y537S, T47D-WT.SO, T47D-Y537S#1, T47D-Y537S#1, T47D-D538G#49 or T47D-D538G#60 cells, except for at a concentration of 10,000nM (Figures 3.7B and 3.32). RU486 targets GR and AR as

well as PR and the effects on growth seen at this high dose are likely to be off-target and not mediated by PR (Whitaker et al. 2014). A second PR antagonist, Onapristone, also had only modest antiproliferative effect on T47D-WT and T47D-Y537S cells, again except at a very high concentration (10,000nM) (Figure 3.7C). Finally, knocking *PGR* down in MCF7, MCF7-Y537S, T47D-WT and T47D-Y537S cells also only resulted in a small inhibition of growth of these cells (Figure 3.8A and C). RU486 also had minimal effect on the expression of PR target genes in MCF7 and MCF7-Y537S cells. Of course, in the MCF7 lines there was little response to the progestogen (P4 and R5020) treatment at the same doses that stimulated expression of PR-regulated genes in the T47D-WT and -Y537S cells. It would therefore be valuable to investigate the effect of RU486, Onapristone and other PR antagonists on expression of genes such as *SGK1, FKBP5* and *MAFB* in the T47D WT and *ESR1* mutant cells, which has not been done in this study.

In contrast, several findings of this thesis suggest that progestogens may have utility in the treatment of endocrine resistant breast cancer. R5020 inhibited proliferation of T47D-Y537S cells in a dose dependent manner (Figure 3.10A) and in the more progestogen-responsive T47D WT and *ESR1* mutant lines provided by Professor Oesterreich, P4 and R5020 clearly inhibited the growth of WT, Y537S and, to a lesser extent, D538G ER cells (Figure 3.32). A further PR agonist, MPA also inhibited the growth of T47D-WT.SO, T47D-Y537S#1 and T47D-Y537S#2 cells but not the T47D-D538G#49 or T47D-D538G#60 cells (except at 10,000nM) (Figure 3.32). The growth inhibition seen with R5020-treated T47D-WT.SO, T47D-Y537S#1 and T47D-Y537S#2 cells was completely abrogated by siRNA-mediated *PGR* knockdown, confirming that the growth effects of this progestogen are mediated through PR. Growth studies in

WT and mutant ER cells treated with a combination of a progestogen and anti-progestin would be helpful to further confirm this. In addition to anti-proliferative effects, R5020 also exhibits anti-migratory effects in both T47D-WT and T47D-Y537S cells (Figure 3.34). It would be important to confirm the effect of R5020 (and other progestogens, anti-progestins and combinations of both) on motility of other ESR1 mutant cells (both in different cell lines and different ER mutant variants) and, as mentioned in section 4.4, extend these studies to see whether PR ligands have any effect on the development of metastases in *ESR1* mutant xenografts. Although the studies presented here suggest that PR agonists are more promising treatments for ER+ breast cancer than PR antagonists, the literature contains reports of growth-inhibitory effects with both progestogen and anti-progestin treatments (discussed in chapter 1, section 8). It may be, therefore, that the modulating effects of PR are dependent on it being ligand-bound, regardless of the agonist/antagonist status of the ligand. The findings of the trials in Table 4.2 may help clarify the activity and tolerability of progestogens and anti-progestins in ER+ breast cancer although there are some limitations to these trials, which are discussed at the end of this section.

Despite being routinely tested for in every patient diagnosed with breast cancer, PR levels still rarely influence treatment decisions. Although evidence is accumulating for the use of PR ligands in PR+ disease, there is very little documented in the literature about PR signalling in PR-negative disease. As PR is an ER-regulated gene, ER+/PR-negative breast cancer is less common (accounting for ~25% of ER+ cases at diagnosis) but is more aggressive with increased treatment resistance and poorer outcomes than ER+/PR+ disease (McGuire and Clark 1986; Arpino et al. 2005; Punglia et al. 2006). In addition, approximately 30% of metastatic ER+ breast cancers

exhibit loss of heterozygosity at the PR locus and therefore lose PR expression later in the disease process, which is also associated with worse outcomes (Mohammed et al. 2015; Knutson and Lange 2014; Cui et al. 2005). This highlights the importance of investigating the effects of modulating PR signalling in the settings of high, medium and low PR levels, as well as in PR-negative breast cancer. Progestogens had very little effect on growth or expression of PR-regulated genes in MCF7 cells or even MCF7-Y537S cells (with their relatively higher *PGR* levels), compared to T47D-WT and T47D-Y537S cells. It would be useful to see whether the low *PGR* mRNA levels in the MCF7 lines also results in an absence of the anti-migratory effects of R5020 seen in the T47D cells. The lack of progestogen-responsiveness in the MCF7 cells suggests that these drugs may have reduced efficacy in low levels or absent PR expression. Sodium Cridanimod (also known as Virexxa) is a type 1 interferon inducer, which increases levels of PR expression (Surkov et al. 1996). It would be interesting to see whether co-treatment with Sodium Cridanimod or overexpression of *PGR* in the MCF7 cell lines would result in them being more sensitive to treatment with PR ligands. Sodium Cridanimod is currently being investigated in a phase II trial in patients with PR-negative recurrent or persistent endometrial cancer in combination with megesterol acetate or MPA (ClinicalTrials.gov Identifier NCT02064725). The results from this will be informative in terms of whether a similar strategy of first increasing PR expression in PR-negative breast cancer before treating with a PR modulating drug may be worth investigating in ER+/PR-negative and perhaps even ER-negative/PR-negative breast cancer.

Downstream targets of PR have also been suggested as treatment targets for ER+ breast cancer. As discussed in chapter 1, section 7.5, receptor activator of NF-κB

(RANKL) is a key mediator of PR's actions and the RANKL inhibitor, Denosumab, is already used widely in many patients with breast cancer to reduce the risk of AI-induced osteoporosis and complications associated with bone metastases. Although the RANKL gene (*TNFSF11)* was not differentially regulated by R5020 (with or without E2) in either T47D-WT or T47D-Y537S cells, the most enriched 'Hallmark' pathway for the genes regulated by R5020 or (R5020+E2) in both these cell lines was 'TNFA Signalling via NF-κB' (Figure 3.28C-D). NF-κB is a downstream effector of RANKL and investigating the genes that are enriched in this pathway following progestogen treatment may provide insights into how RANKL mediates the effects of PR. 'TNFA Signalling via NF-κB' was also the most enriched 'Hallmark' pathway for the 127 genes regulated uniquely in the T47D-Y537S cell line by both R5020 and (R5020+E2) (Figure 3.30C). Interrogating these mutant-specific genes may be helpful in determining whether the RANKL pathway is more active in mutant ER than WT breast cancer. The Phase III ABCSG-18 trial, investigating the effects of Denosumab on survival of patients with ER+/PR+ breast cancer receiving adjuvant AIs, is due to be completed later in 2022 (Gnant et al. 2019). The results from this trial may be helpful in determining whether inhibition of RANKL is worth investigating further as a potential treatment of ER+ breast cancer.

As discussed in section 4.4, WNT pathways were found to be enriched through gene set enrichment analyses for genes regulated by R5020 or (R5020+E2) in T47D-WT and T47D-Y537S cells. After Li et al. 2022 also confirmed the hyperactivation of the WNT pathway in ESR1 mutant breast cancer cells, they studied the effect of LGK974, which prevents WNT ligand secretion, on migration and proliferation of T47D-D538G cells (Li et al. 2022). As a single agent, LGK974 inhibited the migration of T47D-D538G

cells more than WT (by 40% v 20%) but had no effect on growth (Li et al. 2022). Synergy was detected with LGK974 and Fulvestrant combination treatment and inhibition of WNT signalling may reduce the metastatic activity of D538G ER (Li et al. 2022). Li et al. 2022 also observed the rescue of the migratory phenotype of T47D-D538G cells through *FOXA1* knockdown; when *FOXA1* knockdown was performed with concurrent Fulvestrant treatment, E2-independent growth of T47D-D538G cells was inhibited, suggesting a co-regulatory role for ER and FOXA1 in growth (Li et al. 2022). FOXA1 inhibitors are not widely available but, through targeting an upstream regulator (a demethylase, LSD1), modulation of FOXA1 has recently been achieved and it would be valuable to assess the effect of this in ESR1 mutant and WT breast cancer (Omarjee and Carroll 2020; Gao et al. 2020). The downregulation of *FOXA1* seen following progestogen treatment in T47D-Y537S cells was described in section 4.4. Investigating whether there is an additive effect on the inhibition of *FOXA1* through concurrent targeting of LSD1 and progestogen treatment would be interesting. Therefore, a number of downstream targets of PR show promise as therapeutic targets of *ESR1* mutant (and potentially WT) breast cancer and inhibition of some of them (WNT ligand and FOXA1) in combination with anti-estrogens seems to have a greater effect on growth and migration. A valuable addition to this study would be investigating the effects of combined anti-estrogen and progestogen treatment on growth, motility and gene expression in *ESR1* mutant cells and xenografts, to see whether this combination may have utility for patients.

Although many studies and trials have improved our understanding of PR signalling in breast cancer, these and the ongoing studies listed in Table 4.2 have left several questions unanswered in terms of use of PR modulating drugs clinically (Robertson et

al. 1999; Perrault et al. 1996; Jonat et al. 2013). Firstly, the majority of the trial in Table 4.2 are studying a PR-ligand in combination with an AI. Given that the reprogramming of ER by PR into a less tumorigenic profile has been shown to be dependent on the presence of E2, investigating the effects of PR ligands in the absence of E2-lowering AIs will be important (Mohammed et al. 2015). Secondly, most studies and clinical trials use a synthetic progestogen – only two trials are currently investigating the effect of oral, micronized endogenous P4 (Prometrium) in breast cancer. As discussed in chapter 1, section 7, synthetic and natural progestogens have differing effects on the risk of breast cancer when included in HRT, and it is possible that they also have different efficacies in the treatment of breast cancer (Fournier et al. 2005; Fournier et al. 2008). Clinical data on the differences of natural and synthetic progestogens in the treatment of ER+ breast cancer would be helpful. Thirdly, although one trial evaluated 2 different doses of Onapristone, most other clinical trials only use 1 dose (Robertson et al. 1999). As outlined in chapter 1, section 7, high dose progestins have demonstrated anti-tumorigenic effects in metastatic ER+ breast cancer but low doses are associated with the development of breast cancer; trials including a range of doses and long-term follow-up data would be informative (Perrault et al. 1996; Beral 2003; Chlebowski et al. 2015; Hunter et al. 2010). Finally, there is a paucity of evidence on the differential response of mutant variant-specific ER to progestogens/anti-progestins. Since different responses may necessitate different therapies, this has significant implications for the treatment of patients with ESR1 mutations.

The data in this thesis has clinical implications for the treatment of both *ESR1* mutant and WT breast cancer. The use of the MCF7-WT, MCF7-Y537S, T47D-WT, T47D-Y537S, T47D-WT.SO, T47D-Y537S#1, T47D-Y537S#2, T47D-D538G#49 and T47D-

D538G#60 cell lines, provided a means of investigating the effects of modulating PR in both WT and mutant ER settings, as well as in varying levels of *PGR* expression (as discussed in section 4.2). The growth of MCF7-WT and MCF7-Y537S cells was not affected by PR ligands (Figure 3.6), except at the highest concentration tested (10,000nM), which is likely due to off-target effects (Zaurin et al. 2021) When studying the T47D-WT and T47D-Y537S cell lines (which have higher *PGR* levels than the MCF7 cell lines), R5020 was the only PR ligand to have a dose-dependent growth inhibitory effect on the T47D-Y537S line (but not the T47D-WT) (Figure 3.7). However, the T47D-WT.SO line (which has higher levels of *PGR* than the T47D-WT line), as well as the T47D-Y537S#1, T47D-Y537S#2, T47D-D538G#49 and T47D-D538G#60 cell lines were inhibited by the PR agonists P4, R5020 and MPA (but not the PR antagonist RU486) (Figure 3.32). This suggests that the *PGR* expression levels in each cell line dictate their response to progestogen-treatment, rather than simply their mutant or WT ER status. Hence, progestogens may have efficacy in patients with *ESR1* mutant breast cancer but also those with WT ER who have sufficiently high levels of *PGR* expression. In terms of the optimal PR ligand for clinical use in this setting, the data presented here suggests that PR agonists have efficacy whilst PR antagonists do not (Figures 3.7, 3.8 and 3.32). The progestogen with the greatest RBA for PR, R5020, had the greatest effect on growth and target gene expression of all the ligands tested (Figures 3.7, 3.23 and 3.32), but as a synthetic progestin that is not used clinically in the UK, longer term studies will have to be performed to assess its safety should it show promise beyond pre-clinical studies.

Table 4.2 Summary of studies investigating PR modulating drugs in ER+ Breast Cancer

Class	Trial name (ID)	PR Ligand	Combination	Setting	Subtype	Phase
PR Agonist	PIONEER (1)	Megestrol acetate	Letrozole	Early, Window	ER+, HER2-	II
	WinPro (2)	Prometrium#	Letrozole	Early, Window	ER+, PR+, HER-	II
	PEARL	Utrogestan #	Tamoxifen	Early, Window	ER+, PR+, HER2-	II
PR Antagonist	ONAWA (3)	Onapristone ER*	-	Early, window	ER+, PR+, HER2-	I
	Onward 202 (4)	Onapristone ER*	Letrozole + Palbociclib	Metastatic, adaptation to 1st line	ER+, PR+, HER2-	Ib
	SMILE (5)	Onapristone ER*	Fulvestrant	Metastatic, 2nd line	ER+, PR+, HER2-	II

Summary of all registered trials investigating the use of PR ligands on ER+ breast cancer that are registered on ClinicalTrials.gov as active and recruiting, as well as the PEARL study. # - Prometrium and Utrogestan are oral micronized progesterones, * - ER: extended release. ClinicalTrial.gov Identifiers: (1) NCT03306472, (2) NCT0390669, (3) NCT04872608, (4) NCT04738292, (5) NCT04142892.

4.6 Summary

In summary, having confirmed the mutant ER status and characterised the T47D-Y537S cell line, I have shown that both these cells and the MCF7-Y537S line exhibit E2-independent growth and E2-independent expression of ER target genes, including PR. I have demonstrated that the T47D line is superior to the MCF7 cell line for studying the effects of PR modulation, with R5020 exhibiting anti-proliferative effects in T47D-WT, T47D-Y537S, T47D-WT.SO, T47D-Y537S#1, T47D-Y537S#2, T47D-D538G#49 and T47D-D538G#60 cells. Despite reports in the literature of anti-tumorigenic activity following PR inhibition in ER+ breast cancer cells, growth of T47D-WT and T47D-Y537S cells was unaffected by use of anti-progestins (a finding reflected in T47D-WT.SO, T47D-Y537S#1, T47D-Y537S#2, T47D-D538G#49 and T47D-D538G#60 cells) or siRNA-mediated PR knockdown. Using RNA-seq, I have defined a set of PR-regulated genes in T47D-WT cells and, for the first time, in ER mutant cells (T47D-Y537S). In addition, I have identified changes in the expression levels of a number of ER target genes following progestogen-treatment. This will be a valuable resource for further studies of the activity of PR on *ESR1* mutant breast

cancer beyond this thesis, particularly given the proposed mechanism of ligand-bound PR altering the binding profile of ER into a less proliferative pattern. Furthermore, I have highlighted an anti-migratory effect of R5020 on T47D WT and Y537S cells, through scratch wound assays and enrichment of Gene Ontology Biological Process pathways related to motility, which warrants further investigation. These findings are summarised in Figure 4.1. Although several facets of PR signalling are yet to be elucidated, clearly an expanding body of evidence suggests that a role for PR ligands in the treatment of endocrine resistant breast cancer exists, and further research is needed to fully define this.

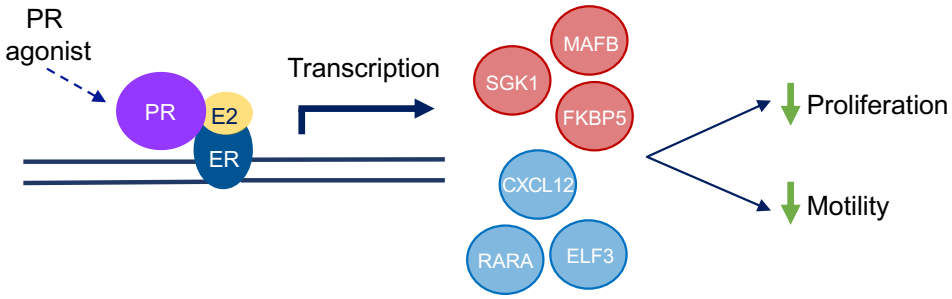


Figure 4.1 PR signalling in ER+ Breast Cancer; Findings of this Thesis

As demonstrated through RNA-seq, progestogen treatment of T47D-WT and T47D-Y537S cells, alters the expression levels of a number of classical PR target genes (in red) and ER target genes (in blue). Progestogens were also observed to inhibit the growth of ER+ cells (ESR1 mutant and WT with sufficient levels of PGR expression). R5020 also inhibited the motility of both T47D-WT and T47D-Y537S cells.

References

Abdel-Hafiz, H., G. S. Takimoto, L. Tung, and K. B. Horwitz. 2002. 'The inhibitory function in human progesterone receptor N termini binds SUMO-1 protein to regulate autoinhibition and transrepression', *J Biol Chem*, 277: 33950-6.

Abdel-Hafiz, Hany A., and Kathryn B. Horwitz. 2014. 'Post-translational modifications of the progesterone receptors', *The Journal of Steroid Biochemistry and Molecular Biology*, 140: 80-89.

Acconcia, Filippo, and Rakesh Kumar. 2006. 'Signaling regulation of genomic and nongenomic functions of estrogen receptors', *Cancer Letters*, 238: 1-14.

Afhüppe, W., J. M. Beekman, C. Otto, D. Korr, J. Hoffmann, U. Fuhrmann, and C. Möller. 2010. 'In vitro characterization of ZK 230211--A type III progesterone receptor antagonist with enhanced antiproliferative properties', *J Steroid Biochem Mol Biol*, 119: 45-55.

Afhüppe, W., A. Sommer, J. Müller, W. Schwede, U. Fuhrmann, and C. Möller. 2009. 'Global gene expression profiling of progesterone receptor modulators in T47D cells provides a new classification system', *J Steroid Biochem Mol Biol*, 113: 105-15.

Africander, Donita, Nicolette Verhoog, and Janet P. Hapgood. 2011. 'Molecular mechanisms of steroid receptor-mediated actions by synthetic progestins used in HRT and contraception', *Steroids*, 76: 636-52.

Al-Hajj, Muhammad, Max S. Wicha, Adalberto Benito-Hernandez, Sean J. Morrison, and Michael F. Clarke. 2003. 'Prospective identification of tumorigenic breast cancer cells', *Proceedings of the National Academy of Sciences*, 100: 3983-88.

Aleskandarany, Mohammad A., Rezvan Abduljabbar, Ibraheem Ashankyty, Ahmed Elmouna, Dena Jerjees, Simak Ali, Laki Buluwela, et al. 2016. 'Prognostic significance of androgen receptor expression in invasive breast cancer: transcriptomic and protein expression analysis', *Breast cancer research and treatment*, 159: 215-27.

Alexieva-Figusch, J., H. A. van Gilse, W. C. Hop, C. H. Phoa, J. Blonk-van der Wijst, and R. E. Treurniet. 1980. 'Progestin therapy in advanced breast cancer: megestrol acetate--an evaluation of 160 treated cases', *Cancer*, 46: 2369-72.

Ali, S., and R. C. Coombes. 2002. 'Endocrine-responsive breast cancer and strategies for combating resistance', *Nat Rev Cancer*, 2: 101-12.

Allen, Edgar, and Edward Adelbert Doisy. 'An Ovarian Hormone: Preliminary Report on Its Localization, Extraction and Partial Purification, and Action in Test Animals', *JAMA*, 250: 2681-83.

Allen, W.M., and W.M. Corner. 1929. 'Physiology of the corpus luteum, III: normal growth and implantation of embryos after very early ablation of the ovaries, and under the influence of extracts of the corpus luteum.', *Am J Physiol*, 88: 340-6.

Allouchery, V., L. Beaussire, A. Perdrix, D. Sefrioui, L. Augusto, C. Guillemet, N. Sarafan-Vasseur, F. Di Fiore, and F. Clatot. 2018. 'Circulating ESR1 mutations at the end of aromatase inhibitor adjuvant treatment and after relapse in breast cancer patients', *Breast Cancer Res*, 20: 40.

An, H. X., M. W. Beckmann, G. Reifenberger, H. G. Bender, and D. Niederacher. 1999. 'Gene amplification and overexpression of CDK4 in sporadic breast carcinomas is associated with high tumor cell proliferation', *The American journal of pathology*, 154: 113-8.

Anbalagan, M., and B. G. Rowan. 2015. 'Estrogen receptor alpha phosphorylation and its functional impact in human breast cancer', *Mol Cell Endocrinol*, 418 Pt 3: 264-72.

Anderson, Elizabeth. 2002. 'Progesterone receptors - animal models and cell signaling in breast cancer: The role of oestrogen and progesterone receptors in human mammary development and tumorigenesis', *Breast Cancer Research*, 4: 197.

Anderson, G. L., R. T. Chlebowski, A. K. Aragaki, L. H. Kuller, J. E. Manson, M. Gass, E. Bluhm, et al. 2012. 'Conjugated equine oestrogen and breast cancer incidence and mortality in postmenopausal women with hysterectomy: extended follow-up of the Women's Health Initiative randomised placebo-controlled trial', *Lancet Oncol*, 13: 476-86.

Anderson, G. L., M. Limacher, A. R. Assaf, T. Bassford, S. A. Beresford, H. Black, D. Bonds, et al. 2004. 'Effects of conjugated equine estrogen in postmenopausal women with hysterectomy: the Women's Health Initiative randomized controlled trial', *Jama*, 291: 1701-12.

André, F., E. M. Ciruelos, D. Juric, S. Loibl, M. Campone, I. A. Mayer, G. Rubovszky, et al. 2021. 'Alpelisib plus fulvestrant for PIK3CA-mutated, hormone receptor-positive, human epidermal growth factor receptor-2-negative advanced breast cancer: final overall survival results from SOLAR-1', *Ann Oncol*, 32: 208-17.

André, Fabrice, Eva Ciruelos, Gabor Rubovszky, Mario Campone, Sibylle Loibl, Hope S. Rugo, Hiroji Iwata, et al. 2019. 'Alpelisib for PIK3CA-Mutated, Hormone Receptor–Positive Advanced Breast Cancer', *New England Journal of Medicine*, 380: 1929-40.

Andreano, Kaitlyn J., Jennifer G. Baker, Sunghee Park, Rachid Safi, Sandeep Artham, Steffi Oesterreich, Rinath Jeselsohn, et al. 2020. 'The Dysregulated Pharmacology of Clinically Relevant ESR1 Mutants is Normalized by Ligand-activated WT Receptor', *Molecular Cancer Therapeutics*, 19: 1395-405.

Anurag, Meenakshi, Matthew J. Ellis, and Svasti Haricharan. 2018. 'DNA damage repair defects as a new class of endocrine treatment resistance driver', *Oncotarget*, 9: 36252-53.

Arnesen, Spencer, Zannel Blanchard, Michelle M. Williams, Kristofer C. Berrett, Zheqi Li, Steffi Oesterreich, Jennifer K. Richer, and Jason Gertz. 2021. 'Estrogen Receptor Alpha Mutations in Breast Cancer Cells Cause Gene Expression Changes through Constant Activity and Secondary Effects', *Cancer Res*, 81: 539-51.

Arnett-Mansfield, Rebecca L., J. Dinny Graham, Adrienne R. Hanson, Patricia A. Mote, Anne Gompel, Lyndee L. Scurr, Natalie Gava, Anna de Fazio, and Christine L. Clarke. 2007. 'Focal Subnuclear Distribution of Progesterone Receptor Is Ligand Dependent and Associated with Transcriptional Activity', *Molecular Endocrinology*, 21: 14-29.

Arpino, Grazia, Heidi Weiss, Adrian V. Lee, Rachel Schiff, Sabino De Placido, C. Kent Osborne, and Richard M. Elledge. 2005. 'Estrogen Receptor–Positive, Progesterone Receptor–Negative Breast Cancer: Association With Growth Factor Receptor Expression and Tamoxifen Resistance', *JNCI: Journal of the National Cancer Institute*, 97: 1254-61.

Ashburner, M., C. A. Ball, J. A. Blake, D. Botstein, H. Butler, J. M. Cherry, A. P. Davis, et al. 2000. 'Gene ontology: tool for the unification of biology. The Gene Ontology Consortium', *Nat Genet*, 25: 25-9.

Asi, Noor, Khaled Mohammed, Qusay Haydour, Michael R. Gionfriddo, Oscar L. Morey Vargas, Larry J. Prokop, Stephanie S. Faubion, and Mohammad Hassan Murad. 2016. 'Progesterone vs. synthetic progestins and the risk of breast cancer: a systematic review and meta-analysis', *Systematic Reviews*, 5: 121.

Asselin-Labat, M. L., M. Shackleton, J. Stingl, F. Vaillant, N. C. Forrest, C. J. Eaves, J. E. Visvader, and G. J. Lindeman. 2006. 'Steroid hormone receptor status of mouse mammary stem cells', *J Natl Cancer Inst*, 98: 1011-4.

Asselin-Labat, M. L., F. Vaillant, J. M. Sheridan, B. Pal, D. Wu, E. R. Simpson, H. Yasuda, et al. 2010. 'Control of mammary stem cell function by steroid hormone signalling', *Nature*, 465: 798-802.

Ataca, Dalya, Patrick Aouad, Céline Constantin, Csaba Laszlo, Manfred Beleut, Marie Shamseddin, Renuga Devi Rajaram, et al. 2020. 'The secreted protease Adamts18 links hormone action to activation of the mammary stem cell niche', *Nature Communications*, 11: 1571-71.

Auchus, Mary Louise, and Richard J. Auchus. 2012. 'Human steroid biosynthesis for the oncologist', *Journal of investigative medicine : the official publication of the American Federation for Clinical Research*, 60: 495-503.

Aupperlee, M. D., and S. Z. Haslam. 2007. 'Differential hormonal regulation and function of progesterone receptor isoforms in normal adult mouse mammary gland', *Endocrinology*, 148: 2290-300.

Aupperlee, Mark D., Jeffrey R. Leipprandt, Jessica M. Bennett, Richard C. Schwartz, and Sandra Z. Haslam. 2013. 'Amphiregulin mediates progesterone-induced mammary ductal development during puberty', *Breast Cancer Research*, 15: R44.

Axlund, S. D., B. H. Yoo, R. B. Rosen, J. Schaack, P. Kabos, D. V. Labarbera, and C. A. Sartorius. 2013. 'Progesterone-inducible cytokeratin 5-positive cells in luminal breast cancer exhibit progenitor properties', *Horm Cancer*, 4: 36-49.

Bachelot, T., C. Bourgier, C. Cropet, I. Ray-Coquard, J. M. Ferrero, G. Freyer, S. Abadie-Lacourtoisie, et al. 2012. 'Randomized phase II trial of everolimus in combination with tamoxifen in patients with hormone receptor-positive, human epidermal growth factor receptor 2-negative metastatic breast cancer with prior exposure to aromatase inhibitors: a GINECO study', *J Clin Oncol*, 30: 2718-24.

Bagamasbad, Pia, and Robert J. Denver. 2011. 'Mechanisms and significance of nuclear receptor auto- and cross-regulation', *General and comparative endocrinology*, 170: 3-17.

Bahreini, Amir, Zheqi Li, Peilu Wang, Kevin M. Levine, Nilgun Tasdemir, Lan Cao, Hazel M. Weir, et al. 2017. 'Mutation site and context dependent effects of ESR1 mutation in genome-edited breast cancer cell models', *Breast Cancer Research*, 19: 60.

Bai, Yongli, and Vincent Giguère. 2003. 'Isoform-Selective Interactions between Estrogen Receptors and Steroid Receptor Coactivators Promoted by Estradiol and ErbB-2 Signaling in Living Cells', *Molecular Endocrinology*, 17: 589-99.

Balk, S. P., and K. E. Knudsen. 2008. 'AR, the cell cycle, and prostate cancer', *Nucl Recept Signal*, 6: e001.

Ballaré, Cecilia, Giancarlo Castellano, Laura Gaveglia, Sonja Althammer, Juan González-Vallinas, Eduardo Eyras, Francois Le Dily, et al. 2013. 'Nucleosome-Driven Transcription Factor Binding and Gene Regulation', *Molecular Cell*, 49: 67-79.

Ballaré, Cecilia, Markus Uhrig, Thomas Bechtold, Elena Sancho, Marina Di Domenico, Antimo Migliaccio, Ferdinando Auricchio, and Miguel Beato. 2003. 'Two Domains of the Progesterone Receptor Interact with the Estrogen Receptor and Are Required for Progesterone Activation of the c-Src/Erk Pathway in Mammalian Cells', *Molecular and cellular biology*, 23: 1994-2008.

Bardia, A., P. Aftimos, T. Bihani, A. T. Anderson-Villaluz, J. Jung, M. G. Conlan, and V. G. Kaklamani. 2019. 'EMERALD: Phase III trial of elacestrant (RAD1901) vs endocrine therapy for previously treated ER+ advanced breast cancer', *Future Oncol*, 15: 3209-18.

Barone, I., D. Iacopetta, K. R. Covington, Y. Cui, A. Tsimelzon, A. Beyer, S. Andò, and S. A. Fuqua. 2010. 'Phosphorylation of the mutant K303R estrogen receptor alpha at serine 305 affects aromatase inhibitor sensitivity', *Oncogene*, 29: 2404-14.

Baselga, J., M. Campone, M. Piccart, H. A. Burris, 3rd, H. S. Rugo, T. Sahmoud, S. Noguchi, et al. 2012a. 'Everolimus in postmenopausal hormone-receptor-positive advanced breast cancer', *N Engl J Med*, 366: 520-9.

Baselga, J., J. Cortés, S. B. Kim, S. A. Im, R. Hegg, Y. H. Im, L. Roman, et al. 2012b. 'Pertuzumab plus trastuzumab plus docetaxel for metastatic breast cancer', *N Engl J Med*, 366: 109-19.

Baselga, J., V. Semiglazov, P. van Dam, A. Manikhas, M. Bellet, J. Mayordomo, M. Campone, et al. 2009. 'Phase II randomized study of neoadjuvant everolimus plus letrozole compared with placebo plus letrozole in patients with estrogen receptor-positive breast cancer', *J Clin Oncol*, 27: 2630-7.

Bautista, S., H. Vallès, R. L. Walker, S. Anzick, R. Zeillinger, P. Meltzer, and C. Theillet. 1998. 'In breast cancer, amplification of the steroid receptor coactivator gene AIB1 is correlated with estrogen and progesterone receptor positivity', *Clin Cancer Res*, 4: 2925-9.

Beato, M., P. Herrlich, and G. Schütz. 1995. 'Steroid hormone receptors: many actors in search of a plot', *Cell*, 83: 851-7.

Beatson, GeorgeThomas. 1896. 'ON THE TREATMENT OF INOPERABLE CASES OF CARCINOMA OF THE MAMMA: SUGGESTIONS FOR A NEW METHOD OF TREATMENT, WITH ILLUSTRATIVE CASES', *The Lancet*, 148: 162-65.

Becher, R., A. A. Miller, K. Höffken, U. Gerhold, H. Hirche, and C. G. Schmidt. 1989. 'High-dose medroxyprogesterone acetate in advanced breast cancer. Clinical and pharmacokinetic study with a combined oral and intramuscular regimen', *Cancer*, 63: 1938-43.

Beck, C. A., N. L. Weigel, M. L. Moyer, S. K. Nordeen, and D. P. Edwards. 1993. 'The progesterone antagonist RU486 acquires agonist activity upon stimulation of cAMP signaling pathways', *Proc Natl Acad Sci U S A*, 90: 4441-45.

Beck, C. A., Y. Zhang, N. L. Weigel, and D. P. Edwards. 1996. 'Two types of anti-progestins have distinct effects on site-specific phosphorylation of human progesterone receptor', *J Biol Chem*, 271: 1209-17.

Beleut, Manfred, Renuga Devi Rajaram, Marian Caikovski, Ayyakkannu Ayyanan, Davide Germano, Yongwon Choi, Pascal Schneider, and Cathrin Brisken. 2010. 'Two distinct mechanisms underlie progesterone-induced proliferation in the mammary gland', *Proc Natl Acad Sci U S A*, 107: 2989-94.

Bendrik, C., and C. Dabrosin. 2009. 'Estradiol increases IL-8 secretion of normal human breast tissue and breast cancer in vivo', *J Immunol*, 182: 371-8.

Benson, J. R. 2002. 'Re: The effects of tamoxifen and estrogen on brain metabolism in elderly women', *J Natl Cancer Inst*, 94: 1336; author reply 36-7.
Bentel, J. M., S. N. Birrell, M. A. Pickering, D. J. Holds, D. J. Horsfall, and W. D. Tilley. 1999. 'Androgen receptor agonist activity of the synthetic progestin, medroxyprogesterone acetate, in human breast cancer cells', *Mol Cell Endocrinol*, 154: 11-20.
Beral, V. 2003. 'Breast cancer and hormone-replacement therapy in the Million Women Study', *Lancet*, 362: 419-27.
Beral, V., E. Banks, and G. Reeves. 2002. 'Evidence from randomised trials on the long-term effects of hormone replacement therapy', *Lancet*, 360: 942-4.
Bergink, E. W., F. van Meel, E. W. Turpijn, and J. van der Vies. 1983. 'Binding of progestagens to receptor proteins in MCF-7 cells', *J Steroid Biochem*, 19: 1563-70.
Bidard, F. C., C. Callens, B. Pistilli, F. Dalenc, T. de La Motte Rouge, R. Sabatier, J. S. Frenel, et al. 2019. 'Emergence of ESR1 mutation in cell-free DNA during first line aromatase inhibitor and palbociclib: An exploratory analysis of the PADA-1 trial', *Annals of Oncology*, 30: v105-v06.
Bidard, François-Clément, Anne-Claire Hardy-Bessard, Florence Dalenc, Thomas Bachelot, Jean-Yves Pierga, Thibault de la Motte Rouge, Renaud Sabatier, et al. 2022. 'Switch to fulvestrant and palbociclib versus no switch in advanced breast cancer with rising ESR1 mutation during aromatase inhibitor and palbociclib therapy (PADA-1): a randomised, open-label, multicentre, phase 3 trial', *The Lancet Oncology*, 23: 1367-77.
BIG1-98. 2005. 'A Comparison of Letrozole and Tamoxifen in Postmenopausal Women with Early Breast Cancer', *New England Journal of Medicine*, 353: 2747-57.
Bines, J., R. Dienstmann, R. M. Obadia, L. G. P. Branco, D. C. Quintella, T. M. Castro, P. G. Camacho, F. A. Soares, and M. E. F. Costa. 2014. 'Activity of megestrol acetate in postmenopausal women with advanced breast cancer after nonsteroidal aromatase inhibitor failure: a phase II trial', *Ann Oncol*, 25: 831-36.
Birrell, S. N., L. M. Butler, J. M. Harris, G. Buchanan, and W. D. Tilley. 2007. 'Disruption of androgen receptor signaling by synthetic progestins may increase risk of developing breast cancer', *FASEB journal : official publication of the Federation of American Societies for Experimental Biology*, 21: 2285-93.
Böcker, W., R. Moll, C. Poremba, R. Holland, P. J. Van Diest, P. Dervan, H. Bürger, et al. 2002. 'Common adult stem cells in the human breast give rise to glandular and myoepithelial cell lineages: a new cell biological concept', *Lab Invest*, 82: 737-46.
Boonyaratanakornkit, Viroj, Margaret Porter Scott, Vered Ribon, Lori Sherman, Steven M. Anderson, James L. Maller, W. Todd Miller, and Dean P. Edwards. 2001. 'Progesterone Receptor Contains a Proline-Rich Motif that Directly Interacts with SH3 Domains and Activates c-Src Family Tyrosine Kinases', *Molecular Cell*, 8: 269-80.
Booth, Brian W., Corinne A. Boulanger, Lisa H. Anderson, Lucia Jimenez-Rojo, Cathrin Brisken, and Gilbert H. Smith. 2010. 'Amphiregulin mediates self-renewal in an immortal mammary epithelial cell line with stem cell characteristics', *Experimental cell research*, 316: 422-32.

Bossis, Guillaume, and Frauke Melchior. 2006. 'SUMO: regulating the regulator', *Cell division*, 1: 13-13.
Boyd, N. F., H. Guo, L. J. Martin, L. Sun, J. Stone, E. Fishell, R. A. Jong, et al. 2007. 'Mammographic density and the risk and detection of breast cancer', *N Engl J Med*, 356: 227-36.
Bradbury, J. M., P. A. Edwards, C. C. Niemeyer, and T. C. Dale. 1995. 'Wnt-4 expression induces a pregnancy-like growth pattern in reconstituted mammary glands in virgin mice', *Dev Biol*, 170: 553-63.
Bradley, Rosie, Jeremy Braybrooke, Richard Gray, Robert K. Hills, Zulian Liu, Hongchao Pan, Richard Peto, et al. 2022. 'Aromatase inhibitors versus tamoxifen in premenopausal women with oestrogen receptor-positive early-stage breast cancer treated with ovarian suppression: a patient-level meta-analysis of 7030 women from four randomised trials', *The Lancet Oncology*, 23: 382-92.
Breuer, Eun-Kyoung, Daniela Fukushiro-Lopes, Annika Dalheim, Miranda Burnette, Jeremiah Zartman, Simon Kaja, Claire Wells, et al. 2019. 'Potassium channel activity controls breast cancer metastasis by affecting β-catenin signaling', *Cell Death & Disease*, 10: 180.
Brisken, C. 2013. 'Progesterone signalling in breast cancer: a neglected hormone coming into the limelight', *Nat Rev Cancer*, 13: 385-96.
Brisken, Cathrin, Ayyakkannu Ayyannan, Cuc Nguyen, Anna Heineman, Ferenc Reinhardt, Tian Jan, S. K. Dey, G. Paolo Dotto, and Robert A. Weinberg. 2002. 'IGF-2 Is a Mediator of Prolactin-Induced Morphogenesis in the Breast', *Developmental Cell*, 3: 877-87.
Brisken, Cathrin, Anna Heineman, Tony Chavarria, Brian Elenbaas, Jian Tan, Sudhansu K. Dey, Jill A. McMahon, Andrew P. McMahon, and Robert A. Weinberg. 2000. 'Essential function of Wnt-4 in mammary gland development downstream of progesterone signaling', *Genes & Development*, 14: 650-54.
Brisken, Cathrin, Sissela Park, Tibor Vass, John P. Lydon, Bert W. O'Malley, and Robert A. Weinberg. 1998. 'A paracrine role for the epithelial progesterone receptor in mammary gland development', *Proceedings of the National Academy of Sciences*, 95: 5076-81.
Brisken, Cathrin, and Valentina Scabia. 2020. '90 YEARS OF PROGESTERONE: Progesterone receptor signaling in the normal breast and its implications for cancer', *Journal of Molecular Endocrinology*, 65: T81-T94.
Burstein, Harold J., Constance T. Cirrincione, William T. Barry, Helen K. Chew, Sara M. Tolaney, Diana E. Lake, Cynthia Ma, Kimberly L. Blackwell, Eric P. Winer, and Clifford A. Hudis. 2014. 'Endocrine therapy with or without inhibition of epidermal growth factor receptor and human epidermal growth factor receptor 2: a randomized, double-blind, placebo-controlled phase III trial of fulvestrant with or without lapatinib for postmenopausal women with hormone receptor-positive advanced breast cancer-CALGB 40302 (Alliance)', *J Clin Oncol*, 32: 3959-66.
Butenandt, A., and U. Westphal. 1934. 'Zur Isolierung und Characterisierung des Corpus-luteum-Hormons.', *Ber chem Ges*, 67: 1440-42.
Buterin, T., C. Koch, and H. Naegeli. 2006. 'Convergent transcriptional profiles induced by endogenous estrogen and distinct xenoestrogens in breast cancer cells', *Carcinogenesis*, 27: 1567-78.
Buzdar, A., J. Douma, N. Davidson, R. Elledge, M. Morgan, R. Smith, L. Porter, J. Nabholtz, X. Xiang, and C. Brady. 2001. 'Phase III, Multicenter, Double-Blind,

Randomized Study of Letrozole, an Aromatase Inhibitor, for Advanced Breast Cancer Versus Megestrol Acetate', *Journal of Clinical Oncology*, 19: 3357-66.
Buzdar, A. U., W. Jonat, A. Howell, S. E. Jones, C. P. Blomqvist, C. L. Vogel, W. Eiermann, et al. 1998. 'Anastrozole versus megestrol acetate in the treatment of postmenopausal women with advanced breast carcinoma: results of a survival update based on a combined analysis of data from two mature phase III trials. Arimidex Study Group', *Cancer*, 83: 1142-52.
Buzdar, Aman, and Anthony Howell. 2001. 'Advances in Aromatase Inhibition', *Clinical Efficacy and Tolerability in the Treatment of Breast Cancer*, 7: 2620-35.
Calle, E. E., C. W. Heath, Jr., H. L. Miracle-McMahill, R. J. Coates, J. M. Liff, S. Franceschi, R. Talamini, et al. 1996. 'Breast cancer and hormonal contraceptives: further results: Collaborative group on hormonal factors in breast cancer', *Contraception*, 54: 1-106.
Campbell, R. A., P. Bhat-Nakshatri, N. M. Patel, D. Constantinidou, S. Ali, and H. Nakshatri. 2001. 'Phosphatidylinositol 3-kinase/AKT-mediated activation of estrogen receptor alpha: a new model for anti-estrogen resistance', *J Biol Chem*, 276: 9817-24.
Cancer Research UK. 'https://www.cancerresearchuk.org/health-professional/cancer-statistics/statistics-by-cancer-type/breast-cancer', Accessed 10th October 2021a.
Cancer Research UK. ‘https://www.cancerresearchuk.org/health-professional/cancer-statistics/statistics-by-cancer-type/breast-cancer/mortality Accessed 1st November 2021b.
Cao, Yixue, Giuseppina Bonizzi, Tiffany N. Seagroves, Florian R. Greten, Randall Johnson, Emmett V. Schmidt, and Michael Karin. 2001. 'IKKα Provides an Essential Link between RANK Signaling and Cyclin D1 Expression during Mammary Gland Development', *Cell*, 107: 763-75.
Cardoso, F., S. Kyriakides, S. Ohno, F. Penault-Llorca, P. Poortmans, I. T. Rubio, S. Zackrisson, and E. Senkus. 2019. 'Early breast cancer: ESMO Clinical Practice Guidelines for diagnosis, treatment and follow-up', *Ann Oncol*, 30: 1674.
Carlini, P, A Frassoldati, S De Marco, A Casali, EM Ruggeri, M Nardi, P Papaldo, A Fabi, F Paoloni, and F Cognetti. 2001. 'Formestane, a steroidal aromatase inhibitor after failure of non-steroidal aromatase inhibitors (anastrozole and letrozole): Is a clinical benefit still achievable?', *Annals of Oncology*, 12: 1539-43.
Carlson, K. E., I. Choi, A. Gee, B. S. Katzenellenbogen, and J. A. Katzenellenbogen. 1997. 'Altered ligand binding properties and enhanced stability of a constitutively active estrogen receptor: evidence that an open pocket conformation is required for ligand interaction', *Biochemistry*, 36: 14897-905.
Carnevale, Romina P., Cecilia J. Proietti, Mariana Salatino, Alejandro Urtreger, Guillermo Peluffo, Dean P. Edwards, Viroj Boonyaratanakornkit, et al. 2007. 'Progestin Effects on Breast Cancer Cell Proliferation, Proteases Activation, and in Vivo Development of Metastatic Phenotype All Depend on Progesterone Receptor Capacity to Activate Cytoplasmic Signaling Pathways', *Molecular Endocrinology*, 21: 1335-58.
Carroll, J. S. 2016. 'Mechanisms of oestrogen receptor (ER) gene regulation in breast cancer', *European journal of endocrinology*, 175: R41-R49.

Carroll, J. S., T. E. Hickey, G. A. Tarulli, M. Williams, and W. D. Tilley. 2017. 'Deciphering the divergent roles of progestogens in breast cancer', *Nat Rev Cancer*, 17: 54-64.
Carroll, J. S., C. A. Meyer, J. Song, W. Li, T. R. Geistlinger, J. Eeckhoute, A. S. Brodsky, et al. 2006. 'Genome-wide analysis of estrogen receptor binding sites', *Nat Genet*, 38: 1289-97.
Carroll, Jason S., X. Shirley Liu, Alexander S. Brodsky, Wei Li, Clifford A. Meyer, Anna J. Szary, Jerome Eeckhoute, et al. 2005. 'Chromosome-Wide Mapping of Estrogen Receptor Binding Reveals Long-Range Regulation Requiring the Forkhead Protein FoxA1', *Cell*, 122: 33-43.
Castellano, I., E. Allia, V. Accortanzo, A. M. Vandone, L. Chiusa, R. Arisio, A. Durando, et al. 2010. 'Androgen receptor expression is a significant prognostic factor in estrogen receptor positive breast cancers', *Breast Cancer Res Treat*, 124: 607-17.
Cella, David, Lesley Fallowfield, Peter Barker, Jack Cuzick, Gershon Locker, Anthony Howell, and Atac Trialistsà Group On behalf of the. 2006. 'Quality of Life of Postmenopausal Women in the ATAC ("Arimidex", Tamoxifen, Alone or in Combination) Trial after Completion of 5 years' Adjuvant Treatment for Early Breast Cancer', *Breast cancer research and treatment*, 100: 273-84.
Cenciarini, M. E., and C. J. Proietti. 2019. 'Molecular mechanisms underlying progesterone receptor action in breast cancer: Insights into cell proliferation and stem cell regulation', *Steroids*, 152: 108503.
CGHFBC. 2019. 'Type and timing of menopausal hormone therapy and breast cancer risk: individual participant meta-analysis of the worldwide epidemiological evidence', *Lancet*, 394: 1159-68.
Chabbert-Buffet, Nathalie, Geri Meduri, Philippe Bouchard, and Irving M. Spitz. 2005. 'Selective progesterone receptor modulators and progesterone antagonists: mechanisms of action and clinical applications', *Human Reproduction Update*, 11: 293-307.
Chandarlapaty, S., D. Chen, W. He, P. Sung, A. Samoila, D. You, T. Bhatt, et al. 2016. 'Prevalence of ESR1 Mutations in Cell-Free DNA and Outcomes in Metastatic Breast Cancer: A Secondary Analysis of the BOLERO-2 Clinical Trial', *JAMA Oncol*, 2: 1310-15.
Chandra, V., P. Huang, Y. Hamuro, S. Raghuram, Y. Wang, T. P. Burris, and F. Rastinejad. 2008. 'Structure of the intact PPAR-gamma-RXR- nuclear receptor complex on DNA', *Nature*, 456: 350-6.
Chatterton, Robert T., John P. Lydon, Rajendra G. Mehta, Esnar T. Mateo, Ashley Pletz, and V. Craig Jordan. 2002. 'Role of the progesterone receptor (PR) in susceptibility of mouse mammary gland to 7,12-dimethylbenz[a]anthracene-induced hormone-independent preneoplastic lesions in vitro', *Cancer Letters*, 188: 47-52.
Chawla, A., J. J. Repa, R. M. Evans, and D. J. Mangelsdorf. 2001. 'Nuclear receptors and lipid physiology: opening the X-files', *Science*, 294: 1866-70.
Cheang, Maggie C.U., David Voduc, Chris Bajdik, Samuel Leung, Steven McKinney, Stephen K. Chia, Charles M. Perou, and Torsten O. Nielsen. 2008. 'Basal-Like Breast Cancer Defined by Five Biomarkers Has Superior Prognostic Value than Triple-Negative Phenotype', *Clinical Cancer Research*, 14: 1368-76.

Chen, C. C., D. B. Hardy, and C. R. Mendelson. 2011. 'Progesterone receptor inhibits proliferation of human breast cancer cells via induction of MAPK phosphatase 1 (MKP-1/DUSP1)', *J Biol Chem*, 286: 43091-102.
Chen, D., T. Riedl, E. Washbrook, P. E. Pace, R. C. Coombes, J. M. Egly, and S. Ali. 2000. 'Activation of estrogen receptor alpha by S118 phosphorylation involves a ligand-dependent interaction with TFIIH and participation of CDK7', *Mol Cell*, 6: 127-37.
Chen, J. D., and R. M. Evans. 1995. 'A transcriptional co-repressor that interacts with nuclear hormone receptors', *Nature*, 377: 454-7.
Chen, Z., X. Lan, D. Wu, B. Sunkel, Z. Ye, J. Huang, Z. Liu, S. K. Clinton, V. X. Jin, and Q. Wang. 2015. 'Ligand-dependent genomic function of glucocorticoid receptor in triple-negative breast cancer', *Nat Commun*, 6: 8323.
Cheung, Shu-Yan, Mong-Ting Yuen, H. L. Choi, H. K. Cheng, Yu Huang, Shiuan Chen, and Franky L. Chan. 2003. 'An expression study of hormone receptors in spontaneously developed, carcinogen-induced and hormone-induced mammary tumors in female Noble rats', *Int J Oncol*, 22: 1383-95.
Chia, S., W. Gradishar, L. Mauriac, J. Bines, F. Amant, M. Federico, L. Fein, et al. 2008. 'Double-blind, randomized placebo controlled trial of fulvestrant compared with exemestane after prior nonsteroidal aromatase inhibitor therapy in postmenopausal women with hormone receptor-positive, advanced breast cancer: results from EFECT', *J Clin Oncol*, 26: 1664-70.
Chlebowski, R. T., S. L. Hendrix, R. D. Langer, M. L. Stefanick, M. Gass, D. Lane, R. J. Rodabough, et al. 2003. 'Influence of estrogen plus progestin on breast cancer and mammography in healthy postmenopausal women: the Women's Health Initiative Randomized Trial', *Jama*, 289: 3243-53.
Chlebowski, R. T., L. H. Kuller, R. L. Prentice, M. L. Stefanick, J. E. Manson, M. Gass, A. K. Aragaki, et al. 2009. 'Breast cancer after use of estrogen plus progestin in postmenopausal women', *N Engl J Med*, 360: 573-87.
Chlebowski, Rowan T., Thomas E. Rohan, JoAnn E. Manson, Aaron K. Aragaki, Andrew Kaunitz, Marcia L. Stefanick, Michael S. Simon, et al. 2015. 'Breast Cancer After Use of Estrogen Plus Progestin and Estrogen Alone: Analyses of Data From 2 Women's Health Initiative Randomized Clinical Trials', *JAMA oncology*, 1: 296-305.
Chung, Hwa Hwa, Siu Kwan Sze, Alvin Shun Long Tay, and Valerie C. L. Lin. 2014a. 'Acetylation at Lysine 183 of Progesterone Receptor by p300 Accelerates DNA Binding Kinetics and Transactivation of Direct Target Genes', *Journal of Biological Chemistry*, 289: 2180-94.
Chung, Hwa Hwa, Siu Kwan Sze, Amanda Rui En Woo, Yang Sun, Kae Hwan Sim, Xue Ming Dong, and Valerie C. L. Lin. 2014b. 'Lysine Methylation of Progesterone Receptor at Activation Function 1 Regulates both Ligand-independent Activity and Ligand Sensitivity of the Receptor *', *Journal of Biological Chemistry*, 289: 5704-22.
Ciarloni, L., S. Mallepell, and C. Brisken. 2007. 'Amphiregulin is an essential mediator of estrogen receptor alpha function in mammary gland development', *Proc Natl Acad Sci U S A*, 104: 5455-60.
Cirillo, L. A., F. R. Lin, I. Cuesta, D. Friedman, M. Jarnik, and K. S. Zaret. 2002. 'Opening of compacted chromatin by early developmental transcription factors HNF3 (FoxA) and GATA-4', *Mol Cell*, 9: 279-89.
Cittelly, D. M., J. Finlay-Schultz, E. N. Howe, N. S. Spoelstra, S. D. Axlund, P. Hendricks, B. M. Jacobsen, C. A. Sartorius, and J. K. Richer. 2013. 'Progestin

suppression of miR-29 potentiates dedifferentiation of breast cancer cells via KLF4', *Oncogene*, 32: 2555-64.
Clare, Susan E., Akash Gupta, MiRan Choi, Manish Ranjan, Oukseub Lee, Jun Wang, David Z. Ivancic, J. Julie Kim, and Seema A. Khan. 2016. 'Progesterone receptor blockade in human breast cancer cells decreases cell cycle progression through G2/M by repressing G2/M genes', *BMC cancer*, 16: 326-26.
Clarke, R. B., A. Howell, C. S. Potten, and E. Anderson. 1997. 'Dissociation between steroid receptor expression and cell proliferation in the human breast', *Cancer Res*, 57: 4987-91.
Clemons, M., and P. Goss. 2001. 'Estrogen and the risk of breast cancer', *N Engl J Med*, 344: 276-85.
Cochrane, D. R., S. Bernales, B. M. Jacobsen, D. M. Cittelly, E. N. Howe, N. C. D'Amato, N. S. Spoelstra, et al. 2014. 'Role of the androgen receptor in breast cancer and preclinical analysis of enzalutamide', *Breast Cancer Res*, 16: R7.
Cochrane, Dawn R., Britta M. Jacobsen, Keith D. Connaghan, Erin N. Howe, David L. Bain, and Jennifer K. Richer. 2012. 'Progestin regulated miRNAs that mediate progesterone receptor action in breast cancer', *Molecular and Cellular Endocrinology*, 355: 15-24.
Cole, M. P., C. T. A. Jones, and I. D. H. Todd. 1971. 'A New Anti-oestrogenic Agent in Late Breast Cancer: An Early Clinical Appraisal of ICI46474', *Br J Cancer*, 25: 270-75.
Condon, Jennifer C., Daniel B. Hardy, Kelly Kovaric, and Carole R. Mendelson. 2006. 'Up-Regulation of the Progesterone Receptor (PR)-C Isoform in Laboring Myometrium by Activation of Nuclear Factor-κB May Contribute to the Onset of Labor through Inhibition of PR Function', *Molecular Endocrinology*, 20: 764-75.
Conneely, Orla M., Biserka Mulac-Jericevic, John P. Lydon, and Francesco J. De Mayo. 2001. 'Reproductive functions of the progesterone receptor isoforms: lessons from knock-out mice', *Molecular and Cellular Endocrinology*, 179: 97-103.
Conway, K., E. Parrish, S. N. Edmiston, D. Tolbert, C. K. Tse, J. Geradts, C. A. Livasy, H. Singh, B. Newman, and R. C. Millikan. 2005. 'The estrogen receptor-alpha A908G (K303R) mutation occurs at a low frequency in invasive breast tumors: results from a population-based study', *Breast Cancer Res*, 7: R871-80.
Cordina-Duverger, E., T. Truong, A. Anger, M. Sanchez, P. Arveux, P. Kerbrat, and P. Guénel. 2013. 'Risk of breast cancer by type of menopausal hormone therapy: a case-control study among post-menopausal women in France', *PloS one*, 8: e78016.
Cork, David M. W., Thomas W. J. Lennard, and Alison J. Tyson-Capper. 2008. 'Alternative splicing and the progesterone receptor in breast cancer', *Breast Cancer Research*, 10: 207.
Corner, G.W., and W.M. Allen. 1929. 'Physiology of the corpus luteum, II: Production of a special uterine reaction (progestational proliferation) by extracts of the corpus luteum.', *Am J Physiol*, 88: 326-99.
Cottu, Paul H., Jacques Bonneterre, Andrea Varga, Mario Campone, Alexandra Leary, Anne Floquet, Dominique Berton-Rigaud, et al. 2018. 'Phase I study of onapristone, a type I antiprogestin, in female patients with previously treated

recurrent or metastatic progesterone receptor-expressing cancers', *PloS one*, 13: e0204973.
Courtin, A., L. Communal, M. Vilasco, D. Cimino, N. Mourra, M. de Bortoli, D. Taverna, et al. 2012. 'Glucocorticoid receptor activity discriminates between progesterone and medroxyprogesterone acetate effects in breast cells', *Breast Cancer Res Treat*, 131: 49-63.
Cowley, S. M., S. Hoare, S. Mosselman, and M. G. Parker. 1997. 'Estrogen receptors alpha and beta form heterodimers on DNA', *J Biol Chem*, 272: 19858-62.
Cristofanilli, M., N. C. Turner, I. Bondarenko, J. Ro, S. A. Im, N. Masuda, M. Colleoni, et al. 2016. 'Fulvestrant plus palbociclib versus fulvestrant plus placebo for treatment of hormone-receptor-positive, HER2-negative metastatic breast cancer that progressed on previous endocrine therapy (PALOMA-3): final analysis of the multicentre, double-blind, phase 3 randomised controlled trial', *Lancet Oncol*, 17: 425-39.
Cui, Jie, Yong Shen, and Rena Li. 2013. 'Estrogen synthesis and signaling pathways during aging: from periphery to brain', *Trends in molecular medicine*, 19: 197-209.
Cui, X., R. Schiff, G. Arpino, C. K. Osborne, and A. V. Lee. 2005. 'Biology of progesterone receptor loss in breast cancer and its implications for endocrine therapy', *J Clin Oncol*, 23: 7721-35.
Cuzick, J., L. Ambroisine, N. Davidson, R. Jakesz, M. Kaufmann, M. Regan, and R. Sainsbury. 2007. 'Use of luteinising-hormone-releasing hormone agonists as adjuvant treatment in premenopausal patients with hormone-receptor-positive breast cancer: a meta-analysis of individual patient data from randomised adjuvant trials', *Lancet*, 369: 1711-23.
Damodaran, Senthil, Paul V. Plourde, Halle C. F. Moore, Ian Churchill Anderson, and David Jay Portman. 2022. 'Open-label, phase 2, multicenter study of lasofoxifene (LAS) combined with abemaciclib (Abema) for treating pre- and postmenopausal women with locally advanced or metastatic ER+/HER2− breast cancer and an ESR1 mutation after progression on prior therapies', *Journal of Clinical Oncology*, 40: 1022-22.
Daniel, A. R., E. J. Faivre, and C. A. Lange. 2007. 'Phosphorylation-dependent antagonism of sumoylation derepresses progesterone receptor action in breast cancer cells', *Mol Endocrinol*, 21: 2890-906.
Daniel, A. R., A. L. Gaviglio, T. P. Knutson, J. H. Ostrander, A. B. D'Assoro, P. Ravindranathan, Y. Peng, G. V. Raj, D. Yee, and C. A. Lange. 2015. 'Progesterone receptor-B enhances estrogen responsiveness of breast cancer cells via scaffolding PELP1- and estrogen receptor-containing transcription complexes', *Oncogene*, 34: 506-15.
Daniel, A.R., Lange, C.A. 2009. 'Protein kinases mediate ligand-independent derepression of sumoylated progesterone receptors in breast cancer cells', *PNAS*, 106: 14287-92.
Daniel, Andrea R., Angela L. Gaviglio, Lauren M. Czaplicki, Christopher J. Hillard, Daniel Housa, and Carol A. Lange. 2010. 'The Progesterone Receptor Hinge Region Regulates the Kinetics of Transcriptional Responses Through Acetylation, Phosphorylation, and Nuclear Retention', *Molecular Endocrinology*, 24: 2126-38.

Daniel, C. W., G. B. Silberstein, and P. Strickland. 1987. 'Direct action of 17 beta-estradiol on mouse mammary ducts analyzed by sustained release implants and steroid autoradiography', *Cancer Res*, 47: 6052-7.
Davies, B. R., H. Greenwood, P. Dudley, C. Crafter, D. H. Yu, J. Zhang, J. Li, et al. 2012. 'Preclinical pharmacology of AZD5363, an inhibitor of AKT: pharmacodynamics, antitumor activity, and correlation of monotherapy activity with genetic background', *Mol Cancer Ther*, 11: 873-87.
Davies, Christina, Hongchao Pan, Jon Godwin, Richard Gray, Rodrigo Arriagada, Vinod Raina, Mirta Abraham, et al. 2013. 'Long-term effects of continuing adjuvant tamoxifen to 10 years versus stopping at 5 years after diagnosis of oestrogen receptor-positive breast cancer: ATLAS, a randomised trial', *Lancet*, 381: 805-16.
De Bosscher, K., S. J. Desmet, D. Clarisse, E. Estébanez-Perpiña, and L. Brunsveld. 2020. 'Nuclear receptor crosstalk - defining the mechanisms for therapeutic innovation', *Nat Rev Endocrinol*, 16: 363-77.
de Lera, A. R., W. Bourguet, L. Altucci, and H. Gronemeyer. 2007. 'Design of selective nuclear receptor modulators: RAR and RXR as a case study', *Nat Rev Drug Discov*, 6: 811-20.
De Savi, C., R. H. Bradbury, A. A. Rabow, R. A. Norman, C. de Almeida, D. M. Andrews, P. Ballard, et al. 2015. 'Optimization of a Novel Binding Motif to (E)-3-(3,5-Difluoro-4-((1R,3R)-2-(2-fluoro-2-methylpropyl)-3-methyl-2,3,4,9-tetrahydro-1H-pyrido[3,4-b]indol-1-yl)phenyl)acrylic Acid (AZD9496), a Potent and Orally Bioavailable Selective Estrogen Receptor Downregulator and Antagonist', *J Med Chem*, 58: 8128-40.
Di Leo, A., G. Jerusalem, L. Petruzelka, R. Torres, I. N. Bondarenko, R. Khasanov, D. Verhoeven, et al. 2010. 'Results of the CONFIRM phase III trial comparing fulvestrant 250 mg with fulvestrant 500 mg in postmenopausal women with estrogen receptor-positive advanced breast cancer', *J Clin Oncol*, 28: 4594-600.
Di Leo, Angelo, Guy Jerusalem, Lubos Petruzelka, Roberto Torres, Igor N. Bondarenko, Rustem Khasanov, Didier Verhoeven, et al. 2014. 'Final Overall Survival: Fulvestrant 500mg vs 250mg in the Randomized CONFIRM Trial', *JNCI: Journal of the National Cancer Institute*, 106: djt337.
Diep, C. H., A. R. Daniel, L. J. Mauro, T. P. Knutson, and C. A. Lange. 2015. 'Progesterone action in breast, uterine, and ovarian cancers', *J Mol Endocrinol*, 54: R31-53.
Dimitrakakis, C., and C. Bondy. 2009. 'Androgens and the breast', *Breast Cancer Res*, 11: 212.
Djerassi, Carl. 1966. 'Steroid Oral Contraceptives', *Science*, 151: 1055-61.
Doan, Tram B., Vanessa Cheung, Colin D. Clyne, Heidi N. Hilton, Natalie Eriksson, Morag J. Young, John W. Funder, et al. 2020. 'A tumour suppressive relationship between mineralocorticoid and retinoic acid receptors activates a transcriptional program consistent with a reverse Warburg effect in breast cancer', *Breast Cancer Research*, 22: 122.
Doane, A. S., M. Danso, P. Lal, M. Donaton, L. Zhang, C. Hudis, and W. L. Gerald. 2006. 'An estrogen receptor-negative breast cancer subset characterized by a hormonally regulated transcriptional program and response to androgen', *Oncogene*, 25: 3994-4008.
Dombernowsky, P., I. Smith, G. Falkson, R. Leonard, L. Panasci, J. Bellmunt, W. Bezwoda, et al. 1998. 'Letrozole, a new oral aromatase inhibitor for advanced

breast cancer: double-blind randomized trial showing a dose effect and improved efficacy and tolerability compared with megestrol acetate', *J Clin Oncol*, 16: 453-61.
Dontu, G., W. M. Abdallah, J. M. Foley, K. W. Jackson, M. F. Clarke, M. J. Kawamura, and M. S. Wicha. 2003. 'In vitro propagation and transcriptional profiling of human mammary stem/progenitor cells', *Genes Dev*, 17: 1253-70.
Dotzlaw, Helmut, Etienne Leygue, Peter H. Watson, and Leigh C. Murphy. 1999. 'Estrogen Receptor-β Messenger RNA Expression in Human Breast Tumor Biopsies', *Relationship to Steroid Receptor Status and Regulation by Progestins*, 59: 529-32.
Dowsett, M., R. C. Stein, and R. C. Coombes. 1992. 'Aromatization inhibition alone or in combination with GnRH agonists for the treatment of premenopausal breast cancer patients', *J Steroid Biochem Mol Biol*, 43: 155-9.
Dressing, Gwen E., Jodi E. Goldberg, Nathan J. Charles, Kathryn L. Schwertfeger, and Carol A. Lange. 2011. 'Membrane progesterone receptor expression in mammalian tissues: a review of regulation and physiological implications', *Steroids*, 76: 11-17.
Dustin, D., G. Gu, and S. A. W. Fuqua. 2019. 'ESR1 mutations in breast cancer', *Cancer*, 125: 3714-28.
Dwyer, Amy R., Thu H. Truong, Julie H. Ostrander, and Carol A. Lange. 2020. '90 YEARS OF PROGESTERONE: Steroid receptors as MAPK signaling sensors in breast cancer: let the fates decide', *Journal of Molecular Endocrinology*, 65: T35-T48.
EBCTCG. 1996. 'Ovarian ablation in early breast cancer: overview of the randomised trials', *The Lancet*, 348: 1189-96.
EBCTCG. 1998. 'Tamoxifen for early breast cancer: an overview of the randomised trials. Early Breast Cancer Trialists' Collaborative Group', *Lancet*, 351: 1451-67.
EBCTCG. 2005. 'Effects of chemotherapy and hormonal therapy for early breast cancer on recurrence and 15-year survival: an overview of the randomised trials', *Lancet*, 365: 1687-717.
EBCTCG. 2015. 'Aromatase inhibitors versus tamoxifen in early breast cancer: patient-level meta-analysis of the randomised trials', *Lancet*, 386: 1341-52.
Edgar, R., M. Domrachev, and A. E. Lash. 2002. 'Gene Expression Omnibus: NCBI gene expression and hybridization array data repository', *Nucleic Acids Res*, 30: 207-10.
Eeckhoute, Jérôme, Jason S. Carroll, Timothy R. Geistlinger, Maria I. Torres-Arzayus, and Myles Brown. 2006. 'A cell-type-specific transcriptional network required for estrogen regulation of cyclin D1 and cell cycle progression in breast cancer', *Genes & Development*, 20: 2513-26.
Eeckhoute, Jérôme, Erika Krasnickas Keeton, Mathieu Lupien, Susan A. Krum, Jason S. Carroll, and Myles Brown. 2007. 'Positive Cross-Regulatory Loop Ties GATA-3 to Estrogen Receptor α Expression in Breast Cancer', *Cancer Res*, 67: 6477-83.
Ellis, M. J., A. Llombart-Cussac, D. Feltl, J. A. Dewar, M. Jasiówka, N. Hewson, Y. Rukazenkov, and J. F. Robertson. 2015. 'Fulvestrant 500 mg Versus Anastrozole 1 mg for the First-Line Treatment of Advanced Breast Cancer: Overall Survival Analysis From the Phase II FIRST Study', *J Clin Oncol*, 33: 3781-7.

Elsheikh, S., A. R. Green, M. A. Aleskandarany, M. Grainge, C. E. Paish, M. B. Lambros, J. S. Reis-Filho, and I. O. Ellis. 2008. 'CCND1 amplification and cyclin D1 expression in breast cancer and their relation with proteomic subgroups and patient outcome', *Breast Cancer Res Treat*, 109: 325-35.
Eng, F. C., H. S. Lee, J. Ferrara, T. M. Willson, and J. H. White. 1997. 'Probing the structure and function of the estrogen receptor ligand binding domain by analysis of mutants with altered transactivation characteristics', *Molecular and cellular biology*, 17: 4644-53.
Esber, N., C. Cherbonnier, M. Resche-Rigon, A. Hamze, M. Alami, J. Fagart, H. Loosfelt, M. Lombès, and N. Chabbert-Buffet. 2016. 'Anti-Tumoral Effects of Anti-Progestins in a Patient-Derived Breast Cancer Xenograft Model', *Horm Cancer*, 7: 137-47.
Espie, M. 1994. 'Megestrol acetate in advanced breast carcinoma', *Oncology*, 51 Suppl 1: 8-12.
Evans, R. M., and D. J. Mangelsdorf. 2014. 'Nuclear Receptors, RXR, and the Big Bang', *Cell*, 157: 255-66.
Fabregat, Antonio, Konstantinos Sidiropoulos, Guilherme Viteri, Pablo Marin-Garcia, Peipei Ping, Lincoln Stein, Peter D'Eustachio, and Henning Hermjakob. 2018. 'Reactome diagram viewer: data structures and strategies to boost performance', *Bioinformatics (Oxford, England)*, 34: 1208-14.
Faivre, E. J., and C. A. Lange. 2007. 'Progesterone receptors upregulate Wnt-1 to induce epidermal growth factor receptor transactivation and c-Src-dependent sustained activation of Erk1/2 mitogen-activated protein kinase in breast cancer cells', *Molecular and cellular biology*, 27: 466-80.
Faivre, Emily J., Andrea R. Daniel, Christopher J. Hillard, and Carol A. Lange. 2008. 'Progesterone Receptor Rapid Signaling Mediates Serine 345 Phosphorylation and Tethering to Specificity Protein 1 Transcription Factors', *Molecular Endocrinology*, 22: 823-37.
Fallowfield, L. 2007. 'Quality of life issues in relation to the aromatase inhibitor', *J Steroid Biochem Mol Biol*, 106: 168-72.
Fallowfield, L. J., L. S. Kilburn, C. Langridge, C. F. Snowdon, J. M. Bliss, and R. C. Coombes. 2012. 'Long-term assessment of quality of life in the Intergroup Exemestane Study: 5 years post-randomisation', *Br J Cancer*, 106: 1062-7.
Fanning, S. W., L. Hodges-Gallagher, D. C. Myles, R. Sun, C. E. Fowler, I. N. Plant, B. D. Green, C. L. Harmon, G. L. Greene, and P. J. Kushner. 2018a. 'Specific stereochemistry of OP-1074 disrupts estrogen receptor alpha helix 12 and confers pure antiestrogenic activity', *Nat Commun*, 9: 2368.
Fanning, S. W., R. Jeselsohn, V. Dharmarajan, C. G. Mayne, M. Karimi, G. Buchwalter, R. Houtman, et al. 2018b. 'The SERM/SERD bazedoxifene disrupts ESR1 helix 12 to overcome acquired hormone resistance in breast cancer cells', *Elife*, 7.
Fanning, Sean W, and Geoffrey L Greene. 2019. 'Next-Generation ERα Inhibitors for Endocrine-Resistant ER+ Breast Cancer', *Endocrinology*, 160: 759-69.
Fanning, Sean W., Christopher G. Mayne, Venkatasubramanian Dharmarajan, Kathryn E. Carlson, Teresa A. Martin, Scott J. Novick, Weiyi Toy, et al. 2016. 'Estrogen receptor alpha somatic mutations Y537S and D538G confer breast cancer endocrine resistance by stabilizing the activating function-2 binding conformation', *Elife*, 5: e12792.
Farhat, Ghada N., Rod Walker, Diana S. M. Buist, Tracy Onega, and Karla Kerlikowske. 2010. 'Changes in Invasive Breast Cancer and Ductal

Carcinoma In Situ Rates in Relation to the Decline in Hormone Therapy Use', *Journal of Clinical Oncology*, 28: 5140-46.
Farmer, Pierre, Herve Bonnefoi, Veronique Becette, Michele Tubiana-Hulin, Pierre Fumoleau, Denis Larsimont, Gaetan MacGrogan, et al. 2005. 'Identification of molecular apocrine breast tumours by microarray analysis', *Oncogene*, 24: 4660-71.
Fata, Jimmie E, Young-Yun Kong, Ji Li, Takehiko Sasaki, Junko Irie-Sasaki, Roger A Moorehead, Robin Elliott, Sheila Scully, Evelyn B Voura, and David L Lacey. 2000. 'The osteoclast differentiation factor osteoprotegerin-ligand is essential for mammary gland development', *Cell*, 103: 41-50.
Fayard, Elisabeth, Kristina Schoonjans, Jean-Sébastien Annicotte, and Johan Auwerx. 2003. 'Liver Receptor Homolog 1 Controls the Expression of Carboxyl Ester Lipase *', *Journal of Biological Chemistry*, 278: 35725-31.
Finlay-Schultz, J., D. M. Cittelly, P. Hendricks, P. Patel, P. Kabos, B. M. Jacobsen, J. K. Richer, and C. A. Sartorius. 2015. 'Progesterone downregulation of miR-141 contributes to expansion of stem-like breast cancer cells through maintenance of progesterone receptor and Stat5a', *Oncogene*, 34: 3676-87.
Finlay-Schultz, J., A. E. Gillen, H. M. Brechbuhl, J. J. Ivie, S. B. Matthews, B. M. Jacobsen, D. L. Bentley, P. Kabos, and C. A. Sartorius. 2017. 'Breast Cancer Suppression by Progesterone Receptors Is Mediated by Their Modulation of Estrogen Receptors and RNA Polymerase III', *Cancer Res*, 77: 4934-46.
Finlay-Schultz, Jessica, Britta M. Jacobsen, Duncan Riley, Kiran V. Paul, Scott Turner, Andrea Ferreira-Gonzalez, J. Chuck Harrell, Peter Kabos, and Carol A. Sartorius. 2020. 'New generation breast cancer cell lines developed from patient-derived xenografts', *Breast Cancer Research*, 22: 68.
Finn, R. S., J. P. Crown, I. Lang, K. Boer, I. M. Bondarenko, S. O. Kulyk, J. Ettl, et al. 2015. 'The cyclin-dependent kinase 4/6 inhibitor palbociclib in combination with letrozole versus letrozole alone as first-line treatment of oestrogen receptor-positive, HER2-negative, advanced breast cancer (PALOMA-1/TRIO-18): a randomised phase 2 study', *Lancet Oncol*, 16: 25-35.
Finn, R. S., J. Dering, D. Conklin, O. Kalous, D. J. Cohen, A. J. Desai, C. Ginther, et al. 2009. 'PD 0332991, a selective cyclin D kinase 4/6 inhibitor, preferentially inhibits proliferation of luminal estrogen receptor-positive human breast cancer cell lines in vitro', *Breast Cancer Res*, 11: R77.
Finn, Richard S., Miguel Martin, Hope S. Rugo, Stephen Jones, Seock-Ah Im, Karen Gelmon, Nadia Harbeck, et al. 2016. 'Palbociclib and Letrozole in Advanced Breast Cancer', *New England Journal of Medicine*, 375: 1925-36.
Fisher, C. R., K. H. Graves, A. F. Parlow, and E. R. Simpson. 1998. 'Characterization of mice deficient in aromatase (ArKO) because of targeted disruption of the cyp19 gene', *Proc Natl Acad Sci U S A*, 95: 6965-70.
Fotovati, A., T. Fujii, M. Yamaguchi, M. Kage, K. Shirouzu, S. Oie, Y. Basaki, M. Ono, H. Yamana, and M. Kuwano. 2006. '17Beta-estradiol induces down-regulation of Cap43/NDRG1/Drg-1, a putative differentiation-related and metastasis suppressor gene, in human breast cancer cells', *Clin Cancer Res*, 12: 3010-8.
Fournier, A., F. Berrino, and F. Clavel-Chapelon. 2008. 'Unequal risks for breast cancer associated with different hormone replacement therapies: results from the E3N cohort study', *Breast Cancer Res Treat*, 107: 103-11.

Fournier, A., F. Berrino, E. Riboli, V. Avenel, and F. Clavel-Chapelon. 2005. 'Breast cancer risk in relation to different types of hormone replacement therapy in the E3N-EPIC cohort', *Int J Cancer*, 114: 448-54.
Fournier, A., S. Mesrine, L. Dossus, M. C. Boutron-Ruault, F. Clavel-Chapelon, and N. Chabbert-Buffet. 2014. 'Risk of breast cancer after stopping menopausal hormone therapy in the E3N cohort', *Breast Cancer Res Treat*, 145: 535-43.
Fox, E. M., M. G. Kuba, T. W. Miller, B. R. Davies, and C. L. Arteaga. 2013. 'Autocrine IGF-I/insulin receptor axis compensates for inhibition of AKT in ER-positive breast cancer cells with resistance to estrogen deprivation', *Breast Cancer Res*, 15: R55.
Francis, Prudence A., Olivia Pagani, Gini F. Fleming, Barbara A. Walley, Marco Colleoni, István Láng, Henry L. Gómez, et al. 2018. 'Tailoring Adjuvant Endocrine Therapy for Premenopausal Breast Cancer', *New England Journal of Medicine*, 379: 122-37.
Fribbens, C., I. Garcia Murillas, M. Beaney, S. Hrebien, B. O'Leary, L. Kilburn, K. Howarth, et al. 2018. 'Tracking evolution of aromatase inhibitor resistance with circulating tumour DNA analysis in metastatic breast cancer', *Ann Oncol*, 29: 145-53.
Fribbens, C., B. O'Leary, L. Kilburn, S. Hrebien, I. Garcia-Murillas, M. Beaney, M. Cristofanilli, et al. 2016. 'Plasma ESR1 Mutations and the Treatment of Estrogen Receptor-Positive Advanced Breast Cancer', *J Clin Oncol*, 34: 2961-8.
Fu, Xiao-Dong, Lorenzo Goglia, Angel Matias Sanchez, Marina Flamini, Maria S. Giretti, Veronica Tosi, Andrea R. Genazzani, and Tommaso Simoncini. 2010. 'Progesterone receptor enhances breast cancer cell motility and invasion via extranuclear activation of focal adhesion kinase', *Endocrine-related cancer*, 17: 431-43.
Fuady, Jerry H., Katrin Gutsche, Sara Santambrogio, Zsuzsanna Varga, David Hoogewijs, and Roland H. Wenger. 2016. 'Estrogen-dependent downregulation of hypoxia-inducible factor (HIF)-2α in invasive breast cancer cells', *Oncotarget*, 7: 31153-65.
Fuhrmann, U., R. Krattenmacher, E. P. Slater, and K. H. Fritzemeier. 1996. 'The novel progestin drospirenone and its natural counterpart progesterone: biochemical profile and antiandrogenic potential', *Contraception*, 54: 243-51.
Fuqua, Suzanne A. W., Guowei Gu, and Yassine Rechoum. 2014. 'Estrogen receptor (ER) α mutations in breast cancer: hidden in plain sight', *Breast cancer research and treatment*, 144: 11-19.
Fuqua, Suzanne A. W., Christoph Wiltschke, Qui X. Zhang, Åke Borg, Carl G. Castles, William E. Friedrichs, Torsten Hopp, et al. 2000. 'A Hypersensitive Estrogen Receptor-α Mutation in Premalignant Breast Lesions', *Cancer Res*, 60: 4026-29.
Gadducci, A., N. Biglia, S. Cosio, P. Sismondi, and A. R. Genazzani. 2009. 'Progestagen component in combined hormone replacement therapy in postmenopausal women and breast cancer risk: a debated clinical issue', *Gynecol Endocrinol*, 25: 807-15.
Gao, Shuai, Sujun Chen, Dong Han, Zifeng Wang, Muqing Li, Wanting Han, Anna Besschetnova, et al. 2020. 'Chromatin binding of FOXA1 is promoted by LSD1-mediated demethylation in prostate cancer', *Nat Genet*, 52: 1011-17.

Gardill, Bernd R., Michael R. Vogl, Hai-Yan Lin, Geoffrey L. Hammond, and Yves A. Muller. 2012. 'Corticosteroid-binding globulin: structure-function implications from species differences', *PloS one*, 7: e52759-e59.
Gates, Leah A., Guowei Gu, Yue Chen, Aarti D. Rohira, Jonathan T. Lei, Ross A. Hamilton, Yang Yu, et al. 2018. 'Proteomic profiling identifies key coactivators utilized by mutant ERα proteins as potential new therapeutic targets', *Oncogene*, 37: 4581-98.
Gazet, J. C., H. T. Ford, R. C. Coombes, J. M. Bland, R. Sutcliffe, J. Quilliam, and S. Lowndes. 1994. 'Prospective randomized trial of tamoxifen vs surgery in elderly patients with breast cancer', *Eur J Surg Oncol*, 20: 207-14.
'The Gene Ontology resource: enriching a GOld mine'. 2021. *Nucleic Acids Res*, 49: D325-d34.
Gennari, A., F. André, C. H. Barrios, J. Cortés, E. de Azambuja, A. DeMichele, R. Dent, et al. 2021. 'ESMO Clinical Practice Guideline for the diagnosis, staging and treatment of patients with metastatic breast cancer', *Ann Oncol*, 32: 1475-95.
Gewirth, Daniel T., and Paul B. Sigler. 1995. 'The basis for half-site specificity explored through a non-cognate steroid receptor-DNA complex', *Nature Structural Biology*, 2: 386-94.
Ghatge, Radhika P., Britta M. Jacobsen, Stephanie A. Schittone, and Kathryn B. Horwitz. 2005. 'The progestational and androgenic properties of medroxyprogesterone acetate: gene regulatory overlap with dihydrotestosterone in breast cancer cells', *Breast Cancer Research*, 7: R1036.
Ghosh, M. G., D. A. Thompson, and R. J. Weigel. 2000. 'PDZK1 and GREB1 are estrogen-regulated genes expressed in hormone-responsive breast cancer', *Cancer Res*, 60: 6367-75.
Ginestier, C., M. H. Hur, E. Charafe-Jauffret, F. Monville, J. Dutcher, M. Brown, J. Jacquemier, et al. 2007. 'ALDH1 is a marker of normal and malignant human mammary stem cells and a predictor of poor clinical outcome', *Cell Stem Cell*, 1: 555-67.
Giordano, Cinzia, Yukun Cui, Ines Barone, Sebastiano Ando, Michael A. Mancini, Valeria Berno, and Suzanne A. W. Fuqua. 2010. 'Growth factor-induced resistance to tamoxifen is associated with a mutation of estrogen receptor alpha and its phosphorylation at serine 305', *Breast cancer research and treatment*, 119: 71-85.
Giulianelli, S., J. P. Vaqué, R. Soldati, V. Wargon, S. I. Vanzulli, R. Martins, E. Zeitlin, et al. 2012. 'Estrogen receptor alpha mediates progestin-induced mammary tumor growth by interacting with progesterone receptors at the cyclin D1/MYC promoters', *Cancer Res*, 72: 2416-27.
Gnant, Michael, Georg Pfeiler, Günther G. Steger, Daniel Egle, Richard Greil, Florian Fitzal, Viktor Wette, et al. 2019. 'Adjuvant denosumab in postmenopausal patients with hormone receptor-positive breast cancer (ABCSG-18): disease-free survival results from a randomised, double-blind, placebo-controlled, phase 3 trial', *The Lancet Oncology*, 20: 339-51.
Godbole, M., T. Togar, K. Patel, B. Dharavath, N. Yadav, S. Janjuha, N. Gardi, et al. 2018. 'Up-regulation of the kinase gene SGK1 by progesterone activates the AP-1-NDRG1 axis in both PR-positive and -negative breast cancer cells', *J Biol Chem*, 293: 19263-76.

Goetz, Matthew P, Masakazu Toi, Mario Campone, Joohyuk Sohn, Shani Paluch-Shimon, Jens Huober, In Hae Park, Olivier Trédan, Shin-Cheh Chen, and Luis Manso. 2017. 'MONARCH 3: abemaciclib as initial therapy for advanced breast cancer', *Journal of Clinical Oncology*, 35.

Goetz, Matthew P., Erika Paige Hamilton, Mario Campone, Sara A. Hurvitz, Javier Cortes, Stephen R. D. Johnston, Guy Heinrich Maria Jerusalem, et al. 2020. 'Acquired genomic alterations in circulating tumor DNA from patients receiving abemaciclib alone or in combination with endocrine therapy', *Journal of Clinical Oncology*, 38: 3519-19.

Goldhirsch, A., E. P. Winer, A. S. Coates, R. D. Gelber, M. Piccart-Gebhart, B. Thürlimann, and H. J. Senn. 2013. 'Personalizing the treatment of women with early breast cancer: highlights of the St Gallen International Expert Consensus on the Primary Therapy of Early Breast Cancer 2013', *Ann Oncol*, 24: 2206-23.

Gompel, Anne, Sonia Somaï, Marc Chaouat, Amani Kazem, Helenius J. Kloosterboer, Ines Beusman, Patricia Forgez, Maurice Mimoun, and William Rostène. 2000. 'Hormonal regulation of apoptosis in breast cells and tissues', *Steroids*, 65: 593-98.

Gonzalez-Suarez, E., D. Branstetter, A. Armstrong, H. Dinh, H. Blumberg, and W. C. Dougall. 2007. 'RANK overexpression in transgenic mice with mouse mammary tumor virus promoter-controlled RANK increases proliferation and impairs alveolar differentiation in the mammary epithelia and disrupts lumen formation in cultured epithelial acini', *Molecular and cellular biology*, 27: 1442-54.

Gonzalez-Suarez, E., A. P. Jacob, J. Jones, R. Miller, M. P. Roudier-Meyer, R. Erwert, J. Pinkas, D. Branstetter, and W. C. Dougall. 2010. 'RANK ligand mediates progestin-induced mammary epithelial proliferation and carcinogenesis', *Nature*, 468: 103-7.

Goodman, C. R., T. Sato, A. R. Peck, M. A. Girondo, N. Yang, C. Liu, A. F. Yanac, et al. 2016. 'Steroid induction of therapy-resistant cytokeratin-5-positive cells in estrogen receptor-positive breast cancer through a BCL6-dependent mechanism', *Oncogene*, 35: 1373-85.

Gou, X., M. Anurag, J. T. Lei, B. J. Kim, P. Singh, S. Seker, D. Fandino, et al. 2021. 'Transcriptional Reprogramming Differentiates Active from Inactive ESR1 Fusions in Endocrine Therapy-Refractory Metastatic Breast Cancer', *Cancer Res*, 81: 6259-72.

Graham, J. D., P. A. Mote, U. Salagame, R. L. Balleine, L. I. Huschtscha, and C. L. Clarke. 2009a. 'Hormone-responsive model of primary human breast epithelium', *J Mammary Gland Biol Neoplasia*, 14: 367-79.

Graham, J. D., P. A. Mote, U. Salagame, J. H. van Dijk, R. L. Balleine, L. I. Huschtscha, R. R. Reddel, and C. L. Clarke. 2009b. 'DNA replication licensing and progenitor numbers are increased by progesterone in normal human breast', *Endocrinology*, 150: 3318-26.

Graham, J. Dinny, Christine Yeates, Rosemary L. Balleine, Suzanna S. Harvey, Jane S. Milliken, A. Michael Bilous, and Christine L. Clarke. 1995. 'Characterization of Progesterone Receptor A and B Expression in Human Breast Cancer', *Cancer Res*, 55: 5063-68.

Green, K. A., and J. S. Carroll. 2007. 'Oestrogen-receptor-mediated transcription and the influence of co-factors and chromatin state', *Nat Rev Cancer*, 7: 713-22.

Greendale, G. A., B. A. Reboussin, S. Slone, C. Wasilauskas, M. C. Pike, and G. Ursin. 2003. 'Postmenopausal hormone therapy and change in mammographic density', *J Natl Cancer Inst*, 95: 30-7.
Grimm, Sandra L., Tiffany N. Seagroves, Elena B. Kabotyanski, Russell C. Hovey, Barbara K. Vonderhaar, John P. Lydon, Keiko Miyoshi, et al. 2002. 'Disruption of Steroid and Prolactin Receptor Patterning in the Mammary Gland Correlates with a Block in Lobuloalveolar Development', *Molecular Endocrinology*, 16: 2675-91.
Gu, G., L. Tian, S. K. Herzog, Y. Rechoum, L. Gelsomino, M. Gao, L. Du, et al. 2021. 'Hormonal modulation of ESR1 mutant metastasis', *Oncogene*, 40: 997-1011.
Gucalp, Ayca, Sara Tolaney, Steven J. Isakoff, James N. Ingle, Minetta C. Liu, Lisa A. Carey, Kimberly Blackwell, et al. 2013. 'Phase II Trial of Bicalutamide in Patients with Androgen Receptor–Positive, Estrogen Receptor–Negative Metastatic Breast Cancer', *Clinical Cancer Research*, 19: 5505-12.
Guerrero-Zotano, Angel L., Thomas P. Stricker, Luigi Formisano, Katherine E. Hutchinson, Daniel G. Stover, Kyung-Min Lee, Luis J. Schwarz, et al. 2018. 'ER⁺ Breast Cancers Resistant to Prolonged Neoadjuvant Letrozole Exhibit an E2F4 Transcriptional Program Sensitive to CDK4/6 Inhibitors', *Clinical Cancer Research*, 24: 2517-29.
Guttery, D. S., K. Page, A. Hills, L. Woodley, S. D. Marchese, B. Rghebi, R. K. Hastings, et al. 2015. 'Noninvasive detection of activating estrogen receptor 1 (ESR1) mutations in estrogen receptor-positive metastatic breast cancer', *Clin Chem*, 61: 974-82.
Gwynne, J. T., and J. F. Strauss, 3rd. 1982. 'The role of lipoproteins in steroidogenesis and cholesterol metabolism in steroidogenic glands', *Endocr Rev*, 3: 299-329.
Hagan, C.R., Lange, C.A. 2014. 'Molecular determinants of context-dependent progesterone receptor action in breast cancer', *BMC Medicine*, 12: 32.
Hagan, Christy R., Todd P. Knutson, and Carol A. Lange. 2013. 'A Common Docking Domain in Progesterone Receptor-B links DUSP6 and CK2 signaling to proliferative transcriptional programs in breast cancer cells', *Nucleic Acids Research*, 41: 8926-42.
Hamilton, Erika P., Javier Cortes, Guy Jerusalem, Peter A. Kaufman, Ozgur Ozyilkan, Roberto Hegg, Lacey M. Litchfield, et al. 2020. 'Abstract 785: Genomic markers of response to monotherapy abemaciclib in the nextMONARCH 1 study', *Cancer Res*, 80: 785-85.
Hamilton, Erika P., Judy S. Wang, Timothy J. Pluard, Stephen R. D. Johnston, Aki Morikawa, Elizabeth Claire Dees, Robert Hugh Jones, et al. 2021. 'Phase I/II study of H3B-6545, a novel selective estrogen receptor covalent antagonist (SERCA), in estrogen receptor positive (ER+), human epidermal growth factor receptor 2 negative (HER2-) advanced breast cancer', *Journal of Clinical Oncology*, 39: 1018-18.
Hamilton, Erika, Linda Vahdat, Hyo S. Han, Jennifer Ranciato, Richard Gedrich, Chi F. Keung, Deborah Chirnomas, and Sara Hurvitz. 2022. 'Abstract PD13-08: First-in-human safety and activity of ARV-471, a novel PROTAC® estrogen receptor degrader, in ER+/HER2- locally advanced or metastatic breast cancer', *Cancer Res*, 82: PD13-08-PD13-08.
Hargrove, J. T., W. S. Maxson, and A. C. Wentz. 1989. 'Absorption of oral progesterone is influenced by vehicle and particle size', *Am J Obstet Gynecol*, 161: 948-51.

Harper-Wynne, C, and RC Coombes. 1999. 'Anastrozole shows evidence of activity in postmenopausal patients who have responded or stabilised on formestane therapy', *European Journal of Cancer*, 35: 744-46.
Harrison, M, A Laight, DA Clarke, P Giles, and R Yates. 2003. "Pharmacokinetics and metabolism of fulvestrant after oral, intravenous and intramuscular administration in healthy volunteers." In *Proc ASCO*, 45.
Harrod, A., J. Fulton, V. T. M. Nguyen, M. Periyasamy, L. Ramos-Garcia, C. F. Lai, G. Metodieva, et al. 2017. 'Genomic modelling of the ESR1 Y537S mutation for evaluating function and new therapeutic approaches for metastatic breast cancer', *Oncogene*, 36: 2286-96.
Hartmaier, R. J., S. E. Trabucco, N. Priedigkeit, J. H. Chung, C. A. Parachoniak, P. Vanden Borre, S. Morley, et al. 2018. 'Recurrent hyperactive ESR1 fusion proteins in endocrine therapy-resistant breast cancer', *Ann Oncol*, 29: 872-80.
Hartmann, M., and A. Wettstein. 1934. 'Ein krystallisiertes Hormon aus Corpus luteum.', *Helv chim Acta*, 17: 878-82.
Harvell, Djuana M. E., Jennifer K. Richer, D. Craig Allred, Carol A. Sartorius, and Kathryn B. Horwitz. 2006. 'Estradiol Regulates Different Genes in Human Breast Tumor Xenografts Compared with the Identical Cells in Culture', *Endocrinology*, 147: 700-13.
Haslam, S. Z., and G. Shyamala. 1979. 'Effect of oestradiol on progesterone receptors in normal mammary glands and its relationship with lactation', *The Biochemical journal*, 182: 127-31.
Haslam, Sandra Z. 1989. 'The ontogeny of mouse mammary gland responsiveness to ovarian steroid hormones', *Endocrinology*, 125: 2766-72.
Haslam, Sandra Z, and G Shyamala. 1981. 'Relative distribution of estrogen and progesterone receptors among the epithelial, adipose, and connective tissue components of the normal mammary gland', *Endocrinology*, 108: 825-30.
Haughian, James M., Mauricio P. Pinto, J. Chuck Harrell, Brian S. Bliesner, Kristiina M. Joensuu, Wendy W. Dye, Carol A. Sartorius, et al. 2012. 'Maintenance of hormone responsiveness in luminal breast cancers by suppression of Notch', *Proceedings of the National Academy of Sciences*, 109: 2742-47.
Hayes, J. H., W. K. Oh, P. W. Kantoff, J. B. Manola, M. R. Smith, E. P. Gelmann, G. Bubley, S. P. Balk, and M. Taplin. 2006. 'Mifepristone (RU-486) in androgen independent prostate cancer', *Journal of Clinical Oncology*, 24: 14508-08.
Heberle, Henry, Gabriela Vaz Meirelles, Felipe R. da Silva, Guilherme P. Telles, and Rosane Minghim. 2015. 'InteractiVenn: a web-based tool for the analysis of sets through Venn diagrams', *BMC Bioinformatics*, 16: 169.
Heinlein, C. A., and C. Chang. 2004. 'Androgen receptor in prostate cancer', *Endocr Rev*, 25: 276-308.
Herynk, M. H., and S. A. Fuqua. 2004. 'Estrogen receptor mutations in human disease', *Endocr Rev*, 25: 869-98.
Herynk, Matthew H., Irma Parra, Yukun Cui, Amanda Beyer, Meng-Fen Wu, Susan G. Hilsenbeck, and Suzanne A. W. Fuqua. 2007. 'Association between the estrogen receptor alpha A908G mutation and outcomes in invasive breast cancer', *Clin Cancer Res*, 13: 3235-43.
Hickey, T. E., J. L. Robinson, J. S. Carroll, and W. D. Tilley. 2012. 'Minireview: The androgen receptor in breast tissues: growth inhibitor, tumor suppressor, oncogene?', *Mol Endocrinol*, 26: 1252-67.

Hickey, T. E., L. A. Selth, K. M. Chia, G. Laven-Law, H. H. Milioli, D. Roden, S. Jindal, et al. 2021. 'The androgen receptor is a tumor suppressor in estrogen receptor-positive breast cancer', *Nat Med*, 27: 310-20.

Hilditch, John R., Jacqueline Lewis, Alice Peter, Barbara van Maris, Alan Ross, Edmée Franssen, Gordon H. Guyatt, Peter G. Norton, and Earl Dunn. 1996. 'A menopause-specific quality of life questionnaire: development and psychometric properties', *Maturitas*, 24: 161-75.

Hilton, Heidi N., N. Santucci, A. Silvestri, S. Kantimm, L. I. Huschtscha, J. D. Graham, and C. L. Clarke. 2014. 'Progesterone stimulates progenitor cells in normal human breast and breast cancer cells', *Breast cancer research and treatment*, 143: 423-33.

Hissom, J. R., and M. R. Moore. 1987. 'Progestin effects on growth in the human breast cancer cell line T-47D--possible therapeutic implications', *Biochem Biophys Res Commun*, 145: 706-11.

Hofseth, L. J., A. M. Raafat, J. R. Osuch, D. R. Pathak, C. A. Slomski, and S. Z. Haslam. 1999. 'Hormone replacement therapy with estrogen or estrogen plus medroxyprogesterone acetate is associated with increased epithelial proliferation in the normal postmenopausal breast', *J Clin Endocrinol Metab*, 84: 4559-65.

Holloran, Sean M., Bakhtiyor Nosirov, Katherine R. Walter, Gloria M. Trinca, Zhao Lai, Victor X. Jin, and Christy R. Hagan. 2020. 'Reciprocal fine-tuning of progesterone and prolactin-regulated gene expression in breast cancer cells', *Molecular and Cellular Endocrinology*, 511: 110859.

Holst, F., P. R. Stahl, C. Ruiz, O. Hellwinkel, Z. Jehan, M. Wendland, A. Lebeau, et al. 2007. 'Estrogen receptor alpha (ESR1) gene amplification is frequent in breast cancer', *Nat Genet*, 39: 655-60.

Hopp, T. A., H. L. Weiss, S. G. Hilsenbeck, Y. Cui, D. C. Allred, K. B. Horwitz, and S. A. Fuqua. 2004. 'Breast cancer patients with progesterone receptor PR-A-rich tumors have poorer disease-free survival rates', *Clin Cancer Res*, 10: 2751-60.

Hörlein, A. J., A. M. Näär, T. Heinzel, J. Torchia, B. Gloss, R. Kurokawa, A. Ryan, et al. 1995. 'Ligand-independent repression by the thyroid hormone receptor mediated by a nuclear receptor co-repressor', *Nature*, 377: 397-404.

Hortobagyi, G. N., S. M. Stemmer, H. A. Burris, Y. S. Yap, G. S. Sonke, S. Paluch-Shimon, M. Campone, et al. 2018. 'Updated results from MONALEESA-2, a phase III trial of first-line ribociclib plus letrozole versus placebo plus letrozole in hormone receptor-positive, HER2-negative advanced breast cancer', *Ann Oncol*, 29: 1541-47.

Horwitz, K. B., and W. L. McGuire. 1975. 'Specific progesterone receptors in human breast cancer', *Steroids*, 25: 497-505.

Horwitz, K. B., M. B. Mockus, and B. A. Lessey. 1982. 'Variant T47D human breast cancer cells with high progesterone-receptor levels despite estrogen and antiestrogen resistance', *Cell*, 28: 633-42.

Horwitz, K. B., and C. A. Sartorius. 2020. '90 YEARS OF PROGESTERONE: Progesterone and progesterone receptors in breast cancer: past, present, future', *J Mol Endocrinol*, 65: T49-t63.

Horwitz, Kathryn B., Wendy W. Dye, Joshua Chuck Harrell, Peter Kabos, and Carol A. Sartorius. 2008. 'Rare steroid receptor-negative basal-like tumorigenic cells in luminal subtype human breast cancer xenografts', *Proceedings of the National Academy of Sciences*, 105: 5774-79.

Howell, A., J. F. Robertson, J. Quaresma Albano, A. Aschermannova, L. Mauriac, U. R. Kleeberg, I. Vergote, B. Erikstein, A. Webster, and C. Morris. 2002. 'Fulvestrant, formerly ICI 182,780, is as effective as anastrozole in postmenopausal women with advanced breast cancer progressing after prior endocrine treatment', *J Clin Oncol*, 20: 3396-403.

Howell, Anthony, John Pippen, Richard M. Elledge, Louis Mauriac, Ignace Vergote, Stephen E. Jones, Steven E. Come, C. Kent Osborne, and John F. R. Robertson. 2005. 'Fulvestrant versus anastrozole for the treatment of advanced breast carcinoma', *Cancer*, 104: 236-39.

Howlin, J., J. McBryan, and F. Martin. 2006. 'Pubertal mammary gland development: insights from mouse models', *J Mammary Gland Biol Neoplasia*, 11: 283-97.

Hu, D. G., L. A. Selth, G. A. Tarulli, R. Meech, D. Wijayakumara, A. Chanawong, R. Russell, et al. 2016. 'Androgen and Estrogen Receptors in Breast Cancer Coregulate Human UDP-Glucuronosyltransferases 2B15 and 2B17', *Cancer Res*, 76: 5881-93.

Hu, X., and M. A. Lazar. 1999. 'The CoRNR motif controls the recruitment of corepressors by nuclear hormone receptors', *Nature*, 402: 93-6.

Huang, Pengxiang, Vikas Chandra, and Fraydoon Rastinejad. 2010. 'Structural overview of the nuclear receptor superfamily: insights into physiology and therapeutics', *Annual review of physiology*, 72: 247-72.

Huggins, C. 1965. 'Two principles in endocrine therapy of cancers: hormone deprival and hormone interference', *Cancer Res*, 25: 1163-7.

Huggins, C., R. C. Moon, and S. Morii. 1962. 'Extinction of experimental mammary cancer. I. Estradiol-17beta and progesterone', *Proc Natl Acad Sci U S A*, 48: 379-86.

Huggins , Charles, Giuliano Briziarelli , and Harold Sutton , Jr. 1959. 'RAPID INDUCTION OF MAMMARY CARCINOMA IN THE RAT AND THE INFLUENCE OF HORMONES ON THE TUMORS', *Journal of Experimental Medicine*, 109: 25-42.

Hulsen, Tim, Jacob de Vlieg, and Wynand Alkema. 2008. 'BioVenn – a web application for the comparison and visualization of biological lists using area-proportional Venn diagrams', *BMC Genomics*, 9: 488.

Hunter, D. J., G. A. Colditz, S. E. Hankinson, S. Malspeis, D. Spiegelman, W. Chen, M. J. Stampfer, and W. C. Willett. 2010. 'Oral contraceptive use and breast cancer: a prospective study of young women', *Cancer Epidemiol Biomarkers Prev*, 19: 2496-502.

Iannone, Camilla, Andy Pohl, Panagiotis Papasaikas, Daniel Soronellas, Guillermo P. Vicent, Miguel Beato, and Juan ValcáRcel. 2015. 'Relationship between nucleosome positioning and progesterone-induced alternative splicing in breast cancer cells', *Rna*, 21: 360-74.

Im, Seock-Ah, Erika P. Hamilton, Antonio Llombart Cussac, Richard D. Baird, Johannes Ettl, Matthew P. Goetz, Hiroji Iwata, et al. 2021. 'SERENA-4: A phase 3 comparison of AZD9833 (camizestrant) plus palbociclib, versus anastrozole plus palbociclib, for patients with ER-positive, HER2-negative advanced breast cancer who have not previously received systemic treatment for advanced disease', *Journal of Clinical Oncology*, 39: TPS1101-TPS01.

Ingle, J. N., D. I. Twito, D. J. Schaid, S. A. Cullinan, J. E. Krook, J. A. Mailliard, L. K. Tschetter, et al. 1991. 'Combination hormonal therapy with tamoxifen plus fluoxymesterone versus tamoxifen alone in postmenopausal women with metastatic breast cancer. An updated analysis', *Cancer*, 67: 886-91.

Izuo, M., Y. Iino, and K. Endo. 1981. 'Oral high-dose medroxyprogesterone acetate (MAP) in treatment of advanced breast cancer. A preliminary report of clinical and experimental studies', *Breast Cancer Res Treat*, 1: 125-30.
Jabara, A. G. 1967. 'Effects of progesterone on 9,10-dimethyl-1,2-benzanthracene-induced mammary tumours in Sprague-Dawley rats', *Br J Cancer*, 21: 418-29.
Jabara, A. G., G. N. Marks, J. E. Summers, and P. S. Anderson. 1979. 'Effects of progesterone on mammary carcinogenesis by DMBA applied directly to rat mammae', *Br J Cancer*, 40: 268-73.
Jacobsen, B. M., J. K. Richer, S. A. Schittone, and K. B. Horwitz. 2002. 'New human breast cancer cells to study progesterone receptor isoform ratio effects and ligand-independent gene regulation', *J Biol Chem*, 277: 27793-800.
Jacobsen, B. M., S. A. Schittone, J. K. Richer, and K. B. Horwitz. 2005. 'Progesterone-independent effects of human progesterone receptors (PRs) in estrogen receptor-positive breast cancer: PR isoform-specific gene regulation and tumor biology', *Mol Endocrinol*, 19: 574-87.
Jacobsen, B. M.; Jambal, P.; Schittone, S. A.; Horwitz, K. B. . 2009. 'ALU repeats in promoters are position-dependent co-response elements (coRE) that enhance or repress transcription by dimeric and monomeric progesterone receptors', *Molecular Endocrinology*, 23: 989-1000.
Jacobsen, Britta M., and Kathryn B. Horwitz. 2012. 'Progesterone receptors, their isoforms and progesterone regulated transcription', *Molecular and Cellular Endocrinology*, 357: 18-29.
Järvinen, T. A., M. Pelto-Huikko, K. Holli, and J. Isola. 2000. 'Estrogen receptor beta is coexpressed with ERalpha and PR and associated with nodal status, grade, and proliferation rate in breast cancer', *The American journal of pathology*, 156: 29-35.
Jensen, Elwood V., Herbert I. Jacobson, Alicia A. Walf, and Cheryl A. Frye. 2010. 'Estrogen action: A historic perspective on the implications of considering alternative approaches', *Physiology & Behavior*, 99: 151-62.
Jerusalem, G., R. H. de Boer, S. Hurvitz, D. A. Yardley, E. Kovalenko, B. Ejlertsen, S. Blau, et al. 2018. 'Everolimus Plus Exemestane vs Everolimus or Capecitabine Monotherapy for Estrogen Receptor-Positive, HER2-Negative Advanced Breast Cancer: The BOLERO-6 Randomized Clinical Trial', *JAMA Oncol*, 4: 1367-74.
Jeselsohn, R., G. Buchwalter, C. De Angelis, M. Brown, and R. Schiff. 2015. 'ESR1 mutations—a mechanism for acquired endocrine resistance in breast cancer', *Nat Rev Clin Oncol*, 12: 573-83.
Jeselsohn, R., H. Guo, R. Rees, W. T. Barry, C. H. Barlett, N. M. Tung, I. E. Krop, M. Brown, and E. P. Winer. 2019. 'Abstract PD1-05: Results from the phase Ib/II clinical trial of bazedoxifene and palbociclib in hormone receptor positive metastatic breast cancer', *Cancer Res*, 79: PD1-05-PD1-05.
Jeselsohn, R., R. Yelensky, G. Buchwalter, G. Frampton, F. Meric-Bernstam, A. M. Gonzalez-Angulo, J. Ferrer-Lozano, et al. 2014. 'Emergence of constitutively active estrogen receptor-alpha mutations in pretreated advanced estrogen receptor-positive breast cancer', *Clin Cancer Res*, 20: 1757-67.
Jeselsohn, Rinath, Johann S. Bergholz, Matthew Pun, MacIntosh Cornwell, Weihan Liu, Agostina Nardone, Tengfei Xiao, et al. 2018. 'Allele-Specific Chromatin Recruitment and Therapeutic Vulnerabilities of ESR1 Activating Mutations', *Cancer cell*, 33: 173-86.e5.

Johnston, S. R. 2009. 'Enhancing the efficacy of hormonal agents with selected targeted agents', *Clin Breast Cancer*, 9 Suppl 1: S28-36.
Johnston, S. R., L. S. Kilburn, P. Ellis, D. Dodwell, D. Cameron, L. Hayward, Y. H. Im, et al. 2013. 'Fulvestrant plus anastrozole or placebo versus exemestane alone after progression on non-steroidal aromatase inhibitors in postmenopausal patients with hormone-receptor-positive locally advanced or metastatic breast cancer (SoFEA): a composite, multicentre, phase 3 randomised trial', *Lancet Oncol*, 14: 989-98.
Jonat, W., T. Bachelot, T. Ruhstaller, I. Kuss, U. Reimann, and J. F. R. Robertson. 2013. 'Randomized phase II study of lonaprisan as second-line therapy for progesterone receptor-positive breast cancer', *Ann Oncol*, 24: 2543-48.
Jonat, W., M. Kaufmann, W. Sauerbrei, R. Blamey, J. Cuzick, M. Namer, I. Fogelman, et al. 2002. 'Goserelin versus cyclophosphamide, methotrexate, and fluorouracil as adjuvant therapy in premenopausal patients with node-positive breast cancer: The Zoladex Early Breast Cancer Research Association Study', *J Clin Oncol*, 20: 4628-35.
Jones, R. H., A. Casbard, M. Carucci, C. Cox, R. Butler, F. Alchami, T. A. Madden, et al. 2020. 'Fulvestrant plus capivasertib versus placebo after relapse or progression on an aromatase inhibitor in metastatic, oestrogen receptor-positive breast cancer (FAKTION): a multicentre, randomised, controlled, phase 2 trial', *Lancet Oncol*, 21: 345-57.
Jordan, V. C. 2003. 'Tamoxifen: a most unlikely pioneering medicine', *Nat Rev Drug Discov*, 2: 205-13.
Jordan, V. C., M. M. Collins, L. Rowsby, and G. Prestwich. 1977. 'A monohydroxylated metabolite of tamoxifen with potent antioestrogenic activity', *J Endocrinol*, 75: 305-16.
Jordan, V. C., and B. W. O'Malley. 2007. 'Selective estrogen-receptor modulators and antihormonal resistance in breast cancer', *J Clin Oncol*, 25: 5815-24.
Joshi, P. A., H. W. Jackson, A. G. Beristain, M. A. Di Grappa, P. A. Mote, C. L. Clarke, J. Stingl, P. D. Waterhouse, and R. Khokha. 2010. 'Progesterone induces adult mammary stem cell expansion', *Nature*, 465: 803-7.
Kabos, P., J. Finlay-Schultz, C. Li, E. Kline, C. Finlayson, J. Wisell, C. A. Manuel, et al. 2012. 'Patient-derived luminal breast cancer xenografts retain hormone receptor heterogeneity and help define unique estrogen-dependent gene signatures', *Breast Cancer Res Treat*, 135: 415-32.
Kahraman, Mehmet, Steven P Govek, Johnny Y Nagasawa, Andiliy Lai, Celine Bonnefous, Karensa Douglas, John Sensintaffar, Nhin Liu, KyoungJin Lee, and Anna Aparicio. 2018. 'Maximizing ER-α degradation maximizes activity in a tamoxifen-resistant breast cancer model: identification of GDC-0927', *ACS medicinal chemistry letters*, 10: 50-55.
Kamaraju, Sailaja, Amy M. Fowler, Elizabeth Weil, Kari B. Wisinski, Thu H. Truong, Martin Lehr, Lubna N. Chaudhary, et al. 2021. 'Leveraging Antiprogestins in the Treatment of Metastatic Breast Cancer', *Endocrinology*, 162: bqab060.
Kariagina, Anastasia, Jianwei Xie, Jeffrey Leipprandt, and Sandra Haslam. 2010. 'Amphiregulin Mediates Estrogen, Progesterone, and EGFR Signaling in the Normal Rat Mammary Gland and in Hormone-Dependent Rat Mammary Cancers', *Hormones & cancer*, 1: 229-44.
Kastner, P., A. Krust, B. Turcotte, U. Stropp, L. Tora, H. Gronemeyer, and P. Chambon. 1990. 'Two distinct estrogen-regulated promoters generate

transcripts encoding the two functionally different human progesterone receptor forms A and B', *Embo j*, 9: 1603-14.
Katzenellenbogen, J. A., C. G. Mayne, B. S. Katzenellenbogen, G. L. Greene, and S. Chandarlapaty. 2018. 'Structural underpinnings of oestrogen receptor mutations in endocrine therapy resistance', *Nat Rev Cancer*, 18: 377-88.
Kaufmann, Manfred, Emilio Bajetta, Luc Yves Dirix, Luis Enrique Fein, Stephen E. Jones, Nicoletta Zilembo, Jean-Louis Dugardyn, et al. 2000. 'Exemestane Is Superior to Megestrol Acetate After Tamoxifen Failure in Postmenopausal Women With Advanced Breast Cancer: Results of a Phase III Randomized Double-Blind Trial', *Journal of Clinical Oncology*, 18: 1399-411.
Keith, Bruce D. 2008. 'Systematic review of the clinical effect of glucocorticoids on nonhematologic malignancy', *BMC cancer*, 8: 84.
Kemppainen, J. A., E. Langley, C. I. Wong, K. Bobseine, W. R. Kelce, and E. M. Wilson. 1999. 'Distinguishing androgen receptor agonists and antagonists: distinct mechanisms of activation by medroxyprogesterone acetate and dihydrotestosterone', *Mol Endocrinol*, 13: 440-54.
Kennedy, B. J. 1965. 'Hormone therapy for advanced breast cancer', *Cancer*, 18: 1551-7.
Khorasanizadeh, S., and F. Rastinejad. 2001. 'Nuclear-receptor interactions on DNA-response elements', *Trends Biochem Sci*, 26: 384-90.
Kiang, D. T., and B. J. Kennedy. 1977. 'Tamoxifen (antiestrogen) therapy in advanced breast cancer', *Ann Intern Med*, 87: 687-90.
Klein-Hitpass, L., A. C. Cato, D. Henderson, and G. U. Ryffel. 1991. 'Two types of antiprogestins identified by their differential action in transcriptionally active extracts from T47D cells', *Nucleic Acids Research*, 19: 1227-34.
Klijn, J. G. M., Frank Jong, G. Bakker, S. W. J. Lamberts, Cees Rodenburg, and J. Alexieva-Figusch. 1989. 'Antiprogestins, a new form of endocrine therapy for human breast cancer', *Cancer Res*, 49: 2851-6.
Klopper, A., and M. Hall. 1971. 'New synthetic agent for the induction of ovulation: preliminary trials in women', *Br Med J*, 1: 152-4.
Knowlden, J. M., I. R. Hutcheson, H. E. Jones, T. Madden, J. M. Gee, M. E. Harper, D. Barrow, A. E. Wakeling, and R. I. Nicholson. 2003. 'Elevated levels of epidermal growth factor receptor/c-erbB2 heterodimers mediate an autocrine growth regulatory pathway in tamoxifen-resistant MCF-7 cells', *Endocrinology*, 144: 1032-44.
Knudsen, Erik S., Steven C. Pruitt, Pamela A. Hershberger, Agnieszka K. Witkiewicz, and David W. Goodrich. 2019. 'Cell Cycle and Beyond: Exploiting New RB1 Controlled Mechanisms for Cancer Therapy', *Trends in cancer*, 5: 308-24.
Knutson, T. P., and C. A. Lange. 2014. 'Tracking progesterone receptor-mediated actions in breast cancer', *Pharmacol Ther*, 142: 114-25.
Knutson, Todd P., Andrea R. Daniel, Danhua Fan, Kevin A. T. Silverstein, Kyle R. Covington, Suzanne A. W. Fuqua, and Carol A. Lange. 2012. 'Phosphorylated and sumoylation-deficient progesterone receptors drive proliferative gene signatures during breast cancer progression', *Breast Cancer Research*, 14: R95.
Knutson, Todd P., Thu H. Truong, Shihong Ma, Nicholas J. Brady, Megan E. Sullivan, Ganesh Raj, Kathryn L. Schwertfeger, and Carol A. Lange. 2017. 'Posttranslationally modified progesterone receptors direct ligand-specific

expression of breast cancer stem cell-associated gene programs', *Journal of hematology & oncology*, 10: 89-89.
Koboldt, Daniel C., Robert S. Fulton, Michael D. McLellan, Heather Schmidt, Joelle Kalicki-Veizer, Joshua F. McMichael, Lucinda L. Fulton, et al. 2012. 'Comprehensive molecular portraits of human breast tumours', *Nature*, 490: 61-70.
Kong, Say Li, Guoliang Li, Siang Lin Loh, Wing-Kin Sung, and Edison T Liu. 2011. 'Cellular reprogramming by the conjoint action of ERα, FOXA1, and GATA3 to a ligand-inducible growth state', *Molecular Systems Biology*, 7: 526.
Kong, Y. Y., H. Yoshida, I. Sarosi, H. L. Tan, E. Timms, C. Capparelli, S. Morony, et al. 1999. 'OPGL is a key regulator of osteoclastogenesis, lymphocyte development and lymph-node organogenesis', *Nature*, 397: 315-23.
Korkmaz, G., Z. Manber, R. Lopes, S. Prekovic, K. Schuurman, Y. Kim, H. Teunissen, et al. 2019. 'A CRISPR-Cas9 screen identifies essential CTCF anchor sites for estrogen receptor-driven breast cancer cell proliferation', *Nucleic Acids Res*, 47: 9557-72.
Kornblum, Noah, Fengmin Zhao, Judith Manola, Paula Klein, Bhuvaneswari Ramaswamy, Adam Brufsky, Phillip J. Stella, et al. 2018. 'Randomized Phase II Trial of Fulvestrant Plus Everolimus or Placebo in Postmenopausal Women With Hormone Receptor–Positive, Human Epidermal Growth Factor Receptor 2–Negative Metastatic Breast Cancer Resistant to Aromatase Inhibitor Therapy: Results of PrE0102', *Journal of Clinical Oncology*, 36: 1556-63.
Kougioumtzi, Anastasia, Panayiotis Tsaparas, and Angeliki Magklara. 2014. 'Deep Sequencing Reveals New Aspects of Progesterone Receptor Signaling in Breast Cancer Cells', *PloS one*, 9: e98404.
Kouros-Mehr, Hosein, Euan M. Slorach, Mark D. Sternlicht, and Zena Werb. 2006. 'GATA-3 Maintains the Differentiation of the Luminal Cell Fate in the Mammary Gland', *Cell*, 127: 1041-55.
Kovacs, L., M. Sas, B. A. Resch, G. Ugocsai, M. L. Swahn, M. Bygdeman, and P. J. Rowe. 1984. 'Termination of very early pregnancy by RU 486 — An antiprogestational compound', *Contraception*, 29: 399-410.
Krop, I. E., I. A. Mayer, V. Ganju, M. Dickler, S. Johnston, S. Morales, D. A. Yardley, et al. 2016. 'Pictilisib for oestrogen receptor-positive, aromatase inhibitor-resistant, advanced or metastatic breast cancer (FERGI): a randomised, double-blind, placebo-controlled, phase 2 trial', *Lancet Oncol*, 17: 811-21.
Kuhl, H. 2005. 'Pharmacology of estrogens and progestogens: influence of different routes of administration', *Climacteric*, 8: 3-63.
Kuiper, G. G., B. Carlsson, K. Grandien, E. Enmark, J. Häggblad, S. Nilsson, and J. A. Gustafsson. 1997. 'Comparison of the ligand binding specificity and transcript tissue distribution of estrogen receptors alpha and beta', *Endocrinology*, 138: 863-70.
Kumar, Sanjeev, Allegra Freelander, and Elgene Lim. 2021. 'Type 1 Nuclear Receptor Activity in Breast Cancer: Translating Preclinical Insights to the Clinic', *Cancers*, 13: 4972.
L'Hermite, M., T. Simoncini, S. Fuller, and A. R. Genazzani. 2008. 'Could transdermal estradiol + progesterone be a safer postmenopausal HRT? A review', *Maturitas*, 60: 185-201.
Lai, Chun-Fui, Koen D. Flach, Xanthippi Alexi, Stephen P. Fox, Silvia Ottaviani, Paul T.R. Thiruchelvam, Fiona J. Kyle, et al. 2013. 'Co-regulated gene expression by oestrogen receptor α and liver receptor homolog-1 is a feature of the

oestrogen response in breast cancer cells', *Nucleic Acids Research*, 41: 10228-40.
Lainé, Muriel, Sean W. Fanning, Ya-Fang Chang, Bradley Green, Marianne E. Greene, Barry Komm, Justyna D. Kurleto, Linda Phung, and Geoffrey L. Greene. 2021. 'Lasofoxifene as a potential treatment for therapy-resistant ER-positive metastatic breast cancer', *Breast Cancer Research*, 23: 54.
Laine, Muriel, Marianne Greene, Ya-fang Chang, Linda Phung, Richard Hiipakka, Barry Komm, and Geoffrey Greene. 2018. 'Lasofoxifene efficacy in a mammary intraductal (MIND) xenograft model of ERα+ breast cancer', *Journal of Clinical Oncology*, 36: e13054-e54.
Lamb, Caroline A, Victoria T Fabris, Britta M Jacobsen, Alfredo Molinolo, and Claudia Lanari. 2018. 'Biological and clinical impact of imbalanced progesterone receptor isoform ratios in breast cancer', *Endocrine-related cancer*, 25: R605-R24.
Lanari, Claudia, Victoria Wargon, Paola Rojas, and Alfredo A. Molinolo. 2012. 'Antiprogestins in breast cancer treatment: are we ready?', *Endocrine-related cancer*, 19: R35-R50.
Lannigan, D. A. 2003. 'Estrogen receptor phosphorylation', *Steroids*, 68: 1-9.
Lapidus, R. G., A. T. Ferguson, Y. L. Ottaviano, F. F. Parl, H. S. Smith, S. A. Weitzman, S. B. Baylin, J. P. Issa, and N. E. Davidson. 1996. 'Methylation of estrogen and progesterone receptor gene 5' CpG islands correlates with lack of estrogen and progesterone receptor gene expression in breast tumors', *Clin Cancer Res*, 2: 805-10.
Leal, Mariana Ferreira, Ben P. Haynes, Eugene Schuster, Belinda Yeo, Maria Afentakis, Lila Zabaglo, Vera Martins, et al. 2019. 'Early Enrichment of ESR1 Mutations and the Impact on Gene Expression in Presurgical Primary Breast Cancer Treated with Aromatase Inhibitors', *Clinical Cancer Research*, 25: 7485-96.
Lee, O., M. E. Sullivan, Y. Xu, C. Rogers, M. Muzzio, I. Helenowski, A. Shidfar, et al. 2020. 'Selective Progesterone Receptor Modulators in Early-Stage Breast Cancer: A Randomized, Placebo-Controlled Phase II Window-of-Opportunity Trial Using Telapristone Acetate', *Clin Cancer Res*, 26: 25-34.
Lee, Sangjun, Syed K. Mohsin, Sufeng Mao, Susan G. Hilsenbeck, Dan Medina, and D. Craig Allred. 2005. 'Hormones, receptors, and growth in hyperplastic enlarged lobular units: early potential precursors of breast cancer', *Breast Cancer Research*, 8: R6.
Lehmann, Brian D., Joshua A. Bauer, Xi Chen, Melinda E. Sanders, A. Bapsi Chakravarthy, Yu Shyr, and Jennifer A. Pietenpol. 2011. 'Identification of human triple-negative breast cancer subtypes and preclinical models for selection of targeted therapies', *The Journal of Clinical Investigation*, 121: 2750-67.
Lei, J. T., J. Shao, J. Zhang, M. Iglesia, D. W. Chan, J. Cao, M. Anurag, et al. 2018. 'Functional Annotation of ESR1 Gene Fusions in Estrogen Receptor-Positive Breast Cancer', *Cell Rep*, 24: 1434-44.e7.
Levitz, M., S. Kadner, and B. K. Young. 1984. 'Intermediary metabolism of estriol in pregnancy', *J Steroid Biochem*, 20: 971-4.
Lewis, J. S., and V. C. Jordan. 2005. 'Selective estrogen receptor modulators (SERMs): mechanisms of anticarcinogenesis and drug resistance', *Mutat Res*, 591: 247-63.

Li, H. W. R., Y. X. Li, T. T. Li, H. Fan, E. H. Ng, W. S. Yeung, P. C. Ho, and K. F. Lee. 2017. 'Effect of ulipristal acetate and mifepristone at emergency contraception dose on the embryo-endometrial attachment using an in vitro human trophoblastic spheroid and endometrial cell co-culture model', *Hum Reprod*, 32: 2414-22.

Li, Li, Ling Lin, Jamunarani Veeraraghavan, Yiheng Hu, Xian Wang, Sanghoon Lee, Ying Tan, Rachel Schiff, and Xiao-Song Wang. 2020. 'Therapeutic role of recurrent ESR1-CCDC170 gene fusions in breast cancer endocrine resistance', *Breast Cancer Research*, 22: 84.

Li, S., D. Shen, J. Shao, R. Crowder, W. Liu, A. Prat, X. He, et al. 2013. 'Endocrine-therapy-resistant ESR1 variants revealed by genomic characterization of breast-cancer-derived xenografts', *Cell Rep*, 4: 1116-30.

Li, Y., M. H. Lambert, and H. E. Xu. 2003. 'Activation of nuclear receptors: a perspective from structural genomics', *Structure*, 11: 741-6.

Li, Z., Y. Wu, M. E. Yates, N. Tasdemir, A. Bahreini, J. Chen, K. M. Levine, et al. 2022. 'Hotspot ESR1 mutations are multimodal and contextual modulators of breast cancer metastasis', *Cancer Res*.

Li, Zheqi, Kevin M. Levine, Amir Bahreini, Peilu Wang, David Chu, Ben Ho Park, Steffi Oesterreich, and Adrian V. Lee. 2018. 'Upregulation of IRS1 Enhances IGF1 Response in Y537S and D538G ESR1 Mutant Breast Cancer Cells', *Endocrinology*, 159: 285-96.

Liberzon, A., C. Birger, H. Thorvaldsdóttir, M. Ghandi, J. P. Mesirov, and P. Tamayo. 2015. 'The Molecular Signatures Database (MSigDB) hallmark gene set collection', *Cell Syst*, 1: 417-25.

Lim, E., F. Vaillant, D. Wu, N. C. Forrest, B. Pal, A. H. Hart, M. L. Asselin-Labat, et al. 2009. 'Aberrant luminal progenitors as the candidate target population for basal tumor development in BRCA1 mutation carriers', *Nat Med*, 15: 907-13.

Lindahl, G., N. Saarinen, A. Abrahamsson, and C. Dabrosin. 2011. 'Tamoxifen, flaxseed, and the lignan enterolactone increase stroma- and cancer cell-derived IL-1Ra and decrease tumor angiogenesis in estrogen-dependent breast cancer', *Cancer Res*, 71: 51-60.

Lippman, M. E., K. A. Krueger, S. Eckert, A. Sashegyi, E. L. Walls, S. Jamal, J. A. Cauley, and S. R. Cummings. 2001. 'Indicators of lifetime estrogen exposure: effect on breast cancer incidence and interaction with raloxifene therapy in the multiple outcomes of raloxifene evaluation study participants', *J Clin Oncol*, 19: 3111-6.

Lonard, David M., and Bert W. O'Malley. 2006. 'The Expanding Cosmos of Nuclear Receptor Coactivators', *Cell*, 125: 411-14.

Lonard, David M., and Bert W. O'Malley. 2007. 'Nuclear Receptor Coregulators: Judges, Juries, and Executioners of Cellular Regulation', *Molecular Cell*, 27: 691-700.

Longacre, T. A., and S. A. Bartow. 1986. 'A correlative morphologic study of human breast and endometrium in the menstrual cycle', *Am J Surg Pathol*, 10: 382-93.

Lønning, Per Eystein, Emilio Bajetta, Robin Murray, Michèle Tubiana-Hulin, Peter D Eisenberg, Elizabeth Mickiewicz, Luigi Celio, Paula Pitt, Monica Mita, and Neil K Aaronson. 2000. 'Activity of exemestane in metastatic breast cancer after failure of nonsteroidal aromatase inhibitors: a phase II trial', *Journal of Clinical Oncology*, 18: 2234-44.

Love, Michael I., Wolfgang Huber, and Simon Anders. 2014. 'Moderated estimation of fold change and dispersion for RNA-seq data with DESeq2', *Genome Biology*, 15: 550.
Lydon, J P, F J DeMayo, C R Funk, S K Mani, A R Hughes, C A Montgomery, G Shyamala, O M Conneely, and B W O'Malley. 1995. 'Mice lacking progesterone receptor exhibit pleiotropic reproductive abnormalities', *Genes & Development*, 9: 2266-78.
Ma, Yan, Ranjana Ambannavar, James Stephans, Jennie Jeong, Andrew Dei Rossi, Mei-Lan Liu, Adam J. Friedman, et al. 2014. "Fusion transcript discovery in formalin-fixed paraffin-embedded human breast cancer tissues reveals a link to tumor progression." In *PloS one*, e94202.
Magee, J. A., L. W. Chang, G. D. Stormo, and J. Milbrandt. 2006. 'Direct, androgen receptor-mediated regulation of the FKBP5 gene via a distal enhancer element', *Endocrinology*, 147: 590-8.
Magnani, L., J. Eeckhoute, and M. Lupien. 2011a. 'Pioneer factors: directing transcriptional regulators within the chromatin environment', *Trends Genet*, 27: 465-74.
Magnani, Luca, Elizabeth B. Ballantyne, Xiaoyang Zhang, and Mathieu Lupien. 2011b. 'PBX1 Genomic Pioneer Function Drives ERα Signaling Underlying Progression in Breast Cancer', *PLOS Genetics*, 7: e1002368.
Magnani, Luca, Gianmaria Frige, Raffaella Maria Gadaleta, Giacomo Corleone, Sonia Fabris, Mannus H. Kempe, Pernette J. Verschure, et al. 2017. 'Acquired CYP19A1 amplification is an early specific mechanism of aromatase inhibitor resistance in ERα metastatic breast cancer', *Nat Genet*, 49: 444-50.
Malbeteau, Lucie, Coralie Poulard, Cécile Languilaire, Ivan Mikaelian, Frédéric Flamant, Muriel Le Romancer, and Laura Corbo. 2020. 'PRMT1 Is Critical for the Transcriptional Activity and the Stability of the Progesterone Receptor', *iScience*, 23.
Mallepell, Sonia, Andrée Krust, Pierre Chambon, and Cathrin Brisken. 2006. 'Paracrine signaling through the epithelial estrogen receptor α is required for proliferation and morphogenesis in the mammary gland', *Proceedings of the National Academy of Sciences*, 103: 2196-201.
Manavathi, Bramanandam, Venkata S. K. Samanthapudi, and Vijay Narasimha Reddy Gajulapalli. 2014. 'Estrogen receptor coregulators and pioneer factors: the orchestrators of mammary gland cell fate and development', *Frontiers in Cell and Developmental Biology*, 2.
Mangelsdorf, D. J., and R. M. Evans. 1995. 'The RXR heterodimers and orphan receptors', *Cell*, 83: 841-50.
Mao, C., M. Livezey, J. E. Kim, and D. J. Shapiro. 2016. 'Antiestrogen Resistant Cell Lines Expressing Estrogen Receptor α Mutations Upregulate the Unfolded Protein Response and are Killed by BHPI', *Sci Rep*, 6: 34753.
Martin, Lesley-Ann, Ricardo Ribas, Nikiana Simigdala, Eugene Schuster, Sunil Pancholi, Tencho Tenev, Pascal Gellert, et al. 2017. 'Discovery of naturally occurring ESR1 mutations in breast cancer cell lines modelling endocrine resistance', *Nature Communications*, 8: 1865.
Martin, Miguel, Elgene Lim, Mariana Chavez Mac Gregor, Mahesh Shivhare, Graham Ross, Monika Patre, Laura Roncoroni, Maria Louka, and Joohyuk Sohn. 2021. 'acelERA Breast Cancer (BC): Phase II study evaluating efficacy and safety of giredestrant (GDC-9545) versus physician's choice of endocrine

monotherapy in patients (pts) with estrogen receptor-positive, HER2-negative (ER+/HER2-) locally advanced or metastatic breast cancer (LA/mBC)', *Journal of Clinical Oncology*, 39: TPS1100-TPS00.
Mason, J. I., and W. E. Rainey. 1987. 'Steroidogenesis in the human fetal adrenal: a role for cholesterol synthesized de novo', *J Clin Endocrinol Metab*, 64: 140-7.
Masters, J. R. W., J. O. Drife, and J. J. Scarisbrick. 1977. 'Cyclic Variation of DNA Synthesis in Human Breast Epithelium', *JNCI: Journal of the National Cancer Institute*, 58: 1263-65.
Mattsson, W. 1983. 'Current status of high dose progestin treatment in advanced breast cancer', *Breast Cancer Res Treat*, 3: 231-5.
McDonnell, D. P., and M. E. Goldman. 1994. 'RU486 exerts antiestrogenic activities through a novel progesterone receptor A form-mediated mechanism', *Journal of Biological Chemistry*, 269: 11945-49.
McDonnell, D. P., M. M. Shahbaz, E. Vegeto, and M. E. Goldman. 1994. 'The human progesterone receptor A-form functions as a transcriptional modulator of mineralocorticoid receptor transcriptional activity', *J Steroid Biochem Mol Biol*, 48: 425-32.
McFall, T., B. McKnight, R. Rosati, S. Kim, Y. Huang, N. Viola-Villegas, and M. Ratnam. 2018. 'Progesterone receptor A promotes invasiveness and metastasis of luminal breast cancer by suppressing regulation of critical microRNAs by estrogen', *J Biol Chem*, 293: 1163-77.
McGuire, W. L., and G. M. Clark. 1986. 'Role of progesterone receptors in breast cancer', *CA Cancer J Clin*, 36: 302-9.
Merenbakh-Lamin, K., N. Ben-Baruch, A. Yeheskel, A. Dvir, L. Soussan-Gutman, R. Jeselsohn, R. Yelensky, et al. 2013. 'D538G mutation in estrogen receptor-alpha: A novel mechanism for acquired endocrine resistance in breast cancer', *Cancer Res*, 73: 6856-64.
Métivier, R., G. Penot, M. R. Hübner, G. Reid, H. Brand, M. Kos, and F. Gannon. 2003. 'Estrogen receptor-alpha directs ordered, cyclical, and combinatorial recruitment of cofactors on a natural target promoter', *Cell*, 115: 751-63.
Michna, H., M. R. Schneider, Y. Nishino, and M. F. el Etreby. 1989. 'Antitumor activity of the antiprogestins ZK 98.299 and RU 38.486 in hormone dependent rat and mouse mammary tumors: mechanistic studies', *Breast Cancer Res Treat*, 14: 275-88.
Migliaccio, Antimo, Domenico Piccolo, Gabriella Castoria, Marina Di Domenico, Antonio Bilancio, Maria Lombardi, Wenrong Gong, Miguel Beato, and Ferdinando Auricchio. 1998. 'Activation of the Src/p21ras/Erk pathway by progesterone receptor via cross-talk with estrogen receptor', *The EMBO Journal*, 17: 2008-18.
Milde-Langosch, Karin, Ana-Maria Bamberger, Gabriele Rieck, Bianca Kelp, and Thomas Löning. 2001. 'Overexpression of the p16 Cell Cycle Inhibitor in Breast Cancer is Associated with a More Malignant Phenotype', *Breast cancer research and treatment*, 67: 61-70.
Miller, W. L. 2017. 'Steroidogenesis: Unanswered Questions', *Trends Endocrinol Metab*, 28: 771-93.
Miller, W. L., and R. J. Auchus. 2011. 'The molecular biology, biochemistry, and physiology of human steroidogenesis and its disorders', *Endocr Rev*, 32: 81-151.
Miranda, Tina B., Ty C. Voss, Myong-Hee Sung, Songjoon Baek, Sam John, Mary Hawkins, Lars Grøntved, R. Louis Schiltz, and Gordon L. Hager. 2013.

'Reprogramming the Chromatin Landscape: Interplay of the Estrogen and Glucocorticoid Receptors at the Genomic Level', *Cancer Res*, 73: 5130-39.
Moelans, C. B., H. N. Monsuur, J. H. de Pinth, R. D. Radersma, R. A. de Weger, and P. J. van Diest. 2010. 'ESR1 amplification is rare in breast cancer and is associated with high grade and high proliferation: a multiplex ligation-dependent probe amplification study', *Anal Cell Pathol (Amst)*, 33: 13-8.
Mohammed, H., I. A. Russell, R. Stark, O. M. Rueda, T. E. Hickey, G. A. Tarulli, A. A. Serandour, et al. 2015. 'Progesterone receptor modulates ERα action in breast cancer', *Nature*, 523: 313-7.
Moore, N. L., T. E. Hickey, L. M. Butler, and W. D. Tilley. 2012. 'Multiple nuclear receptor signaling pathways mediate the actions of synthetic progestins in target cells', *Mol Cell Endocrinol*, 357: 60-70.
Morgan, L. R. 1985. 'Megestrol acetate v tamoxifen in advanced breast cancer in postmenopausal patients', *Semin Oncol*, 12: 43-7.
Mota, André de Lima, Adriane Feijo Evangelista, Taciane Macedo, Renato Oliveira, Cristovam Scapulatempo-Neto, René Aloisio Vieira, and Marcia Maria Chiquitelli Marques. 2017. 'Molecular characterization of breast cancer cell lines by clinical immunohistochemical markers', *Oncology letters*, 13: 4708-12.
Mote, P A, J F Johnston, T Manninen, P Tuohimaa, and C L Clarke. 2001. 'Detection of progesterone receptor forms A and B by immunohistochemical analysis', *Journal of Clinical Pathology*, 54: 624-30.
Mote, P. A., J. D. Graham, and C. L. Clarke. 2007. 'Progesterone receptor isoforms in normal and malignant breast', *Ernst Schering Found Symp Proc*: 77-107.
Mote, PA, S Bartow, N Tran, and CL Clarke. 2002. 'Loss of co-ordinate expression of progesterone receptors A and B is an early event in breast carcinogenesis', *Breast cancer research and treatment*, 72: 163-72.
Mueck, A. O., H. Seeger, and K. J. Bühling. 2009. 'Use of dydrogesterone in hormone replacement therapy', *Maturitas*, 65 Suppl 1: S51-60.
Mueller, Stefan O., James A. Clark, Page H. Myers, and Kenneth S. Korach. 2002. 'Mammary Gland Development in Adult Mice Requires Epithelial and Stromal Estrogen Receptor α', *Endocrinology*, 143: 2357-65.
Mukherjee, Atish, Selma M. Soyal, Jie Li, Yan Ying, Bin He, Francesco J. DeMayo, and John P. Lydon. 2010. 'Targeting RANKL to a specific subset of murine mammary epithelial cells induces ordered branching morphogenesis and alveologenesis in the absence of progesterone receptor expression', *FASEB journal : official publication of the Federation of American Societies for Experimental Biology*, 24: 4408-19.
Mulac-Jericevic, B., J. P. Lydon, F. J. DeMayo, and O. M. Conneely. 2003. 'Defective mammary gland morphogenesis in mice lacking the progesterone receptor B isoform', *Proc Natl Acad Sci U S A*, 100: 9744-9.
Mulac-Jericevic, B., R. A. Mullinax, F. J. DeMayo, J. P. Lydon, and O. M. Conneely. 2000. 'Subgroup of reproductive functions of progesterone mediated by progesterone receptor-B isoform', *Science*, 289: 1751-4.
Musgrove, E. A., and R. L. Sutherland. 2009. 'Biological determinants of endocrine resistance in breast cancer', *Nat Rev Cancer*, 9: 631-43.
Musgrove, E. A., A. Swarbrick, C. S. Lee, A. L. Cornish, and R. L. Sutherland. 1998. 'Mechanisms of cyclin-dependent kinase inactivation by progestins', *Molecular and cellular biology*, 18: 1812-25.

Muss, H. B., L. D. Case, J. N. Atkins, J. D. Bearden, 3rd, M. R. Cooper, J. M. Cruz, D. V. Jackson, Jr., et al. 1994. 'Tamoxifen versus high-dose oral medroxyprogesterone acetate as initial endocrine therapy for patients with metastatic breast cancer: a Piedmont Oncology Association study', *J Clin Oncol*, 12: 1630-8.

Muss, H. B., H. B. Wells, E. H. Paschold, W. R. Black, M. R. Cooper, R. L. Capizzi, R. Christian, et al. 1988. 'Megestrol acetate versus tamoxifen in advanced breast cancer: 5-year analysis--a phase III trial of the Piedmont Oncology Association', *J Clin Oncol*, 6: 1098-106.

Mustacchi, G., R. Ceccherini, S. Milani, A. Pluchinotta, A. De Matteis, L. Maiorino, A. Farris, A. Scanni, and F. Sasso. 2003. 'Tamoxifen alone versus adjuvant tamoxifen for operable breast cancer of the elderly: long-term results of the phase III randomized controlled multicenter GRETA trial', *Ann Oncol*, 14: 414-20.

Nacht, A. Silvina, Roberto Ferrari, Roser Zaurin, Valentina Scabia, José Carbonell-Caballero, Francois Le Dily, Javier Quilez, et al. 2019. 'C/EBPα mediates the growth inhibitory effect of progestins on breast cancer cells', *The EMBO Journal*, 38: e101426.

Nacht, Ana Silvina, Andy Pohl, Roser Zaurin, Daniel Soronellas, Javier Quilez, Priyanka Sharma, Roni H. Wright, Miguel Beato, and Guillermo P. Vicent. 2016. 'Hormone-induced repression of genes requires BRG1-mediated H1.2 deposition at target promoters', *The EMBO Journal*, 35: 1822-43.

Nagy, L., and J. W. Schwabe. 2004. 'Mechanism of the nuclear receptor molecular switch', *Trends Biochem Sci*, 29: 317-24.

Narayanan, R., C. C. Coss, and J. T. Dalton. 2018. 'Development of selective androgen receptor modulators (SARMs)', *Mol Cell Endocrinol*, 465: 134-42.

Nardulli, Ann M., and Benita S. Katzenellenbogen. 1988. 'Progesterone Receptor Regulation in T47D Human Breast Cancer Cells: Analysis by Density Labeling of Progesterone Receptor Synthesis and Degradation and Their Modulation by Progestin*', *Endocrinology*, 122: 1532-40.

Nettles, Kendall W., John B. Bruning, German Gil, Jason Nowak, Sanjay K. Sharma, Johnnie B. Hahm, Kristen Kulp, et al. 2008. 'NFkappaB selectivity of estrogen receptor ligands revealed by comparative crystallographic analyses', *Nature chemical biology*, 4: 241-47.

Ni, Min, Yiwen Chen, Elgene Lim, Hallie Wimberly, Shannon T Bailey, Yuuki Imai, David L Rimm, X. Shirley Liu, and Myles Brown. 2011. 'Targeting Androgen Receptor in Estrogen Receptor-Negative Breast Cancer', *Cancer cell*, 20: 119-31.

Nielsen, K. V., B. Ejlertsen, S. Müller, S. Møller, B. B. Rasmussen, E. Balslev, A. V. Lænkholm, P. Christiansen, and H. T. Mouridsen. 2011. 'Amplification of ESR1 may predict resistance to adjuvant tamoxifen in postmenopausal patients with hormone receptor positive breast cancer', *Breast Cancer Res Treat*, 127: 345-55.

Nielsen, M., J. L. Thomsen, S. Primdahl, U. Dyreborg, and J. A. Andersen. 1987. 'Breast cancer and atypia among young and middle-aged women: a study of 110 medicolegal autopsies', *Br J Cancer*, 56: 814-9.

Nishino, Tsuyuki, Kanako Ishibashi, Christian Hirtreiter, and Yukishige Nishino. 2009. 'Potentiation of the antitumor effect of tamoxifen by combination with the antiprogestin onapristone', *The Journal of Steroid Biochemistry and Molecular Biology*, 116: 187-90.

Nordeen, S. K., B. J. Bona, and M. L. Moyer. 1993. 'Latent agonist activity of the steroid antagonist, RU486, is unmasked in cells treated with activators of protein kinase A', *Mol Endocrinol*, 7: 731-42.
Nuclear Receptors Nomenclature Committee. 1999. 'A Unified Nomenclature System for the Nuclear Receptor Superfamily', *Cell*, 97: 161-63.
O'Leary, Ben, Sarah Hrebien, James P. Morden, Matthew Beaney, Charlotte Fribbens, Xin Huang, Yuan Liu, et al. 2018. 'Early circulating tumor DNA dynamics and clonal selection with palbociclib and fulvestrant for breast cancer', *Nature Communications*, 9: 896-96.
O'Malley, B. W., J. Qin, and R. B. Lanz. 2008. 'Cracking the coregulator codes', *Curr Opin Cell Biol*, 20: 310-5.
O'Malley, B. W., M. R. Sherman, and D. O. Toft. 1970. 'Progesterone "receptors" in the cytoplasm and nucleus of chick oviduct target tissue', *Proc Natl Acad Sci U S A*, 67: 501-08.
Obradović, Milan M. S., Baptiste Hamelin, Nenad Manevski, Joana Pinto Couto, Atul Sethi, Marie-May Coissieux, Simone Münst, et al. 2019. 'Glucocorticoids promote breast cancer metastasis', *Nature*, 567: 540-44.
Oelkers, W. H. 2005. 'Drospirenone in combination with estrogens: for contraception and hormone replacement therapy', *Climacteric*, 8 Suppl 3: 19-27.
Oliveira, Mafalda, Maxine Bennett, Ali Khalil, Richard Mather, Rhiannon Maudsley, Sam McGuinness, Christopher J. Morrow, et al. 2021. 'Abstract OT-09-02: A randomized, open-label, parallel-group, multicenter phase 2 study comparing the efficacy and safety of oral AZD9833 versus fulvestrant in women with advanced ER-positive HER2-negative breast cancer (SERENA-2)', *Cancer Res*, 81: OT-09-02-OT-09-02.
Olsson, H. L., C. Ingvar, and A. Bladström. 2003. 'Hormone replacement therapy containing progestins and given continuously increases breast carcinoma risk in Sweden', *Cancer*, 97: 1387-92.
Omarjee, Soleilmane, and Jason S. Carroll. 2020. 'Targeting LSD1 and FOXA1 in prostate cancer', *Nat Genet*, 52: 1002-03.
Osborne, C. K., V. Bardou, T. A. Hopp, G. C. Chamness, S. G. Hilsenbeck, S. A. Fuqua, J. Wong, D. C. Allred, G. M. Clark, and R. Schiff. 2003. 'Role of the estrogen receptor coactivator AIB1 (SRC-3) and HER-2/neu in tamoxifen resistance in breast cancer', *J Natl Cancer Inst*, 95: 353-61.
Osborne, C. K., J. Pippen, S. E. Jones, L. M. Parker, M. Ellis, S. Come, S. Z. Gertler, et al. 2002. 'Double-blind, randomized trial comparing the efficacy and tolerability of fulvestrant versus anastrozole in postmenopausal women with advanced breast cancer progressing on prior endocrine therapy: results of a North American trial', *J Clin Oncol*, 20: 3386-95.
Osborne, C. K., and R. Schiff. 2011. 'Mechanisms of endocrine resistance in breast cancer', *Annu Rev Med*, 62: 233-47.
Ottaviano, Y. L., J. P. Issa, F. F. Parl, H. S. Smith, S. B. Baylin, and N. E. Davidson. 1994. 'Methylation of the estrogen receptor gene CpG island marks loss of estrogen receptor expression in human breast cancer cells', *Cancer Res*, 54: 2552-5.
Overmoyer, Beth, Pedro Sanz-Altimira, Ann H. Partridge, Martine Extermann, Jane Liu, Eric Winer, Nancy Lin, et al. 2015. 'Abstract P1-13-04: Enobosarm for the treatment of metastatic, estrogen and androgen receptor positive, breast cancer. Final results of the primary endpoint and current progression free survival', *Cancer Res*, 75: P1-13-04-P1-13-04.

Paffenbarger, R. S., Jr., J. B. Kampert, and H. G. Chang. 1980. 'Characteristics that predict risk of breast cancer before and after the menopause', *Am J Epidemiol*, 112: 258-68.
Pagani, Olivia, Meredith M. Regan, Barbara A. Walley, Gini F. Fleming, Marco Colleoni, István Láng, Henry L. Gomez, et al. 2014. 'Adjuvant Exemestane with Ovarian Suppression in Premenopausal Breast Cancer', *New England Journal of Medicine*, 371: 107-18.
Pakdel, F., J. C. Reese, and B. S. Katzenellenbogen. 1993. 'Identification of charged residues in an N-terminal portion of the hormone-binding domain of the human estrogen receptor important in transcriptional activity of the receptor', *Mol Endocrinol*, 7: 1408-17.
Palafox, Marta, Irene Ferrer, Pasquale Pellegrini, Sergi Vila, Sara Hernandez-Ortega, Ander Urruticoechea, Fina Climent, et al. 2012. 'RANK Induces Epithelial–Mesenchymal Transition and Stemness in Human Mammary Epithelial Cells and Promotes Tumorigenesis and Metastasis', *Cancer Res*, 72: 2879-88.
Palmieri, C., S. Cleator, L. S. Kilburn, S. B. Kim, S. H. Ahn, M. Beresford, G. Gong, et al. 2014. 'NEOCENT: a randomised feasibility and translational study comparing neoadjuvant endocrine therapy with chemotherapy in ER-rich postmenopausal primary breast cancer', *Breast Cancer Res Treat*, 148: 581-90.
Palmieri, Carlo, Hannah M. Linden, Stephen Birrell, Elgene Lim, Lee S. Schwartzberg, Hope S. Rugo, Patrick Wayne Cobb, et al. 2021. 'Efficacy of enobosarm, a selective androgen receptor (AR) targeting agent, correlates with the degree of AR positivity in advanced AR+/estrogen receptor (ER)+ breast cancer in an international phase 2 clinical study', *Journal of Clinical Oncology*, 39: 1020-20.
Pan, Deng, Masha Kocherginsky, and Suzanne D. Conzen. 2011. 'Activation of the Glucocorticoid Receptor Is Associated with Poor Prognosis in Estrogen Receptor-Negative Breast Cancer', *Cancer Res*, 71: 6360-70.
Pardo, I., H. A. Lillemoe, R. J. Blosser, M. Choi, C. A. Sauder, D. K. Doxey, T. Mathieson, et al. 2014. 'Next-generation transcriptome sequencing of the premenopausal breast epithelium using specimens from a normal human breast tissue bank', *Breast Cancer Res*, 16: R26.
Paridaens, R. J., L. Y. Dirix, L. V. Beex, M. Nooij, D. A. Cameron, T. Cufer, M. J. Piccart, J. Bogaerts, and P. Therasse. 2008. 'Phase III study comparing exemestane with tamoxifen as first-line hormonal treatment of metastatic breast cancer in postmenopausal women: the European Organisation for Research and Treatment of Cancer Breast Cancer Cooperative Group', *J Clin Oncol*, 26: 4883-90.
Patel, Hitisha K., Nianjun Tao, Kyung-Min Lee, Mariela Huerta, Heike Arlt, Tara Mullarkey, Steven Troy, Carlos L. Arteaga, and Teeru Bihani. 2019. 'Elacestrant (RAD1901) exhibits anti-tumor activity in multiple ER+ breast cancer models resistant to CDK4/6 inhibitors', *Breast Cancer Research*, 21: 146.
Pavlin, Matic, Angelo Spinello, Marzia Pennati, Nadia Zaffaroni, Silvia Gobbi, Alessandra Bisi, Giorgio Colombo, and Alessandra Magistrato. 2018. 'A Computational Assay of Estrogen Receptor α Antagonists Reveals the Key Common Structural Traits of Drugs Effectively Fighting Refractory Breast Cancers', *Scientific reports*, 8: 649-49.

Perou, C. M., T. Sørlie, M. B. Eisen, M. van de Rijn, S. S. Jeffrey, C. A. Rees, J. R. Pollack, et al. 2000. 'Molecular portraits of human breast tumours', *Nature*, 406: 747-52.
Perrault, D., E. A. Eisenhauer, K. I. Pritchard, L. Panasci, B. Norris, T. Vandenberg, and B. Fisher. 1996. 'Phase II study of the progesterone antagonist mifepristone in patients with untreated metastatic breast carcinoma: a National Cancer Institute of Canada Clinical Trials Group study', *J Clin Oncol*, 14: 2709-12.
Peters, A. A., G. Buchanan, C. Ricciardelli, T. Bianco-Miotto, M. M. Centenera, J. M. Harris, S. Jindal, et al. 2009. 'Androgen receptor inhibits estrogen receptor-alpha activity and is prognostic in breast cancer', *Cancer Res*, 69: 6131-40.
Philibert, Daniel, and Jean-Pierre Raynaud. 1974. 'Progesterone Binding in the Immature Rabbit and Guinea Pig Uterus', *Endocrinology*, 94: 627-32.
Piccart, M., G. N. Hortobagyi, M. Campone, K. I. Pritchard, F. Lebrun, Y. Ito, S. Noguchi, et al. 2014. 'Everolimus plus exemestane for hormone-receptor-positive, human epidermal growth factor receptor-2-negative advanced breast cancer: overall survival results from BOLERO-2†', *Ann Oncol*, 25: 2357-62.
Piccart, M., H. Rugo, D. Chen, M. Campone, H. A. Burris, T. Taran, T. Sahmoud, I. Deleu, G. Hortobagyi, and J. Baselga. 2013. 'Assessment of Genetic Alterations in Postmenopausal Women with Hormone Receptor-Positive, HER2-Negative Advanced Breast Cancer from the BOLERO-2 Trial by Next-Generation Sequencing', *Annals of Oncology*, 24: iii25.
Polychronis, A., H. D. Sinnett, D. Hadjiminas, H. Singhal, J. L. Mansi, D. Shivapatham, S. Shousha, et al. 2005. 'Preoperative gefitinib versus gefitinib and anastrozole in postmenopausal patients with oestrogen-receptor positive and epidermal-growth-factor-receptor-positive primary breast cancer: a double-blind placebo-controlled phase II randomised trial', *Lancet Oncol*, 6: 383-91.
Powles, T., P. M. Savage, J. Stebbing, D. Short, A. Young, M. Bower, C. Pappin, P. Schmid, and M. J. Seckl. 2007. 'A comparison of patients with relapsed and chemo-refractory gestational trophoblastic neoplasia', *Br J Cancer*, 96: 732-7.
Presman, D. M., S. Ganguly, R. L. Schiltz, T. A. Johnson, T. S. Karpova, and G. L. Hager. 2016. 'DNA binding triggers tetramerization of the glucocorticoid receptor in live cells', *Proc Natl Acad Sci U S A*, 113: 8236-41.
Presti, D., and E. Quaquarini. 2019. 'The PI3K/AKT/mTOR and CDK4/6 Pathways in Endocrine Resistant HR+/HER2- Metastatic Breast Cancer: Biological Mechanisms and New Treatments', *Cancers (Basel)*, 11.
Proietti, Cecilia J., Wendy Béguelin, María Celeste Díaz Flaqué, Florencia Cayrol, Martín A. Rivas, Mercedes Tkach, Eduardo H. Charreau, Roxana Schillaci, and Patricia V. Elizalde. 2011. 'Novel role of signal transducer and activator of transcription 3 as a progesterone receptor coactivator in breast cancer', *Steroids*, 76: 381-92.
Proverbs-Singh, T., J. L. Feldman, M. J. Morris, K. A. Autio, and T. A. Traina. 2015. 'Targeting the androgen receptor in prostate and breast cancer: several new agents in development', *Endocr Relat Cancer*, 22: R87-r106.
Punglia, R. S., K. M. Kuntz, E. P. Winer, J. C. Weeks, and H. J. Burstein. 2006. 'The impact of tumor progesterone receptor status on optimal adjuvant endocrine therapy for postmenopausal patients with early-stage breast cancer: a decision analysis', *Cancer*, 106: 2576-82.

Puyang, Xiaoling, Craig Furman, Guo Zhu Zheng, Zhenhua J. Wu, Deepti Banka, Kiran Aithal, Sergei Agoulnik, et al. 2018. 'Discovery of Selective Estrogen Receptor Covalent Antagonists for the Treatment of ERα^{WT} and ERα^{MUT} Breast Cancer', *Cancer Discovery*, 8: 1176-93.
Quinkler, M., and S. Diederich. 2002. 'Difference of in vivo and in vitro antimineralocorticoid potency of progesterone', *Endocr Res*, 28: 465-70.
Quinkler, M., B. Meyer, C. Bumke-Vogt, C. Grossmann, U. Gruber, W. Oelkers, S. Diederich, and V. Bahr. 2002. 'Agonistic and antagonistic properties of progesterone metabolites at the human mineralocorticoid receptor', *European journal of endocrinology*, 146: 789-99.
Rae, J. M., M. D. Johnson, J. O. Scheys, K. E. Cordero, J. M. Larios, and M. E. Lippman. 2005. 'GREB 1 is a critical regulator of hormone dependent breast cancer growth', *Breast Cancer Res Treat*, 92: 141-9.
Rajaram, R. D., D. Buric, M. Caikovski, A. Ayyanan, J. Rougemont, J. Shan, S. J. Vainio, O. Yalcin-Ozuysal, and C. Brisken. 2015. 'Progesterone and Wnt4 control mammary stem cells via myoepithelial crosstalk', *Embo j*, 34: 641-52.
Randolph, J. F., Jr., H. Zheng, M. R. Sowers, C. Crandall, S. Crawford, E. B. Gold, and M. Vuga. 2011. 'Change in follicle-stimulating hormone and estradiol across the menopausal transition: effect of age at the final menstrual period', *J Clin Endocrinol Metab*, 96: 746-54.
Razandi, Mahnaz, Ali Pedram, Steven T. Park, and Ellis R. Levin. 2003. 'Proximal Events in Signaling by Plasma Membrane Estrogen Receptors*', *Journal of Biological Chemistry*, 278: 2701-12.
Razavi, Pedram, Matthew T. Chang, Guotai Xu, Chaitanya Bandlamudi, Dara S. Ross, Neil Vasan, Yanyan Cai, et al. 2018. 'The Genomic Landscape of Endocrine-Resistant Advanced Breast Cancers', *Cancer cell*, 34: 427-38.e6.
Read, L D, Catherine E. Snider, J. Scott Miller, Geoffrey L. Greene, and Benita S. Katzenellenbogen. 1988. 'Ligand-modulated regulation of progesterone receptor messenger ribonucleic acid and protein in human breast cancer cell lines', *Molecular Endocrinology*, 2 3: 263-71.
Regan, M. M., O. Pagani, G. F. Fleming, B. A. Walley, K. N. Price, M. Rabaglio, R. Maibach, et al. 2013. 'Adjuvant treatment of premenopausal women with endocrine-responsive early breast cancer: design of the TEXT and SOFT trials', *Breast*, 22: 1094-100.
Reinert, Tomás, Susana Ramalho, Vivian Castro Antunes de Vasconcelos, Leonardo Roberto Silva, Ana Elisa Ribeiro da Silva, Camila Annicchino de Andrade, Maria Beatriz de Paula Leite Kraft, et al. 2020. 'ESR1 Mutations Are Not a Common Mechanism of Endocrine Resistance in Patients With Estrogen Receptor–Positive Breast Cancer Treated With Neoadjuvant Aromatase Inhibitor Therapy', *Frontiers in Oncology*, 10.
Reya, T., S. J. Morrison, M. F. Clarke, and I. L. Weissman. 2001. 'Stem cells, cancer, and cancer stem cells', *Nature*, 414: 105-11.
Ribas, R., S. Pancholi, S. K. Guest, E. Marangoni, Q. Gao, A. Thuleau, N. Simigdala, et al. 2015. 'AKT Antagonist AZD5363 Influences Estrogen Receptor Function in Endocrine-Resistant Breast Cancer and Synergizes with Fulvestrant (ICI182780) In Vivo', *Mol Cancer Ther*, 14: 2035-48.
Richer, J. K., B. M. Jacobsen, N. G. Manning, M. G. Abel, D. M. Wolf, and K. B. Horwitz. 2002. 'Differential gene regulation by the two progesterone receptor isoforms in human breast cancer cells', *J Biol Chem*, 277: 5209-18.

Rimawi, M., J. M. Ferrero, J. de la Haba-Rodriguez, C. Poole, S. De Placido, C. K. Osborne, R. Hegg, V. Easton, C. Wohlfarth, and G. Arpino. 2018. 'First-Line Trastuzumab Plus an Aromatase Inhibitor, With or Without Pertuzumab, in Human Epidermal Growth Factor Receptor 2-Positive and Hormone Receptor-Positive Metastatic or Locally Advanced Breast Cancer (PERTAIN): A Randomized, Open-Label Phase II Trial', *J Clin Oncol*, 36: 2826-35.

Ring, A., and M. Dowsett. 2004. 'Mechanisms of tamoxifen resistance', *Endocr Relat Cancer*, 11: 643-58.

Rioux, N., S. Smith, M. Korpal, M. O'Shea, S. Prajapati, G. Z. Zheng, M. Warmuth, and P. G. Smith. 2019. 'Nonclinical pharmacokinetics and in vitro metabolism of H3B-6545, a novel selective ERα covalent antagonist (SERCA)', *Cancer Chemother Pharmacol*, 83: 151-60.

Robertson, J. F. R., I. M. Bondarenko, E. Trishkina, M. Dvorkin, L. Panasci, A. Manikhas, Y. Shparyk, et al. 2016. 'Fulvestrant 500 mg versus anastrozole 1 mg for hormone receptor-positive advanced breast cancer (FALCON): an international, randomised, double-blind, phase 3 trial', *Lancet*, 388: 2997-3005.

Robertson, J. F. R., and M. Harrison. 2004. 'Fulvestrant: pharmacokinetics and pharmacology', *Br J Cancer*, 90 Suppl 1: S7-S10.

Robertson, J. F., P. C. Willsher, L. Winterbottom, R. W. Blamey, and S. Thorpe. 1999. 'Onapristone, a progesterone receptor antagonist, as first-line therapy in primary breast cancer', *Eur J Cancer*, 35: 214-8.

Robinson, D. R., Y. M. Wu, P. Vats, F. Su, R. J. Lonigro, X. Cao, S. Kalyana-Sundaram, et al. 2013. 'Activating ESR1 mutations in hormone-resistant metastatic breast cancer', *Nat Genet*, 45: 1446-51.

Rocha, R. L., S. G. Hilsenbeck, J. G. Jackson, C. L. VanDenBerg, Cn Weng, A. V. Lee, and D. Yee. 1997. 'Insulin-like growth factor binding protein-3 and insulin receptor substrate-1 in breast cancer: correlation with clinical parameters and disease-free survival', *Clin Cancer Res*, 3: 103-9.

Romieu, G., T. Maudelonde, A. Ulmann, H. Pujol, J. Grenier, G. Cavalie, S. Khalaf, and H. Rochefort. 1987. 'The antiprogestin RU486 in advanced breast cancer: preliminary clinical trial', *Bull Cancer*, 74: 455-61.

Rondón-Lagos, M., L. Verdun Di Cantogno, C. Marchiò, N. Rangel, C. Payan-Gomez, P. Gugliotta, C. Botta, et al. 2014. 'Differences and homologies of chromosomal alterations within and between breast cancer cell lines: a clustering analysis', *Mol Cytogenet*, 7: 8.

Rosati, Rayna, Kailey Oppat, Yanfang Huang, Seongho Kim, and Manohar Ratnam. 2020. 'Clinical association of progesterone receptor isoform A with breast cancer metastasis consistent with its unique mechanistic role in preclinical models', *BMC cancer*, 20: 512.

Ross, R. K., A. Paganini-Hill, P. C. Wan, and M. C. Pike. 2000. 'Effect of hormone replacement therapy on breast cancer risk: estrogen versus estrogen plus progestin', *J Natl Cancer Inst*, 92: 328-32.

Ross-Innes, C. S., R. Stark, K. A. Holmes, D. Schmidt, C. Spyrou, R. Russell, C. E. Massie, S. L. Vowler, M. Eldridge, and J. S. Carroll. 2010. 'Cooperative interaction between retinoic acid receptor-alpha and estrogen receptor in breast cancer', *Genes Dev*, 24: 171-82.

Ross-Innes, Caryn S., Rory Stark, Andrew E. Teschendorff, Kelly A. Holmes, H. Raza Ali, Mark J. Dunning, Gordon D. Brown, et al. 2012. 'Differential

oestrogen receptor binding is associated with clinical outcome in breast cancer', *Nature*, 481: 389-93.
Rossouw, J. E., G. L. Anderson, R. L. Prentice, A. Z. LaCroix, C. Kooperberg, M. L. Stefanick, R. D. Jackson, et al. 2002. 'Risks and benefits of estrogen plus progestin in healthy postmenopausal women: principal results From the Women's Health Initiative randomized controlled trial', *Jama*, 288: 321-33.
Rugo, H. S., F. Lerebours, E. Ciruelos, P. Drullinsky, M. Ruiz-Borrego, P. Neven, Y. H. Park, et al. 2021. 'Alpelisib plus fulvestrant in PIK3CA-mutated, hormone receptor-positive advanced breast cancer after a CDK4/6 inhibitor (BYLieve): one cohort of a phase 2, multicentre, open-label, non-comparative study', *Lancet Oncol*, 22: 489-98.
Rugo, H. S., R. B. Rumble, E. Macrae, D. L. Barton, H. K. Connolly, M. N. Dickler, L. Fallowfield, et al. 2016. 'Endocrine Therapy for Hormone Receptor-Positive Metastatic Breast Cancer: American Society of Clinical Oncology Guideline', *J Clin Oncol*, 34: 3069-103.
Russo, J., X. Ao, C. Grill, and I. H. Russo. 1999. 'Pattern of distribution of cells positive for estrogen receptor alpha and progesterone receptor in relation to proliferating cells in the mammary gland', *Breast Cancer Res Treat*, 53: 217-27.
Rylance, P. B., M. Brincat, K. Lafferty, J. C. De Trafford, S. Brincat, V. Parsons, and J. W. Studd. 1985. 'Natural progesterone and antihypertensive action', *Br Med J (Clin Res Ed)*, 290: 13-4.
Sabnis, G. J., O. Goloubeva, S. Chumsri, N. Nguyen, S. Sukumar, and A. M. Brodie. 2011. 'Functional activation of the estrogen receptor-α and aromatase by the HDAC inhibitor entinostat sensitizes ER-negative tumors to letrozole', *Cancer Res*, 71: 1893-903.
Safe, Stephen. 2001. 'Transcriptional activation of genes by 17β-estradiol through estrogen receptor-Sp1 interactions.' in, *Vitamins & Hormones* (Academic Press).
Salatino, Mariana, Roxana Schillaci, Cecilia J. Proietti, Romina Carnevale, Isabel Frahm, Alfredo A. Molinolo, Adolfo Iribarren, Eduardo H. Charreau, and Patricia V. Elizalde. 2004. 'Inhibition of in vivo breast cancer growth by antisense oligodeoxynucleotides to type I insulin-like growth factor receptor mRNA involves inactivation of ErbBs, PI-3K/Akt and p42/p44 MAPK signaling pathways but not modulation of progesterone receptor activity', *Oncogene*, 23: 5161-74.
Santoro, N., S. L. Crawford, W. L. Lasley, J. L. Luborsky, K. A. Matthews, D. McConnell, J. F. Randolph, Jr., et al. 2008. 'Factors related to declining luteal function in women during the menopausal transition', *J Clin Endocrinol Metab*, 93: 1711-21.
Santoro, N., and J. F. Randolph, Jr. 2011. 'Reproductive hormones and the menopause transition', *Obstet Gynecol Clin North Am*, 38: 455-66.
Santos, Rita, Oleg Ursu, Anna Gaulton, A. Patrícia Bento, Ramesh S. Donadi, Cristian G. Bologa, Anneli Karlsson, et al. 2017. 'A comprehensive map of molecular drug targets', *Nature reviews. Drug discovery*, 16: 19-34.
Sanyal, Amartya, Bryan R. Lajoie, Gaurav Jain, and Job Dekker. 2012. 'The long-range interaction landscape of gene promoters', *Nature*, 489: 109-13.
Sartor, O., and G. B. Cutler, Jr. 1996. 'Mifepristone: treatment of Cushing's syndrome', *Clin Obstet Gynecol*, 39: 506-10.

Sartorius, C. A., S. D. Groshong, L. A. Miller, R. L. Powell, L. Tung, G. S. Takimoto, and K. B. Horwitz. 1994. 'New T47D breast cancer cell lines for the independent study of progesterone B- and A-receptors: only antiprogestin-occupied B-receptors are switched to transcriptional agonists by cAMP', *Cancer Res*, 54: 3868-77.

Sartorius, C. A., L. Tung, G. S. Takimoto, and K. B. Horwitz. 1993. 'Antagonist-occupied human progesterone receptors bound to DNA are functionally switched to transcriptional agonists by cAMP', *J Biol Chem*, 268: 9262-6.

Sartorius, Carol A., Djuana M.E. Harvell, Tianjie Shen, and Kathryn B. Horwitz. 2005. 'Progestins Initiate a Luminal to Myoepithelial Switch in Estrogen-Dependent Human Breast Tumors without Altering Growth', *Cancer Res*, 65: 9779-88.

Sartorius, Carol A., Tianjie Shen, and Kathryn B. Horwitz. 2003. 'Progesterone Receptors A and B Differentially Affect the Growth of Estrogen-Dependent Human Breast Tumor Xenografts', *Breast cancer research and treatment*, 79: 287-99.

Sato, T., T. H. Tran, A. R. Peck, M. A. Girondo, C. Liu, C. R. Goodman, L. M. Neilson, et al. 2014. 'Prolactin suppresses a progestin-induced CK5-positive cell population in luminal breast cancer through inhibition of progestin-driven BCL6 expression', *Oncogene*, 33: 2215-24.

Scarpin, Katherine M., J. Dinny Graham, Patricia A. Mote, and Christine L. Clarke. 2009. 'Progesterone Action in Human Tissues: Regulation by Progesterone Receptor (PR) Isoform Expression, Nuclear Positioning and Coregulator Expression', *Nuclear Receptor Signaling*, 7: nrs.07009.

Schiavon, G., S. Hrebien, I. Garcia-Murillas, R. J. Cutts, A. Pearson, N. Tarazona, K. Fenwick, et al. 2015. 'Analysis of ESR1 mutation in circulating tumor DNA demonstrates evolution during therapy for metastatic breast cancer', *Sci Transl Med*, 7: 313ra182.

Schmid, P., S. E. Pinder, D. Wheatley, J. Macaskill, C. Zammit, J. Hu, R. Price, et al. 2016. 'Phase II Randomized Preoperative Window-of-Opportunity Study of the PI3K Inhibitor Pictilisib Plus Anastrozole Compared With Anastrozole Alone in Patients With Estrogen Receptor-Positive Breast Cancer', *J Clin Oncol*, 34: 1987-94.

Schmid, P., M. Zaiss, C. Harper-Wynne, M. Ferreira, S. Dubey, S. Chan, A. Makris, et al. 2019. 'Fulvestrant Plus Vistusertib vs Fulvestrant Plus Everolimus vs Fulvestrant Alone for Women With Hormone Receptor-Positive Metastatic Breast Cancer: The MANTA Phase 2 Randomized Clinical Trial', *JAMA Oncol*, 5: 1556-64.

Schneider, M. R., H. Michna, U. F. Habenicht, Y. Nishino, H. J. Grill, and K. Pollow. 1992. 'The tumour-inhibiting potential of the progesterone antagonist Onapristone in the human mammary carcinoma T61 in nude mice', *J Cancer Res Clin Oncol*, 118: 187-9.

Schoonen, W. G., G. H. Deckers, M. E. de Gooijer, R. de Ries, and H. J. Kloosterboer. 2000. 'Hormonal properties of norethisterone, 7alpha-methyl-norethisterone and their derivatives', *J Steroid Biochem Mol Biol*, 74: 213-22.

Schoonen, W. G. E. J., R. Dijkema, R. J. H. de Ries, J. L. Wagenaars, J. W. H. Joosten, M. E. de Gooyer, G. H. Deckers, and H. J. Kloosterboer. 1998. 'Human progesterone receptor A and B isoforms in CHO cells. II. Comparison of binding, transactivation and ed50 values of several synthetic (anti)progestagens in vitro in CHO and MCF-7 cells and in vivo in rabbits and rats', *The Journal of Steroid Biochemistry and Molecular Biology*, 64: 157-70.

Schurch, N. J., P. Schofield, M. Gierliński, C. Cole, A. Sherstnev, V. Singh, N. Wrobel, et al. 2016. 'How many biological replicates are needed in an RNA-seq experiment and which differential expression tool should you use?', *Rna*, 22: 839-51.
Schwabe, J. W., L. Chapman, J. T. Finch, and D. Rhodes. 1993. 'The crystal structure of the estrogen receptor DNA-binding domain bound to DNA: how receptors discriminate between their response elements', *Cell*, 75: 567-78.
Seacrist, C. D., G. Kuenze, R. M. Hoffmann, B. E. Moeller, J. E. Burke, J. Meiler, and R. D. Blind. 2020. 'Integrated Structural Modeling of Full-Length LRH-1 Reveals Inter-domain Interactions Contribute to Receptor Structure and Function', *Structure*, 28: 830-46.e9.
Segal, C. V., and M. Dowsett. 2014. 'Estrogen receptor mutations in breast cancer--new focus on an old target', *Clin Cancer Res*, 20: 1724-6.
Segawa, T., M. E. Nau, L. L. Xu, R. N. Chilukuri, M. Makarem, W. Zhang, G. Petrovics, et al. 2002. 'Androgen-induced expression of endoplasmic reticulum (ER) stress response genes in prostate cancer cells', *Oncogene*, 21: 8749-58.
Semiglazov, V. F., V. V. Semiglazov, G. A. Dashyan, E. K. Ziltsova, V. G. Ivanov, A. A. Bozhok, O. A. Melnikova, R. M. Paltuev, A. Kletzel, and L. M. Berstein. 2007. 'Phase 2 randomized trial of primary endocrine therapy versus chemotherapy in postmenopausal patients with estrogen receptor-positive breast cancer', *Cancer*, 110: 244-54.
Sflomos, George, Valerian Dormoy, Tauno Metsalu, Rachel Jeitziner, Laura Battista, Valentina Scabia, Wassim Raffoul, et al. 2016. 'A Preclinical Model for ERα-Positive Breast Cancer Points to the Epithelial Microenvironment as Determinant of Luminal Phenotype and Hormone Response', *Cancer cell*, 29: 407-22.
Shackleton, M., F. Vaillant, K. J. Simpson, J. Stingl, G. K. Smyth, M. L. Asselin-Labat, L. Wu, G. J. Lindeman, and J. E. Visvader. 2006. 'Generation of a functional mammary gland from a single stem cell', *Nature*, 439: 84-8.
Shaffer, Paul L., Arif Jivan, D. Eric Dollins, Frank Claessens, and Daniel T. Gewirth. 2004. 'Structural basis of androgen receptor binding to selective androgen response elements', *Proc Natl Acad Sci U S A*, 101: 4758-63.
Shang, Y., and M. Brown. 2002. 'Molecular determinants for the tissue specificity of SERMs', *Science*, 295: 2465-8.
Shaw, Jacqueline, David Guttery, Allison Hills, Daniel Fernandez Garcia, Karen Page, Brenda Rosales, Kate Goddard, et al. 2016. 'Mutation analysis of cell-free DNA and single circulating tumor cells in metastatic breast cancer patients with high CTC counts', *Clinical Cancer Research*, 23.
Shen, Tianjie, B. Horwitz Kathryn, and A. Lange Carol. 2001. 'Transcriptional Hyperactivity of Human Progesterone Receptors Is Coupled to Their Ligand-Dependent Down-Regulation by Mitogen-Activated Protein Kinase-Dependent Phosphorylation of Serine 294', *Molecular and cellular biology*, 21: 6122-31.
Shiah, Yu-Jia, Pirashaanthy Tharmapalan, Alison E. Casey, Purna A. Joshi, Trevor D. McKee, Hartland W. Jackson, Alexander G. Beristain, et al. 2015. 'A Progesterone-CXCR4 Axis Controls Mammary Progenitor Cell Fate in the Adult Gland', *Stem cell reports*, 4: 313-22.
Shou, Jiang, Suleiman Massarweh, C. Kent Osborne, Alan E. Wakeling, Simale Ali, Heidi Weiss, and Rachel Schiff. 2004. 'Mechanisms of Tamoxifen Resistance:

Increased Estrogen Receptor-HER2/neu Cross-Talk in ER/HER2–Positive Breast Cancer', *JNCI: Journal of the National Cancer Institute*, 96: 926-35.
Sikora, Matthew J. 2016. 'Family Matters: Collaboration and Conflict Among the Steroid Receptors Raises a Need for Group Therapy', *Endocrinology*, 157: 4553-60.
Simpson, Evan R., and Susan R. Davis. 2001. 'Minireview: Aromatase and the Regulation of Estrogen Biosynthesis—Some New Perspectives', *Endocrinology*, 142: 4589-94.
Singhal, H., M. E. Greene, A. L. Zarnke, M. Laine, R. Al Abosy, Y. F. Chang, A. G. Dembo, et al. 2018. 'Progesterone receptor isoforms, agonists and antagonists differentially reprogram estrogen signaling', *Oncotarget*, 9: 4282-300.
Sitruk-Ware, R. 2004. 'Pharmacological profile of progestins', *Maturitas*, 47: 277-83.
Skor, Maxwell N., Erin L. Wonder, Masha Kocherginsky, Anju Goyal, Ben A. Hall, Yi Cai, and Suzanne D. Conzen. 2013. 'Glucocorticoid receptor antagonism as a novel therapy for triple-negative breast cancer', *Clin Cancer Res*, 19: 6163-72.
Slamon, D. J., B. Leyland-Jones, S. Shak, H. Fuchs, V. Paton, A. Bajamonde, T. Fleming, et al. 2001. 'Use of chemotherapy plus a monoclonal antibody against HER2 for metastatic breast cancer that overexpresses HER2', *N Engl J Med*, 344: 783-92.
Slamon, D. J., P. Neven, S. Chia, P. A. Fasching, M. De Laurentiis, S. A. Im, K. Petrakova, et al. 2020. 'Overall Survival with Ribociclib plus Fulvestrant in Advanced Breast Cancer', *N Engl J Med*, 382: 514-24.
Sledge, G. W., Jr., M. Toi, P. Neven, J. Sohn, K. Inoue, X. Pivot, O. Burdaeva, et al. 2020. 'The Effect of Abemaciclib Plus Fulvestrant on Overall Survival in Hormone Receptor-Positive, ERBB2-Negative Breast Cancer That Progressed on Endocrine Therapy-MONARCH 2: A Randomized Clinical Trial', *JAMA Oncol*, 6: 116-24.
Slotta, K., H. Ruschig, and F. Fels. 1934. 'Reindarstellung der Hormone aus dem Corpus luteum', *Ber chem Ges*, 67: 1270-73.
Smith, C. L., Z. Nawaz, and B. W. O'Malley. 1997. 'Coactivator and corepressor regulation of the agonist/antagonist activity of the mixed antiestrogen, 4-hydroxytamoxifen', *Mol Endocrinol*, 11: 657-66.
Smith, Ian, John Robertson, Lucy Kilburn, Maggie Wilcox, Abigail Evans, Chris Holcombe, Kieran Horgan, et al. 2020. 'Long-term outcome and prognostic value of Ki67 after perioperative endocrine therapy in postmenopausal women with hormone-sensitive early breast cancer (POETIC): an open-label, multicentre, parallel-group, randomised, phase 3 trial', *The Lancet Oncology*, 21: 1443-54.
Smyth, L. M., G. Batist, F. Meric-Bernstam, P. Kabos, I. Spanggaard, A. Lluch, K. Jhaveri, et al. 2021. 'Selective AKT kinase inhibitor capivasertib in combination with fulvestrant in PTEN-mutant ER-positive metastatic breast cancer', *NPJ breast cancer*, 7: 44.
Smyth, L. M., K. Tamura, M. Oliveira, E. M. Ciruelos, I. A. Mayer, M. P. Sablin, L. Biganzoli, et al. 2020. 'Capivasertib, an AKT Kinase Inhibitor, as Monotherapy or in Combination with Fulvestrant in Patients with AKT1 (E17K)-Mutant, ER-Positive Metastatic Breast Cancer', *Clin Cancer Res*, 26: 3947-57.
Snyder, Lawrence B., John J. Flanagan, Yimin Qian, Sheryl M. Gough, Monica Andreoli, Mark Bookbinder, Gregory Cadelina, et al. 2021. 'Abstract 44: The discovery of ARV-471, an orally bioavailable estrogen receptor degrading

PROTAC for the treatment of patients with breast cancer', *Cancer Res*, 81: 44-44.
Solano, Maria Emilia, and Petra Clara Arck. 2020. 'Steroids, Pregnancy and Fetal Development', *Frontiers in Immunology*, 10.
Sørlie, T., C. M. Perou, R. Tibshirani, T. Aas, S. Geisler, H. Johnsen, T. Hastie, et al. 2001. 'Gene expression patterns of breast carcinomas distinguish tumor subclasses with clinical implications', *Proc Natl Acad Sci U S A*, 98: 10869-74.
Speirs, V. 2002. 'Oestrogen receptor beta in breast cancer: good, bad or still too early to tell?', *J Pathol*, 197: 143-7.
Spoerke, J. M., S. Gendreau, K. Walter, J. Qiu, T. R. Wilson, H. Savage, J. Aimi, et al. 2016. 'Heterogeneity and clinical significance of ESR1 mutations in ER-positive metastatic breast cancer patients receiving fulvestrant', *Nat Commun*, 7: 11579.
Stampfer, M R, and J C Bartley. 1985. 'Induction of transformation and continuous cell lines from normal human mammary epithelial cells after exposure to benzo[a]pyrene', *Proceedings of the National Academy of Sciences*, 82: 2394-98.
Stanczyk, F. Z., J. P. Hapgood, S. Winer, and D. R. Mishell, Jr. 2013. 'Progestogens used in postmenopausal hormone therapy: differences in their pharmacological properties, intracellular actions, and clinical effects', *Endocr Rev*, 34: 171-208.
Stanczyk, Frank Z. 2003. 'All progestins are not created equal', *Steroids*, 68: 879-90.
Stingl, J., P. Eirew, I. Ricketson, M. Shackleton, F. Vaillant, D. Choi, H. I. Li, and C. J. Eaves. 2006. 'Purification and unique properties of mammary epithelial stem cells', *Nature*, 439: 993-7.
Subramanian, Aravind, Pablo Tamayo, Vamsi K. Mootha, Sayan Mukherjee, Benjamin L. Ebert, Michael A. Gillette, Amanda Paulovich, et al. 2005. 'Gene set enrichment analysis: A knowledge-based approach for interpreting genome-wide expression profiles', *Proceedings of the National Academy of Sciences*, 102: 15545.
Sung, H., J. Ferlay, R. L. Siegel, M. Laversanne, I. Soerjomataram, A. Jemal, and F. Bray. 2021. 'Global Cancer Statistics 2020: GLOBOCAN Estimates of Incidence and Mortality Worldwide for 36 Cancers in 185 Countries', *CA Cancer J Clin*, 71: 209-49.
Surkov, K. G., E. V. Tsyrlina, M. M. Konstantinova, and L. M. Bersteĭn. 1996. '[Neovir, an interferon inductor, modifies expression of steroid hormone receptors in hormone-dependent tissues and restores sensitivity to tamoxifen in patients with inoperable breast cancer]', *Vopr Onkol*, 42: 28-32.
Swain, S. M., D. Miles, S. B. Kim, Y. H. Im, S. A. Im, V. Semiglazov, E. Ciruelos, et al. 2020. 'Pertuzumab, trastuzumab, and docetaxel for HER2-positive metastatic breast cancer (CLEOPATRA): end-of-study results from a double-blind, randomised, placebo-controlled, phase 3 study', *Lancet Oncol*, 21: 519-30.
Takeshita, T., Y. Yamamoto, M. Yamamoto-Ibusuki, T. Inao, A. Sueta, S. Fujiwara, Y. Omoto, and H. Iwase. 2015. 'Droplet digital polymerase chain reaction assay for screening of ESR1 mutations in 325 breast cancer specimens', *Transl Res*, 166: 540-53.e2.
Tan, Si Kee, Zhen Hua Lin, Cheng Wei Chang, Vipin Varang, Kern Rei Chng, You Fu Pan, Eu Leong Yong, Wing Kin Sung, and Edwin Cheung. 2011. 'AP-2γ

regulates oestrogen receptor-mediated long-range chromatin interaction and gene transcription', *The EMBO Journal*, 30: 2569-81.
Tanos, Tamara, George Sflomos, C. Echeverria Pablo, Ayyakkannu Ayyanan, Maria Gutierrez, Jean-Francois Delaloye, Wassim Raffoul, et al. 2013. 'Progesterone/RANKL Is a Major Regulatory Axis in the Human Breast', *Sci Transl Med*, 5: 182ra55-82ra55.
Tecalco-Cruz, A. C., and J. O. Ramírez-Jarquín. 2017. 'Mechanisms that Increase Stability of Estrogen Receptor Alpha in Breast Cancer', *Clin Breast Cancer*, 17: 1-10.
Teulings, F. A., H. A. van Gilse, M. S. Henkelman, H. Portengen, and J. Alexieva-Figusch. 1980. 'Estrogen, androgen, glucocorticoid, and progesterone receptors in progestin-induced regression of human breast cancer', *Cancer Res*, 40: 2557-61.
Theodorou, V., R. Stark, S. Menon, and J. S. Carroll. 2013. 'GATA3 acts upstream of FOXA1 in mediating ESR1 binding by shaping enhancer accessibility', *Genome Res*, 23: 12-22.
Thorat, M. A., and J. Cuzick. 2017. 'Preventing invasive breast cancer using endocrine therapy', *Breast*, 34 Suppl 1: S47-s54.
Toft, D., and J. Gorski. 1966. 'A receptor molecule for estrogens: isolation from the rat uterus and preliminary characterization', *Proceedings of the National Academy of Sciences*, 55: 1574.
Tolaney, Sara, Irfan Cicin, Rafael Betancourt, Arlene Chan, Diego Kaen, Peter Kaufman, Suzette Delaloge, et al. 2021. 'Abstract OT-09-09: AMEERA-3, a phase 2 trial of SAR439859 vs endocrine monotherapy in pre- and post-menopausal, estrogen receptor-positive (ER+)/human epidermal growth factor receptor 2-negative (her2−), locally advanced or metastatic breast cancer (BC) with prior exposure to hormonal therapies', *Cancer Res*, 81: OT-09-09-OT-09-09.
Tomita, S., Z. Zhang, M. Nakano, M. Ibusuki, T. Kawazoe, Y. Yamamoto, and H. Iwase. 2009. 'Estrogen receptor alpha gene ESR1 amplification may predict endocrine therapy responsiveness in breast cancer patients', *Cancer Sci*, 100: 1012-7.
Tosoni, D., P. P. Di Fiore, and S. Pece. 2012. 'Functional purification of human and mouse mammary stem cells', *Methods Mol Biol*, 916: 59-79.
Toy, W., Y. Shen, H. Won, B. Green, R. A. Sakr, M. Will, Z. Li, et al. 2013. 'ESR1 ligand-binding domain mutations in hormone-resistant breast cancer', *Nat Genet*, 45: 1439-45.
Toy, W., H. Weir, P. Razavi, M. Lawson, A. U. Goeppert, A. M. Mazzola, A. Smith, et al. 2017. 'Activating ESR1 Mutations Differentially Affect the Efficacy of ER Antagonists', *Cancer Discov*, 7: 277-87.
Trabert, Britton, Mark E Sherman, Nagarajan Kannan, and Frank Z Stanczyk. 2019. 'Progesterone and Breast Cancer', *Endocr Rev*, 41: 320-44.
Traina, T. A., K. Miller, D. A. Yardley, J. Eakle, L. S. Schwartzberg, J. O'Shaughnessy, W. Gradishar, et al. 2018. 'Enzalutamide for the Treatment of Androgen Receptor-Expressing Triple-Negative Breast Cancer', *J Clin Oncol*, 36: 884-90.
Treeck, Oliver, Claus Lattrich, Anette Springwald, and Olaf Ortmann. 2009. 'Estrogen Receptor beta Exerts Growth-Inhibitory Effects on Human Mammary Epithelial Cells', *Breast cancer research and treatment*, 120: 557-65.

Tripathy, Debu, Seock-Ah Im, Marco Colleoni, Fabio Franke, Aditya Bardia, Nadia Harbeck, Sara A. Hurvitz, et al. 2018. 'Ribociclib plus endocrine therapy for premenopausal women with hormone-receptor-positive, advanced breast cancer (MONALEESA-7): a randomised phase 3 trial', *The Lancet Oncology*, 19: 904-15.

Truong, Thu H, Amy R Dwyer, Caroline H Diep, Hsiangyu Hu, Kyla M Hagen, and Carol A Lange. 2018. 'Phosphorylated Progesterone Receptor Isoforms Mediate Opposing Stem Cell and Proliferative Breast Cancer Cell Fates', *Endocrinology*, 160: 430-46.

Truong, Thu H., and Carol A. Lange. 2018. 'Deciphering Steroid Receptor Crosstalk in Hormone-Driven Cancers', *Endocrinology*, 159: 3897-907.

Tsukamoto, A, R Grosschedl, R Guzman, T Parslow, and H Varmus. 1988. 'Expression of the int-1 gene in transgenic mice is associated with mammary gland hyperplasia and adenocarcinomas in male and female mice', *Cell*, 55: 619-25.

Tung, L., H. Abdel-Hafiz, T. Shen, D. M. Harvell, L. K. Nitao, J. K. Richer, C. A. Sartorius, G. S. Takimoto, and K. B. Horwitz. 2006. 'Progesterone receptors (PR)-B and -A regulate transcription by different mechanisms: AF-3 exerts regulatory control over coactivator binding to PR-B', *Mol Endocrinol*, 20: 2656-70.

Turner, N. C., C. Swift, L. Kilburn, C. Fribbens, M. Beaney, I. Garcia-Murillas, A. U. Budzar, et al. 2020a. 'ESR1 Mutations and Overall Survival on Fulvestrant versus Exemestane in Advanced Hormone Receptor-Positive Breast Cancer: A Combined Analysis of the Phase III SoFEA and EFECT Trials', *Clin Cancer Res*, 26: 5172-77.

Turner, N., S. Howell, K. Jhaveri, H. Gomez, M. Toi, X. Hu, S. Loibl, et al. 2020b. '350TiP A phase III trial of capivasertib and fulvestrant versus placebo and fulvestrant in patients with HR+/HER2− breast cancer (CAPItello-291)', *Annals of Oncology*, 31: S388-S89.

Turner, Nicholas C., Komal L. Jhaveri, Aditya Bardia, Naoki Niikura, Veronique Dieras, Carlos H. Barrios, Seock-Ah Im, et al. 2021. 'persevERA Breast Cancer (BC): Phase III study evaluating the efficacy and safety of giredestrant (GDC-9545) + palbociclib versus letrozole + palbociclib in patients (pts) with estrogen-receptor-positive, HER2-negative locally advanced or metastatic BC (ER+/HER2– LA/mBC)', *Journal of Clinical Oncology*, 39: TPS1103-TPS03.

Turner, Nicholas C., Belinda Kingston, Lucy S. Kilburn, Sarah Kernaghan, Andrew M. Wardley, Iain R. Macpherson, Richard D. Baird, et al. 2020c. 'Circulating tumour DNA analysis to direct therapy in advanced breast cancer (plasmaMATCH): a multicentre, multicohort, phase 2a, platform trial', *The Lancet Oncology*, 21: 1296-308.

Ulrix, W., J. V. Swinnen, W. Heyns, and G. Verhoeven. 1999. 'The differentiation-related gene 1, Drg1, is markedly upregulated by androgens in LNCaP prostatic adenocarcinoma cells', *FEBS Lett*, 455: 23-6.

van Nes, J. G., D. B. Fontein, E. T. Hille, D. W. Voskuil, F. E. van Leeuwen, J. C. de Haes, H. Putter, C. Seynaeve, J. W. Nortier, and C. J. van de Velde. 2012. 'Quality of life in relation to tamoxifen or exemestane treatment in postmenopausal breast cancer patients: a Tamoxifen Exemestane Adjuvant Multinational (TEAM) Trial side study', *Breast Cancer Res Treat*, 134: 267-76.

Verde, G., L. I. De Llobet, R. H. G. Wright, J. Quilez, S. Peiró, F. Le Dily, and M. Beato. 2018. 'Unliganded Progesterone Receptor Governs Estrogen Receptor

Gene Expression by Regulating DNA Methylation in Breast Cancer Cells', *Cancers (Basel)*, 10.
Vignon, F., S. Bardon, D. Chalbos, and H. Rochefort. 1983. 'Antiestrogenic effect of R5020, a synthetic progestin in human breast cancer cells in culture', *J Clin Endocrinol Metab*, 56: 1124-30.
Visakorpi, T., E. Hyytinen, P. Koivisto, M. Tanner, R. Keinänen, C. Palmberg, A. Palotie, T. Tammela, J. Isola, and O. P. Kallioniemi. 1995. 'In vivo amplification of the androgen receptor gene and progression of human prostate cancer', *Nat Genet*, 9: 401-6.
Vogel, Victor G., Joseph P. Costantino, D. Lawrence Wickerham, Walter M. Cronin, Reena S. Cecchini, James N. Atkins, Therese B. Bevers, et al. 2006. 'Effects of Tamoxifen vs Raloxifene on the Risk of Developing Invasive Breast Cancer and Other Disease OutcomesThe NSABP Study of Tamoxifen and Raloxifene (STAR) P-2 Trial', *Jama*, 295: 2727-41.
Vogel, Victor G., Joseph P. Costantino, D. Lawrence Wickerham, Walter M. Cronin, Reena S. Cecchini, James N. Atkins, Therese B. Bevers, et al. 2010. 'Update of the National Surgical Adjuvant Breast and Bowel Project Study of Tamoxifen and Raloxifene (STAR) P-2 Trial: Preventing Breast Cancer', *Cancer Prevention Research*, 3: 696-706.
Voss, Ty C, R. Louis Schiltz, Myong-Hee Sung, Paul M Yen, John A Stamatoyannopoulos, Simon C Biddie, Thomas A Johnson, Tina B Miranda, Sam John, and Gordon L Hager. 2011. 'Dynamic Exchange at Regulatory Elements during Chromatin Remodeling Underlies Assisted Loading Mechanism', *Cell*, 146: 544-54.
Wagenfeld, A., P. T. Saunders, L. Whitaker, and H. O. Critchley. 2016. 'Selective progesterone receptor modulators (SPRMs): progesterone receptor action, mode of action on the endometrium and treatment options in gynecological therapies', *Expert Opin Ther Targets*, 20: 1045-54.
Wakeling, A. E., and J. Bowler. 1988. 'Biology and mode of action of pure antioestrogens', *J Steroid Biochem*, 30: 141-7.
Wakeling, A. E., and J. Bowler. 1992. 'ICI 182,780, a new antioestrogen with clinical potential', *J Steroid Biochem Mol Biol*, 43: 173-7.
Wakeling, A. E., M. Dukes, and J. Bowler. 1991. 'A potent specific pure antiestrogen with clinical potential', *Cancer Res*, 51: 3867-73.
Walker, P., J. E. Germond, M. Brown-Luedi, F. Givel, and W. Wahli. 1984. 'Sequence homologies in the region preceding the transcription initiation site of the liver estrogen-responsive vitellogenin and apo-VLDLII genes', *Nucleic Acids Res*, 12: 8611-26.
Wambach, G., J. R. Higgins, D. C. Kem, and W. Kaufmann. 1979. 'Interaction of synthetic progestagens with renal mineralocorticoid receptors', *Acta Endocrinol (Copenh)*, 92: 560-7.
Wang, P., A. Bahreini, R. Gyanchandani, P. C. Lucas, R. J. Hartmaier, R. J. Watters, A. R. Jonnalagadda, et al. 2016. 'Sensitive Detection of Mono- and Polyclonal ESR1 Mutations in Primary Tumors, Metastatic Lesions, and Cell-Free DNA of Breast Cancer Patients', *Clin Cancer Res*, 22: 1130-7.
Wang, S., L. J. Counterman, and S. Z. Haslam. 1990. 'Progesterone action in normal mouse mammary gland', *Endocrinology*, 127: 2183-9.
Wardell, Suzanne E, Erik R Nelson, Christina A Chao, Holly M Alley, and Donald P McDonnell. 2015. 'Evaluation of the pharmacological activities of RAD1901, a selective estrogen receptor degrader', *Endocrine-related cancer*, 22: 713-24.

Wardell, Suzanne E., Erik R. Nelson, Christina A. Chao, and Donald P. McDonnell. 2013. 'Bazedoxifene Exhibits Antiestrogenic Activity in Animal Models of Tamoxifen-Resistant Breast Cancer: Implications for Treatment of Advanced Disease', *Clinical Cancer Research*, 19: 2420-31.
Watson, P. A., V. K. Arora, and C. L. Sawyers. 2015. 'Emerging mechanisms of resistance to androgen receptor inhibitors in prostate cancer', *Nat Rev Cancer*, 15: 701-11.
Wei, L L, P Hawkins, C Baker, B Norris, P L Sheridan, and P G Quinn. 1996. 'An amino-terminal truncated progesterone receptor isoform, PRc, enhances progestin-induced transcriptional activity', *Molecular Endocrinology*, 10: 1379-87.
Wei, L. L., B. M. Norris, and C. J. Baker. 1997. 'An N-terminally truncated third progesterone receptor protein, PR(C), forms heterodimers with PR(B) but interferes in PR(B)-DNA binding', *J Steroid Biochem Mol Biol*, 62: 287-97.
Wei, Lisa L., Carolina Gonzalez-Aller, William M. Wood, Louise A. Miller, and Kathryn B. Horwitz. 1990. '5′-Heterogeneity in Human Progesterone Receptor Transcripts Predicts a New Amino-Terminal Truncated “C”-Receptor and Unique A-Receptor Messages', *Molecular Endocrinology*, 4: 1833-40.
Weis, K. E., K. Ekena, J. A. Thomas, G. Lazennec, and B. S. Katzenellenbogen. 1996. 'Constitutively active human estrogen receptors containing amino acid substitutions for tyrosine 537 in the receptor protein', *Mol Endocrinol*, 10: 1388-98.
Wellings, S. R., and H. M. Jensen. 1973. 'On the origin and progression of ductal carcinoma in the human breast', *J Natl Cancer Inst*, 50: 1111-8.
Wen, D. X.; Xu, Y. F.; Mais, D. E.: Goldman, M. E., McDonnell, D. P. . 1994. 'The A and B isoforms of the human progesterone receptor operate through distinct signaling pathways within target cells', *Molecular and cellular biology*, 14: 8356-64.
West, Diana C., Deng Pan, Eva Y. Tonsing-Carter, Kyle M. Hernandez, Charles F. Pierce, Sarah C. Styke, Kathleen R. Bowie, Tzintzuni I. Garcia, Masha Kocherginsky, and Suzanne D. Conzen. 2016. 'GR and ER Coactivation Alters the Expression of Differentiation Genes and Associates with Improved ER⁺ Breast Cancer Outcome', *Molecular Cancer Research*, 14: 707-19.
Whitaker, L. H., A. R. Williams, and H. O. Critchley. 2014. 'Selective progesterone receptor modulators', *Curr Opin Obstet Gynecol*, 26: 237-42.
Williams, M. M., N. S. Spoelstra, S. Arnesen, K. I. O'Neill, J. L. Christenson, J. Reese, K. C. Torkko, et al. 2021. 'Steroid Hormone Receptor and Infiltrating Immune Cell Status Reveals Therapeutic Vulnerabilities of ESR1-Mutant Breast Cancer', *Cancer Res*, 81: 732-46.
Wintersteiner, O., and W.M. Allen. 1934. 'Crystalline progestin', *J Biol Chem*, 107: 321-36.
Wolf, I. M., M. D. Heitzer, M. Grubisha, and D. B. DeFranco. 2008. 'Coactivators and nuclear receptor transactivation', *J Cell Biochem*, 104: 1580-6.
Wood, C. E., T. C. Register, C. J. Lees, H. Chen, S. Kimrey, and J. M. Cline. 2007. 'Effects of estradiol with micronized progesterone or medroxyprogesterone acetate on risk markers for breast cancer in postmenopausal monkeys', *Breast Cancer Res Treat*, 101: 125-34.
Yang, Chuanwei, Sally Trent, Viviana Ionescu-Tiba, Lan Lan, Toshi Shioda, Dennis Sgroi, and Emmett V. Schmidt. 2006. 'Identification of Cyclin D1– and

Estrogen-Regulated Genes Contributing to Breast Carcinogenesis and Progression', *Cancer Res*, 66: 11649-58.
Yang, X., D. L. Phillips, A. T. Ferguson, W. G. Nelson, J. G. Herman, and N. E. Davidson. 2001. 'Synergistic activation of functional estrogen receptor (ER)-alpha by DNA methyltransferase and histone deacetylase inhibition in human ER-alpha-negative breast cancer cells', *Cancer Res*, 61: 7025-9.
Yardley, D. A., L. Blakely, B. Hemphill, M. Joseph, W. Liggett, B. Daniel, A. Castrellon, et al. 2017. 'Abstract P4-22-09: A phase 2 open label study of everolimus in combination with endocrine therapy in resistant hormone receptor-positive HER2-negative advanced breast cancer', *Cancer Res*, 77: P4-22-09-P4-22-09.
Yardley, D. A., R. R. Ismail-Khan, B. Melichar, M. Lichinitser, P. N. Munster, P. M. Klein, S. Cruickshank, K. D. Miller, M. J. Lee, and J. B. Trepel. 2013. 'Randomized phase II, double-blind, placebo-controlled study of exemestane with or without entinostat in postmenopausal women with locally recurrent or metastatic estrogen receptor-positive breast cancer progressing on treatment with a nonsteroidal aromatase inhibitor', *J Clin Oncol*, 31: 2128-35.
Yoshida, T., H. Eguchi, K. Nakachi, K. Tanimoto, Y. Higashi, K. Suemasu, Y. Iino, Y. Morishita, and S. Hayashi. 2000. 'Distinct mechanisms of loss of estrogen receptor alpha gene expression in human breast cancer: methylation of the gene and alteration of trans-acting factors', *Carcinogenesis*, 21: 2193-201.
Yu, L., L. Wang, C. Mao, D. Duraki, J. E. Kim, R. Huang, W. G. Helferich, E. R. Nelson, B. H. Park, and D. J. Shapiro. 2019. 'Estrogen-independent Myc overexpression confers endocrine therapy resistance on breast cancer cells expressing ERαY537S and ERαD538G mutations', *Cancer Lett*, 442: 373-82.
Yu, S., T. Kim, K. H. Yoo, and K. Kang. 2017. 'The T47D cell line is an ideal experimental model to elucidate the progesterone-specific effects of a luminal A subtype of breast cancer', *Biochem Biophys Res Commun*, 486: 752-58.
Yung, Rachel L., and Nancy E. Davidson. 2021. 'Optimal adjuvant endocrine therapy for breast cancer', *The Lancet Oncology*, 22: 1357-58.
Zaurin, R., R. Ferrari, A. S. Nacht, J. Carbonell, F. Le Dily, J. Font-Mateu, L. I. de Llobet Cucalon, et al. 2021. 'A set of accessible enhancers enables the initial response of breast cancer cells to physiological progestin concentrations', *Nucleic Acids Res*, 49: 12716-31.
Zhan, T., N. Rindtorff, and M. Boutros. 2017. 'Wnt signaling in cancer', *Oncogene*, 36: 1461-73.
Zhang, Junhui, Francis T. F. Tsai, and David S. Geller. 2006. 'Differential interaction of RU486 with the progesterone and glucocorticoid receptors', *Journal of Molecular Endocrinology*, 37: 163-73.
Zhang, Q. X., A. Borg, D. M. Wolf, S. Oesterreich, and S. A. Fuqua. 1997. 'An estrogen receptor mutant with strong hormone-independent activity from a metastatic breast cancer', *Cancer Res*, 57: 1244-9.
Zhao, Changqing, Akiko Koide, Judith Abrams, Sarah Deighton-Collins, Angela Martinez, Janice A. Schwartz, Shohei Koide, and Debra F. Skafar. 2003. 'Mutation of Leu-536 in Human Estrogen Receptor-α Alters the Coupling between Ligand Binding, Transcription Activation, and Receptor Conformation *', *Journal of Biological Chemistry*, 278: 27278-86.

Appendix

Appendix I – Generation of Y537S knock-in mutation in T47D-Y537S cells

The parental T47D-WT line was transfected with three components: (1) A U6 promoter-driven plasmid expression vector encoding an sgRNA for CRISPR058819 (CRISPR19), which was the single guide RNA (sgRNA) targeting ESR1 exon 8 that was used by Harrod et al. 2017 to generate the MCF7-Y537S cells, (2) a human codon-optimized Cas9 endonuclease and (3) the previously used HDR donor plasmid which encodes the Y537S mutation together with additional silent tracking mutations at L536 (CTG>CTC) that can differentiate targeted from endogenously occurring *ESR1* exon 8 mutations (Martin et al 2017) and silent mutations in the CRISPR19 recognition site, which destroy the CRISPR19 homology and are adjacent to the PAM sequence. These mutations also allowed for the successful integration of the targeting plasmid to be confirmed using a knock-in specific PCR assay, in which a reverse primer was designed to hybridise to the introduced silent changes in the CRISPR19 target sequence, so that it would not amplify the equivalent WT ER sequence. Further confirmation of the successful integration of the targeting plasmid was performed through sequencing of the knock-in specific PCR products, which span across the 5' HDR integration boundary.

The T47D-Y537S cell population was then enriched through subdividing them into smaller pools. This resulted in 2 limited pools enriched for targeted cells. Further genomic DNA (gDNA) sequencing confirmed that the Y537S mutation and CRISPR19 point mutations were present in both pools but limited pool 2 also had additional mutations around the CRISPR19 recognition site. The cells from limited pool 1 were therefore cultured in E2-depleted media as a means of positively selecting them (after

the MCF7-Y537S cells were reported to be E2-independent by Harrod et al. 2017). Dilution culturing was used to generate clones. 20 clones were picked and seeded but only 1 of these showed continued growth. Using gDNA derived from these cells, PCR was performed using forward and reverse *ESR1* exon 8 primers as well as an *ESR1* exon 8 CRISPR19 knock-in specific primer. Sequencing of the resultant product confirmed presence of the Y537S mutation, the silent L536 mutation and the CRISPR19 mutations. Both WT and Y537S sequences were evident in this sequencing, suggesting that the T47D-Y537S line is heterozygous for the Y537S mutation. Further mutations around the CRISPR19 targeting sequence were also noted however, suggesting the presence of insertion-deletion (indel), likely on an additional, third, allele. Analysis of sequencing of cDNA prepared from T47D-Y537S cells supported the conclusion that a third, deletion-derived frameshift allele was present. In keeping with this, *ESR1* exon 8 PCR revealed a smaller PCR product (truncated by 89bp) as well as a PCR product of the expected size. Therefore, it was concluded that the T47D-Y537S line has one *ESR1* Y537S mutant allele, one WT allele and one deletion-derived allele resulting from the erroneous non-homologous DNA end joining pathway. This work was performed by Miss Paula Jiminez and Professor Laki Buluwela.

Appendix II – RNA-seq sample read counts and alignment (%) to reference genome (hg38)

T47D-WT Full Media Replicate 1

23804045 reads; of these:
  23804045 (100.00%) were paired; of these:
    3748874 (15.75%) aligned concordantly 0 times
    18697403 (78.55%) aligned concordantly exactly 1 time
    1357768 (5.70%) aligned concordantly >1 times

    3748874 pairs aligned concordantly 0 times; of these:
      535770 (14.29%) aligned discordantly 1 time

    3213104 pairs aligned 0 times concordantly or discordantly; of these:
      6426208 mates make up the pairs; of these:
        3721506 (57.91%) aligned 0 times
        2424806 (37.73%) aligned exactly 1 time
        279896 (4.36%) aligned >1 times
92.18% overall alignment rate

T47D-WT Full Media Replicate 2

23518621 reads; of these:
  23518621 (100.00%) were paired; of these:
    3534103 (15.03%) aligned concordantly 0 times
    18671080 (79.39%) aligned concordantly exactly 1 time
    1313438 (5.58%) aligned concordantly >1 times

    3534103 pairs aligned concordantly 0 times; of these:
      473506 (13.40%) aligned discordantly 1 time

    3060597 pairs aligned 0 times concordantly or discordantly; of these:
      6121194 mates make up the pairs; of these:
        3663999 (59.86%) aligned 0 times
        2210635 (36.11%) aligned exactly 1 time
        246560 (4.03%) aligned >1 times
92.21% overall alignment rate

T47D-WT Full Media Replicate 3

23496840 reads; of these:
  23496840 (100.00%) were paired; of these:
    3394050 (14.44%) aligned concordantly 0 times
    18737675 (79.75%) aligned concordantly exactly 1 time
    1365115 (5.81%) aligned concordantly >1 times

    3394050 pairs aligned concordantly 0 times; of these:
      415260 (12.23%) aligned discordantly 1 time

    2978790 pairs aligned 0 times concordantly or discordantly; of these:
      5957580 mates make up the pairs; of these:
        3638115 (61.07%) aligned 0 times
        2084653 (34.99%) aligned exactly 1 time
        234812 (3.94%) aligned >1 times
92.26% overall alignment rate

T47D-WT Full Media Replicate 4

24032359 reads; of these:
  24032359 (100.00%) were paired; of these:
    3511109 (14.61%) aligned concordantly 0 times
    19035585 (79.21%) aligned concordantly exactly 1 time
    1485665 (6.18%) aligned concordantly >1 times

    3511109 pairs aligned concordantly 0 times; of these:
      432748 (12.33%) aligned discordantly 1 time

    3078361 pairs aligned 0 times concordantly or discordantly; of these:
      6156722 mates make up the pairs; of these:
        3772823 (61.28%) aligned 0 times
        2122602 (34.48%) aligned exactly 1 time
        261297 (4.24%) aligned >1 times
92.15% overall alignment rate

T47D-WT Full Media Replicate 5

23826804 reads; of these:
  23826804 (100.00%) were paired; of these:
    3791261 (15.91%) aligned concordantly 0 times
    18642970 (78.24%) aligned concordantly exactly 1 time
    1392573 (5.84%) aligned concordantly >1 times

    3791261 pairs aligned concordantly 0 times; of these:
      446199 (11.77%) aligned discordantly 1 time

    3345062 pairs aligned 0 times concordantly or discordantly; of these:
      6690124 mates make up the pairs; of these:
        4082009 (61.02%) aligned 0 times
        2336420 (34.92%) aligned exactly 1 time
        271695 (4.06%) aligned >1 times
91.43% overall alignment rate

T47D-WT Full Media Replicate 6

23423258 reads; of these:
  23423258 (100.00%) were paired; of these:
    3361063 (14.35%) aligned concordantly 0 times
    18688102 (79.78%) aligned concordantly exactly 1 time
    1374093 (5.87%) aligned concordantly >1 times

    3361063 pairs aligned concordantly 0 times; of these:
      439095 (13.06%) aligned discordantly 1 time

    2921968 pairs aligned 0 times concordantly or discordantly; of these:
      5843936 mates make up the pairs; of these:
        3525334 (60.32%) aligned 0 times
        2074592 (35.50%) aligned exactly 1 time
        244010 (4.18%) aligned >1 times
92.47% overall alignment rate

T47D-Y537S Full Media Replicate 1

24062307 reads; of these:
  24062307 (100.00%) were paired; of these:
    3597328 (14.95%) aligned concordantly 0 times
    19045287 (79.15%) aligned concordantly exactly 1 time
    1419692 (5.90%) aligned concordantly >1 times

    3597328 pairs aligned concordantly 0 times; of these:
      465042 (12.93%) aligned discordantly 1 time

    3132286 pairs aligned 0 times concordantly or discordantly; of these:
      6264572 mates make up the pairs; of these:
        3786966 (60.45%) aligned 0 times
        2215208 (35.36%) aligned exactly 1 time
        262398 (4.19%) aligned >1 times
92.13% overall alignment rate

T47D-Y537S Full Media Replicate 2

23779718 reads; of these:
  23779718 (100.00%) were paired; of these:
    3436766 (14.45%) aligned concordantly 0 times
    18931709 (79.61%) aligned concordantly exactly 1 time
    1411243 (5.93%) aligned concordantly >1 times

    3436766 pairs aligned concordantly 0 times; of these:
      432287 (12.58%) aligned discordantly 1 time

    3004479 pairs aligned 0 times concordantly or discordantly; of these:
      6008958 mates make up the pairs; of these:
        3579399 (59.57%) aligned 0 times
        2176404 (36.22%) aligned exactly 1 time
        253155 (4.21%) aligned >1 times
92.47% overall alignment rate

T47D-Y537S Full Media Replicate 3

23457127 reads; of these:
  23457127 (100.00%) were paired; of these:
    3662979 (15.62%) aligned concordantly 0 times
    18436777 (78.60%) aligned concordantly exactly 1 time
    1357371 (5.79%) aligned concordantly >1 times

    3662979 pairs aligned concordantly 0 times; of these:
      485302 (13.25%) aligned discordantly 1 time

    3177677 pairs aligned 0 times concordantly or discordantly; of these:
      6355354 mates make up the pairs; of these:
        3772564 (59.36%) aligned 0 times
        2313576 (36.40%) aligned exactly 1 time
        269214 (4.24%) aligned >1 times
91.96% overall alignment rate

T47D-Y537S Full Media Replicate 4

23789568 reads; of these:
  23789568 (100.00%) were paired; of these:
    3821182 (16.06%) aligned concordantly 0 times
    18617627 (78.26%) aligned concordantly exactly 1 time
    1350759 (5.68%) aligned concordantly >1 times

    3821182 pairs aligned concordantly 0 times; of these:
      493977 (12.93%) aligned discordantly 1 time

    3327205 pairs aligned 0 times concordantly or discordantly; of these:
      6654410 mates make up the pairs; of these:
        3990246 (59.96%) aligned 0 times
        2389105 (35.90%) aligned exactly 1 time
        275059 (4.13%) aligned >1 times
91.61% overall alignment rate

T47D-Y537S Full Media Replicate 5

24079275 reads; of these:
  24079275 (100.00%) were paired; of these:
    3868570 (16.07%) aligned concordantly 0 times
    18857385 (78.31%) aligned concordantly exactly 1 time
    1353320 (5.62%) aligned concordantly >1 times

    3868570 pairs aligned concordantly 0 times; of these:
      526575 (13.61%) aligned discordantly 1 time

    3341995 pairs aligned 0 times concordantly or discordantly; of these:
      6683990 mates make up the pairs; of these:
        3940704 (58.96%) aligned 0 times
        2458622 (36.78%) aligned exactly 1 time
        284664 (4.26%) aligned >1 times
91.82% overall alignment rate

T47D-Y537S Full Media Replicate 6

24105621 reads; of these:
  24105621 (100.00%) were paired; of these:
    3713162 (15.40%) aligned concordantly 0 times
    19034600 (78.96%) aligned concordantly exactly 1 time
    1357859 (5.63%) aligned concordantly >1 times

    3713162 pairs aligned concordantly 0 times; of these:
      489315 (13.18%) aligned discordantly 1 time

    3223847 pairs aligned 0 times concordantly or discordantly; of these:
      6447694 mates make up the pairs; of these:
        3835921 (59.49%) aligned 0 times
        2341730 (36.32%) aligned exactly 1 time
        270043 (4.19%) aligned >1 times
92.04% overall alignment rate

T47D-WT Vehicle (8 hours) Replicate 1

23807893 reads; of these:
  23807893 (100.00%) were paired; of these:
    3957299 (16.62%) aligned concordantly 0 times
    18489855 (77.66%) aligned concordantly exactly 1 time
    1360739 (5.72%) aligned concordantly >1 times

    3957299 pairs aligned concordantly 0 times; of these:
      414059 (10.46%) aligned discordantly 1 time

    3543240 pairs aligned 0 times concordantly or discordantly; of these:
      7086480 mates make up the pairs; of these:
        4536504 (64.02%) aligned 0 times
        2291044 (32.33%) aligned exactly 1 time
        258932 (3.65%) aligned >1 times
90.47% overall alignment rate

T47D-WT Vehicle (8 hours) Replicate 2

24046193 reads; of these:
  24046193 (100.00%) were paired; of these:
    3654584 (15.20%) aligned concordantly 0 times
    18967650 (78.88%) aligned concordantly exactly 1 time
    1423959 (5.92%) aligned concordantly >1 times

    3654584 pairs aligned concordantly 0 times; of these:
      497990 (13.63%) aligned discordantly 1 time

    3156594 pairs aligned 0 times concordantly or discordantly; of these:
      6313188 mates make up the pairs; of these:
        3769548 (59.71%) aligned 0 times
        2265776 (35.89%) aligned exactly 1 time
        277864 (4.40%) aligned >1 times
92.16% overall alignment rate

T47D-WT Vehicle (8 hours) Replicate 3

23952459 reads; of these:
  23952459 (100.00%) were paired; of these:
    3679712 (15.36%) aligned concordantly 0 times
    18876893 (78.81%) aligned concordantly exactly 1 time
    1395854 (5.83%) aligned concordantly >1 times

    3679712 pairs aligned concordantly 0 times; of these:
      517231 (14.06%) aligned discordantly 1 time

    3162481 pairs aligned 0 times concordantly or discordantly; of these:
      6324962 mates make up the pairs; of these:
        3744286 (59.20%) aligned 0 times
        2305244 (36.45%) aligned exactly 1 time
        275432 (4.35%) aligned >1 times
92.18% overall alignment rate

T47D-WT Vehicle (8 hours) Replicate 4

23602193 reads; of these:
  23602193 (100.00%) were paired; of these:
    3352103 (14.20%) aligned concordantly 0 times
    18885092 (80.01%) aligned concordantly exactly 1 time
    1364998 (5.78%) aligned concordantly >1 times

    3352103 pairs aligned concordantly 0 times; of these:
      445024 (13.28%) aligned discordantly 1 time

    2907079 pairs aligned 0 times concordantly or discordantly; of these:
      5814158 mates make up the pairs; of these:
        3472216 (59.72%) aligned 0 times
        2100057 (36.12%) aligned exactly 1 time
        241885 (4.16%) aligned >1 times
92.64% overall alignment rate

T47D-WT Vehicle (8 hours) Replicate 5

23640312 reads; of these:
  23640312 (100.00%) were paired; of these:
    3714431 (15.71%) aligned concordantly 0 times
    18558365 (78.50%) aligned concordantly exactly 1 time
    1367516 (5.78%) aligned concordantly >1 times

    3714431 pairs aligned concordantly 0 times; of these:
      506240 (13.63%) aligned discordantly 1 time

    3208191 pairs aligned 0 times concordantly or discordantly; of these:
      6416382 mates make up the pairs; of these:
        3785711 (59.00%) aligned 0 times
        2354829 (36.70%) aligned exactly 1 time
        275842 (4.30%) aligned >1 times
91.99% overall alignment rate

T47D-WT Vehicle (8 hours) Replicate 6

24052007 reads; of these:
  24052007 (100.00%) were paired; of these:
    3774214 (15.69%) aligned concordantly 0 times
    18835923 (78.31%) aligned concordantly exactly 1 time
    1441870 (5.99%) aligned concordantly >1 times

    3774214 pairs aligned concordantly 0 times; of these:
      528439 (14.00%) aligned discordantly 1 time

    3245775 pairs aligned 0 times concordantly or discordantly; of these:
      6491550 mates make up the pairs; of these:
        3852385 (59.34%) aligned 0 times
        2351860 (36.23%) aligned exactly 1 time
        287305 (4.43%) aligned >1 times
91.99% overall alignment rate

T47D-WT 10nM E2 (8 hours) Replicate 1

23613464 reads; of these:
  23613464 (100.00%) were paired; of these:
    3420087 (14.48%) aligned concordantly 0 times
    18871582 (79.92%) aligned concordantly exactly 1 time
    1321795 (5.60%) aligned concordantly >1 times

    3420087 pairs aligned concordantly 0 times; of these:
      450769 (13.18%) aligned discordantly 1 time

    2969318 pairs aligned 0 times concordantly or discordantly; of these:
      5938636 mates make up the pairs; of these:
        3552087 (59.81%) aligned 0 times
        2148737 (36.18%) aligned exactly 1 time
        237812 (4.00%) aligned >1 times

T47D-WT 10nM E2 (8 hours) Replicate 2

23666942 reads; of these:
  23666942 (100.00%) were paired; of these:
    3496866 (14.78%) aligned concordantly 0 times
    18795383 (79.42%) aligned concordantly exactly 1 time
    1374693 (5.81%) aligned concordantly >1 times

    3496866 pairs aligned concordantly 0 times; of these:
      506368 (14.48%) aligned discordantly 1 time

    2990498 pairs aligned 0 times concordantly or discordantly; of these:
      5980996 mates make up the pairs; of these:
        3541554 (59.21%) aligned 0 times
        2181853 (36.48%) aligned exactly 1 time
        257589 (4.31%) aligned >1 times
92.52% overall alignment rate

T47D-WT 10nM E2 (8 hours) Replicate 3

23989052 reads; of these:
  23989052 (100.00%) were paired; of these:
    3662272 (15.27%) aligned concordantly 0 times
    18955846 (79.02%) aligned concordantly exactly 1 time
    1370934 (5.71%) aligned concordantly >1 times

    3662272 pairs aligned concordantly 0 times; of these:
      510619 (13.94%) aligned discordantly 1 time

    3151653 pairs aligned 0 times concordantly or discordantly; of these:
      6303306 mates make up the pairs; of these:
        3752934 (59.54%) aligned 0 times
        2284302 (36.24%) aligned exactly 1 time
        266070 (4.22%) aligned >1 times
92.18% overall alignment rate

T47D-WT 10nM E2 (8 hours) Replicate 4

23984024 reads; of these:
  23984024 (100.00%) were paired; of these:
    3843161 (16.02%) aligned concordantly 0 times
    18778448 (78.30%) aligned concordantly exactly 1 time
    1362415 (5.68%) aligned concordantly >1 times

    3843161 pairs aligned concordantly 0 times; of these:
      556556 (14.48%) aligned discordantly 1 time

    3286605 pairs aligned 0 times concordantly or discordantly; of these:
      6573210 mates make up the pairs; of these:
        3886571 (59.13%) aligned 0 times
        2396793 (36.46%) aligned exactly 1 time
        289846 (4.41%) aligned >1 times
91.90% overall alignment rate

T47D-WT 10nM E2 (8 hours) Replicate 5

23664300 reads; of these:
  23664300 (100.00%) were paired; of these:
    3801581 (16.06%) aligned concordantly 0 times
    18507793 (78.21%) aligned concordantly exactly 1 time
    1354926 (5.73%) aligned concordantly >1 times

    3801581 pairs aligned concordantly 0 times; of these:
      566905 (14.91%) aligned discordantly 1 time

    3234676 pairs aligned 0 times concordantly or discordantly; of these:
      6469352 mates make up the pairs; of these:
        3756008 (58.06%) aligned 0 times
        2423869 (37.47%) aligned exactly 1 time
        289475 (4.47%) aligned >1 times
92.06% overall alignment rate

T47D-WT 10nM E2 (8 hours) Replicate 6

23845650 reads; of these:
  23845650 (100.00%) were paired; of these:
    3639303 (15.26%) aligned concordantly 0 times
    18716149 (78.49%) aligned concordantly exactly 1 time
    1490198 (6.25%) aligned concordantly >1 times

    3639303 pairs aligned concordantly 0 times; of these:
      492892 (13.54%) aligned discordantly 1 time

    3146411 pairs aligned 0 times concordantly or discordantly; of these:
      6292822 mates make up the pairs; of these:
        3697054 (58.75%) aligned 0 times
        2296957 (36.50%) aligned exactly 1 time
        298811 (4.75%) aligned >1 times
92.25% overall alignment rate

T47D-Y537S Vehicle (8 hours) Replicate 1

24004614 reads; of these:
  24004614 (100.00%) were paired; of these:
    3691702 (15.38%) aligned concordantly 0 times
    18916127 (78.80%) aligned concordantly exactly 1 time
    1396785 (5.82%) aligned concordantly >1 times

    3691702 pairs aligned concordantly 0 times; of these:
      541621 (14.67%) aligned discordantly 1 time

    3150081 pairs aligned 0 times concordantly or discordantly; of these:
      6300162 mates make up the pairs; of these:
        3610867 (57.31%) aligned 0 times
        2395808 (38.03%) aligned exactly 1 time
        293487 (4.66%) aligned >1 times
92.48% overall alignment rate

T47D-Y537S Vehicle (8 hours) Replicate 2

24092885 reads; of these:
  24092885 (100.00%) were paired; of these:
    3649759 (15.15%) aligned concordantly 0 times
    19034687 (79.01%) aligned concordantly exactly 1 time
    1408439 (5.85%) aligned concordantly >1 times

    3649759 pairs aligned concordantly 0 times; of these:
      543446 (14.89%) aligned discordantly 1 time

    3106313 pairs aligned 0 times concordantly or discordantly; of these:
      6212626 mates make up the pairs; of these:
        3532368 (56.86%) aligned 0 times
        2387901 (38.44%) aligned exactly 1 time
        292357 (4.71%) aligned >1 times
92.67% overall alignment rate

T47D-Y537S Vehicle (8 hours) Replicate 3

24007932 reads; of these:
  24007932 (100.00%) were paired; of these:
    3513473 (14.63%) aligned concordantly 0 times
    19057691 (79.38%) aligned concordantly exactly 1 time
    1436768 (5.98%) aligned concordantly >1 times

    3513473 pairs aligned concordantly 0 times; of these:
      491186 (13.98%) aligned discordantly 1 time

    3022287 pairs aligned 0 times concordantly or discordantly; of these:
      6044574 mates make up the pairs; of these:
        3500129 (57.91%) aligned 0 times
        2263425 (37.45%) aligned exactly 1 time
        281020 (4.65%) aligned >1 times
92.71% overall alignment rate

T47D-Y537S Vehicle (8 hours) Replicate 4

23421223 reads; of these:
  23421223 (100.00%) were paired; of these:
    3299278 (14.09%) aligned concordantly 0 times
    18737994 (80.00%) aligned concordantly exactly 1 time
    1383951 (5.91%) aligned concordantly >1 times

    3299278 pairs aligned concordantly 0 times; of these:
      490532 (14.87%) aligned discordantly 1 time

    2808746 pairs aligned 0 times concordantly or discordantly; of these:
      5617492 mates make up the pairs; of these:
        3228480 (57.47%) aligned 0 times
        2128137 (37.88%) aligned exactly 1 time
        260875 (4.64%) aligned >1 times
93.11% overall alignment rate

T47D-Y537S Vehicle (8 hours) Replicate 5

23880012 reads; of these:
  23880012 (100.00%) were paired; of these:
    3667060 (15.36%) aligned concordantly 0 times
    18706157 (78.33%) aligned concordantly exactly 1 time
    1506795 (6.31%) aligned concordantly >1 times

    3667060 pairs aligned concordantly 0 times; of these:
      436905 (11.91%) aligned discordantly 1 time

    3230155 pairs aligned 0 times concordantly or discordantly; of these:
      6460310 mates make up the pairs; of these:
        4021996 (62.26%) aligned 0 times
        2160938 (33.45%) aligned exactly 1 time
        277376 (4.29%) aligned >1 times
91.58% overall alignment rate

T47D-Y537S Vehicle (8 hours) Replicate 6

23969652 reads; of these:
  23969652 (100.00%) were paired; of these:
    3353160 (13.99%) aligned concordantly 0 times
    19207808 (80.13%) aligned concordantly exactly 1 time
    1408684 (5.88%) aligned concordantly >1 times

    3353160 pairs aligned concordantly 0 times; of these:
      380599 (11.35%) aligned discordantly 1 time

    2972561 pairs aligned 0 times concordantly or discordantly; of these:
      5945122 mates make up the pairs; of these:
        3682202 (61.94%) aligned 0 times
        2029558 (34.14%) aligned exactly 1 time
        233362 (3.93%) aligned >1 times
92.32% overall alignment rate

T47D-Y537S 10nM E2 (8 hours) Replicate 1

23598915 reads; of these:
  23598915 (100.00%) were paired; of these:
    3385933 (14.35%) aligned concordantly 0 times
    18849215 (79.87%) aligned concordantly exactly 1 time
    1363767 (5.78%) aligned concordantly >1 times

    3385933 pairs aligned concordantly 0 times; of these:
      521203 (15.39%) aligned discordantly 1 time

    2864730 pairs aligned 0 times concordantly or discordantly; of these:
      5729460 mates make up the pairs; of these:
        3271291 (57.10%) aligned 0 times
        2194742 (38.31%) aligned exactly 1 time
        263427 (4.60%) aligned >1 times
93.07% overall alignment rate

T47D-Y537S 10nM E2 (8 hours) Replicate 2

23585267 reads; of these:
  23585267 (100.00%) were paired; of these:
    3204100 (13.59%) aligned concordantly 0 times
    19028659 (80.68%) aligned concordantly exactly 1 time
    1352508 (5.73%) aligned concordantly >1 times

    3204100 pairs aligned concordantly 0 times; of these:
      462917 (14.45%) aligned discordantly 1 time

    2741183 pairs aligned 0 times concordantly or discordantly; of these:
      5482366 mates make up the pairs; of these:
        3137675 (57.23%) aligned 0 times
        2104455 (38.39%) aligned exactly 1 time
        240236 (4.38%) aligned >1 times
93.35% overall alignment rate

T47D-Y537S 10nM E2 (8 hours) Replicate 3

23797833 reads; of these:
  23797833 (100.00%) were paired; of these:
    3203269 (13.46%) aligned concordantly 0 times
    19206933 (80.71%) aligned concordantly exactly 1 time
    1387631 (5.83%) aligned concordantly >1 times

    3203269 pairs aligned concordantly 0 times; of these:
      480684 (15.01%) aligned discordantly 1 time

    2722585 pairs aligned 0 times concordantly or discordantly; of these:
      5445170 mates make up the pairs; of these:
        3103508 (57.00%) aligned 0 times
        2095142 (38.48%) aligned exactly 1 time
        246520 (4.53%) aligned >1 times
93.48% overall alignment rate

T47D-Y537S 10nM E2 (8 hours) Replicate 4

23806250 reads; of these:
  23806250 (100.00%) were paired; of these:
    3311147 (13.91%) aligned concordantly 0 times
    19101718 (80.24%) aligned concordantly exactly 1 time
    1393385 (5.85%) aligned concordantly >1 times

    3311147 pairs aligned concordantly 0 times; of these:
      502248 (15.17%) aligned discordantly 1 time

    2808899 pairs aligned 0 times concordantly or discordantly; of these:
      5617798 mates make up the pairs; of these:
        3170062 (56.43%) aligned 0 times
        2186191 (38.92%) aligned exactly 1 time
        261545 (4.66%) aligned >1 times
93.34% overall alignment rate

T47D-Y537S 10nM E2 (8 hours) Replicate 5

24000486 reads; of these:
  24000486 (100.00%) were paired; of these:
    3036888 (12.65%) aligned concordantly 0 times
    19519408 (81.33%) aligned concordantly exactly 1 time
    1444190 (6.02%) aligned concordantly >1 times

    3036888 pairs aligned concordantly 0 times; of these:
      429132 (14.13%) aligned discordantly 1 time

    2607756 pairs aligned 0 times concordantly or discordantly; of these:
      5215512 mates make up the pairs; of these:
        2928822 (56.16%) aligned 0 times
        2048753 (39.28%) aligned exactly 1 time
        237937 (4.56%) aligned >1 times
93.90% overall alignment rate

T47D-Y537S 10nM E2 (8 hours) Replicate 6

23387831 reads; of these:
  23387831 (100.00%) were paired; of these:
    3530067 (15.09%) aligned concordantly 0 times
    18448946 (78.88%) aligned concordantly exactly 1 time
    1408818 (6.02%) aligned concordantly >1 times

    3530067 pairs aligned concordantly 0 times; of these:
      471454 (13.36%) aligned discordantly 1 time

    3058613 pairs aligned 0 times concordantly or discordantly; of these:
      6117226 mates make up the pairs; of these:
        3545221 (57.95%) aligned 0 times
        2287190 (37.39%) aligned exactly 1 time
        284815 (4.66%) aligned >1 times
92.42% overall alignment rate

T47D-WT Vehicle (16 hours) Replicate 1

22423800 reads; of these:
  22423800 (100.00%) were paired; of these:
    3032894 (13.53%) aligned concordantly 0 times
    18200667 (81.17%) aligned concordantly exactly 1 time
    1190239 (5.31%) aligned concordantly >1 times

    3032894 pairs aligned concordantly 0 times; of these:
      373938 (12.33%) aligned discordantly 1 time

    2658956 pairs aligned 0 times concordantly or discordantly; of these:
      5317912 mates make up the pairs; of these:
        3203647 (60.24%) aligned 0 times
        1917240 (36.05%) aligned exactly 1 time
        197025 (3.70%) aligned >1 times
92.86% overall alignment rate

T47D-WT Vehicle (16 hours) Replicate 2

22024185 reads; of these:
  22024185 (100.00%) were paired; of these:
    2383056 (10.82%) aligned concordantly 0 times
    18448162 (83.76%) aligned concordantly exactly 1 time
    1192967 (5.42%) aligned concordantly >1 times

    2383056 pairs aligned concordantly 0 times; of these:
      274527 (11.52%) aligned discordantly 1 time

    2108529 pairs aligned 0 times concordantly or discordantly; of these:
      4217058 mates make up the pairs; of these:
        2531655 (60.03%) aligned 0 times
        1530216 (36.29%) aligned exactly 1 time
        155187 (3.68%) aligned >1 times
94.25% overall alignment rate

T47D-WT Vehicle (16 hours) Replicate 3

22256803 reads; of these:
  22256803 (100.00%) were paired; of these:
    2766769 (12.43%) aligned concordantly 0 times
    18309080 (82.26%) aligned concordantly exactly 1 time
    1180954 (5.31%) aligned concordantly >1 times

    2766769 pairs aligned concordantly 0 times; of these:
      357382 (12.92%) aligned discordantly 1 time

    2409387 pairs aligned 0 times concordantly or discordantly; of these:
      4818774 mates make up the pairs; of these:
        2852533 (59.20%) aligned 0 times
        1781790 (36.98%) aligned exactly 1 time
        184451 (3.83%) aligned >1 times
93.59% overall alignment rate

T47D-WT Vehicle (16 hours) Replicate 4

21965889 reads; of these:
  21965889 (100.00%) were paired; of these:
    2931465 (13.35%) aligned concordantly 0 times
    17868020 (81.34%) aligned concordantly exactly 1 time
    1166404 (5.31%) aligned concordantly >1 times

    2931465 pairs aligned concordantly 0 times; of these:
      408236 (13.93%) aligned discordantly 1 time

    2523229 pairs aligned 0 times concordantly or discordantly; of these:
      5046458 mates make up the pairs; of these:
        3002619 (59.50%) aligned 0 times
        1849530 (36.65%) aligned exactly 1 time
        194309 (3.85%) aligned >1 times
93.17% overall alignment rate

T47D-WT Vehicle (16 hours) Replicate 5

22181080 reads; of these:
  22181080 (100.00%) were paired; of these:
    3117424 (14.05%) aligned concordantly 0 times
    18084341 (81.53%) aligned concordantly exactly 1 time
    979315 (4.42%) aligned concordantly >1 times

    3117424 pairs aligned concordantly 0 times; of these:
      423517 (13.59%) aligned discordantly 1 time

    2693907 pairs aligned 0 times concordantly or discordantly; of these:
      5387814 mates make up the pairs; of these:
        3241075 (60.16%) aligned 0 times
        1910822 (35.47%) aligned exactly 1 time
        235917 (4.38%) aligned >1 times
92.69% overall alignment rate

T47D-WT Vehicle (16 hours) Replicate 6

22325795 reads; of these:
  22325795 (100.00%) were paired; of these:
    2982675 (13.36%) aligned concordantly 0 times
    18335496 (82.13%) aligned concordantly exactly 1 time
    1007624 (4.51%) aligned concordantly >1 times

    2982675 pairs aligned concordantly 0 times; of these:
      364379 (12.22%) aligned discordantly 1 time

    2618296 pairs aligned 0 times concordantly or discordantly; of these:
      5236592 mates make up the pairs; of these:
        3149697 (60.15%) aligned 0 times
        1854352 (35.41%) aligned exactly 1 time
        232543 (4.44%) aligned >1 times
92.95% overall alignment rate

T47D-WT 10nM E2 (16 hours) Replicate 1

22053756 reads; of these:
  22053756 (100.00%) were paired; of these:
    2940718 (13.33%) aligned concordantly 0 times
    17947092 (81.38%) aligned concordantly exactly 1 time
    1165946 (5.29%) aligned concordantly >1 times

    2940718 pairs aligned concordantly 0 times; of these:
      439229 (14.94%) aligned discordantly 1 time

    2501489 pairs aligned 0 times concordantly or discordantly; of these:
      5002978 mates make up the pairs; of these:
        2858300 (57.13%) aligned 0 times
        1939855 (38.77%) aligned exactly 1 time
        204823 (4.09%) aligned >1 times
93.52% overall alignment rate

T47D-WT 10nM E2 (16 hours) Replicate 2

22325220 reads; of these:
  22325220 (100.00%) were paired; of these:
    2767698 (12.40%) aligned concordantly 0 times
    18369856 (82.28%) aligned concordantly exactly 1 time
    1187666 (5.32%) aligned concordantly >1 times

    2767698 pairs aligned concordantly 0 times; of these:
      390238 (14.10%) aligned discordantly 1 time

    2377460 pairs aligned 0 times concordantly or discordantly; of these:
      4754920 mates make up the pairs; of these:
        2746027 (57.75%) aligned 0 times
        1817197 (38.22%) aligned exactly 1 time
        191696 (4.03%) aligned >1 times
93.85% overall alignment rate

T47D-WT 10nM E2 (16 hours) Replicate 3

22375192 reads; of these:
  22375192 (100.00%) were paired; of these:
    2744851 (12.27%) aligned concordantly 0 times
    18414793 (82.30%) aligned concordantly exactly 1 time
    1215548 (5.43%) aligned concordantly >1 times

    2744851 pairs aligned concordantly 0 times; of these:
      362806 (13.22%) aligned discordantly 1 time

    2382045 pairs aligned 0 times concordantly or discordantly; of these:
      4764090 mates make up the pairs; of these:
        2787269 (58.51%) aligned 0 times
        1789536 (37.56%) aligned exactly 1 time
        187285 (3.93%) aligned >1 times
93.77% overall alignment rate

T47D-WT 10nM E2 (16 hours) Replicate 4

22280333 reads; of these:
  22280333 (100.00%) were paired; of these:
    2695885 (12.10%) aligned concordantly 0 times
    18342714 (82.33%) aligned concordantly exactly 1 time
    1241734 (5.57%) aligned concordantly >1 times

    2695885 pairs aligned concordantly 0 times; of these:
      377110 (13.99%) aligned discordantly 1 time

    2318775 pairs aligned 0 times concordantly or discordantly; of these:
      4637550 mates make up the pairs; of these:
        2756458 (59.44%) aligned 0 times
        1698853 (36.63%) aligned exactly 1 time
        182239 (3.93%) aligned >1 times
93.81% overall alignment rate

T47D-WT 10nM E2 (16 hours) Replicate 5

21733718 reads; of these:
  21733718 (100.00%) were paired; of these:
    2617467 (12.04%) aligned concordantly 0 times
    17938630 (82.54%) aligned concordantly exactly 1 time
    1177621 (5.42%) aligned concordantly >1 times

    2617467 pairs aligned concordantly 0 times; of these:
      381957 (14.59%) aligned discordantly 1 time

    2235510 pairs aligned 0 times concordantly or discordantly; of these:
      4471020 mates make up the pairs; of these:
        2560690 (57.27%) aligned 0 times
        1725024 (38.58%) aligned exactly 1 time
        185306 (4.14%) aligned >1 times
94.11% overall alignment rate

T47D-WT 10nM E2 (16 hours) Replicate 6

22114080 reads; of these:
  22114080 (100.00%) were paired; of these:
    2786432 (12.60%) aligned concordantly 0 times
    18127343 (81.97%) aligned concordantly exactly 1 time
    1200305 (5.43%) aligned concordantly >1 times

    2786432 pairs aligned concordantly 0 times; of these:
      378167 (13.57%) aligned discordantly 1 time

    2408265 pairs aligned 0 times concordantly or discordantly; of these:
      4816530 mates make up the pairs; of these:
        2812239 (58.39%) aligned 0 times
        1812442 (37.63%) aligned exactly 1 time
        191849 (3.98%) aligned >1 times
93.64% overall alignment rate

T47D-WT 1nM P4 Replicate 4

22407094 reads; of these:
  22407094 (100.00%) were paired; of these:
    2755884 (12.30%) aligned concordantly 0 times
    18429372 (82.25%) aligned concordantly exactly 1 time
    1221838 (5.45%) aligned concordantly >1 times

    2755884 pairs aligned concordantly 0 times; of these:
      321898 (11.68%) aligned discordantly 1 time

    2433986 pairs aligned 0 times concordantly or discordantly; of these:
      4867972 mates make up the pairs; of these:
        2951705 (60.64%) aligned 0 times
        1736645 (35.67%) aligned exactly 1 time
        179622 (3.69%) aligned >1 times
93.41% overall alignment rate

T47D-WT 1nM P4 Replicate 5

22396665 reads; of these:
  22396665 (100.00%) were paired; of these:
    2885796 (12.88%) aligned concordantly 0 times
    18307134 (81.74%) aligned concordantly exactly 1 time
    1203735 (5.37%) aligned concordantly >1 times

    2885796 pairs aligned concordantly 0 times; of these:
      361354 (12.52%) aligned discordantly 1 time

    2524442 pairs aligned 0 times concordantly or discordantly; of these:
      5048884 mates make up the pairs; of these:
        3021814 (59.85%) aligned 0 times
        1834839 (36.34%) aligned exactly 1 time
        192231 (3.81%) aligned >1 times
93.25% overall alignment rate

T47D-WT 1nM P4 Replicate 6

22244466 reads; of these:
  22244466 (100.00%) were paired; of these:
    3049931 (13.71%) aligned concordantly 0 times
    18008945 (80.96%) aligned concordantly exactly 1 time
    1185590 (5.33%) aligned concordantly >1 times

    3049931 pairs aligned concordantly 0 times; of these:
      360727 (11.83%) aligned discordantly 1 time

    2689204 pairs aligned 0 times concordantly or discordantly; of these:
      5378408 mates make up the pairs; of these:
        3247064 (60.37%) aligned 0 times
        1932355 (35.93%) aligned exactly 1 time
        198989 (3.70%) aligned >1 times
92.70% overall alignment rate

T47D-WT 1nM R5020 Replicate 1

22266010 reads; of these:
  22266010 (100.00%) were paired; of these:
    2968316 (13.33%) aligned concordantly 0 times
    18112244 (81.34%) aligned concordantly exactly 1 time
    1185450 (5.32%) aligned concordantly >1 times

    2968316 pairs aligned concordantly 0 times; of these:
      377719 (12.73%) aligned discordantly 1 time

    2590597 pairs aligned 0 times concordantly or discordantly; of these:
      5181194 mates make up the pairs; of these:
        3095968 (59.75%) aligned 0 times
        1888288 (36.45%) aligned exactly 1 time
        196938 (3.80%) aligned >1 times
93.05% overall alignment rate

T47D-WT 1nM R5020 Replicate 2

22034078 reads; of these:
  22034078 (100.00%) were paired; of these:
    2880726 (13.07%) aligned concordantly 0 times
    17993091 (81.66%) aligned concordantly exactly 1 time
    1160261 (5.27%) aligned concordantly >1 times

    2880726 pairs aligned concordantly 0 times; of these:
      404037 (14.03%) aligned discordantly 1 time

    2476689 pairs aligned 0 times concordantly or discordantly; of these:
      4953378 mates make up the pairs; of these:
        2960927 (59.78%) aligned 0 times
        1801411 (36.37%) aligned exactly 1 time
        191040 (3.86%) aligned >1 times
93.28% overall alignment rate

T47D-WT 1nM R5020 Replicate 3

22370104 reads; of these:
  22370104 (100.00%) were paired; of these:
    2839247 (12.69%) aligned concordantly 0 times
    18318676 (81.89%) aligned concordantly exactly 1 time
    1212181 (5.42%) aligned concordantly >1 times

    2839247 pairs aligned concordantly 0 times; of these:
      326934 (11.51%) aligned discordantly 1 time

    2512313 pairs aligned 0 times concordantly or discordantly; of these:
      5024626 mates make up the pairs; of these:
        3055406 (60.81%) aligned 0 times
        1785045 (35.53%) aligned exactly 1 time
        184175 (3.67%) aligned >1 times
93.17% overall alignment rate

T47D-WT 1nM R5020 Replicate 4

20177301 reads; of these:
  20177301 (100.00%) were paired; of these:
    2552292 (12.65%) aligned concordantly 0 times
    16558123 (82.06%) aligned concordantly exactly 1 time
    1066886 (5.29%) aligned concordantly >1 times

    2552292 pairs aligned concordantly 0 times; of these:
      342657 (13.43%) aligned discordantly 1 time

    2209635 pairs aligned 0 times concordantly or discordantly; of these:
      4419270 mates make up the pairs; of these:
        2651534 (60.00%) aligned 0 times
        1602055 (36.25%) aligned exactly 1 time
        165681 (3.75%) aligned >1 times
93.43% overall alignment rate

T47D-WT 1nM R5020 Replicate 5

22340630 reads; of these:
  22340630 (100.00%) were paired; of these:
    3007174 (13.46%) aligned concordantly 0 times
    18162569 (81.30%) aligned concordantly exactly 1 time
    1170887 (5.24%) aligned concordantly >1 times

    3007174 pairs aligned concordantly 0 times; of these:
      413019 (13.73%) aligned discordantly 1 time

    2594155 pairs aligned 0 times concordantly or discordantly; of these:
      5188310 mates make up the pairs; of these:
        3039506 (58.58%) aligned 0 times
        1946310 (37.51%) aligned exactly 1 time
        202494 (3.90%) aligned >1 times
93.20% overall alignment rate

T47D-WT 1nM R5020 Replicate 6

22430614 reads; of these:
  22430614 (100.00%) were paired; of these:
    3051606 (13.60%) aligned concordantly 0 times
    18192502 (81.11%) aligned concordantly exactly 1 time
    1186506 (5.29%) aligned concordantly >1 times

    3051606 pairs aligned concordantly 0 times; of these:
      435595 (14.27%) aligned discordantly 1 time

    2616011 pairs aligned 0 times concordantly or discordantly; of these:
      5232022 mates make up the pairs; of these:
        3048092 (58.26%) aligned 0 times
        1973164 (37.71%) aligned exactly 1 time
        210766 (4.03%) aligned >1 times
93.21% overall alignment rate

T47D-WT (1nM P4+10nM E2) Replicate 1

21712713 reads; of these:
  21712713 (100.00%) were paired; of these:
    2873509 (13.23%) aligned concordantly 0 times
    17700864 (81.52%) aligned concordantly exactly 1 time
    1138340 (5.24%) aligned concordantly >1 times

    2873509 pairs aligned concordantly 0 times; of these:
      428573 (14.91%) aligned discordantly 1 time

    2444936 pairs aligned 0 times concordantly or discordantly; of these:
      4889872 mates make up the pairs; of these:
        2802919 (57.32%) aligned 0 times
        1887532 (38.60%) aligned exactly 1 time
        199421 (4.08%) aligned >1 times
93.55% overall alignment rate

T47D-WT (1nM P4+10nM E2) Replicate 2

22305046 reads; of these:
  22305046 (100.00%) were paired; of these:
    2924408 (13.11%) aligned concordantly 0 times
    18189551 (81.55%) aligned concordantly exactly 1 time
    1191087 (5.34%) aligned concordantly >1 times

    2924408 pairs aligned concordantly 0 times; of these:
      406687 (13.91%) aligned discordantly 1 time

    2517721 pairs aligned 0 times concordantly or discordantly; of these:
      5035442 mates make up the pairs; of these:
        2938106 (58.35%) aligned 0 times
        1898010 (37.69%) aligned exactly 1 time
        199326 (3.96%) aligned >1 times
93.41% overall alignment rate

T47D-WT (1nM P4+10nM E2) Replicate 3

22196871 reads; of these:
  22196871 (100.00%) were paired; of these:
    2855284 (12.86%) aligned concordantly 0 times
    18148052 (81.76%) aligned concordantly exactly 1 time
    1193535 (5.38%) aligned concordantly >1 times

    2855284 pairs aligned concordantly 0 times; of these:
      391626 (13.72%) aligned discordantly 1 time

    2463658 pairs aligned 0 times concordantly or discordantly; of these:
      4927316 mates make up the pairs; of these:
        2881697 (58.48%) aligned 0 times
        1852458 (37.60%) aligned exactly 1 time
        193161 (3.92%) aligned >1 times
93.51% overall alignment rate

T47D-WT (1nM P4+10nM E2) Replicate 4

22428198 reads; of these:
  22428198 (100.00%) were paired; of these:
    2846734 (12.69%) aligned concordantly 0 times
    18376384 (81.93%) aligned concordantly exactly 1 time
    1205080 (5.37%) aligned concordantly >1 times

    2846734 pairs aligned concordantly 0 times; of these:
      370967 (13.03%) aligned discordantly 1 time

    2475767 pairs aligned 0 times concordantly or discordantly; of these:
      4951534 mates make up the pairs; of these:
        2905476 (58.68%) aligned 0 times
        1853366 (37.43%) aligned exactly 1 time
        192692 (3.89%) aligned >1 times
93.52% overall alignment rate

T47D-WT (1nM P4+10nM E2) Replicate 5

22381692 reads; of these:
  22381692 (100.00%) were paired; of these:
    2795953 (12.49%) aligned concordantly 0 times
    18372168 (82.09%) aligned concordantly exactly 1 time
    1213571 (5.42%) aligned concordantly >1 times

    2795953 pairs aligned concordantly 0 times; of these:
      376318 (13.46%) aligned discordantly 1 time

    2419635 pairs aligned 0 times concordantly or discordantly; of these:
      4839270 mates make up the pairs; of these:
        2836202 (58.61%) aligned 0 times
        1812347 (37.45%) aligned exactly 1 time
        190721 (3.94%) aligned >1 times
93.66% overall alignment rate

T47D-WT (1nM P4+10nM E2) Replicate 6

22134050 reads; of these:
  22134050 (100.00%) were paired; of these:
    2808030 (12.69%) aligned concordantly 0 times
    18136890 (81.94%) aligned concordantly exactly 1 time
    1189130 (5.37%) aligned concordantly >1 times

    2808030 pairs aligned concordantly 0 times; of these:
      374770 (13.35%) aligned discordantly 1 time

    2433260 pairs aligned 0 times concordantly or discordantly; of these:
      4866520 mates make up the pairs; of these:
        2867419 (58.92%) aligned 0 times
        1810278 (37.20%) aligned exactly 1 time
        188823 (3.88%) aligned >1 times
93.52% overall alignment rate

T47D-WT (1nM R5020+10nM E2) Replicate 1

21908554 reads; of these:
  21908554 (100.00%) were paired; of these:
    2811293 (12.83%) aligned concordantly 0 times
    17916732 (81.78%) aligned concordantly exactly 1 time
    1180529 (5.39%) aligned concordantly >1 times

    2811293 pairs aligned concordantly 0 times; of these:
      378191 (13.45%) aligned discordantly 1 time

    2433102 pairs aligned 0 times concordantly or discordantly; of these:
      4866204 mates make up the pairs; of these:
        2899845 (59.59%) aligned 0 times
        1779444 (36.57%) aligned exactly 1 time
        186915 (3.84%) aligned >1 times
93.38% overall alignment rate

T47D-WT (1nM R5020+10nM E2) Replicate 2

22358013 reads; of these:
  22358013 (100.00%) were paired; of these:
    2867022 (12.82%) aligned concordantly 0 times
    18291058 (81.81%) aligned concordantly exactly 1 time
    1199933 (5.37%) aligned concordantly >1 times

    2867022 pairs aligned concordantly 0 times; of these:
      377299 (13.16%) aligned discordantly 1 time

    2489723 pairs aligned 0 times concordantly or discordantly; of these:
      4979446 mates make up the pairs; of these:
        2918028 (58.60%) aligned 0 times
        1867100 (37.50%) aligned exactly 1 time
        194318 (3.90%) aligned >1 times
93.47% overall alignment rate

T47D-WT (1nM R5020+10nM E2) Replicate 3

22296949 reads; of these:
  22296949 (100.00%) were paired; of these:
    2794310 (12.53%) aligned concordantly 0 times
    18310825 (82.12%) aligned concordantly exactly 1 time
    1191814 (5.35%) aligned concordantly >1 times

    2794310 pairs aligned concordantly 0 times; of these:
      372921 (13.35%) aligned discordantly 1 time

    2421389 pairs aligned 0 times concordantly or discordantly; of these:
      4842778 mates make up the pairs; of these:
        2831558 (58.47%) aligned 0 times
        1823882 (37.66%) aligned exactly 1 time
        187338 (3.87%) aligned >1 times
93.65% overall alignment rate

T47D-WT (1nM R5020+10nM E2) Replicate 4

21940731 reads; of these:
  21940731 (100.00%) were paired; of these:
    2863850 (13.05%) aligned concordantly 0 times
    17907122 (81.62%) aligned concordantly exactly 1 time
    1169759 (5.33%) aligned concordantly >1 times

    2863850 pairs aligned concordantly 0 times; of these:
      365093 (12.75%) aligned discordantly 1 time

    2498757 pairs aligned 0 times concordantly or discordantly; of these:
      4997514 mates make up the pairs; of these:
        2937634 (58.78%) aligned 0 times
        1870805 (37.43%) aligned exactly 1 time
        189075 (3.78%) aligned >1 times
93.31% overall alignment rate

T47D-WT (1nM R5020+10nM E2) Replicate 5

22279331 reads; of these:
  22279331 (100.00%) were paired; of these:
    2966908 (13.32%) aligned concordantly 0 times
    18132476 (81.39%) aligned concordantly exactly 1 time
    1179947 (5.30%) aligned concordantly >1 times

    2966908 pairs aligned concordantly 0 times; of these:
      440246 (14.84%) aligned discordantly 1 time

    2526662 pairs aligned 0 times concordantly or discordantly; of these:
      5053324 mates make up the pairs; of these:
        2881082 (57.01%) aligned 0 times
        1966742 (38.92%) aligned exactly 1 time
        205500 (4.07%) aligned >1 times
93.53% overall alignment rate

T47D-WT (1nM R5020+10nM E2) Replicate 6

22366310 reads; of these:
  22366310 (100.00%) were paired; of these:
    2863893 (12.80%) aligned concordantly 0 times
    18280715 (81.73%) aligned concordantly exactly 1 time
    1221702 (5.46%) aligned concordantly >1 times

    2863893 pairs aligned concordantly 0 times; of these:
      367785 (12.84%) aligned discordantly 1 time

    2496108 pairs aligned 0 times concordantly or discordantly; of these:
      4992216 mates make up the pairs; of these:
        2949472 (59.08%) aligned 0 times
        1849010 (37.04%) aligned exactly 1 time
        193734 (3.88%) aligned >1 times
93.41% overall alignment rate

T47D-Y537S Vehicle (16 hours) Replicate 1

22128626 reads; of these:
  22128626 (100.00%) were paired; of these:
    2784450 (12.58%) aligned concordantly 0 times
    18132095 (81.94%) aligned concordantly exactly 1 time
    1212081 (5.48%) aligned concordantly >1 times

    2784450 pairs aligned concordantly 0 times; of these:
      361753 (12.99%) aligned discordantly 1 time

    2422697 pairs aligned 0 times concordantly or discordantly; of these:
      4845394 mates make up the pairs; of these:
        2846385 (58.74%) aligned 0 times
        1807141 (37.30%) aligned exactly 1 time
        191868 (3.96%) aligned >1 times
93.57% overall alignment rate

T47D-Y537S Vehicle (16 hours) Replicate 2

22308519 reads; of these:
  22308519 (100.00%) were paired; of these:
    2745731 (12.31%) aligned concordantly 0 times
    18326381 (82.15%) aligned concordantly exactly 1 time
    1236407 (5.54%) aligned concordantly >1 times

    2745731 pairs aligned concordantly 0 times; of these:
      346449 (12.62%) aligned discordantly 1 time

    2399282 pairs aligned 0 times concordantly or discordantly; of these:
      4798564 mates make up the pairs; of these:
        2789833 (58.14%) aligned 0 times
        1817004 (37.87%) aligned exactly 1 time
        191727 (4.00%) aligned >1 times
93.75% overall alignment rate

T47D-Y537S Vehicle (16 hours) Replicate 3

22277147 reads; of these:
  22277147 (100.00%) were paired; of these:
    2674132 (12.00%) aligned concordantly 0 times
    18377651 (82.50%) aligned concordantly exactly 1 time
    1225364 (5.50%) aligned concordantly >1 times

    2674132 pairs aligned concordantly 0 times; of these:
      362203 (13.54%) aligned discordantly 1 time

    2311929 pairs aligned 0 times concordantly or discordantly; of these:
      4623858 mates make up the pairs; of these:
        2640461 (57.11%) aligned 0 times
        1791633 (38.75%) aligned exactly 1 time
        191764 (4.15%) aligned >1 times
94.07% overall alignment rate

T47D-Y537S Vehicle (16 hours) Replicate 4

22184719 reads; of these:
  22184719 (100.00%) were paired; of these:
    2840809 (12.81%) aligned concordantly 0 times
    18122842 (81.69%) aligned concordantly exactly 1 time
    1221068 (5.50%) aligned concordantly >1 times

    2840809 pairs aligned concordantly 0 times; of these:
      383692 (13.51%) aligned discordantly 1 time

    2457117 pairs aligned 0 times concordantly or discordantly; of these:
      4914234 mates make up the pairs; of these:
        2809774 (57.18%) aligned 0 times
        1900924 (38.68%) aligned exactly 1 time
        203536 (4.14%) aligned >1 times
93.67% overall alignment rate

T47D-Y537S Vehicle (16 hours) Replicate 5

22443709 reads; of these:
  22443709 (100.00%) were paired; of these:
    2663072 (11.87%) aligned concordantly 0 times
    18540392 (82.61%) aligned concordantly exactly 1 time
    1240245 (5.53%) aligned concordantly >1 times

    2663072 pairs aligned concordantly 0 times; of these:
      367249 (13.79%) aligned discordantly 1 time

    2295823 pairs aligned 0 times concordantly or discordantly; of these:
      4591646 mates make up the pairs; of these:
        2596065 (56.54%) aligned 0 times
        1801523 (39.23%) aligned exactly 1 time
        194058 (4.23%) aligned >1 times
94.22% overall alignment rate

T47D-Y537S Vehicle (16 hours) Replicate 6

22445042 reads; of these:
  22445042 (100.00%) were paired; of these:
    2712250 (12.08%) aligned concordantly 0 times
    18488891 (82.37%) aligned concordantly exactly 1 time
    1243901 (5.54%) aligned concordantly >1 times

    2712250 pairs aligned concordantly 0 times; of these:
      353690 (13.04%) aligned discordantly 1 time

    2358560 pairs aligned 0 times concordantly or discordantly; of these:
      4717120 mates make up the pairs; of these:
        2707022 (57.39%) aligned 0 times
        1816484 (38.51%) aligned exactly 1 time
        193614 (4.10%) aligned >1 times
93.97% overall alignment rate

T47D-Y537S 10nM E2 (16 hours) Replicate 1

22453824 reads; of these:
  22453824 (100.00%) were paired; of these:
    2679510 (11.93%) aligned concordantly 0 times
    18539621 (82.57%) aligned concordantly exactly 1 time
    1234693 (5.50%) aligned concordantly >1 times

    2679510 pairs aligned concordantly 0 times; of these:
      403426 (15.06%) aligned discordantly 1 time

    2276084 pairs aligned 0 times concordantly or discordantly; of these:
      4552168 mates make up the pairs; of these:
        2539920 (55.80%) aligned 0 times
        1812332 (39.81%) aligned exactly 1 time
        199916 (4.39%) aligned >1 times
94.34% overall alignment rate

T47D-Y537S 10nM E2 (16 hours) Replicate 2

22241226 reads; of these:
  22241226 (100.00%) were paired; of these:
    2686658 (12.08%) aligned concordantly 0 times
    18327390 (82.40%) aligned concordantly exactly 1 time
    1227178 (5.52%) aligned concordantly >1 times

    2686658 pairs aligned concordantly 0 times; of these:
      376593 (14.02%) aligned discordantly 1 time

    2310065 pairs aligned 0 times concordantly or discordantly; of these:
      4620130 mates make up the pairs; of these:
        2618809 (56.68%) aligned 0 times
        1804844 (39.06%) aligned exactly 1 time
        196477 (4.25%) aligned >1 times
94.11% overall alignment rate

T47D-Y537S 10nM E2 (16 hours) Replicate 3

22153058 reads; of these:
  22153058 (100.00%) were paired; of these:
    2638520 (11.91%) aligned concordantly 0 times
    18289217 (82.56%) aligned concordantly exactly 1 time
    1225321 (5.53%) aligned concordantly >1 times

    2638520 pairs aligned concordantly 0 times; of these:
      383154 (14.52%) aligned discordantly 1 time

    2255366 pairs aligned 0 times concordantly or discordantly; of these:
      4510732 mates make up the pairs; of these:
        2560415 (56.76%) aligned 0 times
        1757194 (38.96%) aligned exactly 1 time
        193123 (4.28%) aligned >1 times
94.22% overall alignment rate

T47D-Y537S 10nM E2 (16 hours) Replicate 4

21731354 reads; of these:
  21731354 (100.00%) were paired; of these:
    2694918 (12.40%) aligned concordantly 0 times
    17841002 (82.10%) aligned concordantly exactly 1 time
    1195434 (5.50%) aligned concordantly >1 times

    2694918 pairs aligned concordantly 0 times; of these:
      368008 (13.66%) aligned discordantly 1 time

    2326910 pairs aligned 0 times concordantly or discordantly; of these:
      4653820 mates make up the pairs; of these:
        2640236 (56.73%) aligned 0 times
        1816657 (39.04%) aligned exactly 1 time
        196927 (4.23%) aligned >1 times
93.93% overall alignment rate

T47D-Y537S 10nM E2 (16 hours) Replicate 5

22335475 reads; of these:
  22335475 (100.00%) were paired; of these:
    2812248 (12.59%) aligned concordantly 0 times
    18292925 (81.90%) aligned concordantly exactly 1 time
    1230302 (5.51%) aligned concordantly >1 times

    2812248 pairs aligned concordantly 0 times; of these:
      375297 (13.35%) aligned discordantly 1 time

    2436951 pairs aligned 0 times concordantly or discordantly; of these:
      4873902 mates make up the pairs; of these:
        2754734 (56.52%) aligned 0 times
        1913716 (39.26%) aligned exactly 1 time
        205452 (4.22%) aligned >1 times
93.83% overall alignment rate

T47D-Y537S 10nM E2 (16 hours) Replicate 6

21984570 reads; of these:
  21984570 (100.00%) were paired; of these:
    2682169 (12.20%) aligned concordantly 0 times
    18062630 (82.16%) aligned concordantly exactly 1 time
    1239771 (5.64%) aligned concordantly >1 times

    2682169 pairs aligned concordantly 0 times; of these:
      398190 (14.85%) aligned discordantly 1 time

    2283979 pairs aligned 0 times concordantly or discordantly; of these:
      4567958 mates make up the pairs; of these:
        2619034 (57.33%) aligned 0 times
        1751704 (38.35%) aligned exactly 1 time
        197220 (4.32%) aligned >1 times
94.04% overall alignment rate

T47D-Y537S 1nM P4 Replicate 1

22444187 reads; of these:
  22444187 (100.00%) were paired; of these:
    2681772 (11.95%) aligned concordantly 0 times
    18525673 (82.54%) aligned concordantly exactly 1 time
    1236742 (5.51%) aligned concordantly >1 times

    2681772 pairs aligned concordantly 0 times; of these:
      321994 (12.01%) aligned discordantly 1 time

    2359778 pairs aligned 0 times concordantly or discordantly; of these:
      4719556 mates make up the pairs; of these:
        2758129 (58.44%) aligned 0 times
        1776090 (37.63%) aligned exactly 1 time
        185337 (3.93%) aligned >1 times
93.86% overall alignment rate

T47D-Y537S 1nM P4 Replicate 2

21976529 reads; of these:
  21976529 (100.00%) were paired; of these:
    2660871 (12.11%) aligned concordantly 0 times
    18115445 (82.43%) aligned concordantly exactly 1 time
    1200213 (5.46%) aligned concordantly >1 times

    2660871 pairs aligned concordantly 0 times; of these:
      380247 (14.29%) aligned discordantly 1 time

    2280624 pairs aligned 0 times concordantly or discordantly; of these:
      4561248 mates make up the pairs; of these:
        2634717 (57.76%) aligned 0 times
        1737510 (38.09%) aligned exactly 1 time
        189021 (4.14%) aligned >1 times
94.01% overall alignment rate

T47D-Y537S 1nM P4 Replicate 3

21852812 reads; of these:
  21852812 (100.00%) were paired; of these:
    2601286 (11.90%) aligned concordantly 0 times
    18057222 (82.63%) aligned concordantly exactly 1 time
    1194304 (5.47%) aligned concordantly >1 times

    2601286 pairs aligned concordantly 0 times; of these:
      363580 (13.98%) aligned discordantly 1 time

    2237706 pairs aligned 0 times concordantly or discordantly; of these:
      4475412 mates make up the pairs; of these:
        2530754 (56.55%) aligned 0 times
        1755893 (39.23%) aligned exactly 1 time
        188765 (4.22%) aligned >1 times
94.21% overall alignment rate

T47D-Y537S 1nM P4 Replicate 4

21785467 reads; of these:
  21785467 (100.00%) were paired; of these:
    2796654 (12.84%) aligned concordantly 0 times
    17782439 (81.63%) aligned concordantly exactly 1 time
    1206374 (5.54%) aligned concordantly >1 times

    2796654 pairs aligned concordantly 0 times; of these:
      371400 (13.28%) aligned discordantly 1 time

    2425254 pairs aligned 0 times concordantly or discordantly; of these:
      4850508 mates make up the pairs; of these:
        2773770 (57.19%) aligned 0 times
        1874605 (38.65%) aligned exactly 1 time
        202133 (4.17%) aligned >1 times
93.63% overall alignment rate

T47D-Y537S 1nM P4 Replicate 5

22129681 reads; of these:
  22129681 (100.00%) were paired; of these:
    2758932 (12.47%) aligned concordantly 0 times
    18164436 (82.08%) aligned concordantly exactly 1 time
    1206313 (5.45%) aligned concordantly >1 times

    2758932 pairs aligned concordantly 0 times; of these:
      384282 (13.93%) aligned discordantly 1 time

    2374650 pairs aligned 0 times concordantly or discordantly; of these:
      4749300 mates make up the pairs; of these:
        2718042 (57.23%) aligned 0 times
        1832856 (38.59%) aligned exactly 1 time
        198402 (4.18%) aligned >1 times
93.86% overall alignment rate

T47D-Y537S 1nM P4 Replicate 6

21834004 reads; of these:
  21834004 (100.00%) were paired; of these:
    2641069 (12.10%) aligned concordantly 0 times
    17984872 (82.37%) aligned concordantly exactly 1 time
    1208063 (5.53%) aligned concordantly >1 times

    2641069 pairs aligned concordantly 0 times; of these:
      327071 (12.38%) aligned discordantly 1 time

    2313998 pairs aligned 0 times concordantly or discordantly; of these:
      4627996 mates make up the pairs; of these:
        2678058 (57.87%) aligned 0 times
        1765054 (38.14%) aligned exactly 1 time
        184884 (3.99%) aligned >1 times
93.87% overall alignment rate

T47D-Y537S 1nM R5020 Replicate 1

22445449 reads; of these:
  22445449 (100.00%) were paired; of these:
    2766709 (12.33%) aligned concordantly 0 times
    18444078 (82.17%) aligned concordantly exactly 1 time
    1234662 (5.50%) aligned concordantly >1 times

    2766709 pairs aligned concordantly 0 times; of these:
      369748 (13.36%) aligned discordantly 1 time

    2396961 pairs aligned 0 times concordantly or discordantly; of these:
      4793922 mates make up the pairs; of these:
        2747339 (57.31%) aligned 0 times
        1847940 (38.55%) aligned exactly 1 time
        198643 (4.14%) aligned >1 times
93.88% overall alignment rate

T47D-Y537S 1nM R5020 Replicate 2

22256893 reads; of these:
  22256893 (100.00%) were paired; of these:
    2885297 (12.96%) aligned concordantly 0 times
    18167890 (81.63%) aligned concordantly exactly 1 time
    1203706 (5.41%) aligned concordantly >1 times

    2885297 pairs aligned concordantly 0 times; of these:
      401756 (13.92%) aligned discordantly 1 time

    2483541 pairs aligned 0 times concordantly or discordantly; of these:
      4967082 mates make up the pairs; of these:
        2806665 (56.51%) aligned 0 times
        1951532 (39.29%) aligned exactly 1 time
        208885 (4.21%) aligned >1 times
93.69% overall alignment rate

T47D-Y537S 1nM R5020 Replicate 3

22433653 reads; of these:
  22433653 (100.00%) were paired; of these:
    2840794 (12.66%) aligned concordantly 0 times
    18355970 (81.82%) aligned concordantly exactly 1 time
    1236889 (5.51%) aligned concordantly >1 times

    2840794 pairs aligned concordantly 0 times; of these:
      357878 (12.60%) aligned discordantly 1 time

    2482916 pairs aligned 0 times concordantly or discordantly; of these:
      4965832 mates make up the pairs; of these:
        2865015 (57.69%) aligned 0 times
        1898540 (38.23%) aligned exactly 1 time
        202277 (4.07%) aligned >1 times
93.61% overall alignment rate

T47D-Y537S 1nM R5020 Replicate 4

22369812 reads; of these:
  22369812 (100.00%) were paired; of these:
    2626194 (11.74%) aligned concordantly 0 times
    18513309 (82.76%) aligned concordantly exactly 1 time
    1230309 (5.50%) aligned concordantly >1 times

    2626194 pairs aligned concordantly 0 times; of these:
      338701 (12.90%) aligned discordantly 1 time

    2287493 pairs aligned 0 times concordantly or discordantly; of these:
      4574986 mates make up the pairs; of these:
        2645100 (57.82%) aligned 0 times
        1743695 (38.11%) aligned exactly 1 time
        186191 (4.07%) aligned >1 times
94.09% overall alignment rate

T47D-Y537S 1nM R5020 Replicate 5

22410050 reads; of these:
  22410050 (100.00%) were paired; of these:
    2697908 (12.04%) aligned concordantly 0 times
    18479401 (82.46%) aligned concordantly exactly 1 time
    1232741 (5.50%) aligned concordantly >1 times

    2697908 pairs aligned concordantly 0 times; of these:
      334032 (12.38%) aligned discordantly 1 time

    2363876 pairs aligned 0 times concordantly or discordantly; of these:
      4727752 mates make up the pairs; of these:
        2764846 (58.48%) aligned 0 times
        1774851 (37.54%) aligned exactly 1 time
        188055 (3.98%) aligned >1 times
93.83% overall alignment rate

T47D-Y537S 1nM R5020 Replicate 6

21796758 reads; of these:
  21796758 (100.00%) were paired; of these:
    2739483 (12.57%) aligned concordantly 0 times
    17867938 (81.98%) aligned concordantly exactly 1 time
    1189337 (5.46%) aligned concordantly >1 times

    2739483 pairs aligned concordantly 0 times; of these:
      368999 (13.47%) aligned discordantly 1 time

    2370484 pairs aligned 0 times concordantly or discordantly; of these:
      4740968 mates make up the pairs; of these:
        2762097 (58.26%) aligned 0 times
        1787488 (37.70%) aligned exactly 1 time
        191383 (4.04%) aligned >1 times
93.66% overall alignment rate

T47D-Y537S (1nM P4+10nM E2) Replicate 1

22308845 reads; of these:
  22308845 (100.00%) were paired; of these:
    2765829 (12.40%) aligned concordantly 0 times
    18312425 (82.09%) aligned concordantly exactly 1 time
    1230591 (5.52%) aligned concordantly >1 times

    2765829 pairs aligned concordantly 0 times; of these:
      355050 (12.84%) aligned discordantly 1 time

    2410779 pairs aligned 0 times concordantly or discordantly; of these:
      4821558 mates make up the pairs; of these:
        2771672 (57.48%) aligned 0 times
        1852607 (38.42%) aligned exactly 1 time
        197279 (4.09%) aligned >1 times
93.79% overall alignment rate

T47D-Y537S (1nM P4+10nM E2) Replicate 2

21945785 reads; of these:
  21945785 (100.00%) were paired; of these:
    2589345 (11.80%) aligned concordantly 0 times
    18149825 (82.70%) aligned concordantly exactly 1 time
    1206615 (5.50%) aligned concordantly >1 times

    2589345 pairs aligned concordantly 0 times; of these:
      360995 (13.94%) aligned discordantly 1 time

    2228350 pairs aligned 0 times concordantly or discordantly; of these:
      4456700 mates make up the pairs; of these:
        2557022 (57.37%) aligned 0 times
        1717669 (38.54%) aligned exactly 1 time
        182009 (4.08%) aligned >1 times
94.17% overall alignment rate

T47D-Y537S (1nM P4+10nM E2) Replicate 3

22052963 reads; of these:
  22052963 (100.00%) were paired; of these:
    2609833 (11.83%) aligned concordantly 0 times
    18237709 (82.70%) aligned concordantly exactly 1 time
    1205421 (5.47%) aligned concordantly >1 times

    2609833 pairs aligned concordantly 0 times; of these:
      385775 (14.78%) aligned discordantly 1 time

    2224058 pairs aligned 0 times concordantly or discordantly; of these:
      4448116 mates make up the pairs; of these:
        2513817 (56.51%) aligned 0 times
        1744942 (39.23%) aligned exactly 1 time
        189357 (4.26%) aligned >1 times
94.30% overall alignment rate

T47D-Y537S (1nM P4+10nM E2) Replicate 4

22331737 reads; of these:
  22331737 (100.00%) were paired; of these:
    2953444 (13.23%) aligned concordantly 0 times
    18172144 (81.37%) aligned concordantly exactly 1 time
    1206149 (5.40%) aligned concordantly >1 times

    2953444 pairs aligned concordantly 0 times; of these:
      450435 (15.25%) aligned discordantly 1 time

    2503009 pairs aligned 0 times concordantly or discordantly; of these:
      5006018 mates make up the pairs; of these:
        2768110 (55.30%) aligned 0 times
        2018821 (40.33%) aligned exactly 1 time
        219087 (4.38%) aligned >1 times
93.80% overall alignment rate

T47D-Y537S (1nM P4+10nM E2) Replicate 5

22223688 reads; of these:
  22223688 (100.00%) were paired; of these:
    2810713 (12.65%) aligned concordantly 0 times
    18205229 (81.92%) aligned concordantly exactly 1 time
    1207746 (5.43%) aligned concordantly >1 times

    2810713 pairs aligned concordantly 0 times; of these:
      411996 (14.66%) aligned discordantly 1 time

    2398717 pairs aligned 0 times concordantly or discordantly; of these:
      4797434 mates make up the pairs; of these:
        2684593 (55.96%) aligned 0 times
        1907176 (39.75%) aligned exactly 1 time
        205665 (4.29%) aligned >1 times
93.96% overall alignment rate

T47D-Y537S (1nM P4+10nM E2) Replicate 6

22223509 reads; of these:
  22223509 (100.00%) were paired; of these:
    2681085 (12.06%) aligned concordantly 0 times
    18335724 (82.51%) aligned concordantly exactly 1 time
    1206700 (5.43%) aligned concordantly >1 times

    2681085 pairs aligned concordantly 0 times; of these:
      396090 (14.77%) aligned discordantly 1 time

    2284995 pairs aligned 0 times concordantly or discordantly; of these:
      4569990 mates make up the pairs; of these:
        2583097 (56.52%) aligned 0 times
        1793145 (39.24%) aligned exactly 1 time
        193748 (4.24%) aligned >1 times
94.19% overall alignment rate

T47D-Y537S (1nM R5020+10nM E2) Replicate 1

22054354 reads; of these:
  22054354 (100.00%) were paired; of these:
    2817113 (12.77%) aligned concordantly 0 times
    18040105 (81.80%) aligned concordantly exactly 1 time
    1197136 (5.43%) aligned concordantly >1 times

    2817113 pairs aligned concordantly 0 times; of these:
      415430 (14.75%) aligned discordantly 1 time

    2401683 pairs aligned 0 times concordantly or discordantly; of these:
      4803366 mates make up the pairs; of these:
        2706979 (56.36%) aligned 0 times
        1891906 (39.39%) aligned exactly 1 time
        204481 (4.26%) aligned >1 times
93.86% overall alignment rate

T47D-Y537S (1nM R5020+10nM E2) Replicate 2

22116469 reads; of these:
  22116469 (100.00%) were paired; of these:
    2655564 (12.01%) aligned concordantly 0 times
    18245954 (82.50%) aligned concordantly exactly 1 time
    1214951 (5.49%) aligned concordantly >1 times

    2655564 pairs aligned concordantly 0 times; of these:
      353896 (13.33%) aligned discordantly 1 time

    2301668 pairs aligned 0 times concordantly or discordantly; of these:
      4603336 mates make up the pairs; of these:
        2654820 (57.67%) aligned 0 times
        1762625 (38.29%) aligned exactly 1 time
        185891 (4.04%) aligned >1 times
94.00% overall alignment rate

T47D-Y537S (1nM R5020+10nM E2) Replicate 3

22326220 reads; of these:
  22326220 (100.00%) were paired; of these:
    2788951 (12.49%) aligned concordantly 0 times
    18297555 (81.96%) aligned concordantly exactly 1 time
    1239714 (5.55%) aligned concordantly >1 times

    2788951 pairs aligned concordantly 0 times; of these:
      348164 (12.48%) aligned discordantly 1 time

    2440787 pairs aligned 0 times concordantly or discordantly; of these:
      4881574 mates make up the pairs; of these:
        2831099 (58.00%) aligned 0 times
        1853150 (37.96%) aligned exactly 1 time
        197325 (4.04%) aligned >1 times
93.66% overall alignment rate

T47D-Y537S (1nM R5020+10nM E2) Replicate 4

22190801 reads; of these:
  22190801 (100.00%) were paired; of these:
    2699956 (12.17%) aligned concordantly 0 times
    18260894 (82.29%) aligned concordantly exactly 1 time
    1229951 (5.54%) aligned concordantly >1 times

    2699956 pairs aligned concordantly 0 times; of these:
      356935 (13.22%) aligned discordantly 1 time

    2343021 pairs aligned 0 times concordantly or discordantly; of these:
      4686042 mates make up the pairs; of these:
        2689190 (57.39%) aligned 0 times
        1802887 (38.47%) aligned exactly 1 time
        193965 (4.14%) aligned >1 times
93.94% overall alignment rate

T47D-Y537S (1nM R5020+10nM E2) Replicate 5

22447941 reads; of these:
  22447941 (100.00%) were paired; of these:
    2667537 (11.88%) aligned concordantly 0 times
    18531018 (82.55%) aligned concordantly exactly 1 time
    1249386 (5.57%) aligned concordantly >1 times

    2667537 pairs aligned concordantly 0 times; of these:
      337341 (12.65%) aligned discordantly 1 time

    2330196 pairs aligned 0 times concordantly or discordantly; of these:
      4660392 mates make up the pairs; of these:
        2685646 (57.63%) aligned 0 times
        1785098 (38.30%) aligned exactly 1 time
        189648 (4.07%) aligned >1 times
94.02% overall alignment rate

T47D-Y537S (1nM R5020+10nM E2) Replicate 6

21993430 reads; of these:
  21993430 (100.00%) were paired; of these:
    2680065 (12.19%) aligned concordantly 0 times
    18110359 (82.34%) aligned concordantly exactly 1 time
    1203006 (5.47%) aligned concordantly >1 times

    2680065 pairs aligned concordantly 0 times; of these:
      356782 (13.31%) aligned discordantly 1 time

    2323283 pairs aligned 0 times concordantly or discordantly; of these:
      4646566 mates make up the pairs; of these:
        2685063 (57.79%) aligned 0 times
        1773597 (38.17%) aligned exactly 1 time
        187906 (4.04%) aligned >1 times
93.90% overall alignment rate

Appendix III – GSEA lists

Full Media: T47D-WT vs T47D-Y537S (Figure 3.15C)

Hallmark

Pathway	Total genes	Genes in list	Enrichment FDR	Fold Enrichment
HALLMARK ESTROGEN RESPONSE EARLY	200	104	1.97E-34	3.603015198
HALLMARK ESTROGEN RESPONSE LATE	200	92	1.63E-25	3.187282675
HALLMARK P53 PATHWAY	200	79	3.88E-17	2.736905775
HALLMARK MTORC1 SIGNALING	199	72	2.03E-13	2.506929786
HALLMARK CHOLESTEROL HOMEOSTASIS	73	35	9.14E-11	3.322063538
HALLMARK GLYCOLYSIS	198	65	3.62E-10	2.274630807
HALLMARK TNFA SIGNALING VIA NFKB	199	62	8.11E-09	2.158745093
HALLMARK UNFOLDED PROTEIN RESPONSE	112	42	8.11E-09	2.598328267
HALLMARK MITOTIC SPINDLE	197	59	9.12E-08	2.075145418
HALLMARK UV RESPONSE UP	158	49	3.94E-07	2.148828441
HALLMARK ADIPOGENESIS	199	57	7.08E-07	1.984652747
HALLMARK HYPOXIA	200	57	7.81E-07	1.974729483
HALLMARK EPITHELIAL MESENCHYMAL TRAN	200	56	1.74E-06	1.940085106
HALLMARK ANDROGEN RESPONSE	99	34	1.92E-06	2.379613767
HALLMARK G2M CHECKPOINT	198	55	2.51E-06	1.924687606
HALLMARK APICAL JUNCTION	200	55	3.32E-06	1.905440729
HALLMARK UV RESPONSE DN	143	43	3.57E-06	2.083507981
HALLMARK APOPTOSIS	161	46	6.67E-06	1.97967868
HALLMARK MYOGENESIS	200	54	6.67E-06	1.870796353
HALLMARK MYC TARGETS V1	199	53	1.17E-05	1.84537887
HALLMARK HEME METABOLISM	197	50	8.26E-05	1.758597812
HALLMARK E2F TARGETS	200	50	0.000115004	1.732218845
HALLMARK XENOBIOTIC METABOLISM	200	50	0.000115004	1.732218845
HALLMARK WNT BETA CATENIN SIGNALING	42	16	0.00028034	2.639571573
HALLMARK HEDGEHOG SIGNALING	36	13	0.002041162	2.502093887
HALLMARK TGF BETA SIGNALING	54	16	0.005869409	2.053000113
HALLMARK FATTY ACID METABOLISM	158	36	0.005869409	1.578731099
HALLMARK IL2 STAT5 SIGNALING	199	43	0.006961126	1.497194178
HALLMARK PEROXISOME	104	25	0.010679763	1.665595043
HALLMARK APICAL SURFACE	44	13	0.012527237	2.047167726

T47D-WT and T47D-Y537S: Vehicle vs 10nM E2, upregulated genes (Figure 3.17B)

Hallmark

Pathway	Total genes	Genes in list	Enrichment FDR
MSigDB:HALLMARK ESTROGEN RESPONSE EARLY	197	25	1.68E-29
MSigDB:HALLMARK ESTROGEN RESPONSE LATE	198	15	2.54E-14
MSigDB:HALLMARK HYPOXIA	194	5	0.005209813
MSigDB:HALLMARK EPITHELIAL MESENCHYMAL TRA	197	5	0.005209813

Curated MSigDB

Pathway	Total genes	Genes in list	Enrichment FDR
MSigDB:CREIGHTON ENDOCRINE THERAPY RESISTANCE 4	277	25	1.92E-24
MSigDB:BHAT ESR1 TARGETS NOT VIA AKT1 UP	205	23	1.92E-24
MSigDB:BHAT ESR1 TARGETS VIA AKT1 UP	269	24	2.02E-23
MSigDB:DUTERTRE ESTRADIOL RESPONSE 6HR UP	220	22	1.58E-22
MSigDB:MASSARWEH TAMOXIFEN RESISTANCE DN	231	22	3.77E-22
MSigDB:MASSARWEH RESPONSE TO ESTRADIOL	58	14	1.10E-19
MSigDB:DUTERTRE ESTRADIOL RESPONSE 24HR UP	310	18	3.83E-14
MSigDB:SMID BREAST CANCER BASAL DN	654	23	9.89E-14
MSigDB:WILLIAMS ESR1 TARGETS UP	26	8	5.38E-12
MSigDB:MASRI RESISTANCE TO TAMOXIFEN AND AROMATASE INHIBITORS UP	20	7	6.46E-11
MSigDB:CREIGHTON ENDOCRINE THERAPY RESISTANCE 1	491	17	7.27E-10
MSigDB:STEIN ESTROGEN RESPONSE NOT VIA ESRRA	18	6	3.38E-09
MSigDB:FRASOR RESPONSE TO ESTRADIOL UP	37	7	6.23E-09
MSigDB:STOSSI RESPONSE TO ESTRADIOL	48	7	3.99E-08
MSigDB:STEIN ESR1 TARGETS	82	8	6.11E-08
MSigDB:SMID BREAST CANCER LUMINAL A UP	80	7	1.36E-06
MSigDB:DOANE BREAST CANCER ESR1 UP	106	7	8.98E-06
MSigDB:SMID BREAST CANCER LUMINAL B UP	160	8	9.76E-06
MSigDB:VANTVEER BREAST CANCER ESR1 UP	161	8	9.76E-06
MSigDB:BOQUEST STEM CELL UP	256	9	3.05E-05
MSigDB:PID HES HEY PATHWAY	48	5	4.16E-05
MSigDB:BENPORATH EED TARGETS	1017	16	8.84E-05
MSigDB:MOHANKUMAR TLX1 TARGETS UP	389	10	0.000104284
MSigDB:PEDERSEN METASTASIS BY ERBB2 ISOFORM 4	104	6	0.000104284
MSigDB:DUAN PRDM5 TARGETS	77	5	0.000367573
MSigDB:RIGGINS TAMOXIFEN RESISTANCE DN	209	7	0.000534936
MSigDB:BENPORATH ES WITH H3K27ME3	1063	15	0.000545369
MSigDB:ZHU CMV 24 HR DN	89	5	0.000663359
MSigDB:BOQUEST STEM CELL CULTURED VS FRESH UP	405	9	0.000836955
MSigDB:BERNARD PPAPDC1B TARGETS DN	52	4	0.001163471

Gene Ontology Molecular Function

Pathway	Total genes	Genes in list	Enrichment FDR
RNA polymerase II proximal promoter sequence-specific DNA binding	542	8	0.036786268
Proximal promoter sequence-specific DNA binding	556	8	0.036786268
Steroid hormone receptor activity	61	3	0.036786268
Nuclear receptor activity	52	3	0.036786268
Signaling receptor binding	1819	17	0.036786268
Potassium channel activity	131	4	0.036786268
Steroid binding	101	4	0.036786268
Lipid binding	761	11	0.036786268
Transcription factor activity, direct ligand regulated sequence-specific DNA binding	52	3	0.036786268

T47D-WT and T47D-Y537S: Vehicle vs 1nM R5020, upregulated genes (Figure 3.28C)

Hallmark

Pathway	Total genes	Genes in list	Enrichment FDR
MSigDB:HALLMARK TNFA SIGNALING VIA NFKB	198	8	3.57E-06
MSigDB:HALLMARK HYPOXIA	194	6	0.000206121
MSigDB:HALLMARK ESTROGEN RESPONSE EARLY	197	6	0.000206121
MSigDB:HALLMARK UV RESPONSE DN	141	5	0.000343086
MSigDB:HALLMARK ANDROGEN RESPONSE	97	4	0.000811568
MSigDB:HALLMARK ESTROGEN RESPONSE LATE	198	4	0.009507972
MSigDB:HALLMARK ANGIOGENESIS	36	2	0.01279366
MSigDB:HALLMARK WNT BETA CATENIN SIGNALING	42	2	0.015110531
MSigDB:HALLMARK EPITHELIAL MESENCHYMAL TRANSITION	197	3	0.034897904
MSigDB:HALLMARK P53 PATHWAY	196	3	0.034897904
MSigDB:HALLMARK KRAS SIGNALING UP	194	3	0.034897904

Gene Ontology Molecular Function

Pathway	Total genes	Genes in list	Enrichment FDR
DNA-binding transcription factor activity, RNA polymerase II-specific	1673	15	0.015691581
Regulatory region nucleic acid binding	1002	10	0.015691581
DNA-binding transcription repressor activity, RNA polymerase II-specific	242	5	0.015691581
DNA-binding transcription factor activity	1793	15	0.015691581
Voltage-gated potassium channel activity	94	4	0.015691581
Cation channel activity	337	6	0.015691581
Potassium channel activity	131	4	0.015691581
Gated channel activity	367	6	0.015691581
Ion gated channel activity	358	6	0.015691581
Voltage-gated cation channel activity	151	4	0.015691581
Sequence-specific DNA binding	1189	11	0.015691581
Transcription regulatory region DNA binding	1000	10	0.015691581
Transcription regulator activity	2183	16	0.015691581
Transcription regulatory region sequence-specific DNA binding	875	9	0.019426
Potassium ion transmembrane transporter activity	170	4	0.020966256
Phospholipid-translocating ATPase activity	23	2	0.022013683
Sequence-specific double-stranded DNA binding	920	9	0.02244019
DNA-binding transcription activator activity, RNA polymerase II-specific	441	6	0.023290671
Ion channel activity	446	6	0.023324103
Substrate-specific channel activity	459	6	0.025507687
RNA polymerase II regulatory region sequence-specific DNA binding	816	8	0.025932497
RNA polymerase II regulatory region DNA binding	823	8	0.025932497
Calcium activated cation channel activity	31	2	0.025932497
Voltage-gated ion channel activity	211	4	0.025932497
Channel activity	488	6	0.025932497
Passive transmembrane transporter activity	490	6	0.025932497
Voltage-gated channel activity	211	4	0.025932497
Delayed rectifier potassium channel activity	34	2	0.027264582
Double-stranded DNA binding	1029	9	0.027390618
Inorganic molecular entity transmembrane transporter activity	878	8	0.032739225

T47D-WT and T47D-Y537S: Vehicle vs (1nM R5020+10nM E2), upregulated genes (Figure 3.28D)

Hallmark

Pathway	Total genes	Genes in list	Enrichment FDR
MSigDB:HALLMARK TNFA SIGNALING VIA NFKB	198	15	2.94E-11
MSigDB:HALLMARK ESTROGEN RESPONSE EARLY	197	11	4.16E-07
MSigDB:HALLMARK NOTCH SIGNALING	32	5	1.13E-05
MSigDB:HALLMARK WNT BETA CATENIN SIGNALING	42	4	0.000768721
MSigDB:HALLMARK ESTROGEN RESPONSE LATE	198	7	0.001052786
MSigDB:HALLMARK HYPOXIA	194	6	0.005048062
MSigDB:HALLMARK UV RESPONSE DN	141	5	0.006160008
MSigDB:HALLMARK ANDROGEN RESPONSE	97	4	0.009217695
MSigDB:HALLMARK KRAS SIGNALING DN	191	5	0.017551849

Gene Ontology Molecular Function

Pathway	Total genes	Genes in list	Enrichment FDR
Wnt-activated receptor activity	18	4	0.000759542
Regulatory region nucleic acid binding	1002	18	0.002353139
Transcription regulatory region DNA binding	1000	18	0.002353139
Transcription regulatory region sequence-specific DNA binding	875	16	0.003337383
Wnt-protein binding	38	4	0.003337383
RNA polymerase II proximal promoter sequence-specific DNA binding	542	12	0.003711717
Proximal promoter sequence-specific DNA binding	556	12	0.003711717
Sequence-specific double-stranded DNA binding	920	16	0.003711717
Stem cell factor receptor binding	4	2	0.005007373
Voltage-gated potassium channel activity	94	5	0.005539137
DNA-binding transcription activator activity, RNA polymerase II-specific	441	10	0.006672292
RNA polymerase II regulatory region sequence-specific DNA binding	816	14	0.007201788
RNA polymerase II regulatory region DNA binding	823	14	0.007201788
Double-stranded DNA binding	1029	16	0.007201788
Potassium ion transmembrane transporter activity	170	6	0.008211284
Kinase binding	754	13	0.008524181
Enzyme binding	2353	27	0.009032441
Protein kinase binding	673	12	0.009032441
Sequence-specific DNA binding	1189	17	0.009032441
DNA-binding transcription factor activity, RNA polymerase II-specific	1673	21	0.010665764
DNA-binding transcription factor activity	1793	22	0.010665764
Delayed rectifier potassium channel activity	34	3	0.010665764
Potassium channel activity	131	5	0.010934887
Transcription regulator activity	2183	25	0.011055133
Growth factor receptor binding	137	5	0.012270843
Prostanoid receptor activity	10	2	0.012694772
Voltage-gated cation channel activity	151	5	0.017406012
Channel activity	488	9	0.021268698
Passive transmembrane transporter activity	490	9	0.021268698
Icosanoid receptor activity	16	2	0.026861518

T47D-Y537S unique: (Vehicle vs 1nM R5020) and (10nM E2 vs (1nM R5020+10nM E2)), (Figure 3.29F)

Gene Ontology Molecular Function

Pathway	Total genes	Genes in list	Enrichment FDR
Regulatory region nucleic acid binding	1002	54	1.57E-10
Transcription regulatory region DNA binding	1000	54	1.57E-10
Transcription regulatory region sequence-specific DNA binding	875	48	1.01E-09
RNA polymerase II regulatory region sequence-specific DNA binding	816	46	1.01E-09
RNA polymerase II regulatory region DNA binding	823	46	1.07E-09
Sequence-specific DNA binding	1189	56	3.26E-09
Sequence-specific double-stranded DNA binding	920	48	3.26E-09
RNA polymerase II proximal promoter sequence-specific DNA binding	542	34	1.91E-08
Proximal promoter sequence-specific DNA binding	556	34	2.96E-08
Double-stranded DNA binding	1029	49	2.96E-08
DNA-binding transcription factor activity, RNA polymerase II-specific	1673	64	3.14E-07
DNA-binding transcription activator activity, RNA polymerase II-specific	441	28	3.14E-07
DNA-binding transcription factor activity	1793	67	3.14E-07
Transcription regulator activity	2183	77	3.14E-07
Enzyme binding	2353	74	4.43E-05
Protein kinase binding	673	31	5.63E-05
Kinase binding	754	33	7.45E-05
DNA binding	2718	78	0.00053563
Transcription factor binding	689	29	0.000547358
DNA-binding transcription repressor activity, RNA polymerase II-specific	242	15	0.000769908
Chromatin binding	575	24	0.002706577
Lipid binding	761	29	0.002706577
Transcription coregulator activity	613	24	0.006487301
Phospholipid binding	441	19	0.007988222
Protein heterodimerization activity	551	22	0.007988222
G-protein alpha-subunit binding	23	4	0.010910547
Protein domain specific binding	766	27	0.01223448
Sodium:potassium-exchanging ATPase activity	11	3	0.012374158
Beta-catenin binding	86	7	0.013090661
Potassium-transporting ATPase activity	12	3	0.015192621

T47D-Y537S unique: Vehicle vs 1nM R5020 only, (Figure 3.30A)

Hallmark

Pathway	Total genes	Genes in list	Enrichment FDR
MSigDB:HALLMARK NOTCH SIGNALING	32	6	1.14E-06
MSigDB:HALLMARK TNFA SIGNALING VIA NFKB	198	9	3.98E-05
MSigDB:HALLMARK HYPOXIA	194	9	3.98E-05
MSigDB:HALLMARK ESTROGEN RESPONSE EARLY	197	8	0.000231818
MSigDB:HALLMARK INFLAMMATORY RESPONSE	197	7	0.001320985
MSigDB:HALLMARK APOPTOSIS	159	6	0.002241664
MSigDB:HALLMARK ESTROGEN RESPONSE LATE	198	6	0.00524311
MSigDB:HALLMARK IL2 STAT5 SIGNALING	195	6	0.00524311
MSigDB:HALLMARK WNT BETA CATENIN SIGNALING	42	3	0.006875119
MSigDB:HALLMARK G2M CHECKPOINT	195	5	0.018835571
MSigDB:HALLMARK APICAL JUNCTION	194	5	0.018835571
MSigDB:HALLMARK UV RESPONSE UP	154	4	0.035986217

Gene Ontology Biological Process

Pathway	Total genes	Genes in list	Enrichment FDR
Regulation of cell migration	883	23	1.25E-05
Regulation of cell motility	946	23	1.95E-05
Positive regulation of cell migration	521	17	1.95E-05
Positive regulation of cell motility	544	17	2.73E-05
Positive regulation of cellular component movement	558	17	3.14E-05
Regulation of locomotion	1041	23	3.17E-05
Positive regulation of locomotion	576	17	3.17E-05
Regulation of cellular component movement	1028	23	3.17E-05
Positive regulation of multicellular organismal process	1911	32	4.49E-05
Regulation of multicellular organismal development	2138	34	5.18E-05
Regulation of multicellular organismal process	3382	45	5.71E-05
Intracellular signal transduction	3113	42	0.000103459
Response to ischemia	50	6	0.000103459
Regulation of localization	2905	40	0.00011029
Circulatory system development	1077	22	0.000122832
Regulation of signal transduction	3529	45	0.000132107
Regulation of cell proliferation	1756	29	0.000133093
Negative regulation of multicellular organismal process	1286	24	0.000153038
Regulation of protein phosphorylation	1503	26	0.00020314
Locomotion	1921	30	0.000225355
Cell proliferation	2165	32	0.000279055
Regulation of cell differentiation	1954	30	0.000279055
Alpha-beta T cell differentiation	101	7	0.000279055
Regulation of response to stimulus	4820	54	0.000279055
Regulation of signaling	3952	47	0.000291922
Negative regulation of cellular biosynthetic process	1658	27	0.000291922
Regulation of interleukin-1 beta production	103	7	0.000291922
Cell motility	1670	27	0.000291922
Localization of cell	1670	27	0.000291922
Protein phosphorylation	2093	31	0.000294399

T47D-Y537S unique: (E2 vs (1nM R5020+10nM E2)) only, (Figure 3.30B)

Gene Ontology Molecular Function

Pathway	Total genes	Genes in list	Enrichment FDR
Transcription regulatory region sequence-specific DNA binding	875	23	6.11E-07
RNA polymerase II regulatory region sequence-specific DNA binding	816	22	6.11E-07
RNA polymerase II regulatory region DNA binding	823	22	6.11E-07
Sequence-specific double-stranded DNA binding	920	23	7.08E-07
Regulatory region nucleic acid binding	1002	23	2.24E-06
Transcription regulatory region DNA binding	1000	23	2.24E-06
Sequence-specific DNA binding	1189	25	2.61E-06
Double-stranded DNA binding	1029	23	2.71E-06
RNA polymerase II proximal promoter sequence-specific DNA binding	542	16	6.69E-06
Proximal promoter sequence-specific DNA binding	556	16	8.45E-06
DNA-binding transcription factor activity, RNA polymerase II-specific	1673	28	2.68E-05
DNA-binding transcription factor activity	1793	29	3.07E-05
DNA-binding transcription activator activity, RNA polymerase II-specific	441	13	6.34E-05
Transcription regulator activity	2183	31	0.000158222
DNA binding	2718	33	0.001696385
Superoxide dismutase activity	6	2	0.006043861
Oxidoreductase activity, acting on superoxide radicals as acceptor	6	2	0.006043861
Nucleoside-triphosphatase regulator activity	372	9	0.006043861
Enzyme activator activity	552	11	0.00727836
Sodium ion binding	8	2	0.009819435
Sodium:potassium-exchanging ATPase activity	11	2	0.018143521
GTPase activator activity	290	7	0.018972266
Potassium-transporting ATPase activity	12	2	0.018972266
Potassium ion binding	12	2	0.018972266
Steroid hormone receptor binding	97	4	0.024216205
GTPase regulator activity	327	7	0.033256653
Enzyme regulator activity	1132	15	0.033774777
Alkali metal ion binding	17	2	0.033774777
Enzyme binding	2353	25	0.039083304
Ankyrin binding	21	2	0.046537114

Gene Ontology Biological Process

Pathway	Total genes	Genes in list	Enrichment FDR
Positive regulation of transcription, DNA-templated	1599	29	0.000140047
Positive regulation of transcription by RNA polymerase II	1255	25	0.000140047
Positive regulation of RNA metabolic process	1789	31	0.000140047
Positive regulation of RNA biosynthetic process	1695	29	0.000195632
Positive regulation of nucleic acid-templated transcription	1694	29	0.000195632
Positive regulation of gene expression	2060	32	0.000319913
Positive regulation of nucleobase-containing compound metabolic process	1993	31	0.000407166
Negative regulation of transcription by RNA polymerase II	876	19	0.000491441
Regulation of transcription by RNA polymerase II	2830	38	0.000603204
Positive regulation of macromolecule biosynthetic process	1978	30	0.000721007
Cognition	325	11	0.000957752
Transcription by RNA polymerase II	2992	38	0.001443104
Positive regulation of cellular biosynthetic process	2082	30	0.001443104
Negative regulation of photoreceptor cell differentiation	8	3	0.001443104
Animal organ morphogenesis	1099	20	0.001726925
Positive regulation of biosynthetic process	2113	30	0.001726925
Negative regulation of transcription, DNA-templated	1298	22	0.001726925
Regulation of photoreceptor cell differentiation	9	3	0.001726925
Regulation of cell differentiation	1954	28	0.002372493
Negative regulation of RNA biosynthetic process	1355	22	0.002590706
Negative regulation of nucleic acid-templated transcription	1353	22	0.002590706
Regulation of developmental process	2763	35	0.002590706
Epithelial cell proliferation involved in prostate gland development	11	3	0.002590706
Regulation of multicellular organismal development	2138	29	0.003592792
Negative regulation of cellular macromolecule biosynthetic process	1511	23	0.004205971
Regulation of neurogenesis	844	16	0.004946548
Negative regulation of cellular biosynthetic process	1658	24	0.005408767
Regulation of RNA metabolic process	4163	45	0.005408767
Negative regulation of RNA metabolic process	1446	22	0.005408767
Negative regulation of biosynthetic process	1681	24	0.006456581

T47D-Y537S unique: (Vehicle vs 1nM R5020) and (E2 vs (1nM R5020+10nM E2)), (Figure 3.30C)

Hallmark

Pathway	Total genes	Genes in list	Enrichment FDR
MSigDB:HALLMARK TNFA SIGNALING VIA NFKB	198	10	3.80E-06
MSigDB:HALLMARK ESTROGEN RESPONSE EARLY	197	6	0.008694753
MSigDB:HALLMARK UV RESPONSE DN	141	5	0.008694753
MSigDB:HALLMARK TGF BETA SIGNALING	54	3	0.018868948

Gene Ontology Molecular Function

Pathway	Total genes	Genes in list	Enrichment FDR
Regulatory region nucleic acid binding	1002	18	0.001238622
Transcription regulatory region DNA binding	1000	18	0.001238622
Protein kinase binding	673	14	0.001726792
Sequence-specific DNA binding	1189	19	0.001759245
DNA-binding transcription factor activity, RNA polymerase II-specific	1673	23	0.002059836
Transcription regulator activity	2183	27	0.002153005
Chromatin binding	575	12	0.002185842
Kinase binding	754	14	0.002185842
Chromatin DNA binding	125	6	0.002185842
RNA polymerase II regulatory region sequence-specific DNA binding	816	14	0.002829545
RNA polymerase II regulatory region DNA binding	823	14	0.002829545
DNA-binding transcription activator activity, RNA polymerase II-specific	441	10	0.002829545
DNA-binding transcription factor activity	1793	23	0.002829545
Transcription coregulator activity	613	12	0.002829545
Phospholipid binding	441	10	0.002829545
Enzyme binding	2353	27	0.002829545
Transcription regulatory region sequence-specific DNA binding	875	14	0.004796076
Neurotrophin TRK receptor binding	6	2	0.005058511
Neurotrophin TRKA receptor binding	6	2	0.005058511
Cytoskeletal protein binding	1004	15	0.005151614
Double-stranded DNA binding	1029	15	0.006082383
Sequence-specific double-stranded DNA binding	920	14	0.006082383
Transcription corepressor activity	264	7	0.006569728
Lipid binding	761	12	0.010164317
Neurotrophin receptor binding	10	2	0.011365605
DNA-binding transcription repressor activity, RNA polymerase II-specific	242	6	0.019565923
Phosphatidylinositol binding	249	6	0.02170249
Glucocorticoid receptor binding	15	2	0.023249335
RNA polymerase II proximal promoter sequence-specific DNA binding	542	9	0.02489824
Proximal promoter sequence-specific DNA binding	556	9	0.025840585

Appendix IV - List of genes in Heatmap clusters

Heatmap of 295 genes differentially expressed by 10nM E2 in T47D-WT and T47D-Y537S cells (Figure 3.18):

Cluster 1 genes

AOC1	FAM83E	LIMD2	TM4SF18	PCBP1	IL17REL	PPP3CB-AS1
SLC9A3	COL7A1	ARHGAP24	ABCA1	TMEM37	C15orf62	CEBPD
TP63	DLX2	CYP1A1	NYAP1	LCN12	SP6	ZNF492
PKP1	HOXC12	IGFBP3	RCOR2	MST1P2	TPM2	FEZF1-AS1
BIK	KLHDC7B	EXTL1	DDIT4	MST1L	SLC6A10P	YJEFN3
						WASH9P

Cluster 2 genes

ITGAL	CISH	IL6ST	NEIL2	DSCAM	SPRY4	HEATR4
SEMA3G	TFCP2L1	SPOCD1	PDLIM3	CYP4F22	DSCAM	SPRY4
BIRC3	IGFBP5	C5AR2	PPM1J	ZNF556	CYP4F22	THSD4
SH2D2A	FHL2	HEY2	RMND1	MBOAT1	ZNF556	TPRG1
FLT4	TPSG1	PKIB	SUSD3	NIPAL4	MBOAT1	SMTNL2
VCAN	NCF2	ANKRD36	CIART	FAM86B3P	NIPAL4	GREB1
PTGER3	OLFML3	GATA4	RUNX1	CD34	FAM86B3P	ASB13
CCDC85A	MREG	MYC	PGLYRP2	PDZK1	CD34	CACNA1H
CCN5	MYB	THBS1	SCGB3A1	AMZ1	PDZK1	ARID5A
NTN1	CSF3R	PLCB2	ADCY9	DOK7	AMZ1	PELI1
MPPED2	DUSP4	MYOF	KCNF1	TENM3-AS1	DOK7	ELOVL2
CELSR1	SPINK4	ESR2	SERPINI1	EGR3	TENM3-AS1	TMEM229B
FOSL2	KCNK15	IGFBP4	PPM1K	SSTR2	EGR3	C2CD4A
PGR	CHST8	SLC47A1	TIPARP	MAP6D1	SSTR2	NOS1AP
EPB41L3	RUNX2	KCNH1	GRIK3	SIAH2	MAP6D1	DISP3
NKAIN1	GRPR	ETNK2	NPY1R	YBEY	SIAH2	INSYN1
TFAP4	FGD3	AFF3	RANBP3L	NXPH3	YBEY	ATP10A
ESR1	EPS15L1	ARMT1	KCNK5	TSKU	NXPH3	COLQ
SEC14L2	KDM4B	PXDNL	CARD19	ABAT	TSKU	IGKC
XBP1	LRFN1	UGCG	RET	TMEM121B	ABAT	PLAC9P1
RBBP8	MGAT3	ST8SIA6	SYNPO2L	GPR132	TMEM121B	CT62
SGK3	A4GALT	GRIK4	NOD2	PSG9	GPR132	LINC00511
CXCL12	LIF	ADRA2A	CYP2S1	ZNF703	PSG9	EMSLR
INPP4B	NXNL2	MAT1A	PXK	KIRREL1	ZNF703	CYP2T1P
NEDD9	OLFM1	THRSP	KCTD6	ZBTB40	KIRREL1	DSCAM-AS1
PHACTR1	RARA	HSPB8	ACOX2	WT1	ZBTB40	RNF223
RBM24	CHSY1	GJA1	SERPINA6	MAFF	WT1	C1orf226
HBEGF	STARD13	CMTM7	PFKFB3	MYBL1	MAFF	IFITM10
LNPEP	LARGE1	ANKFN1	GPR27	KCNQ5	MYBL1	LINC00992
STC2	SAA2	ANKH	FGG	HEATR4	KCNQ5	FMN1
						CYP2B7P
						LINC02298
						LINC02568
						LINC00565

Cluster 3 genes

APBB1IP	IL1R1	FAIM2	ADGRF1	TCP11L2	B3GNT8	STPG3
NRP1	GRIN3B	SPAG8	WNT3A	PPFIBP2	PCED1B	MAFB
KLF5	CCN2	POU2F3	TSC22D3	BMERB1	SOX2	SMIM5
BMF	MTERF2	VAMP1	LMOD1	ANGPTL4	BPIFA4P	CRIP1
DBP	CCR2	RDH16	ELF3	CHRM1	KCNK12	LINC02015
TMEM205	DNAI1	NKD1	CRELD1	PCDH7	FAM43A	ZNF737
ITGB8	ID1	GRB7	SPRY1	KRT2	PLEKHG7	LINC02701
RNF43	KCNC1	TINAGL1	CITED2	ARL4D	CYSRT1	CCDC177
WNT5A	VSTM2L	FAM83A	PKNOX2	RNF152	CCDC154	LINC02560
						RNF225
						SCO2
						PERCC1

Cluster 4 genes

GREB1L	ANKRD1	FOS	NCMAP	KRT18P17
SYBU	GEM	HSD11B2	ARC	EGLN2

Heatmap of 371 genes differentially expressed by 1nM R5020 in T47D-WT and T47D-Y537S cells (Figure 3.26):

Cluster 1 genes

ADM	BMP4	EFNA5	GRB7	LMOD1	PIK3R3	SLC40A1
AJUBA	CCL2	ELF3	GRHL3	LRATD2	PLAU	SMIM5
AKAP12	CCL20	ELL2	HIVEP1	MAP3K8	PLK2	SRGAP2B
AMOTL2	CDC42EP3	EPGN	HS3ST1	MB21D2	PXDC1	STON2
ANKRD50	CDKN2B	F2R	IRAK2	MTMR9	RGS16	STYK1
ARHGAP42	CPA4	FOXA1	IRF1	N4BP3	RHOV	TIFA
ARID5B	CSF1	FRMD4B	IRF2BPL	NAV2	RND1	TMCC3
ATF3	CX3CL1	G2E3-AS1	IRX2	NFKBIZ	RND3	TNFSF15
BACH2	DENND1B	GABRQ	ITPRIPL2	NKX1-2	RNF222	TNS4
BBC3	DISP1	GASK1B	JAG1	NUAK2	RUSC2	WNT5A
BCL2	DUSP10	GCNT2	KCNB1	OVOL1	SERTAD4	ZBED5
BCL3	DUSP5	GEM	KLF10	PCDH7	SHROOM3	ZBTB16
BHLHE40	EFNA1	GPAT3	LIF	PDE4B	SLC25A6P2	ZNF217
						ZNF441
						ZNF812P
						ZNF823

Cluster 2 genes

ABTB2	CLDN8	FZD5	KCNG1	NBPF25P	RANBP3L	SSR4P1
ACER2	CMTM7	FZD8	KCNH1	NCALD	RAPGEF6	STAMBPL1
ADAMTS15	CRY2	G6PC	KDF1	NET1	RASL10A	STARD8
ADAMTS8	CSRNP1	GAS6-AS1	KIAA0040	NEURL1B	RBM24	STAT5A
ADGRA2	DGKH	GATA6	KLF15	NOG	RCOR2	SYNM
ANGPT1	DIPK2A	GJB2	KLF4	NOTCH2	RERE	TADA2B
ANKRD22	DNAJB4	GJB3	LEF1	NPIPB15	RGMA	TAF5L
ANKRD35	DTX2	GPR153	LINC00482	NXPE3	RHOBTB2	TBXA2R
ANKRD63	DUSP1	GPR63	LINC00511	NXPH3	RHOU	TCAF2
APLN	EEF2K	GPSM2	LINC01018	OGFRL1	RREB1	TFCP2L1
ARL4A	ERICD	GREB1	LINC01588	OTULINL	RUNX1	TGFBR3
ATP10A	ERN1	GRHL2	LMO7	PACSIN1	S1PR5	TIPARP
ATP1A4	ERRFI1	HERC5	LRIG1	PAG1	SAP30	TMEM158
ATP8B3	F3	HES2	MAFB	PDK4	SDR39U1	TMEM63C
AZGP1P1	FAM104A	HILPDA	MAN1A1	PER2	SEC14L2	TNFAIP8L3
BCL2L11	FAM53B	HS3ST3B1	MARVELD3	PIK3R1	SGK1	TNFRSF10A
BCL6	FAXDC2	HSD11B2	MEX3B	PIM2	SGPP2	TRAF5
C2CD4A	FCRLB	HSPA2	MIR1915HG	PISD	SH3BP5	TRIM22
CBR3-AS1	FGD4	IL17C	MIRLET7BHG	PKP1	SH3TC2	TRNP1
CBX4	FGF18	IL17D	MMP25	PLA2G3	SKIDA1	TSKU
CCND1	FHL3	IL20RA	MPHOSPH10	PLA2G4E	SLC25A18	UACA
CDYL2	FKBP5	ITGA10	MPP3	PPM1L	SMKR1	ULK2
CECR2	FNDC4	KANK1	MRAS	PPTC7	SNAI1	USP54
CHAC1	FOXO4	KANK3	MSX1	PRDM1	SNX30	VWA5B2
CHST3	FRK	KCNC4	MTCL1	PRKAB2	SPATC1	YTHDF1
CISH	FRS3	KCNE4	MTSS1	PXK	SPRED1	ZFP36
CITED4	FZD1	KCNF1	NBPF10	PXYLP1	SPSB1	ZFPM1
						ZIC2
						ZNF189
						ZNF563
						ZNF652
						ZNF703

Cluster 3 genes

BARX2	ETS2	JAK2	POC5	RGS2	SPATA13
CPEB4	FHDC1	KCNK5	PRICKLE1	RNF223	SYBU
DISP3	GADD45B	MAP1B	RAB11FIP1	SCUBE2	SYT8
DIXDC1	GLUL	PHLDA1	RARA	SOX4	THBS1

Cluster 4 genes

ADD3	C15orf39	EGFR	KLF9	PRR15	SASH1	SRGAP2C
AHNAK	C9orf152	ENPP3	LRRC31	PRR15L	SCNN1G	ST8SIA1
AMIGO2	CCDC177	FIGN	MIR3142HG	PTCH1	SIK1	TBC1D8
ANGPTL4	CLVS2	KCNJ11	MYO10	PTPRJ	SLC37A2	TENT5B
AQP3	CORO2A	KCNMA1	NBPF14	PUS10	SMAD3	TFEB
ARHGEF37	CYP1B1	KIAA0232	NDRG1	PXMP4	SMPD5	TLR5
ARL4C	DDIT4	KIAA0513	PER1	RBBP8NL	SNTB2	TSC22D3
B3GNT8	EGF	KIF13B	PLLP	RPS6KA5	SOWAHA	VAV3
						ZC3H12A
						ZCCHC2
						ZFHX3

Heatmap of 467 genes differentially expressed by (1nM R5020+10nM E2) in T47D-WT and T47D-Y537S cells (Figure 3.27):

Cluster 1 genes

A4GALT	CEBPD	FZD1	KCNG1	MTSS1	RAB11FIP1	SPRED2
ABTB2	CFAP20	FZD5	KCNH1	NBPF25P	RANBP3L	SPSB1
ACER2	CHAC1	FZD8	KCNK5	NET1	RARA	SSR4P1
ACOT6	CHST3	G6PC	KCTD6	NEURL1B	RBM24	STARD13
ADAMTS15	CISH	GADD45A	KIAA0040	NOG	RBP2	SYBU
ADAMTS8	CITED4	GADD45B	KLF15	NOTCH2	RCL1	SYNM
ADGRA2	CLDN8	GAS6-AS1	KLF4	NXPE3	RERE	TADA2B
ADPRM	CLK4	GATA6	KLF7	NXPH3	RGMA	TAF5L
ADRB2	CMTM7	GJB2	LCOR	OGFRL1	RGS2	TFAP2E
ANGPT1	CPM	GJB3	LEF1	OTULINL	RHOBTB2	TFCP2L1
ANKRD22	DIPK2A	GLIPR1	LINC00511	PACSIN1	RNF122	TGFBR3
ANKRD35	DISP3	GNA12	LINC01018	PAG1	RNF14	TGM2
ANKRD63	DIXDC1	GPR132	LINC01588	PANK1	RRS1-AS1	THBS1
APLN	DLX1	GPR153	LMO7	PDK4	RUNX1	TIPARP
ARC	DLX2	GPR63	LRCH1	PER2	S1PR5	TMCC2
ARL4A	DNAJB4	GPSM2	LRIG1	PGC	SEC14L2	TMEM266
ATP10A	ERICD	HEATR4	LRIG3	PGF	SGK1	TMEM63C
ATP1A4	ERN1	HERC5	MAFB	PHLDA1	SGPP2	TNFAIP8L3
ATP8B3	ERRFI1	HES2	MAN1A1	PI15	SH3BP5	TNFRSF10A
AZGP1P1	F3	HILPDA	MAP1B	PIK3R1	SKIDA1	TRIM17
BAG3	FAM104A	HOXA5	MARVELD3	PIM2	SLC16A9	TRNP1
BARX2	FAM43A	HS3ST3B1	MGAT3	PISD	SLC25A18	TSC22D2
BCL2L11	FAM53B	HSD11B2	MID1	PLA2G3	SLC25A25	TSKU
BCL6	FGD4	HSPA2	MIR1915HG	PLA2G4E	SNAI1	UACA
C1orf116	FGF18	HSPA6	MMP15	PLAUR	SNX30	USP54
C2CD4A	FHL3	IL17C	MMP24	PPM1L	SNX8	VWA5B2
CACUL1	FJX1	IL20RA	MMP25	PPTC7	SOD2	VWCE
CAVIN2	FKBP5	IMPDH1	MPHOSPH10	PRDM1	SOS1	WTAP
CCDC71L	FNDC4	IRS2	MPP3	PRICKLE1	SOWAHD	YTHDF1
CCND1	FOXO4	JAK2	MRAS	PRKAB2	SOX4	ZFP36
CD83	FOXP2	KCNE4	MRTFA	PXK	SPATA13	ZIC2
CDYL2	FRK	KCNF1	MTCL1	PXYLP1	SPRED1	ZNF189
						ZNF341
						ZNF563
						ZNF703
						ZSWIM3

Cluster 2 genes

ARHGAP42	DISP1	FAM107B	GPAT3	KLF10	MYB	PTGER4
BACH2	EFHC2	FBXL3	GRHL3	LHX4	NAV2	RCAN1
CCDC96	EFNA5	FGD6	HAS3	LIF	NKX1-2	RN7SL1
CCN2	EFNB2	GABRQ	HUNK	MAP3K8	NOTCH1	RND3
CDC42EP3	EPGN	GEM	IGFBPL1	MBOAT2	OVOL1	STMND1
CPEB4	ETS2	GLUL	JAG1	MTMR9	POC5	STYK1
						TIFA
						ZBTB16
						ZNF812P

Cluster 3 genes

AFDN	CBR3-AS1	DUSP1	KANK3	NBPF14	RAPGEF6	SMAD3
ARID3A	CBX4	EGFR	KIAA0232	NCALD	RCOR2	SOX9
ARL4D	CRY2	FIGN	LINC00482	PHF21A	RHOU	SP110
ATP1A1	CSRNP1	GRHL2	MAST3	PKP1	RIPK4	STAT5A
BRWD3	DOP1B	ITGA10	MYO10	PLEKHF1	RUSC1-AS1	TBXA2R
C3orf70	DTX2	KANK1	NBPF10	PPL	SH3TC2	TCAF2
						TMEM158
						TRIM22
						TSC22D3
						ZNF248
						ZNF652

Cluster 4 genes

ACOX1	C15orf39	FAM83B	KCNJ11	PAX9	RND1	ST8SIA1
ADD3	C9orf152	FOXA1	KCNMA1	PCDH7	RNF222	STING1
ADGRF1	CCDC177	FOXO1	KIAA0513	PDGFB	RORC	STOM
ADM	CDON	FOXO6	KIF13B	PER1	RPS6KA5	TBC1D8
AK4	CHRM1	FRMD4A	KLF5	PIK3R3	SALL2	TBX2
AKAP12	CLEC7A	FRMD4B	KLF9	PLAU	SASH1	TENT5B
AMIGO2	CLVS2	GCSAM	KLHDC7A	PLK2	SCNN1G	TFEB
AMOTL2	CORO2A	GULP1	LINC02361	PLLP	SERTAD1	TMC7
ANKRD50	CPEB3	HIVEP1	LRRC31	PPARGC1B	SH2B2	TMCC3
AQP3	CSF1	HOTAIR	LURAP1L	PPP1R26-AS1	SHROOM3	TMPRSS2
ARHGAP31	CYP1B1	HOXB2	MIR3142HG	PRR15	SLC22A23	TNRC6C
ARHGEF37	DBP	HOXB3	MMD	PRR15L	SLC40A1	TSHZ1
ARID5B	DDIT4	IL17RD	MSX1	PUS10	SLFN5	VAV3
ARL4C	DENND1B	IRAK2	N4BP3	PXDC1	SMAD6	ZBED5
ARMCX2	DUSP5	IRF2BP2	NAT1	PXMP4	SNPH	ZCCHC24
ASCL2	EFNA1	IRF2BPL	NDRG1	RBBP8NL	SOD3	ZFHX2
ATP1B1	EGF	IRX2	NKX3-1	RDH16	SOWAHA	ZFHX3
BCL3	ELF3	ITPRIPL2	NOL4L	RGS14	SRGAP1	ZKSCAN3
BCORL1	EPHB3	JUN	NRARP	RGS16	SRGAP2B	ZMAT3
BHLHE40	FAM110C	KCNB1	NUAK2	RHOV	SSH2	ZNF433
BMP4	FAM78A	KCNC4	PARD6B	RIN1	ST3GAL1	ZNF823